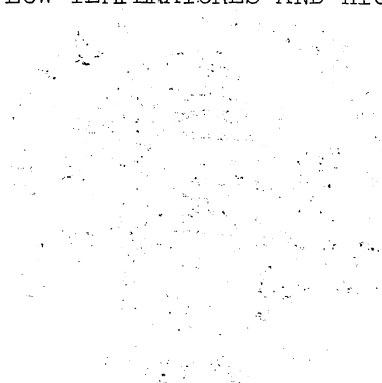


THE UNIVERSITY OF MICHIGAN  
INDUSTRY PROGRAM OF THE COLLEGE OF ENGINEERING

EXPERIMENTAL DETERMINATION OF THE THERMODYNAMIC PROPERTIES  
OF GASES AT LOW TEMPERATURES AND HIGH PRESSURES



Richard C. Faulkner, Jr.

A dissertation submitted in partial fulfillment  
of the requirements for the degree of  
Doctor of Philosophy in the  
University of Michigan  
1959

May, 1959

IP-368

Engr  
UMR  
1436

Doctoral Committee:

Professor Donald L. Katz, Chairman

Professor Joseph J. Martin

Professor Gordon J. Van Wylene

Professor Edgar F. Westrum, Jr.

Professor G. Brymer Williams

## ACKNOWLEDGEMENTS

I want to thank all of the many people who helped me during my doctorate work.

I am especially grateful to Dr. D. L. Katz, my committee chairman, for providing a great deal of leadership and encouragement during my thesis work.

I wish to express my gratitude to the other members of my committee, all of whom were called upon for advice and counsel. They are: Drs. J. J. Martin, G. J. Van Wylen, E. F. Westrum, Jr., and G. B. Williams.

I would like to thank those who assisted me in the construction of the equipment: Lawrason Thomas and Alex Robertson, graduate students; Herbert Senecal of the U.M.R.I. Instrument Shop; Frank Drogosz and Cleatis Bollen of the Chemical and Metallurgical Engineering Department. I would like to especially thank Millard Jones, the next investigator, who assisted me both in construction and operation of the equipment.

I am indebted to a number of persons for advice, aid, and counsel during my doctorate work: Dr. G. T. Furukawa of the U. S. Bureau of Standards, Dr. Riki Kobayashi of Rice Institute, Dr. J. R. Roebuck of the University of Wisconsin, Dr. B. H. Sage of California Institute of Technology, Dr. R. B. Scott of the U. S. Cryogenic Laboratory, and Mr. Guy Waddington of the U. S. Bureau of Mines.

I wish to gratefully acknowledge several organizations and persons who contributed financial support to this research:

The Chemical and Metallurgical Engineering Dept. Special Fund for a contribution toward equipment purchases.

The Horace H. Rackham School of Graduate Studies for a grant toward the purchase of a compressor.

The National Science Foundation for a grant without which the project could not have proceeded.

The Petroleum Research Fund of the American Chemical Society for a continuing support of the research, and for granting a fellowship.

The Socony Mobil Oil Co. for personal financial aid in the form of two fellowships, and a grant toward equipment purchases.

I want to thank the following people and organizations for donations of material, equipment, and facilities:

Dr. J. R. Roebuck for the loan of a pressure balance.

Dr. G. J. Van Wylen and Mr. W. H. Graves of the University of Michigan for making available the working space at the Automotive Laboratory.

Dr. E. F. Westrum, Jr. for the use of equipment and the gift of a large number of miscellaneous items.

Dow Chemical Company for donating a large quantity of Styrofoam insulation.

Gulf Oil Corporation for a 10 hp explosion-proof AC motor, and the provision of facilities to evacuate, purge, fill, and transport a number of gas cylinders.

Phillips Petroleum Company for the gift of some isopentane.

Tennessee Gas Transmission Company and Phillips Petroleum Company for the gift of a large quantity of very pure methane.

Wolverine Fin Tube for a gift of some finned tubing.

## TABLE OF CONTENTS

	<u>Page</u>
ACKNOWLEDGEMENTS.....	iii
LIST OF TABLES.....	viii
LIST OF FIGURES.....	x
ABSTRACT.....	xii
NOMENCLATURE.....	xiv
INTRODUCTION.....	1
THERMODYNAMIC PROPERTIES OF FLUIDS: AN APPROACH FOR THE EXPERIMENTAL INVESTIGATOR.....	6
Solution or Heat of Mixing Effects.....	7
Isobaric, Constant Composition Effect of Temperature Upon Enthalpy.....	14
Isothermal, Constant Composition Effect of Pressure Upon Enthalpy.....	17
Latent Heats of Liquid-Vapor Transition.....	24
The Combined Method.....	28
EXPERIENCE OF PREVIOUS INVESTIGATORS.....	35
Heat Capacities and Latent Heats.....	35
Joule-Thomson Measurements.....	44
The Thermodynamic Properties of the Pure Light Hydrocarbons.....	46
Properties of Light Hydrocarbon Systems Under Pressure.....	49
DESCRIPTION OF THE FLOW SYSTEM.....	51
Circulation, Purification, and Gas Storage.....	56
Refrigeration, Temperature and Pressure Control.....	59
Specific Heat and Latent Heat Measurements.....	63
Joule-Thomson Measurements.....	66
Flow Metering.....	66
Control Panel.....	69
Physical Layout and Facilities.....	71
Utilities and Safety Precautions.....	71
ISOBARIC SPECIFIC HEAT MEASUREMENTS ON NITROGEN.....	75
Discussion of System Performance.....	75
Data Obtained.....	84
Calculation of Specific Heat from Data.....	84
Comparison with Literature Values.....	89
Discussion of Results and Consideration of Errors.....	94

TABLE OF CONTENTS ( CONT'D )

	<u>Page</u>
RECOMMENDATIONS FOR FUTURE WORK.....	101
SUMMARY AND CONCLUSIONS.....	104
APPENDIX A.....	105
DESIGNING THE FLOW SYSTEM.....	106
Maintenance of Steady Conditions at the Calorimeter and Joule-Thomson Throttle.....	107
The Total Cooling Requirements of the System and the Time Required to Reach a Condition of Steady State Operation...	111
Sizing the System.....	114
Accuracy of Measurement of the Several Problem Variables; Selection of Magnitude of the Variable and Method of Measurement.....	117
DETAILED EQUIPMENT DESIGN AND DESCRIPTION.....	126
Hofer Compressor.....	126
Secondary Oil Separator.....	128
Liquid Nitrogen Cooler.....	129
Interchanger.....	131
Low Temperature (Calorimeter) Bath.....	131
Isobaric Specific Heat Calorimeter.....	137
Joule-Thomson Throttle.....	160
Vacuum System.....	175
Precision Electrical Measurements.....	175
Calorimeter Power Supply and Power Measurement.....	181
Measurement of the Operating Temperature of the Low Temperature Bath.....	185
Measurement of Flow Rate.....	187
Measurement of System Pressures.....	193
Measurement of System Temperatures.....	196
MECHANICAL DESIGN.....	197
Piping and Vessels.....	197
Pressure Testing.....	199
AC Power.....	199
Low Temperature, High Pressure Mechanical Problems.....	202
Low Temperature Insulation.....	207
Low Temperature Freeze-Ups.....	208
APPENDIX B.....	209
CALIBRATION OF THE EQUIPMENT.....	210
Linear Flow Metering Equipment.....	210

TABLE OF CONTENTS (CONT'D)

	<u>Page</u>
Main Calorimeter Thermocouple.....	221
Low Temperature Bath Platinum Resistance Thermometer.....	226
Standard Electrical Resistors.....	228
Heise Bourdon Tube Gauge.....	228
Potentiometer Standard Cell.....	228
Differential Pressure Balance Weights.....	228
APPENDIX C.....	229
MEASUREMENTS ERROR ANALYSIS.....	230
Power Measurement.....	230
Measurement of $\Delta T$ .....	234
Flow Rate Measurement.....	239
APPENDIX D.....	244
SAMPLE CALCULATION OF ISOBARIC SPECIFIC HEAT.....	245
Calculation of Mass Flow Rate, F.....	246
Calculation of Measured Heat Addition, Q.....	251
Calculation of Fluid Temperature Rise, $\Delta T$ .....	252
Calculation of Joule-Thomson Correction Term, $\delta T$ .....	255
Calculation of Isobaric Specific Heat, $C_p$ , from Apparent Isobaric Specific Heat, $(C_p)_F$ .....	255
APPENDIX E.....	257
BIBLIOGRAPHY.....	265



LIST OF TABLES

<u>Table</u>		<u>Page</u>
I	Principal References on Experimental Methods.....	36
II	References to Tabulations of Thermodynamic Properties of the Light Hydrocarbons.....	47
III	Typical Set of Readings for Calorimeter Difference Thermocouples.....	83
IV	Summary of Isobaric Specific Heat Data on Nitrogen.....	85
V	Comparison of Isobaric Specific Heat Data for Nitrogen with Literature Values.....	90
VI	Estimate of Maximum Measurement Errors.....	99
VII	Potentiometric Switch Positions.....	178
VIII	Analysis of Gas Used in Calibrating Flow Meter.....	211
IX	Main Calorimeter Thermocouple Calibration Data.....	227
X	Main Calorimeter Thermocouple Calibration Constants.....	227
XI	Summary of Data: -50°F, 294 psia, Flow 1.....	245
XII	Intermediate Mass Flow Rate Variables for Example Calculation.....	251
XIII	Summary of Variables Used in Computing $C_p$ for Example Calculation.....	255
XIV	Calibration Constants for Platinum Resistance Thermometer, Serial No. 1216653.....	258
XV	Calibrated Resistances of Standard Resistors.....	258
XVI	First Calibration of Heise Gauge.....	259
XVII	Second Heise Gauge Calibration.....	260
XVIII	Calibration of Potentiometer Standard Cell.....	260
XIX	Temperature Corrections to Barometric Pressure.....	261
XX	Analysis of Nitrogen Used in Isobaric Specific Heat Measurements.....	261

LIST OF TABLES (CONT'D)

<u>Table</u>		<u>Page</u>
XXI	Raw Data Nitrogen Specific Heats.....	262
XXII	Intermediate Calculations, Nitrogen Specific Heat Data.....	263
XXIII	Characteristics of Leeds and Northrup Model K3 Potentiometer.....	264

LIST OF FIGURES

<u>Figure</u>		<u>Page</u>
1	Isenthalpic Throttling Curves by Two Experimental Techniques.....	21
2	Combined Application of Isenthalpic Data and Data on Isobaric Specific Heats.....	23
3	<u>H</u> -T Diagram for a Hydrocarbon Mixture.....	26
4	<u>H</u> -P Diagram for a Hydrocarbon Mixture.....	27
5	P-T Diagram for a Hydrocarbon Mixture.....	29
6	Simplified Flow Diagram of the System.....	52
7	System Flow Diagram.....	53-55
8	Compressor Supply Tank, Compressor, Oil Separator, and High Pressure Cylinders.....	58
9	Liquid Nitrogen Transfer.....	61
10	Low Temperature (Calorimeter) Bath, Carbon Dioxide Cooler, Liquid Nitrogen Cooler, and Interchanger.....	64
11	Constant Temperature Metering Bath and Differential Dead Weight Pressure Balance.....	68
12	Control Panel.....	70
13	Liquid Nitrogen Machine.....	72
14	Overall View of Test Cell 247.....	73
15	Calorimeter Assembly Drawing.....	81
16	Linear Approximation for Heat Leakage Correction in a Flow Calorimeter.....	87
17	Variation of Isobaric Specific Heat of Nitrogen with Pressure at -50°F, -100°F, and -150°F.....	92
18	Variation of $C_P/C_{P_0}$ for Nitrogen with Pressure at -50°F, -100°F, and -150°F.....	93
19	Calorimeter Detail Drawings.....	142-151
20	Modified Calorimeter Heater Capsule Closure.....	152

LIST OF FIGURES (CONT'D)

<u>Figure</u>		<u>Page</u>
21	Modified Calorimeter Thermocouple Wells.....	153
22	Joule-Thomson Throttle Assembly Drawing.....	163
23	Joule-Thomson Throttle Detail Drawings.....	171-174
24	Calorimeter Heater Circuit.....	182
25	Platinum Resistance Thermometer Circuit.....	186
26	Calorimeter and Joule-Thomson Pressure Measurements...	194
27	Primary Distribution of AC Power in Test Cell 247.....	200
28	115 VAC Single Phase Circuitry in Test Cell 247.....	201
29	Pressure Correction to Methane Viscosity for Flowmeter Calibration.....	215
30	Compressibility Factors for Methane at 20°C.....	216
31	Pressure Correction to Flowmetering Calibration Constants at 20°C.....	218
32	Calibration Curves for Linear Flowmeter at 20°C and Several Pressures.....	220
33	Deviations of Calorimeter Thermocouple Data from a Fitted Curve.....	237

EXPERIMENTAL DETERMINATION OF THE THERMODYNAMIC PROPERTIES  
OF GASES AT LOW TEMPERATURES AND HIGH PRESSURES

Richard Campbell Faulkner, Jr.

ABSTRACT

The purpose of this work was to (1) design and construct equipment suitable for determining experimentally the enthalpy of light hydrocarbon mixtures over the temperature range from 70°F to -280°F, over the pressure range from atmospheric to 2500 psia, (2) mechanically test and calibrate the equipment, and (3) obtain sufficient data on a gaseous substance to evaluate the performance of the system.

In order to deliver fluid to a flow calorimeter or expansion device at a specified temperature and pressure, a compressor for circulation, equipment for continuous purification, means for stabilization and control of pressure and flow rate, and a cooling system employing dry ice and liquid nitrogen, were incorporated in a closed flow cycle. A linear flow meter was installed on the intake side of the compressor in a portion of the system operating at ambient temperature and at pressures from 60 to 100 psia. The flow meter was placed in a constant temperature liquid bath.

A high pressure flow calorimeter was constructed to measure isobaric specific heats of liquids, gases, or single phase systems above their critical pressures, and to measure isobaric integral latent heats of vaporization of mixtures. An expansion device employing radial porous plugs, often described as a Joule-Thomson throttle, was constructed to measure isenthalpic throttling.

Both the calorimeter and expansion device were located in a constant temperature liquid bath. The temperature of the bath was measured with a platinum resistance thermometer. A pressure balance was installed

for measuring absolute pressures or pressure differences at the calorimeter or expansion device. An electronically regulated DC power supply, having a capacity of 60 watts, furnished the energy for calorimetric measurements at 0 to 100 volts. Electrical energy to the calorimeter was measured with a potentiometer, standard resistors, and attendant circuitry. Multiple junction copper-constantan thermocouples were provided for measuring temperature changes in the calorimeter or expansion device.

Prior to taking measurements the flow system, calorimeter, and expansion device were mechanically tested and calibrations were performed for the measuring devices including the flow meter and calorimeter thermocouple.

The flow system and calorimeter were operationally tested by measuring the isobaric specific heat of nitrogen at pressures from 294 to 1176 psia and temperatures from -50°F to -150°F employing mass flow rates from .16 to the maximum system flow rate of .30 pounds per minute. Measured energy additions ranged from .9 to 2.9 Btu's per minute, causing a temperature rise of 18 to 20°F for the fluid.

The majority of the experimentally measured values of the isobaric specific heat of nitrogen agreed with literature values within 2%.

Based on experience gained during operation of the equipment, it was concluded that modifications should be undertaken by the next investigator to reduce the length of time required to obtain data and to eliminate sources of inaccuracy which became apparent. It is believed that measurements of isobaric specific heats of light hydrocarbon mixtures from 70°F to -280°F, from atmospheric pressure to 2500 psia with an accuracy of 1%, or better, would then be possible.

## NOMENCLATURE

a	A calibration constant for the linear flowmeter
a	A calibration constant for the main calorimeter thermocouple
a	A calibration constant for standard electrical resistors
b	A calibration constant for the linear flowmeter
b	A calibration constant for the main calorimeter thermocouple
B	Barometric pressure
c	A calibration constant for the main calorimeter thermocouple
$C_P$	Isobaric specific heat
$(C_P)_F$	Apparent isobaric specific heat measured at flow rate F
$C_{P,x}$	Isobaric specific heat measured at constant composition
d	A calibration constant for the main calorimeter thermocouple
E	Emf or voltage
$E_C$	IR drop across calorimeter heater
$E_{L_1}, \dots, E_{L_{10}}, E_{R_1}, \dots, E_{R_{11}}$	Potentiometric voltage measurement at switch positions $L_1, \dots, L_{10}, R_1, \dots, R_{11}$ (Table VII)
$E_P$	Voltage drop across the platinum resistance thermometer
$E_T$	Emf of main calorimeter thermocouple at temperature T with one set of junctions at the ice point temperature
F	Mass flow rate
g	Gravitational acceleration
$g_l$	Local gravitational acceleration
G	Any thermodynamic property G, per mol
$\Delta h$	Differences in liquid levels in a U-tube as measured by a cathetometer
H	Enthalpy

## NOMENCLATURE (CONT'D)

$\underline{H}$	Enthalpy of a pure substance or a mixture, per mol
$\underline{H}_K$	Enthalpy of pure component K at the temperature and pressure of a mixture, per mol
$\bar{H}_j$	Enthalpy of component J in a mixture
$\Delta \underline{H}_{P,x}$	Enthalpy change at constant pressure and composition, per mol
$\Delta \underline{H}_{T,x}$	Enthalpy change at constant temperature and composition, per mol
I	Electrical current
$I_C$	Current passing through calorimeter heater
$I_M$	Current passing through a voltage multiplying circuit
$I_P$	Current passing through platinum resistance thermometer
$I_T$	Current flowing through the calorimeter power supply
m	Mass
m	Number of moles
$M_w$	Molecular weight
P	Pressure
$\Delta P$	Pressure difference
$\Delta P$	Pressure drop across a linear flowmeter, inches of water at 20°C
$\Delta P$	Pressure difference measured during isenthalpic measurements
Q	Heat added to a system
Q	Measured addition of energy to a flow calorimeter
$\delta Q$	Heat added to a system
$\delta Q$	(Unmeasured) heat leakage, generally across the boundaries of a system
R	Electrical resistance



## NOMENCLATURE (CONT'D)

R	Universal gas constant
$R_a, \dots, R_f$	Standard electrical resistances
$R_0$	Electrical resistance at a reference temperature, $T_0$
$R_T$	An electrical resistance at temperature, T
T	Temperature
$\Delta T$	A temperature change
$\Delta T$	Temperature rise of fluid in a flow calorimeter, upon addition of energy
$\delta T$	A temperature correction for the Joule-Thomson effect in a flow calorimeter
u	Linear velocity
V	Volume
$\frac{V}{n}$	Volume per mole of a pure component or mixture
$\dot{V}$	Volumetric flow rate
W	Electrical power
$W_C$	Power dissipation in the calorimeter heater, watts
$\delta W$	Mechanical work done by a system
$x_A, \dots, x_K$	Mole fraction of component A, ..., K in a mixture
Z	Compressibility factor
Z	Elevation above a reference plane
$\alpha$	Integrated mean coefficient of resistivity
$\beta$	A calibration constant for the platinum resistance thermometer
$\beta$	A calibration constant for standard electrical resistors
$\delta$	A calibration constant for the platinum resistance
$\epsilon_1, \dots, \epsilon_9$	Estimated uncertainties in a measurement
$\rho$	Density

NOMENCLATURE (CONT'D)

$\rho_0$	Density at one atmosphere pressure and temperature T
$\mu$	Viscosity
$\mu_{1,T}$	Viscosity at one atmosphere pressure and temperature T
$\mu_{P,T}$	Viscosity at pressure P and temperature T
$\mu^*$	Joule-Thomson coefficient

## INTRODUCTION

The purpose of the present investigation was to design, construct, test, and operate equipment which would be capable of direct measurement of the enthalpy properties of single pure light hydrocarbons or light hydrocarbon mixtures over the temperature range from 70°F to -280°F, and over the pressure range from atmospheric to 2,500 psia. The question of type and amount of experimental data to be taken in the present research was not immediately established in view of the anticipated magnitude of the equipment problem. It was intended that this investigation should lay the ground work for several future theses dealing with thermodynamic properties of the light hydrocarbons.

Equipment was designed, constructed, and mechanically tested which is thought to be suitable for obtaining the desired information. This equipment includes a calorimeter for measuring isobaric enthalpy changes with temperature and a Joule-Thomson porous plug expansion device for the purpose of measuring isenthalpic throttling. Both devices were incorporated in a closed flow cycle which includes equipment for circulation of the fluid being tested, refrigeration, storage, flow rate control, flow rate measurement, pressure control, temperature control, and measurement of pressure and temperature. The entire apparatus was operationally tested to the extent of measuring the specific heat of nitrogen as a function of pressure and temperature and comparing the resultant values with the literature. It was concluded that the values of  $C_p$  obtained for nitrogen were of about the same accuracy as values with which they were compared.

Information concerning the behavior of the light hydrocarbons at low temperatures and under high pressures is of great importance. At the present, this is particularly true because of the increasing emphasis being placed on low temperature separation and purification of natural gas constituents. There is a steadily increasing demand for these constituents as raw materials in a large number of industrial chemical processes. At the same time, because of the high cost of refrigeration necessary in carrying out low temperature operations, a demand exists for a better knowledge of the physical properties of the light hydrocarbons upon which to base design calculations and to better optimize operating conditions.

It appears that the information which is most necessary for the satisfactory solution of a large majority of the existing problems is a knowledge of the enthalpy properties of the light hydrocarbons in mixtures under both single phase and two phase liquid-gas conditions, together with liquid-gas equilibrium data. Equilibrium studies of binary, ternary, and multicomponent light hydrocarbon systems together with hydrogen and nitrogen are being conducted at the University of Michigan and elsewhere.

At the present time satisfactory information is not available concerning the thermodynamic behavior of the light hydrocarbons, particularly when present in mixtures with other light hydrocarbons over a wide range of low temperatures and high pressures.

The values of properties which are available for the pure components under these conditions have been constructed from related information though complicated calculational procedures. In the process of constructing these values from PVT, vapor pressure measurements, etc., a

great deal of loss in original accuracy of the experimental measurements has occurred. Furthermore, in some regions of interest, good experimental data upon which to base calculations of the thermodynamic properties are not in existence.

In the case of light hydrocarbon mixtures, the situation is much worse. By and large, calculational procedures have either neglected the mixing effects or have employed procedures of combining the properties of single components which have not for the most part been verified experimentally or have been shown to be only approximate. Few PVT or thermodynamic data for light hydrocarbon mixtures existed under the experimental conditions which were proposed for this research.

It was felt that one satisfactory experimental program for ascertaining the required information concerning the enthalpy properties of light hydrocarbon mixtures would be to measure, at constant composition, isobaric specific heat as a function of pressure and temperature by direct flow calorimetry, measure also by direct flow calorimetry values of isobaric integral latent heat of vaporization, and determine by the Joule-Thomson porous plug method a series of isenthalpic throttling curves. All of these measurements are consistent with the operation of a flow system.

The flow system, operating as a closed cycle, was constructed for the purpose of incorporating the measurements mentioned. A calorimeter suitable for measuring specific heats at constant pressure of light hydrocarbon liquids, gases, and single phase systems above the critical point was constructed. The calorimeter and associated equipment, after slight modification, will be suitable for measuring large enthalpy changes at constant pressure such as isobaric integral latent heats or specific heats

very near the critical points of pure components or mixtures. A Joule-Thomson expansion device, using radial porous plugs, was also constructed and will be capable of measuring isenthalpic throttling over a wide range of conditions.

In the initial stage of the broad program which was planned, the majority of all equipment design, construction, mechanical testing, and calibration, was completed. The flow system was operationally tested and the calorimeter proved by measuring values of the specific heat of nitrogen and comparing them with literature values. Isobaric specific heat measurements were made on nitrogen at temperatures of  $-50^{\circ}\text{F}$ ,  $-100^{\circ}\text{F}$ , and  $-150^{\circ}\text{F}$ , and at pressures from 294 psia to 1176 psia. The majority of the measurements agreed with literature values within 2%. The accuracy of the measurements was thought to be 2 to 3%. It was concluded that with slight modification of the system an accuracy of better than 1% can be attained in specific heat determinations.

Future work, which will constitute other doctoral programs, will include measurements of specific heats at constant pressure, isenthalpic throttling, and isobaric integral latent heats of vaporization for a series of mixtures at constant composition. These measurements will be carried out first for a series of binary mixtures of the light hydrocarbons at low temperatures and high pressures. Later, measurements will be made with more complex systems and possibly with hydrogen and nitrogen as components. At constant composition, specific heat and Joule-Thomson measurements will serve to determine the change of the enthalpy property with pressure and temperature in single phase regions. Below the mixture critical point, direct measurements of the constant pressure heat of vaporization will supply the necessary information for directly relating liquid and gaseous enthalpy values.

It will be possible from a study of a number of mixtures to deduce the effect of composition in a system composed of a certain set of components. It is hoped that given this information for a number of systems, the enthalpy values in arbitrary complex mixtures can be constructed as a function of pressure, temperature, and at least one composition correlating factor -- but without the necessity of considering all of the phase variables and hence destroying any generality. Such generalized correlations exist at the present time; however, they suffer from lack of basic data upon which to base a test of the correlation.

It is important to point out that the method described for determining the enthalpy property is not the only satisfactory one. The present method does represent a very direct approach to the problem of determining the enthalpy property. The method is less direct if it is desired to obtain various other thermodynamic information. In any event, it is highly desirable to make use of other additional information that may become available -- such as PVT data for mixtures. With a great deal of related information, it is possible to employ a number of cross-checks in arriving at the complete thermodynamic network. Also, for the purpose of ascertaining properties it is frequently advisable to employ information obtained from different techniques in different regions. One method may be superior under certain experimental conditions, another preferable under other experimental conditions.

THERMODYNAMIC PROPERTIES OF FLUIDS:  
AN APPROACH FOR THE EXPERIMENTAL INVESTIGATOR

The enthalpy of a solution in a single homogeneous phase is defined by the state of the substance. The variables which define this state are those which exert an appreciable influence on the enthalpy function. Except in very special systems the variables of importance are pressure, temperature, and chemical composition. Since the value of the enthalpy function is determined from its state, the change in enthalpy with a change in the variables which define it may be expressed as an exact differential. In other words, the change in the enthalpy function from one state to another is determined from a knowledge of the two states and is in no way dependent upon the manner in which this change may be carried out.

The statements which have been made concerning enthalpy can be expressed mathematically for a single homogeneous phase by the equation:

$$dH = \left(\frac{\partial H}{\partial T}\right)_{P, x_A, x_B, \dots} dT + \left(\frac{\partial H}{\partial P}\right)_{T, x_A, x_B, \dots} dP + \left(\frac{\partial H}{\partial x_A}\right)_{P, T, x_B, \dots} dx_A + \dots \quad (1)$$

H = Enthalpy of solution containing several components per mole

T = Temperature

P = Pressure

$x_I$  = Mole fraction of component I

In practice, the absolute value of the enthalpy function is never known. Its value relative to an arbitrary state is sufficient for



its practical use, however. Equation (1) can be integrated to express the change in the enthalpy function from one state to another within any single homogeneous phase region defined by the variables P, T,  $x_1$ :

$$\Delta H_{12} = H_{P, x_A, x_B, \dots} \Big|_{T_1}^{T_2} + H_{T, x_A, x_B, \dots} \Big|_{P_1}^{P_2} + H_{P, T, x_B, \dots} \Big|_{x_{A_1}}^{x_{A_2}} + \dots \quad (2)$$

Equation (2) expresses the total change in enthalpy from state 1 to state 2 as the sum of the changes along a set of convenient paths.

Let us consider the problem of determining experimentally the necessary information for evaluating the change in the enthalpy function along the various paths indicated in Equation (1).

#### Solution or Heat of Mixing Effects

The problem of experimentally evaluating the terms in Equation (1) which involved enthalpy change due to changes in composition was given some consideration. Unfortunately, however, such effects are not amenable to a fairly simple and reliable experimental determination under the conditions imposed by this research. It is necessary before discussing the problem of evaluating solution effects to review certain basic principles regarding the behavior of different kinds of systems.

Certain systems under proper conditions of temperature and pressure tend to exhibit what is termed ideal system behavior. Ideal system behavior implies that the properties of the system are simply a combination of the properties of the chemical species which comprise the solution, weighted according to chemical composition. Thus, if G

represents the value of any property per unit quantity of the mixture and  $G_A, G_B, \dots$  are the values of this property per unit quantity for the pure components under the conditions at which the mixture exists, then:

$$G = x_A G_A + x_B G_B + \dots \quad (3)$$

where  $x_A, x_B$  are the fractions of A, B, ... in the system.

An ideal system has been defined by Hougen and Watson<sup>(50)</sup>, for example, to be "a group of components which tend to form ideal liquid solutions at low temperatures where the saturated vapor of each component behaves as an ideal gas". A non-ideal system is defined by the same authors to be a system that does not exhibit ideal liquid solution behavior at any temperature.

In general, chemical homologs tend to exhibit ideal system behavior. Substances in solutions which are chemically dissimilar, however, often as measured by the polarity of the compounds, are not likely to form ideal systems.

While chemical homologs do tend to form ideal systems, these systems do not necessarily exhibit ideal solution behavior under all conditions. This is explained frequently by the difference in size of the several molecules making up the system. Non-ideal systems show this kind of non-ideal behavior in addition to that caused by chemical dissimilarity. It has been pointed out by Hougen and Watson<sup>(50)</sup> that liquid systems involving chemical dissimilarity tend to become more ideal as temperature increases, whereas for liquid systems exhibiting non-ideal behavior-due chiefly to the differences in molecular size - the degree of non-ideality tends to decrease with a decrease in temperature.

In the case of a system composed of hydrocarbons, particularly if they are of the same type, e.g., aliphatic, liquid solutions tend to approach ideal solution behavior at some low temperature. This temperature depends on the composition of the solution and the pressure exerted on the system. Nevertheless, it can be stated that when all of the components in the liquid solution would exist in a stable liquid state under the pressure and temperature of the solution, that ideal solution behavior is being approached. Hougen and Watson<sup>(50)</sup> have suggested that when all of the components in an ideal system present in a liquid phase are below a certain reduced temperature, suggested to be on the average about 0.9, that ideal solution behavior is to be expected.

Measurements of liquid-vapor equilibrium have indicated that in systems composed of a homologous series of hydrocarbons that a wide deviation from ideality occurs when components lighter than the solution average are present. Since if a solution is non-ideal in one respect, it is non-ideal in all others, this clearly indicates that solution values of internal energy, enthalpy, etc., can be expected to deviate from ideal solution values. The effect of pressure on this non-ideality of a low temperature liquid system is important insofar as it may promote the presence of a volatile material in the mixture under conditions in which the pure volatile component would not be stable. At sufficiently low temperature, the pressure effect on the thermodynamic properties, as in the case of pure component liquid phases, is small.

In the case of mixtures of hydrocarbon homologs in a gaseous phase, in general, the assumption of ideal solution behavior is much more nearly true than is the assumption of the applicability of the

ideal gas law. At low pressures, where gases approach ideal gas law behavior, the assumption of ideal solution behavior may be quite good. However, if less volatile components are present in a gas which under the same temperature and pressure would be liquefied in the pure state, difficulties analogous to those encountered for light components dissolved in liquids may be expected to occur. Hougen and Watson<sup>(50)</sup> have suggested that such difficulties will definitely occur at pseudo-reduced temperatures of the mixture of the order of 1.0 or less. At higher temperatures, well removed from the critical temperature of all of the components, ideal solution behavior tends to be approximated to much higher pressures. In view of the fact that ideal gas behavior is approached at very high temperatures, regardless of pressure, it is assumed that ideal solution behavior would also be approximated under these conditions.

It is desirable now to return to the discussion of the experimental determination of heat of mixing effects.

It should be pointed out that the ultimate aims in studying the enthalpy properties of mixtures are:

1. Report mixture enthalpies on a common "basis" so that they may be used in conjunction with other mixture enthalpies.
2. Obtain information which will constitute the justification or proof for generalized methods of treating mixture problems - thus avoiding the necessity of investigating a vast number of systems.

One experimental possibility which would provide the necessary information would be to study a number of different mixtures of a set of

components -- each experiment being conducted, however, at constant composition. This would consist of studying the isobaric temperature effect and the isothermal pressure effect on the enthalpy of fixed composition solutions. If no composition change occurs during an experiment:

$$\Delta H_{12} = H_{P, X_A, X_B, \dots} \Big|_{T_2} + H_{T, X_A, X_B, \dots} \Big|_{P_2} - H_{P, X_A, X_B, \dots} \Big|_{T_1} - H_{T, X_A, X_B, \dots} \Big|_{P_1} \quad (4)$$

and the experimental problem in determining pressure and temperature effects upon the enthalpy of a particular mixture would be exactly the same as for a single pure substance.

In view of the discussion of non-ideal solution behavior in an ideal system, such as is approximated by at least the aliphatic light hydrocarbons, it is apparent that we can select a reference state for the enthalpy of a mixture of light hydrocarbons in which the solution approximates ideal solution behavior. This might be a state in which the gas phase behaves according to the ideal gas law or it might be a low temperature saturated liquid state in which the components form a nearly ideal solution.

If such a reference state were selected, the various light hydrocarbon mixture enthalpies at a particular temperature and pressure, in a series of systems composed of the same components, could easily be referred to a common basis of temperature and pressure. If, however, a reference state were selected where ideal solution behavior was not closely approximated, it would be necessary to know the solution heat effects associated with the formation of each mixture at the reference

temperature and pressure. In such a case, or if no ideal solution state existed, it would be mandatory to conduct more or less direct measurements of the solution effects in order to be able to relate enthalpy information for different mixtures of the same components.

It is, of course, alternately theoretically possible to measure the enthalpy change of the pure components from any base reference state (defined for pure components by pressure and temperature in all but special systems) to a desired final pressure and temperature and then measure the "heat of mixing" or solution effects at this pressure and temperature resulting from a combination of the components to form a particular system. For the light hydrocarbons, however, the regions of particular practical interest make such measurements extremely difficult. Under conditions of high pressures and frequently low temperatures such measurements are practically impossible.

A few investigations, for example, by Sage and Lacey<sup>(17)</sup> and Miller<sup>(71)</sup> have been conducted to determine the heat effects associated with the solution or dissolution of a volatile material from a relatively non-volatile liquid.

A number of measurements of mixing effects have been made for systems composed of components normally all in the liquid state at atmospheric pressure and near room temperature. Even under these mild conditions, the experimental techniques usually employed for such measurements frequently do not produce good data.<sup>(79)</sup> Examples of solution effect studies conducted in the liquid state are the work of Kemp and Brown<sup>(53)</sup> with mixtures of n-pentane and benzene (an almost ideal system), the work of Tsao and Smith<sup>(132)</sup> with binary and ternary mixtures of methanol, n-heptane, and toluene (not an ideal system).

Some time prior to the work of Tsao and Smith, Scatchard<sup>(116,117)</sup> had presented, from the fundamental point of view of intermolecular forces existing in liquid mixtures, equations to predict heats of mixing. Unfortunately, it was necessary for Scatchard to make so many assumptions regarding certain of the forces in order to make the equations usable, that the resulting equations were applicable only to very simple, nearly ideal solutions. As a result of the failure of this and similar theoretical treatments to adequately describe complex solution behavior the approach to predicting heats of mixing has been generally empirical. This kind of situation is not restricted to heats of mixing; difficulty has been experienced in most theoretical attempts to describe thermodynamic behavior of pure components or mixtures except under relatively mild conditions or near conditions of ideality. In general, more success has resulted from mathematical predictions in regions of lower fluid density, e.g., gas behavior based on the kinetic theory of gases, than for liquid systems.

A great deal of effort in recent investigations concerning non-ideal behavior of mixtures has been directed toward the study of vapor-liquid equilibrium in non-ideal systems. This has been true because of the increasingly important roles of azeotropic and extractive distillation processes. Guggenheim<sup>(44,45)</sup>, Redlich and Kister<sup>(89-91)</sup>, and Scatchard and Raymond<sup>(118)</sup> have correlated equilibrium data on the basis of the concept of "excess free energy of mixing". A number of correlations of varying complexity have been used for this purpose. Wohl<sup>(147)</sup> proposed a four-suffix equation which it was claimed included as special cases most of the empirical equations which had been proposed.

The concept of excess free energy of mixing was extended by Redlich and Kister<sup>(89-91)</sup> and Scatchard and Tichnor<sup>(119)</sup> to a method of correlating enthalpies of mixing. In the case of absence of ternary or multicomponent heat of mixing data, methods have been proposed for predicting these effects from binary data using the empirical schemes mentioned.

The results of such investigations indicate one way in which the solution enthalpy effects (which are apparent in various light hydrocarbon mixtures when referred to a common basis and compared) might be correlated. For the purpose of establishing a convenient correlation for multicomponent systems the concept of excess free energy of mixing is not thought to be the best approach, however. This matter will be discussed in greater detail at another point in the discussion.

Isobaric, Constant Composition Effect  
of Temperature Upon Enthalpy

Examination of Equation (1) reveals that for a single uniform phase of constant composition that the effect of pressure and temperature on enthalpy must be determined.

Experimentally it is convenient to evaluate the differential coefficient,  $\left(\frac{\partial H}{\partial T}\right)_{P, X_A, X_B, \dots}$  as well as the integral temperature effect upon enthalpy,  $\Delta H_{P, X_A, X_B, \dots}$ . This coefficient, termed the specific heat at constant pressure and composition as a function of pressure and temperature, is valuable for a number of thermodynamic calculations.

A variety of methods, some rather direct, others less direct have been employed in the determination of heat capacities. A number of these methods have been reviewed by Partington and Schilling<sup>(81)</sup> and



by Masi<sup>(66)</sup> and include:

1. Flow calorimetry.
2. Constant volume calorimetry.
3. Heat exchange method.
4. Explosion method.
5. Isentropic expansion method.
6. Velocity of sound method.
7. Resonance method.
8. Self-sustained oscillation method.
9. Flow comparison method.
10. Constant volume method.

In addition, ideal gas heat capacities of simple molecules may now be calculated statistically with probably equal or better accuracy than they can be measured.<sup>(66)</sup>

Not all of the methods mentioned determine  $C_{P,x}$ . Some result in the determination of constant volume specific heats or ratios of constant pressure to constant volume specific heats.

Simultaneous consideration of the following difficulties:

1. Limited range of reliable applicability,
2. Other information necessary to convert experimental results to values of  $C_{P,x}$ ,
3. Applicability to mixtures, and
4. Accuracy of measurements,

led the author to feel that direct flow calorimetry represented the best method of determining  $C_{P,x}$  over a range of temperatures and pressures.

The direct flow method of calorimetry consists of measuring the temperature change of a flowing fluid at constant pressure when a known amount of electrical energy is added to the fluid, and at the same time determining the mass rate of flow.

The energy balance for a flow system may be stated in one form as (65):

$$\left[ \left( H + \frac{u^2}{2} + gz \right) dm \right]_{in} - \left[ \left( H + \frac{u^2}{2} + gz \right) dm \right]_{out} + \delta Q - \delta W = d \left[ \left( H + \frac{u^2}{2} + gz \right) m \right]_{\text{system}} \quad (5)$$

$u$  = Velocity

$z$  = Elevation above reference plane

$m$  = Number of mols

$\delta Q$  = Heat input to the system

$\delta W$  = Mechanical work done by the system

If we select a flow calorimeter as a system, the term  $d \left[ \left( H + \frac{u^2}{2} + gz \right) m \right]_{\text{system}}$  is zero for steady operation. Furthermore, in flow calorimetry changes in potential or kinetic energy are made negligible, there is no shaft work crossing the boundaries of the system, and mass into the calorimeter is equal to mass out of the calorimeter per unit time. Under these conditions from Equation (5) the enthalpy change of the fluid at constant pressure is equal to the energy addition to the system at constant pressure:

$$\Delta H_{P, X_A, X_B, \dots} = \delta Q_{P, X_A, X_B, \dots} \quad (6)$$

In the practical execution of this experiment it was necessary to make corrections for heat leaks and for the failure of the process to be exactly isobaric. The calculation  $C_{P,x}$  from  $\Delta \underline{H}_{P,x}$  is straightforward. The only requirement experimentally is that of maintaining a sufficiently small temperature increment so that the integrated mean  $C_{P,x}$  which is calculated is very nearly the same as the value for the arithmetic mean heat capacity over the temperature increment.

Isothermal, Constant Composition Effect  
of Pressure Upon Enthalpy

The evaluation of the isothermal change in enthalpy with pressure may also be evaluated by a number of experimental procedures.

One very direct method has been termed the Eucken method. The experiment consists of imposing a pressure drop upon a flowing fluid while at the same time supplying sufficient energy so that the process will be isothermal. The flow process is conducted in a steady state manner, no shaft work is allowed to cross the boundaries of the system, no appreciable kinetic or potential energy effects are permitted. Under these conditions, from Equation (5), it is seen that

$$\Delta H_{T,x_A,x_B,\dots} = \int \delta Q_{T,x_A,x_B,\dots} \quad (7)$$

While very direct, this method has certain disadvantages, the principle disadvantage being the practical difficulties in carrying out such an experiment. A satisfactory flow rate must be established and measured. A variable pressure drop must be imposed without engendering problems of translational or rotational kinetic energy effect. A trial and error addition of heat must be made and heat leaks must be minimized in the system.

Some consideration was given to the possibility of conducting measurements of single phase pressure effects and temperature effects upon enthalpy as well as isobaric integral latent heat measurements in a single experimental device, but this possibility was abandoned due to mechanical problems.

Another very common way of determining the isothermal pressure effect upon enthalpy is that of measuring PVT properties. This method has been very commonly employed in the determination of a number of thermodynamic effects in pure substances. It is equally applicable to constant composition mixtures and has been used, for example, by Sage and Lacey<sup>(112)</sup> in conjunction with other methods to report the thermodynamic properties of light hydrocarbon binaries above room temperature and under pressure. From PVT measurements the differential coefficient  $\left(\frac{\partial H}{\partial P}\right)_{T,x}$  may be evaluated from the relation:

$$\left(\frac{\partial H}{\partial P}\right)_{T,x} = \left[ V - T \left(\frac{\partial V}{\partial T}\right)_P \right]_x \quad (8)$$

One disadvantage in such a procedure lies in the extreme accuracy with which the PVT measurements must be made, since errors in experimental measurements may be magnified many fold in differentiation processes. In many cases PVT data is fitted with an appropriate equation of state in order to facilitate analytical treatment. In general, in the processes of smoothing and fitting over a wide range of conditions, considerable accuracy is lost in the description of the PVT data unless an extremely complicated equation of state is employed. For example, it has been

estimated that in order to obtain an accuracy of one percent in representation of PVT data for densities up to 1.5 times the critical density, using a pressure explicit equation of state, requires from 8 to 10 constants.<sup>(65)</sup> Most equations of state tend to fail at densities much greater than that of the critical density. It has been claimed that the Benedict-Webb-Rubin<sup>(7)</sup> equation represents the liquid phase fairly successfully. This is open to question.

Another method for measuring the isothermal pressure effect upon enthalpy, and the one used in the present investigation, is the method of measurement of isenthalpic expansion.

This experiment consists of introducing a pressure drop into a flowing fluid and measuring the resulting temperature change under conditions of steady flow, no shaft work, negligible potential and kinetic energy effects, no transfer of heat to the system surroundings. Under these conditions Equation (5) indicates that  $H_1 = H_2$  or that the process is isenthalpic. What is measured is the ratio of  $\left(\frac{\Delta T}{\Delta P}\right)_{H,x}$ . In the limit as  $\Delta P \rightarrow 0$  this quantity approaches the Joule-Thomson coefficient,  $\mu^*$ , i.e.:

$$\mu^* = \lim_{\Delta P \rightarrow 0} \left(\frac{\Delta T}{\Delta P}\right)_{H,x} = \left(\frac{\partial T}{\partial P}\right)_{H,x} \quad (9)$$

The differential coefficient  $\left(\frac{\partial H}{\partial P}\right)_{T,x}$  is given by:

$$\left(\frac{\partial H}{\partial P}\right)_{T,x} = -\left(\frac{\partial T}{\partial P}\right)_{H,x} \left(\frac{\partial H}{\partial T}\right)_{P,x} \quad (10)$$

Therefore, substituting the quantity  $C_{P,x}$  for its equivalent

$$\left(\frac{\partial H}{\partial P}\right)_{T,x} = -\mu^*(P,T) C_{P,x}(P,T) \quad (11)$$

It is clear from this relation that a knowledge of specific heat at constant pressure and the Joule-Thomson coefficient as a function of pressure and temperature at constant composition would permit integrating to obtain the integral isothermal enthalpy change with pressure:

$$\Delta H_{T,x} = -\int [\mu^* C_P]_x dP_T dT_P \quad (12)$$

There are two general experimental methods for isenthalpic measurements without regard to the many differences in individual experimental techniques.

One method is illustrated by the work of Sage, Lacey, and co-workers (13-16,55,109-111) This method consists of expanding from an initial pressure and temperature to a slightly lower pressure, measuring the resulting temperature change, and then readjusting the initial conditions of another measurement to the final conditions of the previous measurement (Figure 1). Such a procedure has certain advantages and disadvantages. It is apparent that by taking small pressure increments an integral average Joule-Thomson coefficient which is not greatly different from the Joule-Thomson coefficient at the arithmetic average conditions may be reported. However, it is experimentally difficult often to readjust the initial conditions of a successive measurement to the final conditions of a previous measurement. Furthermore, since  $\Delta T$  and  $\Delta P$  are small they must be measured with high absolute accuracy.

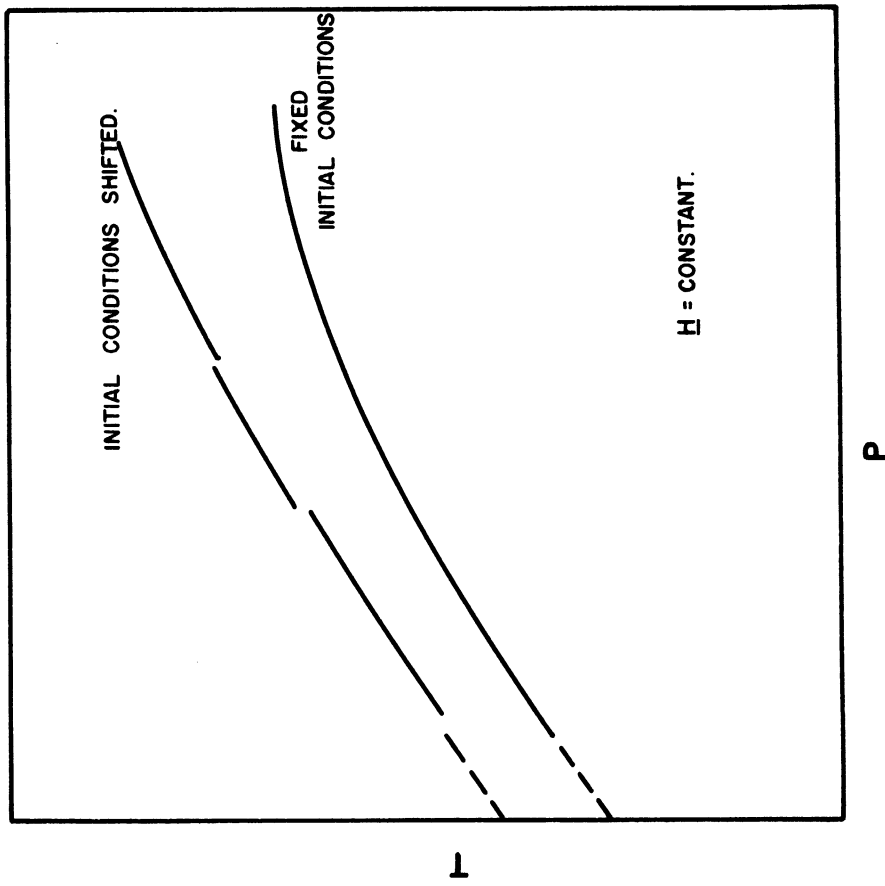


Figure 1. Isenthalpic Throttling Curves by Two Experimental Techniques

The second method of measuring isenthalpic throttling, the one adopted for the present investigation, is that of making continuous expansions (Figure 1). The second method will be discussed in conjunction with the problem of determining the combination of temperature and pressure effects upon enthalpy.

Figure 2 shows a number of isenthalpic throttling curves labeled  $H_1$ ,  $H_2$ , etc. These curves may be established by expanding continuously from a fixed initial temperature and pressure to a wide range of lower pressures. Such a procedure has the advantage of producing a smooth connected curve without the problem of "matching" segments. The quantity  $\mu^*$  may be determined, if desired, by differentiation of the integral curve. Primary interest of this investigation was in the integral expansion curve, however.

If values could be assigned to the isenthalpic curves in Figure 2, the combined effect of pressure and temperature upon the enthalpy of a pure substance or a mixture at constant composition would be established. One procedure for accomplishing this would be to extrapolate appropriate isenthalpic curves to near atmospheric pressure (normally they cannot be experimentally extended to very low pressures because of kinetic energy effects) and apply along a line of constant pressure, values of low pressure heat capacity to refer the curves to a chosen low pressure and arbitrary temperature. For pure substances having a relatively simple molecular structure ideal gas heat capacities would often be known with a high degree of accuracy.

Since within the scope of the overall program which has been initiated  $C_{P,x}$ ,  $\Delta H_{-P,x}$ , and latent heats will be studied as a function of



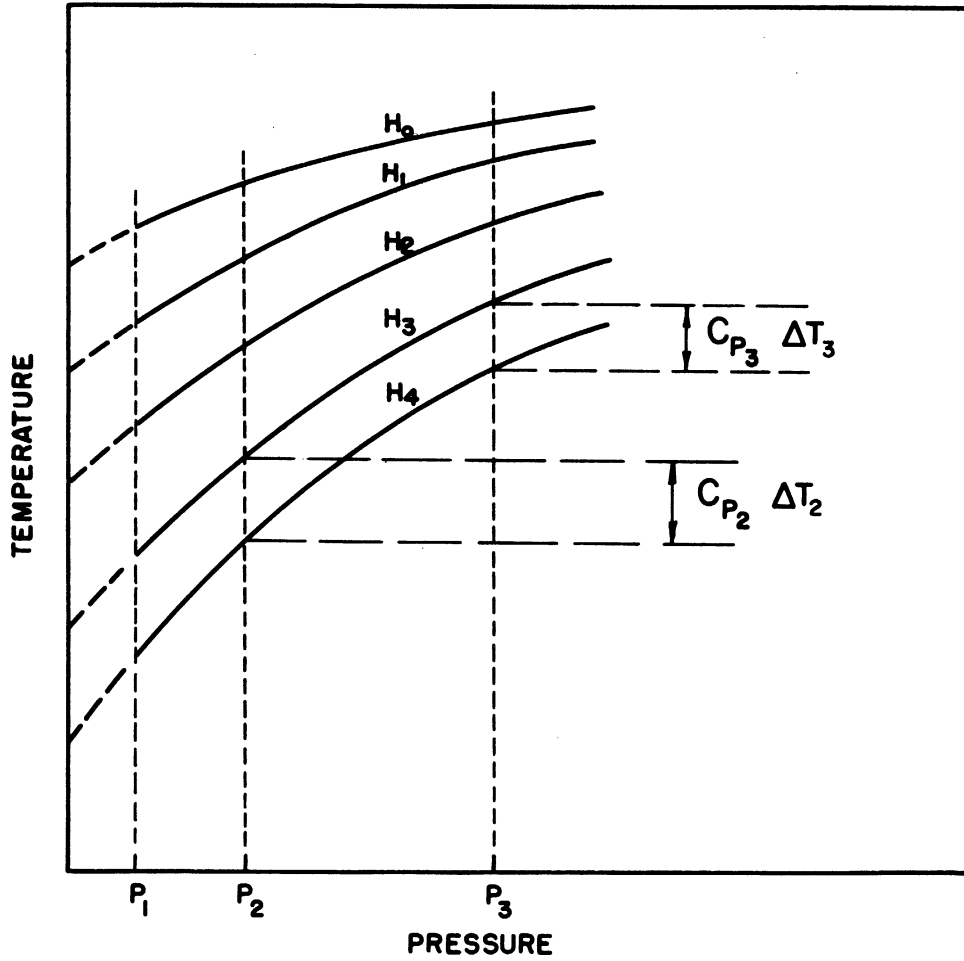


Figure 2. Combined Application of Isenthalpic Data and Data on Isobaric Specific Heats

pressure and temperature it will be possible to establish the relative enthalpy of the various isenthalpic curves with respect to any chosen base. The isobaric enthalpy change between successive isenthalpic curves, referenced by means of data at one pressure, will serve as a cross check on values of  $\Delta H_{P,x}$  and  $C_{P,x}$  measured independently at other pressures (See Figure 2).

### Latent Heats of Liquid-Vapor Transition

Thus far in the discussion, we have considered the problem of determining enthalpy as a function of pressure, temperature, and composition in any single phase region. It is also necessary to establish experimentally the change in enthalpy resulting from the heat of phase change from liquid to vapor at pressures below the critical of a pure component or mixture.

It was thought that the latent heat of phase change of a mixture could be evaluated experimentally using the same calorimeter which was employed for determining isobaric enthalpy changes in single phase regions. This procedure was followed, for example, by Brown and Associates (39,53,62,64,73,82,131) in their calorimetric and Joule-Thomson investigations on a number of systems.

The quantity measured in the vaporization experiments would be the isobaric integral latent heat of phase change for a constant composition mixture.

Latent heats for a mixture may be differential or integral. The differential heat of vaporization corresponds to the heat effect for the vaporization of a differential amount of saturated liquid to form the equilibrium vapor with no appreciable change in liquid composition.

Differential vaporization of a mixture occurs at constant pressure and constant temperature. The integral latent heat of a mixture is the heat effect associated with complete vaporization of a liquid mixture to form a vapor of the same composition. Integral vaporization of a mixture may be carried out at constant temperature or constant pressure (Figures 3,4).

The differential heat of vaporization or condensation of a mixture or the partial differential heat effects for individual components may be calculated from PVT and phase equilibrium measurements as described by Dodge<sup>(30)</sup>, Canjar and Edmister<sup>(22)</sup>, Weber<sup>(141)</sup>, and Stiehl, Hobson, and Weber<sup>(128)</sup>. Differential heats may be employed to calculate integral heats as described by Stiehl, Hobson, and Weber.<sup>(128)</sup>

The isothermal integral latent heat may also be calculated from PVT and equilibrium measurements as discussed by Balke and Kay<sup>(5)</sup>, Weber<sup>(141)</sup>, Sage and Lacey<sup>(112)</sup>, and Bloomer, Eakin, Ellington, and Gami<sup>(10)</sup>.

The isobaric integral latent heat for a mixture may also be calculated, but this has not been accomplished rigorously because of the extent and nature of experimental PVT and equilibrium data necessary.<sup>(128)</sup> Dodge<sup>(31)</sup> develops an expression for the isobaric integral latent heat effect, but includes a heat of mixing term which cannot be calculated. Recently Edmister<sup>(32)</sup> has presented a simplified, approximate solution for the isobaric integral latent heat in terms of equilibrium data. In addition to PVT and equilibrium data, heat of mixing data would be necessary for calculation of the latent heat effects in a non-ideal system (non-ideal solution behavior is allowed).

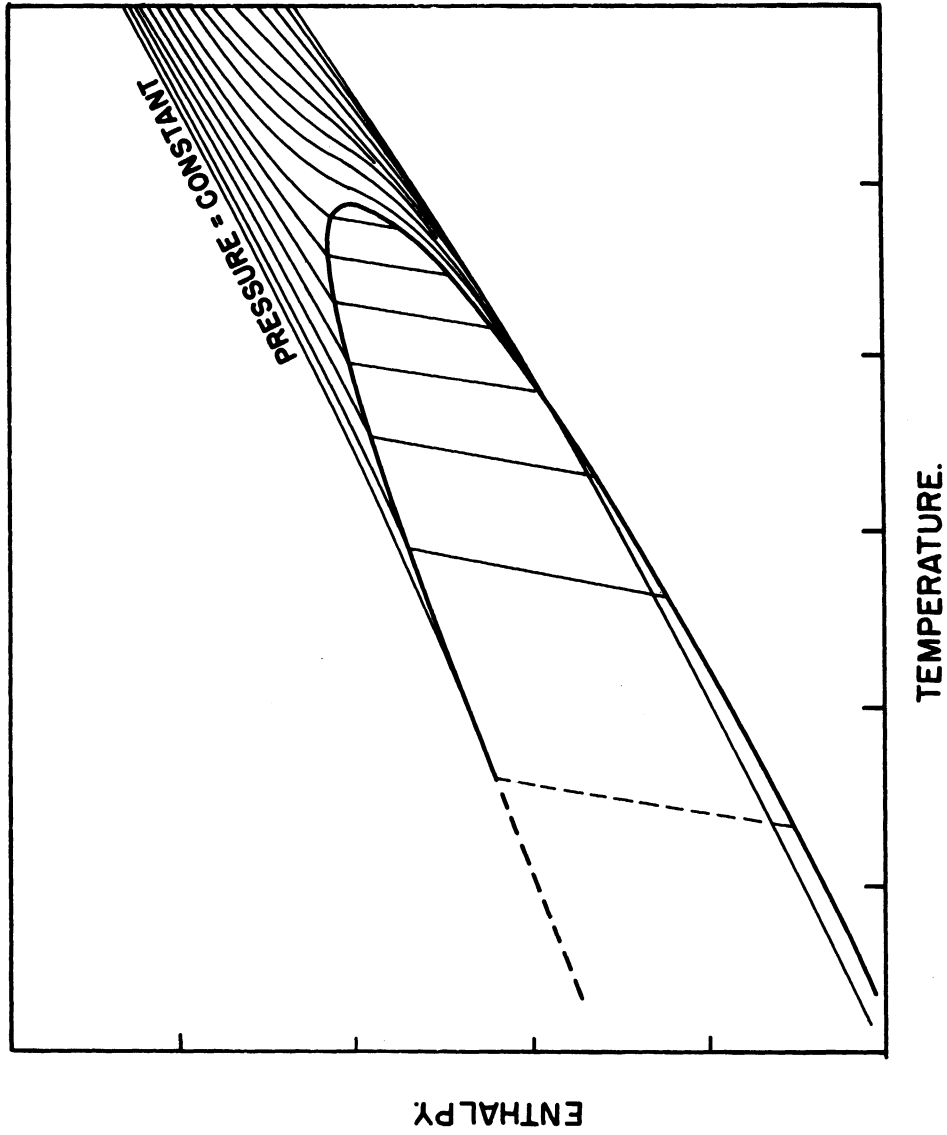


Figure 3. H-T Diagram for a Hydrocarbon Mixture

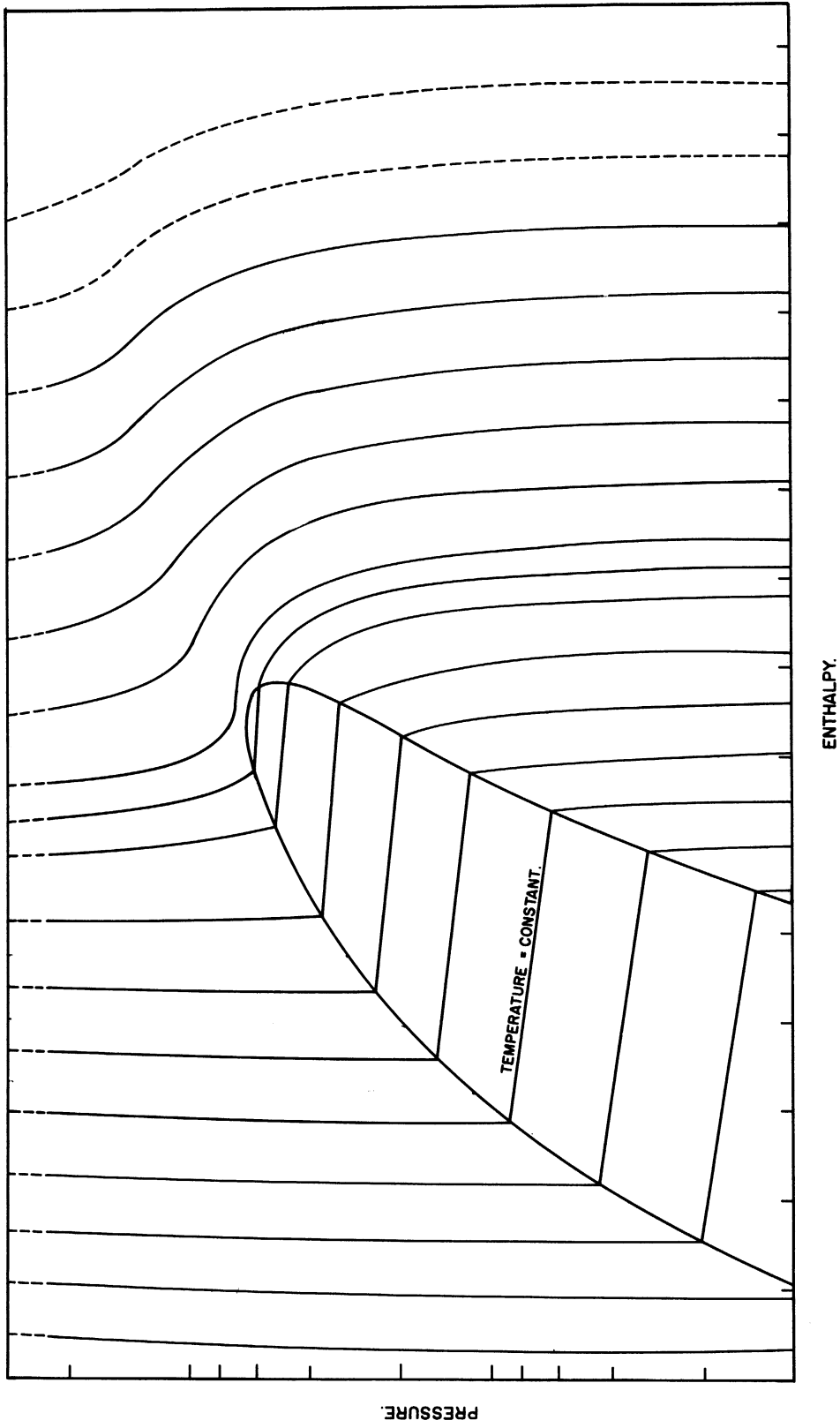


Figure 4. H-P Diagram for a Hydrocarbon Mixture

The Combined Method

From the series of measurements which have been described the enthalpy, relative to an ideal solution state, may be established for a series of mixtures of various binary, ternary, and multicomponent mixtures of the light hydrocarbons. From this kind of data other information for mixtures at constant composition may be calculated including the PVT behavior of the mixture and thermodynamic properties other than enthalpy.

Specific volume as a function of pressure and temperature for a constant composition mixture may be established from the relation:

$$\left(\frac{V}{T}\right)_X = \left[ \frac{V_0}{T_0} + \int_{T_0}^T \frac{1}{T^2} \left(\frac{\partial H}{\partial P}\right)_T dT \right]_X \quad (13)$$

or a thermodynamically equivalent one, if volume is known as a function of pressure along any isotherm. This information exists for light hydrocarbon binaries from the work of Sage and Lacey<sup>(112)</sup> or may be approximated in a state which approaches ideal solution behavior. Phase boundaries of mixtures may be conveniently verified by isenthalpic expansion (Figure 5).

A number of thermodynamically equivalent expressions are available for calculation of such quantities as internal energy,  $\underline{E}$ ; entropy,  $\underline{S}$ ; etc., relative to a selected base, from the measurements which have been described and other information which may be available.

In general, calculations of information other than enthalpy from the measurements described would introduce considerable additional uncertainty arising in calculation procedures -- such as differentiation of

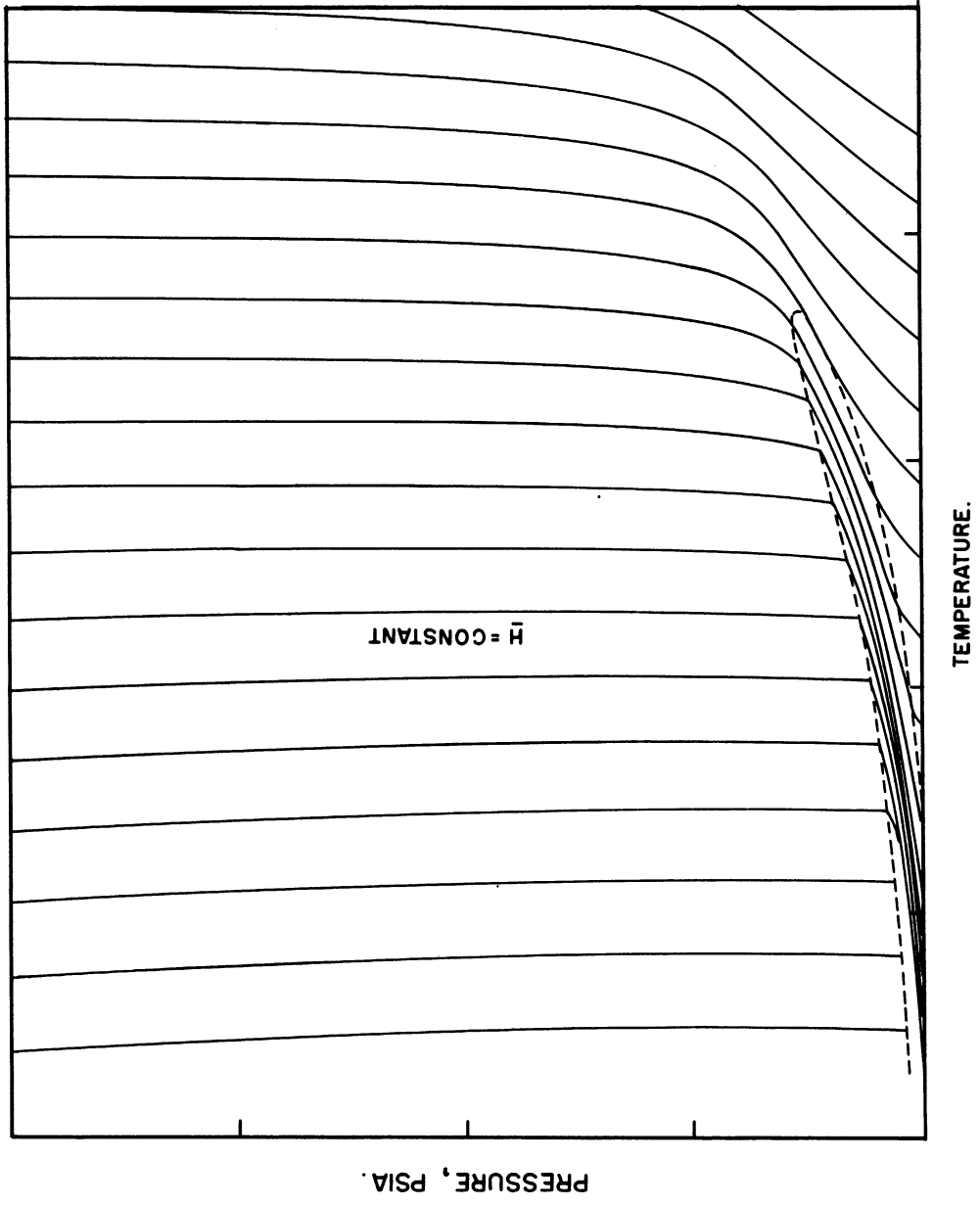


Figure 5. P-T Diagram for a Hydrocarbon Mixture

the data. It is beyond the scope of this thesis to discuss the magnitude of errors associated with various possible calculational procedures.

For the purpose of establishing the properties of a pure component or mixture over a wide range of conditions it is, of course, desirable to make use of as much different, independent information as may be available. Certain calculational procedures may be inherently more accurate in one range, while another may be better elsewhere. Sage and Lacey discuss this matter.<sup>(112)</sup> Also with independent measurements of several thermodynamic quantities, a number of tests for consistency became available. This is discussed to some extent by Sage and Lacey<sup>(112)</sup>; a discussion is found in any good thermodynamics textbook.

Having established the enthalpy property for mixtures at constant composition, the ultimate goal of the overall project is to provide some means of correlating and generalizing this specific mixture data so that it may be used in the calculation of the properties of complex and arbitrary light hydrocarbon systems. While it is not within the scope of the present work to predict how such a generalization may be accomplished, some discussion of this matter is necessary in order to justify the approach to the investigation of mixtures which has been initiated.

It is thought that the best approach to the problem would be through the concept of partial molal properties. Partial molal properties are merely the properties of a component when present in a mixture. The concept of partial molal quantities and their calculation according to various procedures is discussed in a number of textbooks, including Glasstone<sup>(43)</sup> and Lewis and Randall<sup>(63)</sup>. The partial molal enthalpy of



component J in a mixture is defined, for example, by the equation:

$$\bar{H}_J \triangleq \left( \frac{\partial H}{\partial x_J} \right)_{T, P, x_I (I \neq J)} \quad (14)$$

$\bar{H}_J$  = partial molal enthalpy of component J in a mixture at temperature T and pressure P.

$H$  = enthalpy of the mixture relative to a selected reference state per mole

$x_I$  = mole fractions of other components I

Calculation of partial molal enthalpies from the solution data would be in principle:

$$\Delta H = H - \sum_{K=A}^I x_K H_K \quad (15)$$

$\Delta H$  = the difference in enthalpy of a mixture at a particular pressure and temperature and the ideal solution enthalpy at the same pressure and temperature (per mole)

$H_K$  = enthalpy of pure component K at the mixture temperature and pressure per mole

$x_K$  = mole fraction of component K

and

$$\bar{H}_J = H_J + \left[ \frac{\partial(\Delta H)}{\partial x_J} \right]_{T, P, x_I} \quad (15a)$$

Once partial molal enthalpies for a series of mixtures and systems have been established, they might be correlated as a function of temperature, pressure, and one or more composition variables. The problems of representing complex solution behavior with less than

the number of phase variables theoretically required has been discussed by Benham.<sup>(9)</sup> If composition dependent variables can be found which correlate the behavior of a particular n component system, the extension to other n component systems and to systems of more than n components depends on the sensitiveness of the variables chosen. This problem of selecting composition dependent correlating variables for complex vapor-liquid equilibria correlations has been reviewed by Benham.<sup>(9)</sup>

Canjar and Edmister<sup>(22)</sup> have correlated partial molal enthalpies of light hydrocarbon systems as a function of reduced temperature, reduced pressure and boiling point ratio

$$\left( \frac{\text{molal average boiling point of mixture}}{\text{component boiling point}} \right)$$

above the component critical temperatures. Below the critical temperature of the components, it was necessary to employ a residual, since apparently latent heats of vaporization could not be correlated satisfactorily with these variables. Canjar and Edmister<sup>(22)</sup> found that reduced temperature was the most important independent variable. In the liquid phase the next most important variable was reduced pressure, and least important was boiling point ratio. In the vapor phase boiling point ratios were more important than reduced pressures.

Calculation of the enthalpy of an arbitrary mixture from partial molal enthalpies for components is based on the principle that:

$$H = \sum_{K=A}^I x_K \bar{H}_K \quad (16)$$

One would expect that the error in the partial molal enthalpy of minor components, present in small amounts in the mixture, and obtained from

a generalized correlation, would be relatively large. However, the contribution of these constituents to the overall solution enthalpy would be relatively small and therefore would not seriously affect the total enthalpy. In general, the properties of constituents having properties near the average of the solution would be known much more accurately for such a correlation.

Canjar and Edmister<sup>(21)</sup> and Papadopoulos, Pigford and Friend<sup>(79)</sup> calculated partial molal enthalpies of the light hydrocarbons by means of the Benedict-Webb-Rubin equation of state using different calculational procedures. The constants for the equation of state were based on weighted averages for the pure components. The accuracy of the results of these calculations is limited, however, by the lack of experimental data upon which to base a weighting of the constants, reliability of pure component and mixture PVT measurements, and applicability of the equation of state at high fluid densities. Furthermore, apparently different processes used in smoothing and differentiating the data led to disagreement between the two sets of results based on the same equation of state.

Recently Canjar and Peterka<sup>(24)</sup> have suggested that an isothermal pressure correction based on the behavior of pure light hydrocarbons may be applied to the total enthalpy of the ideal solution mixture to determine the pressure effect on enthalpy for the mixture. They state that a mixture of homologous hydrocarbons which has an average molal boiling point equal to the boiling point of a pure component will exhibit the same PVT and derived thermodynamic property behavior as the pure component. This suggested method is similar to other calculational procedures which

have been used for light hydrocarbon mixtures. Canjar and Edmister<sup>(21)</sup> reviewed a number of these procedures; all are subject to experimental verification.

## EXPERIENCE OF PREVIOUS INVESTIGATORS

A review of the literature is made for the methods of experimental measurement of heat capacity, latent heat, and isenthalpic throttling.

### Heat Capacities and Latent Heats

The principal references of concern in this investigation along with selected articles on other experimental techniques are given in Table I.

#### Constant Volume or Batch Calorimetry

Constant volume calorimetry is discussed both historically and comprehensively by White<sup>(143)</sup> and Weissberger.<sup>(142)</sup> Although this investigation used a flow rather than a constant volume technique, a brief statement on the application of the constant volume method is included.

A large majority of the more accurate liquid heat capacity and latent heat determinations for the light hydrocarbons (and most other materials) have been carried out in a constant volume apparatus. A controlled removal of saturated vapor has been provided for in the case of latent heat measurements. A calorimeter of this type consists, basically, of a vessel into which a known weight of subcooled liquid is placed. A measured quantity of electrical energy is introduced into the vessel and means are provided for measuring the temperature and pressure of the fluid in the vessel and also the condition of any material leaving the vessel as a function of time. Elaborate precautions are normally taken for preventing undesired heat transfer. These may include an insulating vacuum around the calorimeter, isothermal shielding, the use of highly reflective

TABLE I  
 PRINCIPAL REFERENCES ON EXPERIMENTAL METHODS

Experimental Method or Measurement	Investigators or Authors	Date of Publication	Reference No.
Constant Volume Calorimetry	Osborne, N.S.	1930	74
	Osborne, N.S. and Ginnings, D.C.	1947	76
	Weissberger, A.	1949	142
	White, W.P.	1928	143
Flow Calorimetry	De Vries, T. and Collins, B.T.	1941	29
	Masi, J.F. and Petkof, B.	1952	67
	Montgomery, T.B. and Devries, T.	1942	72
	Osborne, N.S., Stimson, H.F., and Sligh, T.S., Jr.	1925	78
	Partington, J.R. and Shilling, N.G.	1924	81
	Pitzer, K.S.	1941	84
	Schrock, V.E.	1952	123
	Scott, R.B.	1956	124
	Scott, R.B. and Mellors, J.W.	1945	126
	Wacker, P.F., Cheney, R.K., and Scott, R.B.	1947	136
	Waddington, G.	1956	137
	Waddington, G., Todd, S.S., and Huffman, H.M.	1947	138
	Isenthalpic Expansions	Budenholzer, R.A., Sage, B.N., and Lacey, W.N.	1939
Burnett, E.S. and Roebuck, J.R.		1910	19
Roebuck, J.R.		1925	95
Roebuck, J.R.		1930	96
Roebuck, J.R.		1957	94
Roebuck, J.R. and Osberberg, H.		1933	102

surfaces, techniques for preventing heat leakage along electrical wires and other accessories which must enter the calorimeter, and a great many other refinements.

The basic advantage that the "batch" method possesses is that the mass of fluid entering into the necessary heat and material balances can usually be determined with very great accuracy. Regarding the calorimeter, and vapor collection system if material is removed, as a system, the sample weight(s) involved normally are weighed directly using a tare method.

The constant volume method as applied to organic liquid heat capacities and latent heats has normally been carried out at approximately atmospheric pressure because of experimental difficulties associated with higher pressure operation. It should be mentioned, however, that a constant volume technique is applicable to heat capacity measurements, gas or liquid, over a range of pressure provided that the heat capacity of the sample is large in comparison to the heat capacity of the calorimeter.

The fact that  $C_V$ , rather than  $C_P$ , is normally the result of a constant volume technique may become an important factor in high pressure gaseous heat capacity measurements if high accuracy is desired.

The constant volume method is also applicable to latent heat measurements over a range of pressures.<sup>(77)</sup> However, if it is desired to measure latent heats of a mixture, the removal of material of a changing composition from the calorimeter may involve serious computational problems.

The mathematical analysis of a very elaborate device used by the National Bureau of Standards for moderate and high temperature measurement of the enthalpy of saturated liquid, saturated vapor, and superheated vapor

for the substance water is given by Osborne.<sup>(74)</sup> The operation of a similar device for moderate temperature measurements of saturated heat capacities and latent heats of a number of hydrocarbons is given by Osborne and Ginnings.<sup>(76)</sup>

White<sup>(143)</sup> and Weissberger<sup>(142)</sup> have discussed in detail the Nernst-Diague and adiabatic type calorimeters employed in most of the low temperature, light hydrocarbon liquid specific heat investigations. Both of these references contain a great deal of information about calorimetric methods. Although the methods of the present investigation were entirely different than much of the work discussed by White and Weissberger, a great deal of information about experimental calorimetric techniques was gained from these sources. A number of the references to particular investigations given by these authors was valuable for more detailed discussions of these techniques.

#### Gaseous Heat Capacities

Literature on gaseous heat capacities has been reviewed by Partington and Shilling<sup>(81)</sup>, including essentially all of the published experimental techniques and data concerning heat capacities in gaseous systems carried out prior to 1924. Included are the classical techniques of direct flow calorimetry, as well as many of the more indirect methods which had been employed.

Masi<sup>(66)</sup> has reviewed much of the experimental heat capacity work which has taken place between 1925 and 1952. Ten experimental methods of heat capacity determination are discussed: 1. direct flow calorimetry, 2. direct constant volume calorimetry, 3. a heat exchange method, 4. a so-called explosion method, 5. a method of isentropic expansion, 6. a



velocity of sound method, 7. a resonance method, 8. a method of self-sustained oscillation, 9. a flow comparison method, 10. a constant volume comparison method. Masi has also tabulated for ten technically important gases: the method of measurement, temperature and pressure range of investigation, and estimated accuracy of measurements for investigations between 1925 and 1952.

Another method of very high accuracy for molecularly simple pure gases which Masi<sup>(66)</sup> does not include (because it is not actually experimental) is that of statistical determination. Ideal gas heat capacities for single substances can be calculated from spectroscopic measurement, provided that molecular structure is not too complicated, with an accuracy of better than 0.1 percent. Simplifications of the statistical method have been frequently attempted for more complex molecules where all significant energy levels could not be identified or the calculation became extremely complicated. In such cases lower accuracies are obtained.

#### Flow Calorimetry

The flow method of calorimetry which was used in the present investigation was employed by Callendar and Barnes<sup>(20)</sup> in the measurement of liquid heat capacities. One of the first extensions of this method to measurements involving gases and vapors was the classical work of Scheele and Heuse<sup>(121,122)</sup> described by Partington and Schilling.<sup>(81)</sup>

Direct flow calorimetry consists, basically, of introducing a measured quantity of energy into a fluid flowing at known mass flow rate, normally at constant pressure, and determining the change in conditions, i.e., change in temperature or change from saturated liquid to saturated vapor, which are produced. The calorimeter is so constructed that heat

leakage is virtually eliminated or a satisfactory correction for this effect is made. If a true steady flow condition is approached, the heat capacity of the calorimeter is not a factor in the measurements.

The vast majority of the more accurate applications of flow calorimetry have been made at essentially atmospheric pressure<sup>(66,81)</sup> because of experimental difficulties that arise at higher pressures. Most measurements of this type have also been made at temperatures above room temperature.<sup>(66,81)</sup>

Holborn and Jacob<sup>(49)</sup> measured the isobaric specific heat of air at 59°C and at pressures to 200 atm in a flow calorimeter built to withstand 400 atm. The device was extremely massive and not well protected against heat leakage. At flow rates of 10 to 30 kilograms per hour the heat leakage was equivalent to 10 percent of the smallest electrical power addition. Nevertheless, the authors were able to correct for this effect well and the reported values of specific heat may have an accuracy of 1 - 2 percent.

Schrock<sup>(123)</sup> measured the isobaric specific heat of carbon dioxide at pressures as high as 1000 psig and temperatures from 339 to 951°F in a flow calorimeter with an estimated accuracy of 0.5 percent. The material was supplied to the calorimeter from a bank of high pressure cylinders. The pressure at the calorimeter was controlled by means of automatic regulators and by heating the cylinders. Flow rate was varied by means of a high pressure metering valve. The volume of material passing through the calorimeter was measured near atmospheric pressure in a gasometer. Electrical energy, measured by means of a precision wattmeter, was added to the gas. The resultant temperature rise was measured by thermocouples. The calorimeter was evacuated and radiation shields employed to reduce heat leakage.

The most accurate direct flow calorimetry over a wide range of temperatures and pressures was undoubtedly the investigation of the specific heat of ammonia by Osborne, Stimson, and Sligh<sup>(78)</sup> conducted in 1925 at the National Bureau of Standards. These investigators constructed an extremely elaborate adiabatic flow calorimeter which was designed to withstand 100 atm. It was found experimentally that the corrections for heat leakage for the calorimeter did not exceed 0.2 - 0.3 percent of the measured energy addition and an overall accuracy of 0.1 percent was reported for the heat capacities of ammonia over a 20 atm range in pressure. Their work served as a standard for the present investigation.

The supply of ammonia to the calorimeter built by Osborne, Stimson, and Sligh was made steady by a combination of a controlled evaporation of condensed ammonia, the use of automatically operated supply valves, and a back pressure system of orifices after the calorimeter. The weight of material which had passed through the calorimeter was determined by a procedure of recondensing the ammonia, collecting and weighing it. Energy was added to the ammonia by means of a DC electrical resistance element in the calorimeter. The current source consisted of wet-cell batteries. The portion of the calorimeter in which energy was being accounted for was protected against heat leakage by the use of an insulating vacuum, a series of isothermal shields, and a number of special procedures which are described<sup>(78)</sup> in the literature. The temperature rise of the gas passing through the calorimeter was ascertained by means of two platinum thermometer. A large number of thermocouples were used for the purpose of surveying the temperature distribution in the calorimeter and for proper regulation of the main radiation shield. The effect of heat leakage was determined

by varying the flow rate and power input while keeping the temperature rise of the gas constant. An empirical expression was developed for predicting this correction.

Other investigators at the National Bureau of Standards<sup>(67,136)</sup> have obtained an accuracy of approximately 0.1 percent in direct flow heat capacity measurements using simpler calorimeters than employed by Osborne, Stimson, and Sligh. Such investigations, however, have been limited to essentially atmospheric pressure.

Montgomery and De Vries<sup>(72)</sup>, De Vries and Collins<sup>(29)</sup>, Pitzer<sup>(84)</sup> and Waddington, Todd and Huffman<sup>(138)</sup> have conducted low pressure flow calorimetric measurements in glass calorimeters. The materials being studied in all of these investigations were pure compounds and could be condensed near atmospheric pressure, at the temperatures involved. Supply of gas to the calorimeters was, therefore, accomplished by controlling the rate of evaporation of the condensed material. Waddington, Todd, and Huffman<sup>(138)</sup> incorporated accurate measurement of latent heat by using the supply vessel as a second calorimeter and measuring the electrical energy input to maintain a constant measured rate of evaporation.

The investigations of Montgomery and De Vries<sup>(72)</sup>, De Vries and Collins<sup>(29)</sup>, and Pitzer<sup>(84)</sup> represent simplifications of the elaborate procedure used by the investigators at the Bureau of Standards and the results are generally of a lower accuracy. Waddington, Todd, and Huffman<sup>(138)</sup> improved the experimental techniques used by Pitzer<sup>(84)</sup> and obtained an accuracy of close to 0.1 percent.

In addition to experimental measurements of heat capacity, Montgomery and De Vries<sup>(72)</sup> studied the problem of the dependence of heat

leakage on flow rate in several adiabatic flow calorimeters of different designs.

Brown and Associates(39,53,62,64,73,82,131) at the University of Michigan conducted a series of flow experiments with hydrocarbon systems in which the effect of pressure as well as temperature upon heat content was investigated. Calorimetric measurements of liquid and gaseous enthalpy and latent heat were made. These investigations were all made at or above room temperature in a heat exchange device which compared the properties of the material being investigated to those of water -- which it was felt were well known. In this respect, the procedure is different from what Masi(67) has referred to as flow calorimetry and may be termed a heat exchange method. The materials investigated by Pattee and Brown, normal pentane and a naptha(82), Lindsay and Brown, benzene(64), Konz and Brown, normal pentane(62), Fekula and Brown, three naphthas(39), Kemp and Brown, four pentane-benzene mixtures(53), Tripathi and Brown, orthodichlorobenzene(131), and Moore and Brown, acetone(73) were all liquid at room temperature and atmospheric pressure. For this reason, it was practicable to supply the calorimeter by a very constant pumping from a reservoir. A heater, which consisted of a series of electrically heated tubes, was used to bring the temperature of the material being studied to the desired level. The materials could be vaporized, if desired, and brought to the calorimeter as a gas. In the calorimeter, the material was cooled by heat exchange with cold water. The temperature rise and mass flow rate of the water were measured, the latter by direct weighing, and the energy transferred to the water calculated. The material of unknown heat capacity after passing through the calorimeter was re-condensed and weighed. Necessary temperatures and pressures were also measured.

### Joule-Thomson Measurements

The most comprehensive and accurate measurement of the Joule-Thomson effect over a wide range of conditions has undoubtedly been the work of Roebuck and co-workers. The investigations included measurements on air(95,96), helium(102,103), argon(93), nitrogen(105), mixtures of helium and nitrogen(100), mixtures of helium and argon(101), and carbon dioxide.(99)

Roebuck employed the radial porous plug method for producing the desired throttling effect. The theory of the method was first described by Burnett and Roebuck(19) and later in more detail by Roebuck.(95,96) The radial plug technique avoids many of the difficulties of heat leakage and kinetic energy effects which are frequently encountered in work of this nature.

The technique of measurement was to expand from a fixed initial temperature and pressure continuously to lower pressures until a pressure near atmospheric was reached.

Roebuck employed a large compressor to supply gas to the Joule-Thomson device and maintained constancy of flow rate and pressure before and after the throttle by means of "barostats". The barostats were designed by Roebuck and provided for a continuously varying bleed from the system. The use of these barostats and an ingenious means of temperature control permitted Roebuck to virtually eliminate the problems of perturbation and drift which have long plagued investigators in this area of experimental measurement. The temperature change of the fluid flowing through the porous plug was measured by platinum thermometers. The pressure drop across the plugs was measured in the earlier work by a differential pressure

balance. Later a multiple-leg manometer<sup>(98)</sup> was constructed capable of an amazing accuracy of .01 percent at a static pressure of 200 atm. The overall accuracy of Roebuck's measurements is probably better than 1 percent over a wide range of conditions and materials.

A detailed description of Roebuck's equipment was given in several papers.<sup>(95,96,102)</sup> The author was fortunate, however, to be able to inspect this very elaborate and extensive equipment first-hand and to discuss the measurement of the Joule-Thomson effect on several occasions with Dr. Roebuck at the University of Wisconsin in Madison, Wisconsin. This aided immeasurably in a detailed appreciation of the problems and techniques involved.

Brown and associates<sup>(39,53,62,64,73,82,131)</sup> incorporated in the calorimetric system previously described a device for measuring the Joule-Thomson effect. This device contained a series of interchangeable orifices. In general, the technique of holding initial pressure and temperature constant was employed. Difficulties were encountered in holding these conditions constant in some regions, however, and the method of successive expansions had to be used. The pressure drop and static pressure were measured by means of Bourdon tube gauges, the temperatures by means of thermocouples. The device was heavily insulated, but this did not prevent serious difficulties due to heat leakage. A large flow rate was employed to offset this effect. Unaccounted-for difficulties undoubtedly arose also because of "streaking" or translational kinetic effects through the orifices. Nevertheless, the values of enthalpy as a function of pressure and temperature obtained by the combination of throttling and calorimetric measurements were probably of an accuracy of  $\pm 5$  percent.

Sage, Lacey and co-workers (13,14,15,16,55,109,110,111) have conducted a number of investigations of the Joule-Thomson effect in light hydrocarbon gases in the temperature range of 70°F to 300°F and at pressures as high as 1500 psi. These investigations employed the technique of using a series of small pressure drops, with shifting initial conditions relative to a particular isenthalp. Gas was supplied to a porous "thimble" by means of a compressor. An automatically operated valve and volume damping before and after the thimble were employed to stabilize flow. The pressure drop across the thimble was measured by a high pressure mercury manometer with electrical sensing contacts. The temperature change of the fluid passing through the thimble was determined by a multiple junction difference thermocouple. Sage and Lacey's measurements were of an accuracy of about  $\pm 3$  percent.

The Thermodynamic Properties  
of the Pure Light Hydrocarbons

Table II lists the references that are considered by the author to be the most complete tabulations of the thermodynamic properties of the pure light hydrocarbons. These tables and charts were all prepared from a great number of different types of information, often quite scattered. The tabulation of the properties of methane by Matthews and Hurd<sup>(68)</sup>, for example, was derived from the measurements which included:

1. Specific volumes of the liquid.
2. Vapor pressure measurements.
3. PVT data.
4. Liquid heat capacity measurements.
5. Ideal gas thermodynamic properties
6. Determinations of the critical constants.



TABLE II  
REFERENCES TO TABULATIONS OF THERMODYNAMIC  
PROPERTIES OF THE LIGHT HYDROCARBONS

Substance	Authors	Reference No.
Methane	Matthews, C.S. and Hurd, C.O.	68
Ethane	Barkeley, C.H., Valentine, J.L. and Hurd, C.O.	6
Ethylene	York, R., Jr., and White, E.F., Jr.	148
Propane	Chu, I.C., Muller, N.F., Bunche, R.M. and Jennings, A.S.	25
	Stearns, W.V. and George, E.J.	127
Propylene	Canjar, L.N., Goldman, M. and Marchman, H.	23
n-Butane	Prengle, H.W., Greenhaus, L.R. and York, R.J.	88
	Sage, B.H., Webster, D.C. and Lacey, W.N.	113
iso-Butane	Sage, B.H., and Lacey, W.N.	111
Butene-1	Weber, J.H.	140

#### Ideal Gas Heat Capacities

Zero pressure heat capacities of many of the light hydrocarbons are well known over a range of temperatures. Determination of molecular constants for the simpler molecules, from spectroscopic measurement, has permitted statistical calculation of heat capacity as a function of temperature. Some uncertainty is encountered at higher temperatures because of anharmonicity. A number of other experimental determinations of heat capacity using a variety of techniques, including flow calorimetry, has served to establish a reliable set of molecular constants for the more complicated substances. Once a reliable set of constants are available,

the zero pressure heat capacity may be calculated very accurately over a wide range of low and intermediate temperatures. National Bureau of Standards Circular C461<sup>(133)</sup>, National Bureau of Standard Circular 500<sup>(134)</sup>, and a publication of the American Petroleum Institute<sup>(1)</sup> report values of ideal gaseous heat capacity for the light hydrocarbons at 25°C as well as a number of other properties. Low pressure gaseous heat capacities have been reported in the literature for methane<sup>(28,35,36,47,70,83,115)</sup>, ethane<sup>(12b, 26,37,38,60,83,110,145)</sup>, propane<sup>(26,58,59,83,114)</sup>, normal butane<sup>(26,83,85,108,129)</sup>, isobutane<sup>(26,114,136)</sup>, ethylene<sup>(12b, 18,37,57)</sup>, propylene<sup>(57,61)</sup>, butene-1<sup>(3,57,136)</sup>.

Values of saturated or subcooled liquid heat capacities at one atmosphere pressure have been determined by several investigations using generally the low-temperature, adiabatic, constant volume type calorimeter discussed by White<sup>(143)</sup> and Weissberger<sup>(142)</sup> and described in detail by other investigators. These investigations include measurements for methane<sup>(144)</sup>, ethane<sup>(145,146)</sup>, propane<sup>(27,44)</sup>, normal butane<sup>(27,69,108)</sup>, isobutane.<sup>(80)</sup>

#### Latent Heat of Vaporization

Measurements of latent heat of vaporization of the pure light hydrocarbon include values for: methane<sup>(1,40,41)</sup>, ethane<sup>(86,146)</sup>, propane<sup>(1,27,44,107)</sup>, normal butane<sup>(1,4,27,113)</sup>, isobutane<sup>(27,114)</sup>, ethylene<sup>(1,33)</sup>, propylene<sup>(87)</sup>, butene-1<sup>(1,3)</sup>. Frequently the measurements were made at only one temperature.

#### Effect of Pressure on Thermodynamic Properties

No published heat capacity measurements for the light hydrocarbons above two or three atmospheres were discovered by the author.

The pressure dependence of the thermodynamic properties above room temperature has generally been ascertained by means of PVT data, Joule-Thomson measurements, or Eucken isothermal throttling experiments.

A discussion of the accuracy and adequacy of existing PVT data for calculating the various thermodynamic properties for different temperature and pressure regions is beyond the scope of this thesis. In general, it is observed that more PVT data exists near room temperature and above than at the lower temperatures.

Experimental Measurements of Joule-Thomson coefficients above 70°F for pure light hydrocarbons have been reported by Sage, Lacey, and co-workers: methane<sup>(14)</sup>, ethane<sup>(110)</sup>, propane<sup>(109)</sup>, normal butane<sup>(55)</sup>, isobutane<sup>(111)</sup>. No published Joule-Thomson data was found for temperatures below approximately ambient temperature for the light hydrocarbons.

#### Properties of Light Hydrocarbon Systems Under Pressure

Experimental and theoretical investigations of the phase behavior of light hydrocarbon systems have been made by several investigators. The PVT measurements of Sage and Lacey at temperatures above 70°F, reviewed by Katz<sup>(52)</sup>, and the work of Bloomer and associates<sup>(10,11)</sup>, represent efforts to compute thermodynamic properties of hydrocarbon systems from PVT data. Joule-Thomson measurements for light hydrocarbon mixtures under pressure and at temperatures above 70°F by Sage, Lacey, and co-workers include the binaries: methane-ethane<sup>(15)</sup>, methane-propane<sup>(13)</sup>, and methane-butane.<sup>(16)</sup>

Extension of calculations to lower temperatures for light hydrocarbon systems is now generally accomplished by means of the Benedict-Webb-Rubin equation of state.

Canjar and Edmister<sup>(21)</sup> and Papadopoulos, Pigford, and Friend<sup>(79)</sup> have tabulated partial molal enthalpies calculated from the Benedict-Webb-Rubin equation using estimated values of equation-constants for mixtures.

## DESCRIPTION OF THE FLOW SYSTEM

The design, procurement, and construction of the equipment necessary for making direct measurements of several of the thermodynamic properties of the light hydrocarbons at low temperature and under super-atmospheric pressures proved to be a very formidable task. More than a year was spent in designing the equipment and ordering the components. It was believed that a thorough study was necessary, if an accurate flow calorimetric system was to be constructed. The following principal items were considered at length:

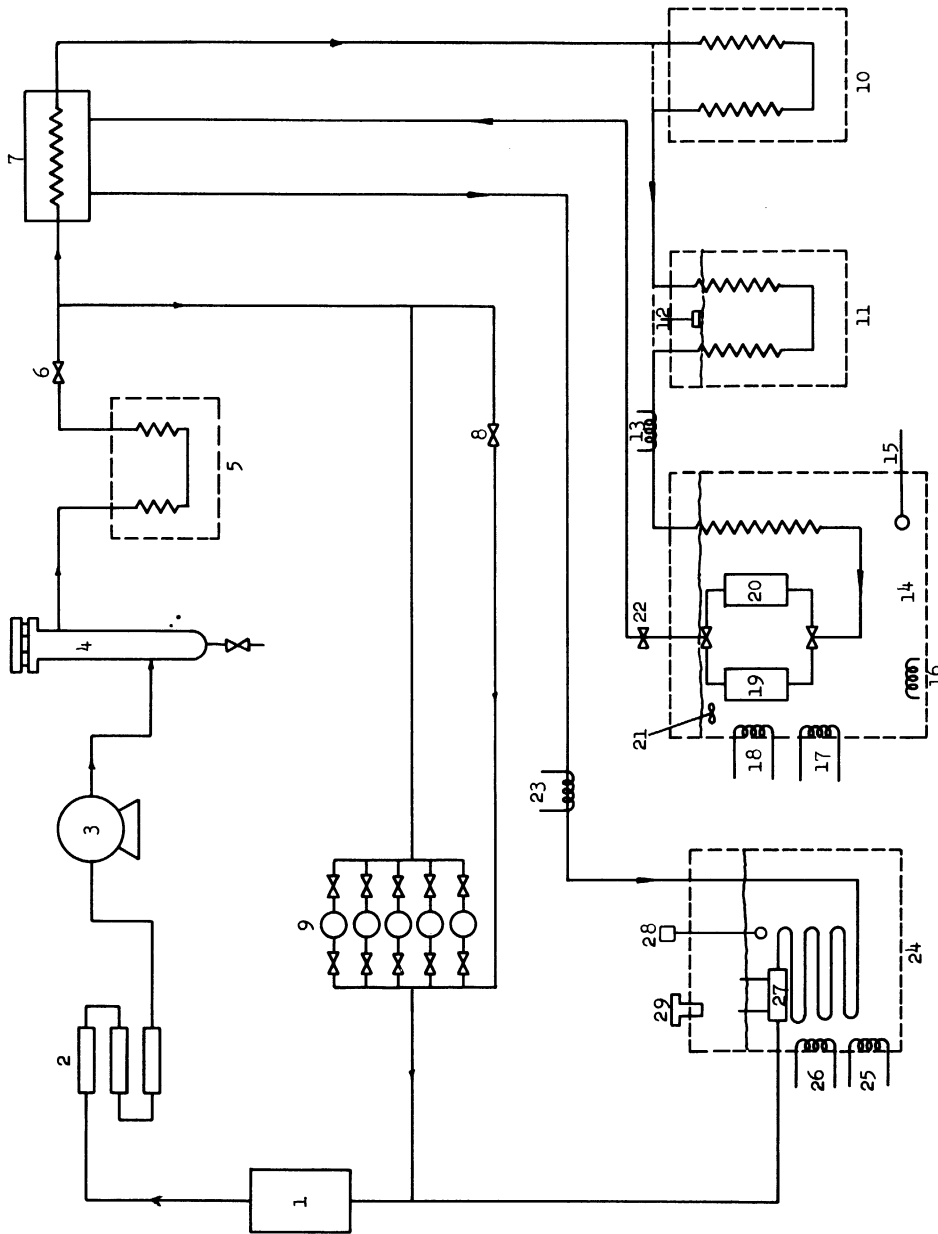
1. Flow rate and sizing of the system.
2. Design of the calorimeter.
3. Design of the Joule-Thomson throttle.
4. Precise control of pressure, temperature, and flow rate.
5. The effect of the accuracy of individual measurements on the final thermodynamic data.

These items are discussed in detail in Appendix A of the thesis.

It is the purpose of this section of the thesis to describe, in a relatively brief manner, the essential features of the equipment. More detailed discussions are given in Appendix A.

The essential features of the overall operation may be seen schematically in Figures 6 and 7. They include circulation; purification; gas storage; control of pressure, flow rate, and temperature; refrigeration; the calorimeter and Joule-Thomson throttle; and the various measuring instruments.

The collection of equipment making up the low temperature apparatus constitutes a closed flow cycle. During operation the fluid



1. Compressor Supply Tank
2. Purification System
3. Höfer Compressor
4. Oil Separator
5. Ice Cooler
6. Throttling Valves
7. Interchanger
8. Throttling Valves
9. Gas Storage and Buffering
10. Carbon Dioxide Cooler
11. Liquid Nitrogen Cooler
12. Liquid Nitrogen Level Control
13. Electrical Heater
14. Low Temperature (Calorimeter) Bath
15. Platinum Resistance Thermometer
16. Bath Controller Sensing Element
17. Electrical Heaters
18. Liquid Nitrogen Cooling Coil
19. Calorimeter
20. Joule-Thomson Throttle
21. Stirrer
22. Throttling Valves
23. Electrical Heater
24. Constant Temperature Metering Bath
25. Cooling Coil
26. Electrical Heaters
27. Flowmeter
28. Thermoregulator and Relay
29. Centrififugal Stirrer

Figure 6. Simplified Flow Diagram of the System

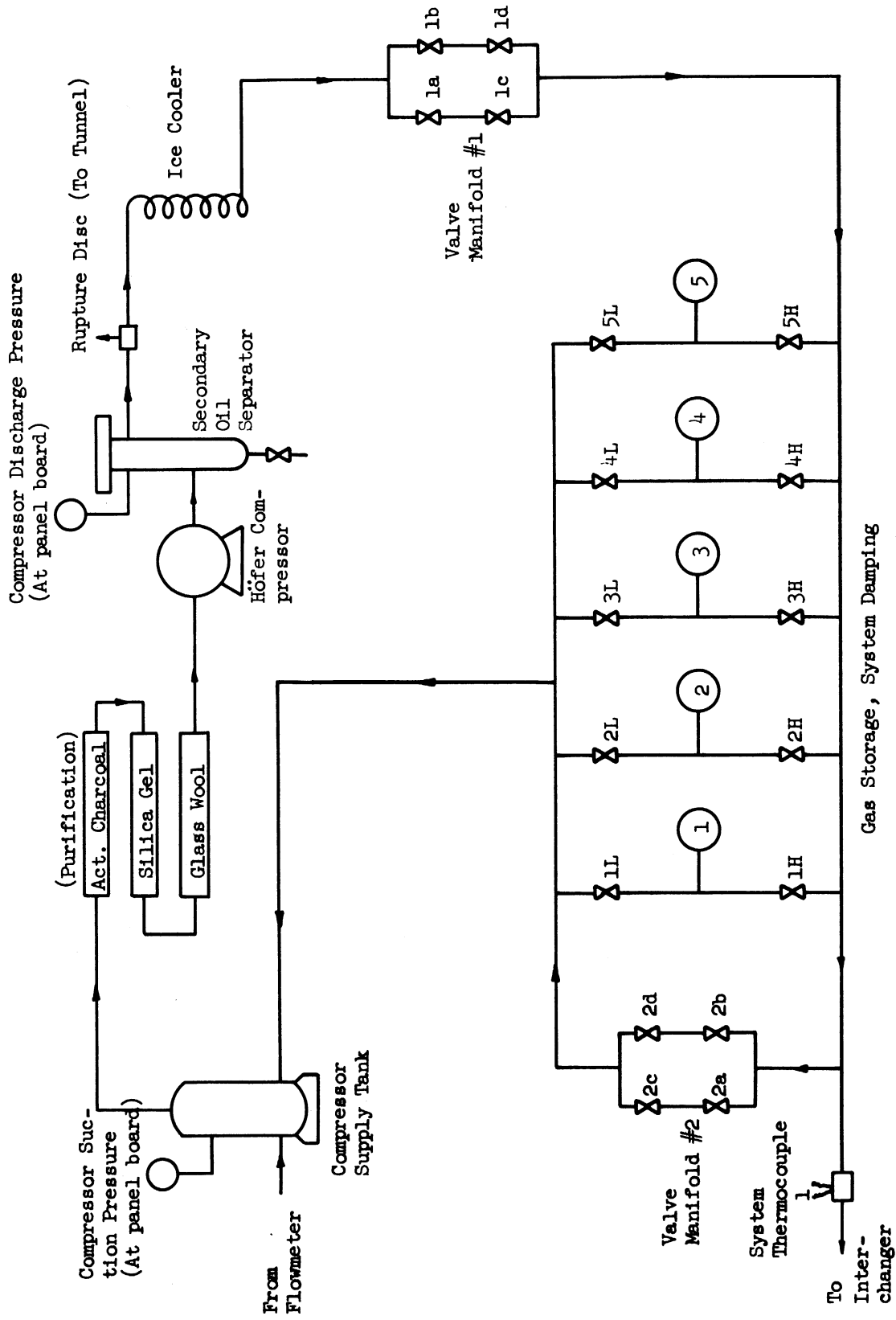
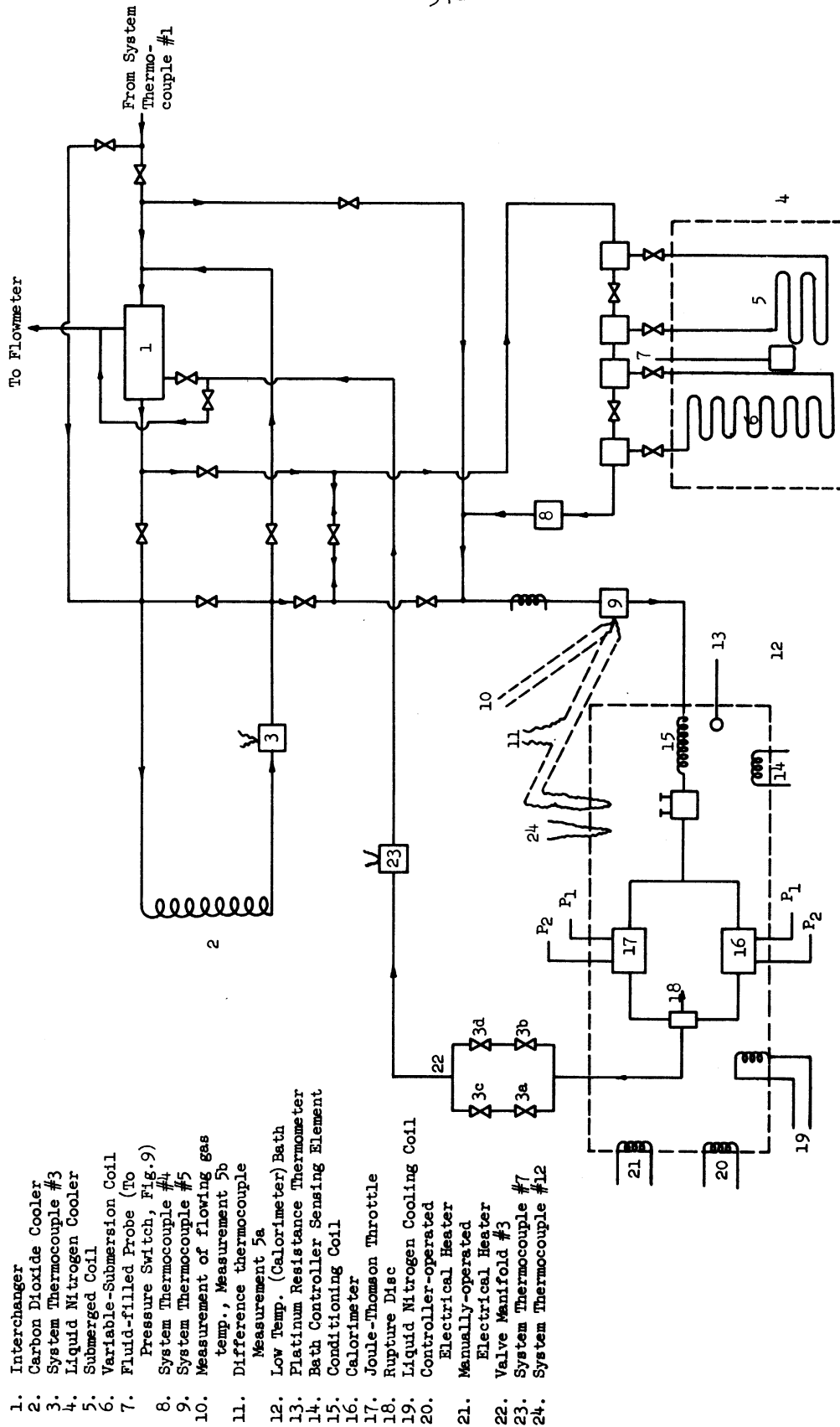


Figure 7. System Flow Diagram



1. Interchanger
2. Carbon Dioxide Cooler
3. System Thermocouple #3
4. Liquid Nitrogen Cooler
5. Submerged Coil
6. Variable-Submersion Coil
7. Fluid-filled Probe (To Pressure Switch, Fig. 9)
8. System Thermocouple #4
9. System Thermocouple #5
10. Measurement of flowing gas temp., Measurement 5b
11. Difference thermocouple Measurement 5a
12. Low Temp. (Calorimeter) Bath
13. Platinum Resistance Thermometer
14. Bath Controller Sensing Element
15. Conditioning Coil
16. Calorimeter
17. Joule-Thomson Throttle
18. Rupture Disc
19. Liquid Nitrogen Cooling Coil
20. Controller-operated Electrical Heater
21. Manually-operated Electrical Heater
22. Valve Manifold #3
23. System Thermocouple #7
24. System Thermocouple #12

Figure 7. System Flow Diagram (Cont'd)



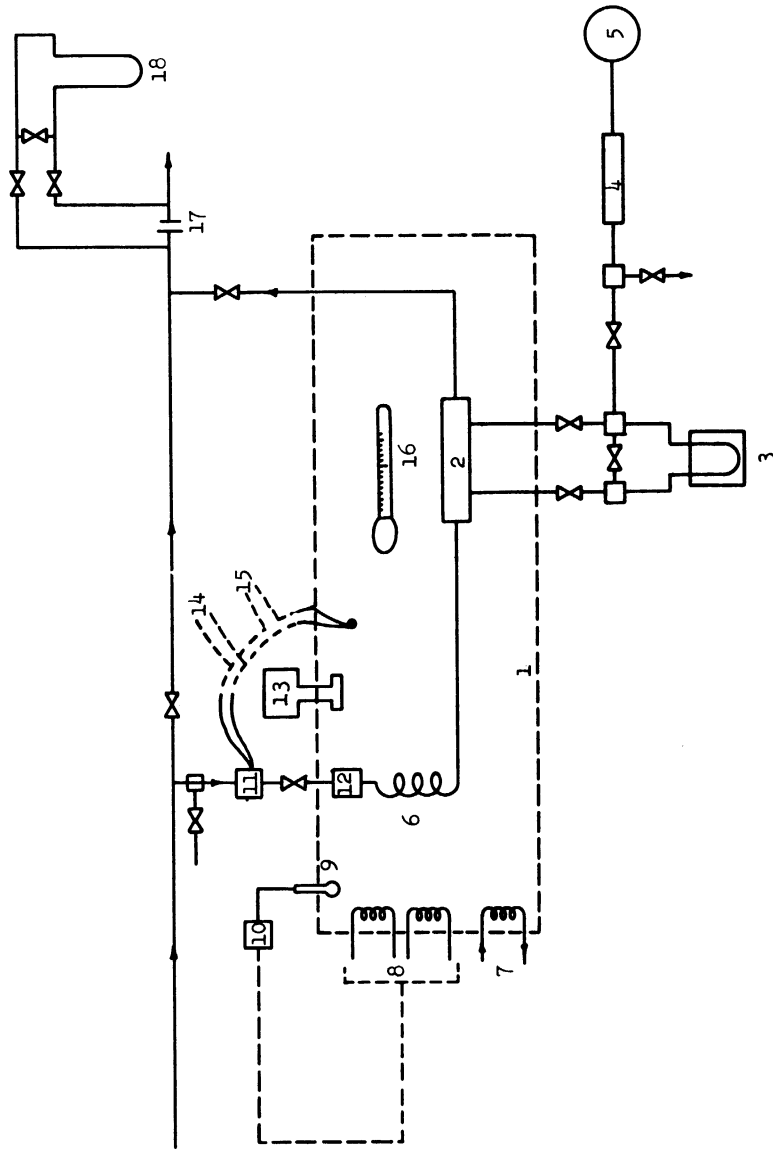


Figure 7. System Flow Diagram (Cont'd)

1. Constant Temp. Metering Bath
2. Linear Flowmeter
3. U-Tube and Cathetometer
4. "Gauge Saver"
5. Heise Bourdon Tube Gauge
6. Conditioning Coil
7. Cooling Coil
8. 2-250 Watt Electrical Heaters
9. Thermoregulator
10. Fisher Relay
11. System Thermocouple #8
12. Filter
13. Centrifugal Stirrer
14. Measurement of Flowing Gas temp., Measurement 8b
15. Difference Thermocouple Measurement 8a
16. Mercury-in-Glass Thermometer
17. Orifice
18. High Pressure Manometer

being studied is circulated by means of a compressor, brought to a specified low temperature and high pressure for calorimetric measurements, and then reheated and throttled for the purposes of flow metering and recirculation. The mass of material in the system remains constant during this process, as material is neither added nor removed.

An understanding of the operation is best gained by following a typical unit mass of material as it moves through a complete cycle.

#### Circulation, Purification, and Gas Storage

Beginning at the compressor supply tank, gas which is to be compressed and circulated flows to the intake side of the compressor.

The compressor supply tank has the function of insuring stable operation of the compressor. It does this by preventing short-term surges in the supply of gas to the compressor intake. Normally, the pressure at this point varies between about 4 and 7 atmospheres absolute, depending on several factors.

The gas on its way to the compressor from the compressor supply tank passes through three filters in series: activated carbon, silica gel, and finally glass wool. These are for the purpose of removing oil, water, and other impurities.

Circulation in the system is obtained by means of a three-stage Höfer compressor. It has a maximum discharge pressure rating of about 2600 psia and a volumetric capacity of 1.63 cubic meters per hour at a suction pressure of 6.5 atmospheres absolute. The compressor is driven by a ten horsepower AC squirrel cage motor.

The gas passing through the compressor is boosted to a pressure which at steady state is dependent upon the total quantity of fluid

in the closed system, the temperature profile in the system, and the flow resistances imposed by valves and other equipment. The gas is cooled after each compressor stage and finally passes from the third stage into an oil separator integral to the compressor. Here, part of the oil added during compressor operation is removed by gravity separation. The remainder of the oil is removed in a secondary oil separator which operates by a combination of gravity separation and filtering action through activated carbon and glass wool. Figure 8 is a photograph of the compressor supply tank, compressor, secondary oil separator, and storage cylinders.

After compression, the gas is further cooled by passage through a coil submerged in crushed ice and then throttled to a somewhat lower pressure by means of valve manifold #1. The throttling serves to level out small short term fluctuations in pressure and flow rate due to compressor operation and provides one of the points at which flow resistance can be changed in the system.

Following passage through valve manifold #1, part of the gas may be recycled to the compressor intake through valve manifold #2. This represents a means of altering the flow rate to the calorimeter or Joule-Thomson throttle.

Cylinders 1 through 5 in Figure 8 have two functions:

1. They serve as gas storage for the system. Gas may be either added to or removed from the system for the purpose of altering the pressure profile in the system.
2. During operation, any of the cylinders 1 through 5 may be open to either the high or low pressure side of the system for the purpose of buffering (all of the system at

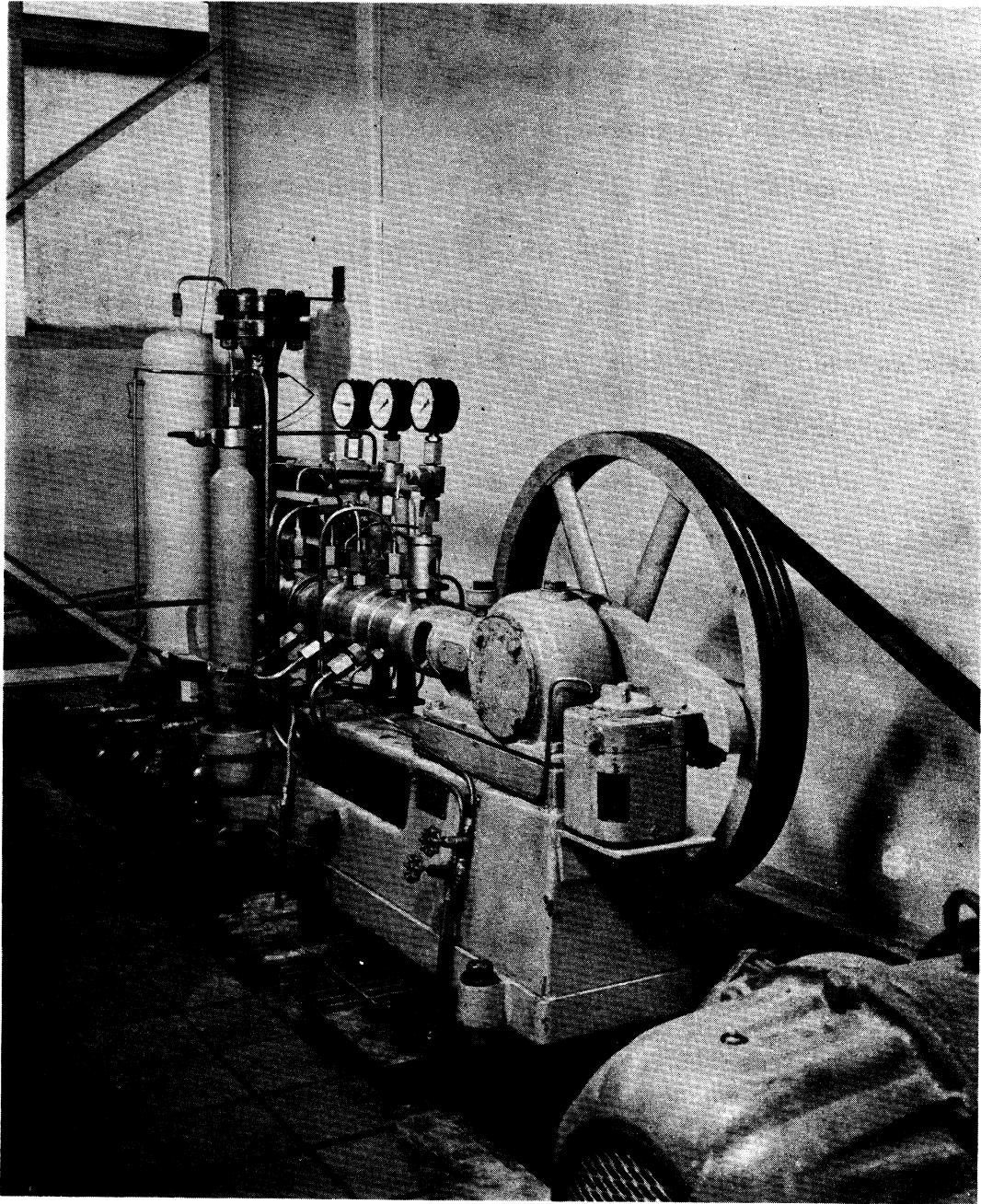


Figure 8. Compressor Supply Tank, Compressor, Oil Separator, and High Pressure Cylinders

essentially compressor suction pressure being designated low pressure for this purpose and the remainder of the system being designated high pressure). This results in steadier system operation. The short term oscillation in flow rate and pressure due principally to compressor action are very materially reduced; the longer term variations or drifting are spread over a much longer period of time.

#### Refrigeration, Temperature and Pressure Control

After passing system thermocouple 1, the gas may take one of a number of routes through a cooling system before arriving at the low temperature bath where the calorimeter and Joule-Thomson throttle are located. The choice of paths depends on the temperature at which specific heat or Joule-Thomson measurements are being made and the location of that temperature with respect to the sublimation temperature of carbon dioxide. The different flow paths offer the possibility of mixing several fluid streams at different temperatures in order to bring the fluid as closely as possible to the temperature at which measurements are being made.

At higher operating temperatures, only dry ice cooling and heat exchange with the cold fluid leaving the low temperature bath is necessary to cool the incoming fluid. At the lower temperatures, these operations provide pre-cooling, and additional cooling is provided by liquid nitrogen.

The exchanger (Figure 7) is operated countercurrently, with the fluid leaving the low temperature bath receiving heat from the fluid being cooled.

The carbon dioxide cooler (Figure 7) consists simply of a high pressure coil submerged in dry ice.

The liquid nitrogen cooler (Figure 7) consists of two high-pressure coils. One is completely submerged in liquid nitrogen; the other is in the form of a helix and is several feet in length. It is possible by means of liquid leveling equipment to adjust the degree of submersion of the second coil in order to vary the heat removal from the fluid flowing through it. The necessary transfer of liquid nitrogen to the cooler is accomplished by means of gas pressure on an evacuated and insulated liquid nitrogen tank or Dewar. The gas pressure on the liquid nitrogen Dewar is regulated by the height of a dip-stick containing a volatile material. Variation in the pressure of this volatile material operates a combination of a pressure switch and a solenoid valve to supply pressure to the liquid nitrogen Dewar (Figure 9).

The fluid passing through the cooling system eventually converges at a point just before the line heater at system thermocouple 5 in Figure 7. Here, the fluid which is slightly below the operating temperature of the low temperature bath is adjusted by a manually controlled line heater to approximately the low temperature bath operating conditions. The approach to low temperature bath operating conditions is followed by system thermocouple 5 (fluid temperature just before the low temperature bath) and system thermocouple 12 (located in the low temperature bath) on a Honeywell multiple point indicating potentiometer. Junction 5 and a second junction located in the low temperature bath may also be operated as a difference thermocouple for closer adjustment. This measurement is designated 5a in Figure 7.

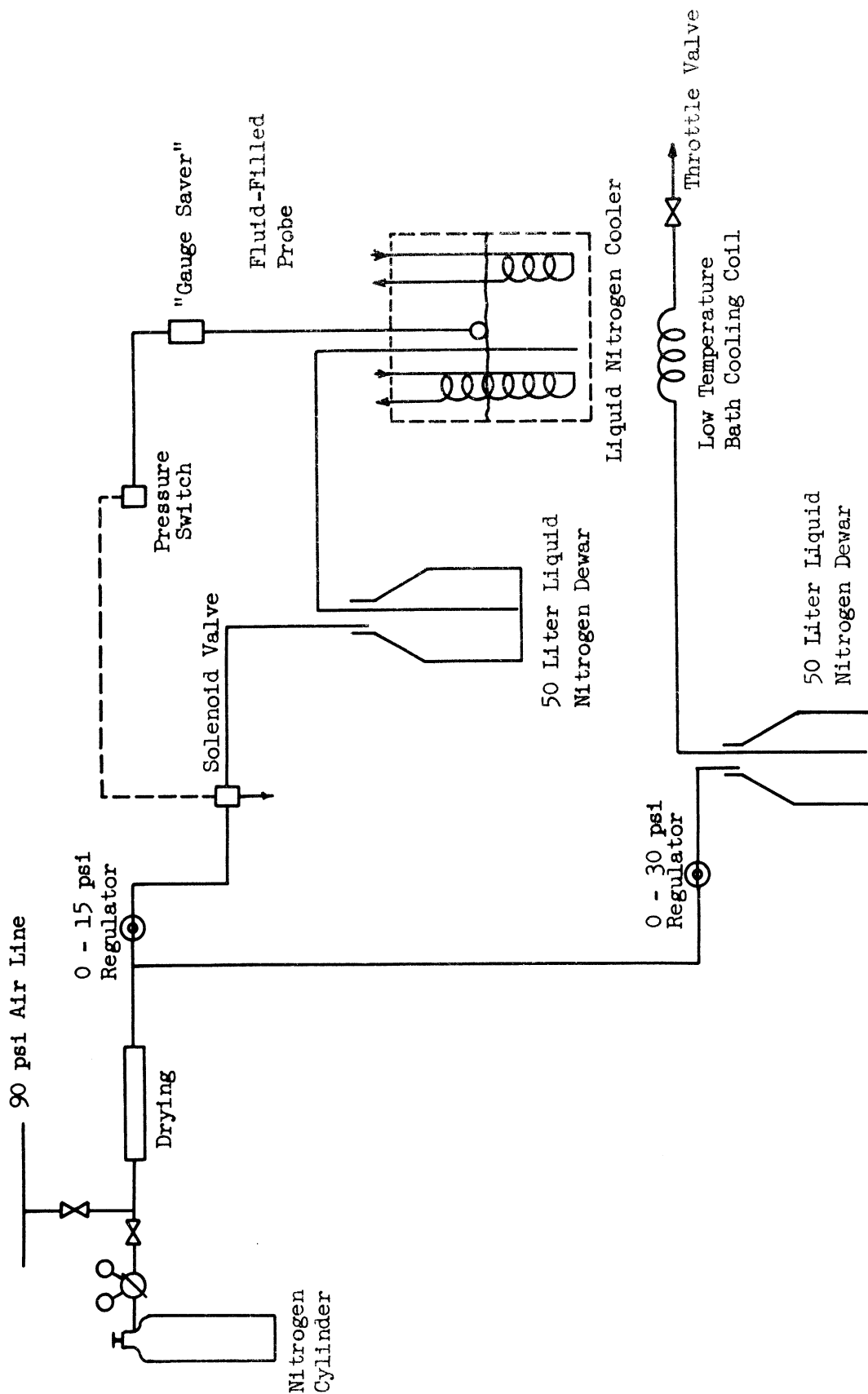


Figure 9. Liquid Nitrogen Transfer

After temperature adjustment and prior to entering the calorimeter or Joule-Thomson throttle, the fluid passes through a conditioning coil in the low temperature bath for the purpose of bringing it exactly to bath conditions.

The low temperature bath is a parallelepiped tank containing a vigorously agitated liquid in which the calorimeter, Joule-Thomson throttle, conditioning coil, and other items necessary for temperature control are submerged. The temperature of the bath liquid is controlled to 0.025°F at all times, and is the initial temperature of the fluid entering the calorimeter or Joule-Thomson throttle.

The low temperature bath is cooled by a liquid nitrogen coil. Gas pressure causing nitrogen flow is controlled manually (Figure 9). Final temperature adjustment is made by two electrical heaters, one manually operated and the other under automatic control. A thermocouple and a platinum resistance thermometer are employed to measure the temperature of the bath.

After bringing the low temperature bath to the proper temperature, the cooling and heating rates are adjusted so that the bath tends to cool slowly if left alone. At this time the automatic heater is put into operation to hold the bath temperature at the desired point. The output of this heater is regulated by a Brown Air-O-Line controller model 152. This controller is a combination Wheatstone Bridge-pneumatic instrument. One leg of the Wheatstone Bridge is located in the low temperature bath in the form of a nickel resistance and serves as the primary sensing element. As the temperature of the bath shifts from the desired control point, the temperature coefficient of resistivity of



the nickel causes a bridge unbalance in the controller. The resulting error signal which is produced is converted from DC to AC, amplified, and through mechanical linkage, controls a pneumatic signal from the control instrument. The pneumatic signal operates a piston-positioned variac which controls the automatic low temperature bath heater operation.

The fluid is brought to the calorimeter or Joule-Thomson device at the desired temperature, in the manner described. The pressure entering the calorimeter or Joule-Thomson throttle depends on the amount of fluid in the system, the temperature profile in the system, and the setting of various flow resistances. The flow rate is also a function of these variables. A constant compressor displacement is assumed.

The cooling system and low temperature bath are shown in Figure 10. The smallest of the insulated boxes nearest the reader in Figure 10 contains the low temperature bath, the next, the carbon dioxide cooling coil, the third, the liquid nitrogen cooling coils, and the box in the background contains the interchanger. Also visible are the Dewars for supplying liquid nitrogen and, overhead, a large box which contains innerconnecting high pressure tubing which must be insulated.

#### Specific Heat and Latent Heat Measurements

If calorimetric measurements are being made, a controlled addition of heat is made to the fluid by means of a 60 watt, maximum output electronically regulated, DC power supply. The calorimeter heater circuit is shown in Figure 24. The current supplied to the heater from the constant voltage source, normally operated at 90 to 100 VDC, is controlled by several rheostates in series. The current flowing through

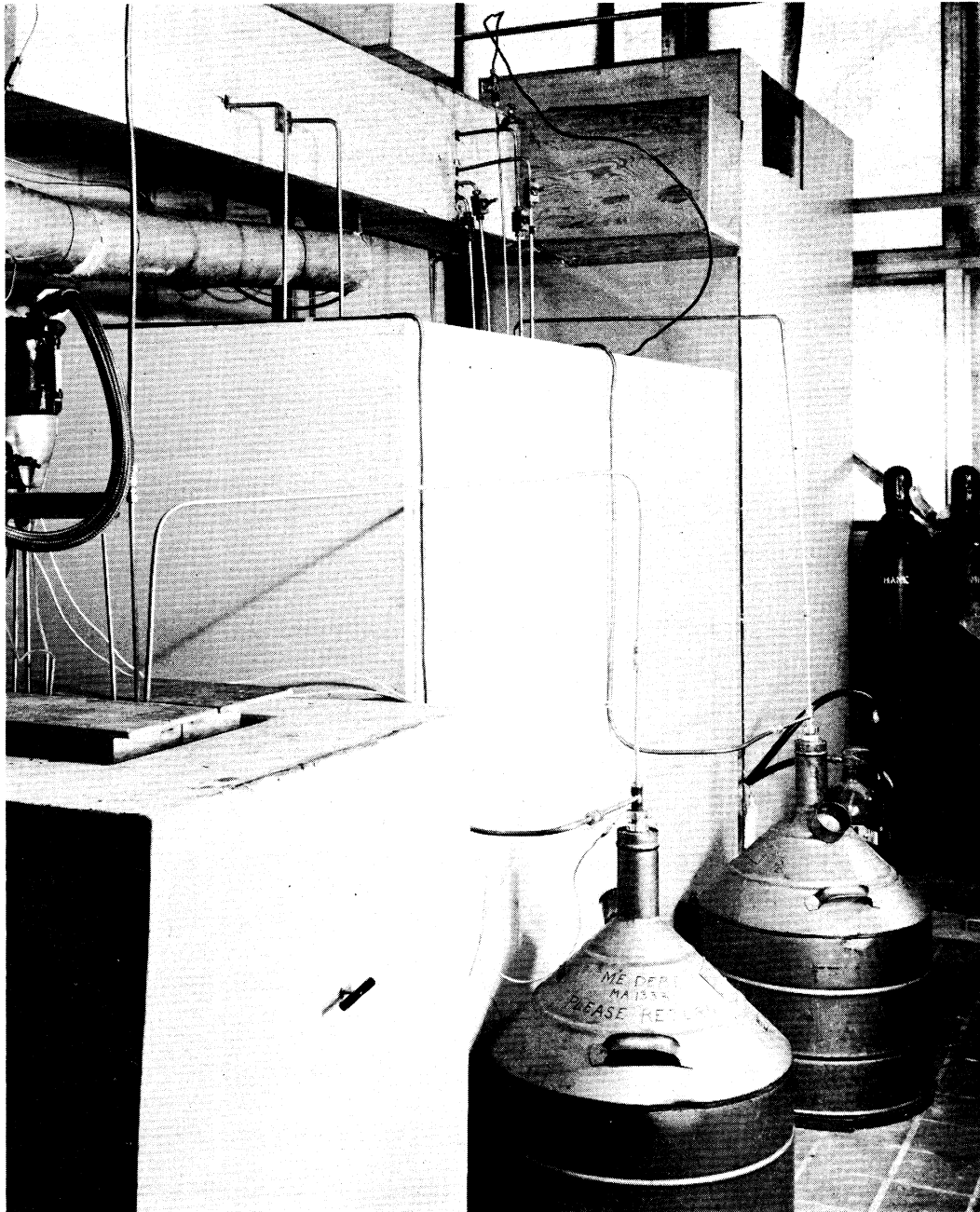


Figure 10. Low Temperature (Calorimeter) Bath, Carbon Dioxide Cooler, Liquid Nitrogen Cooler, and Interchanger

the calorimeter heater and the IR drop across it, are determined by measuring voltage drops across standard resistors with a Leeds and Northrup K-3 potentiometer. The actual voltages measured are scaled, of course, to the potentiometer ranges. From these measurements of calorimeter current and IR drop, the power dissipation in the calorimeter heater can be easily calculated.

The corresponding temperature change of the fluid passing through the calorimeter is measured by a 6-junction copper-constantan difference thermocouple between entering and exiting thermocouple wells.

The portion of the calorimeter in which energy is being accounted for is protected against undesired heat exchange by controlling the temperature of the calorimeter surroundings, suitably isolating components of the calorimeter, employing a radiation shield and an insulating vacuum. (Certain other refinements for preventing heat leakage in the calorimeter are discussed in Appendix A.)

From a knowledge of the flow rate, the temperature change, and the energy addition to the fluid, it is possible after applying certain corrections to calculate the average specific heat at constant pressure of the fluid over the temperature increment employed. These corrections include a small correction for Joule-Thomson effect due to the slight pressure drop in the calorimeter and a correction for undesired heat leakage to the fluid. The former correction is determined by making blank runs in which there is no electrical addition of heat. The latter correction is determined by varying the flow rate while keeping the initial temperature and pressure of the fluid and its temperature change constant. The initial or final pressure and the pressure drop through the calorimeter are measured by means of a dead weight pressure balance system.

Measurements of isobaric integral latent heat may be made in the calorimeter provided that the present calorimetric system is modified to supply the necessarily larger heat inputs.

#### Joule-Thomson Measurements

Joule-Thomson measurements may also be made in the low temperature bath by passing the fluid through a Joule-Thomson expansion device containing one of a series of interchangeable porous plugs. Joule-Thomson measurements were not carried out in the present investigation although the necessary Joule-Thomson expansion device was constructed.

The fluid will probably be expanded from an initial pressure and temperature to progressively lower pressures in continuous steps. The porous plugs selected for a particular set of measurements will depend on the flow rates desired over this pressure range. Use of several plugs for a given set of measurements will insure independence of the measurements with respect to flow rate.

The temperature change of the fluid passing through the Joule-Thomson device will be determined by a multiple-junction copper-constantan difference thermocouple. The initial and final pressure and the pressure drop will be found by means of the dead weight differential pressure balance.

#### Flow Metering

After leaving the calorimeter or Joule-Thomson expansion device, the fluid is throttled to a pressure near that of the compressor suction pressure through valve manifold #3. This manifold holds the required final pressure at the calorimeter or Joule-Thomson throttle. The

fluid then flows through the shell side of the interchanger in order to pre-cool fluid moving toward the low temperature bath. From here it goes to the metering equipment.

For preliminary system adjustments in calorimetric determinations, the fluctuations in flow rate and pressure may be detected by means of an orifice and mercury manometer (Figure 7). This aids in properly setting the degree of system damping (by floating cylinders 1 through 5 on either the low or high pressure side of the system).

The flow rate through the calorimeter or Joule-Thomson device is measured by channeling the flow through a linear flow meter. The mass flow rate through this instrument is determined by measuring the pressure drop through the meter and the pressure and temperature at this point. It is desirable and practicable to maintain a constant metering temperature. This is accomplished by locating the flow meter in a constant temperature water bath (Figure 11). The pressure at the meter necessarily varies so that a variety of flow rates and pressure profiles in the system may be obtained. The pressure entering the meter (normally 75 to 100 psia) is determined using a 16-inch Heise Bourdon tube gauge. The pressure drop through the meter is measured with a U-tube containing water and a cathetometer.

Prior to being metered, the fluid temperature is adjusted to 20°C by means of a manually operated line heater. The temperature just before entering the meter is measured by system thermocouple 8 and read on a Honeywell indicating potentiometer. This measurement is designated 8b in Figure 7. The difference between the temperature at this point and the metering temperature is more accurately determined with a difference thermocouple. This measurement is designated 8a in Figure 7. A

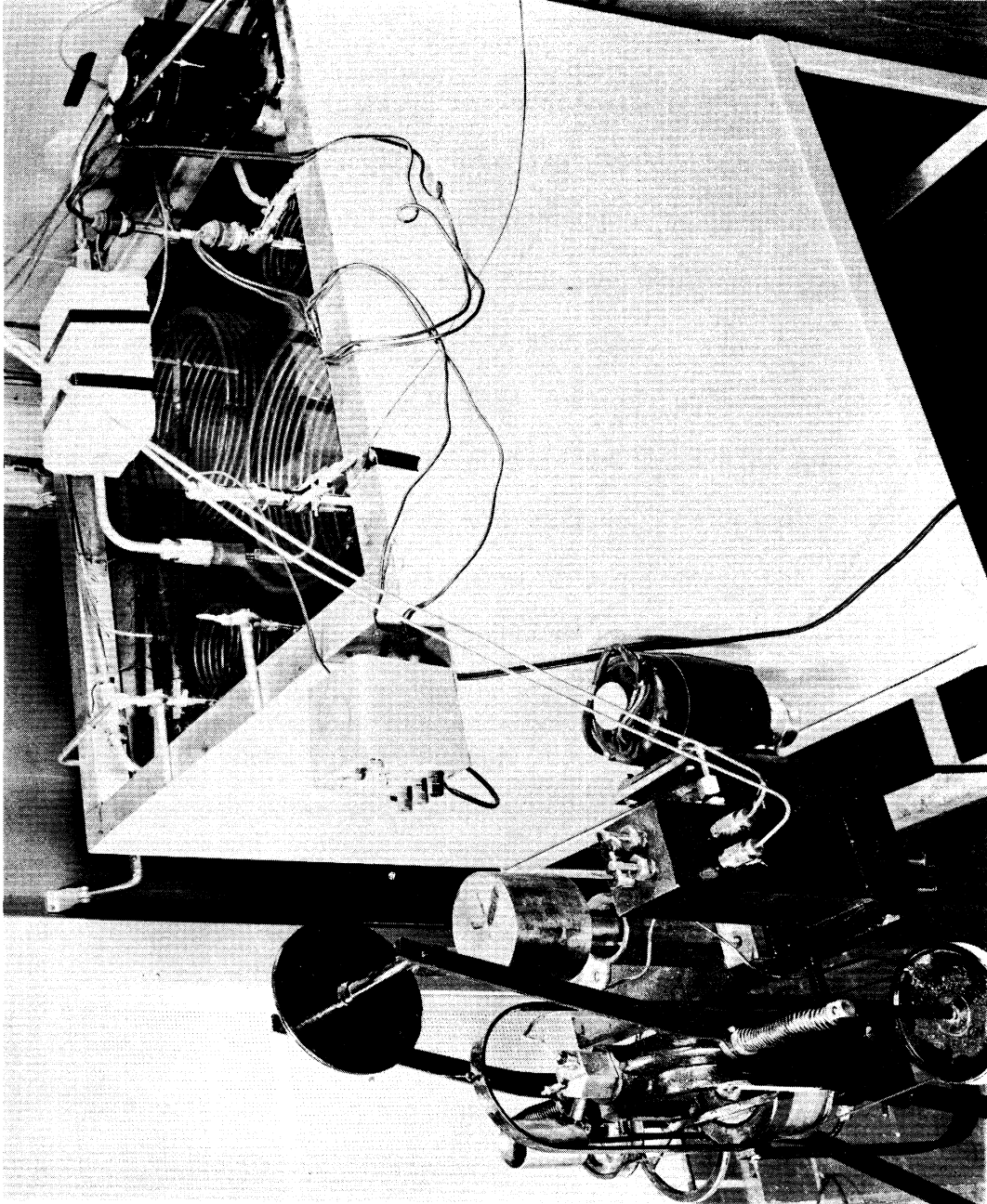


Figure 11. Constant Temperature Metering Bath and Differential Dead Weight Pressure Balance

conditioning coil in the water bath is responsible for a final precise adjustment to 20°C.

After metering, the fluid returns to the compressor supply tank, the point of origin, at essentially metering pressure and temperature.

### Control Panel

Figure 12 is a view of the control panel from where operations are conducted. This panel consists of two parts, a one-eighth inch steel section supported vertically by angle iron at about 2 feet from the barricade and an inclined wooden desk top extending down and away from the bottom of the steel. Much of the equipment is located between this panel and the barricade -- including all flush-mounted equipment in the panel, as well as the vacuum system, standard electrical resistors, main air and water lines, accessories, the pneumatic rheostat, a constant-voltage AC transformer, fusing, and most of the electrical wiring for the system. At the end of the panel from which the picture (Figure 12) was taken can be seen the calorimeter power supply, the potentiometer, and some of the electrical controls for platinum thermometer operation, calorimeter heater control, and operation of many of the system's AC instruments. A number of control rheostats are located beneath the inclined desk top in which the potentiometer is flush-mounted. Other items visible in Figure 12 include a McLeod gauge, the U-tube and cathetometer, the mercury manometer, and at the extreme end of the steel panel, the Honeywell controller and indicating potentiometer. In one area of the panel are seen a large number of valves and fittings. This is the valve switchboard where most of the valves in the system are located. This arrangement allows convenience

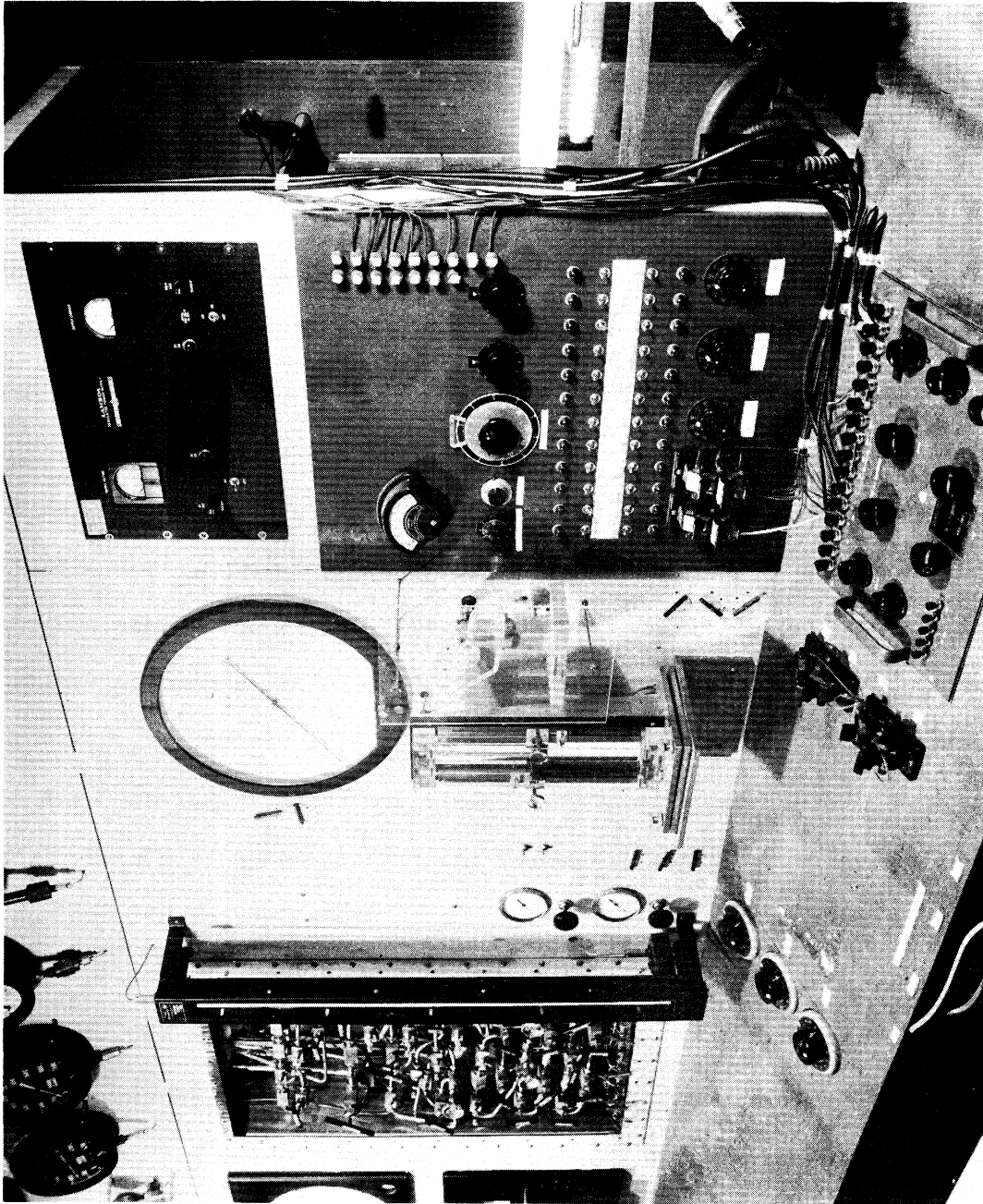


Figure 12. Control Panel



in operation and maintenance of much of the system piping. Several pressure gauges, for determining compressor discharge and suction pressures and the pressures available at cylinders 1 through 5 are also visible.

#### Physical Layout and Facilities

The entire apparatus is located in the Automotive Engineering Building on the North Campus. The equipment which the author has constructed is located in Test Cell 247, a 30 foot by 17 foot room.

The source of low temperature coolant for the project, a 25 liter per hour liquid nitrogen machine (Figure 13) operated by the Mechanical Engineering Department, is located in an adjacent cell. Another facility of particular value to the present investigation was a large, well-equipped instrument shop operated by the University of Michigan Research Institute at the Automotive Engineering Building. A great deal of the equipment construction was accomplished in this shop.

Figure 14 is an overall view of test cell 247. In it can be seen the steel barricade which surrounds much of the equipment to protect operating personnel from the hazard of fire or rupture of the system. At the rear of the cell are a number of large glass windows (blacked out in Figure 14) which provide some assurance of pressure relief in case of an explosion.

#### Utilities and Safety Precautions

Utilities not already in the test cell at the time of initiation of the low temperature project, which were installed include:

1. An air supply at 90 pounds per square inch.

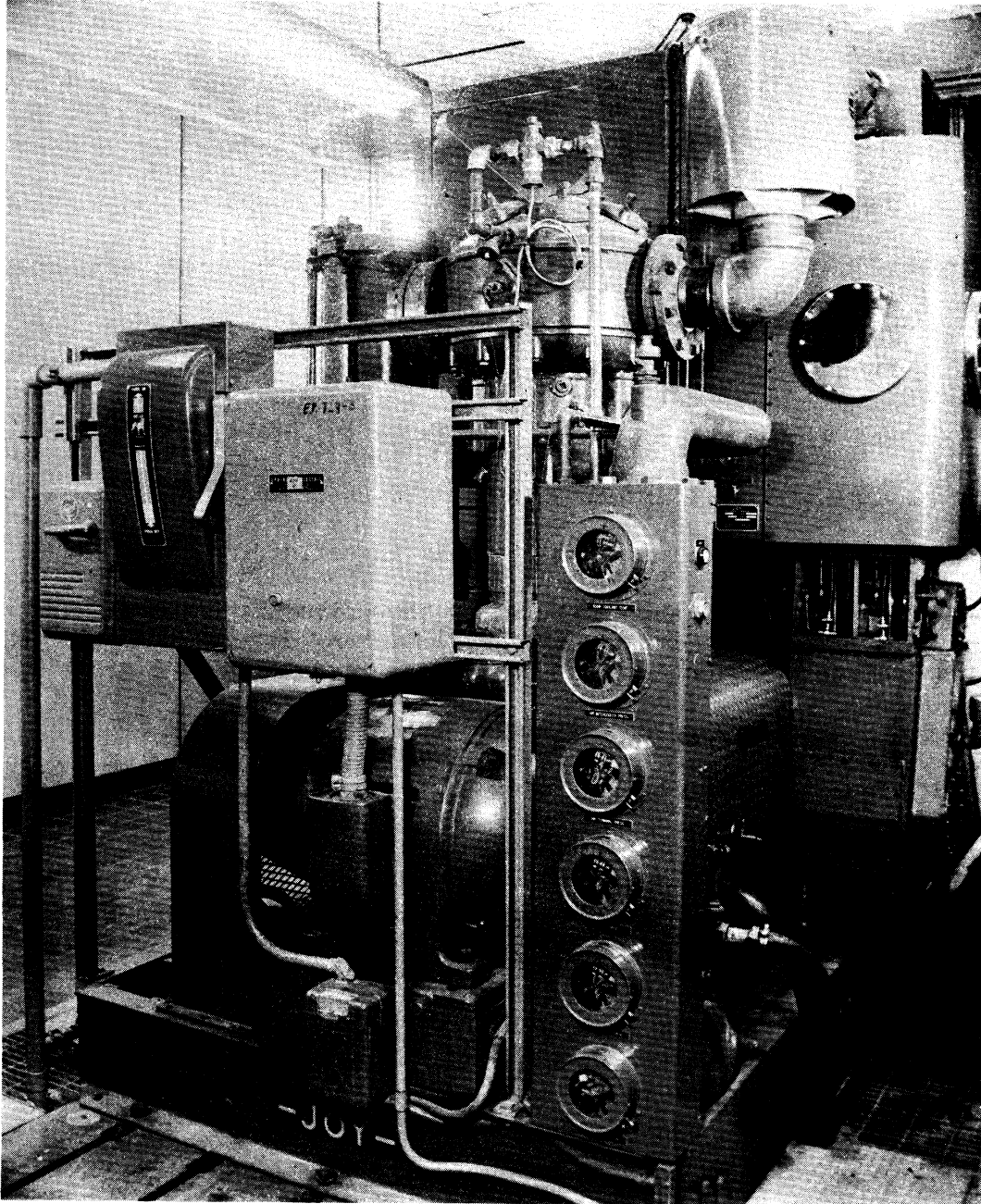


Figure 13. Liquid Nitrogen Machine

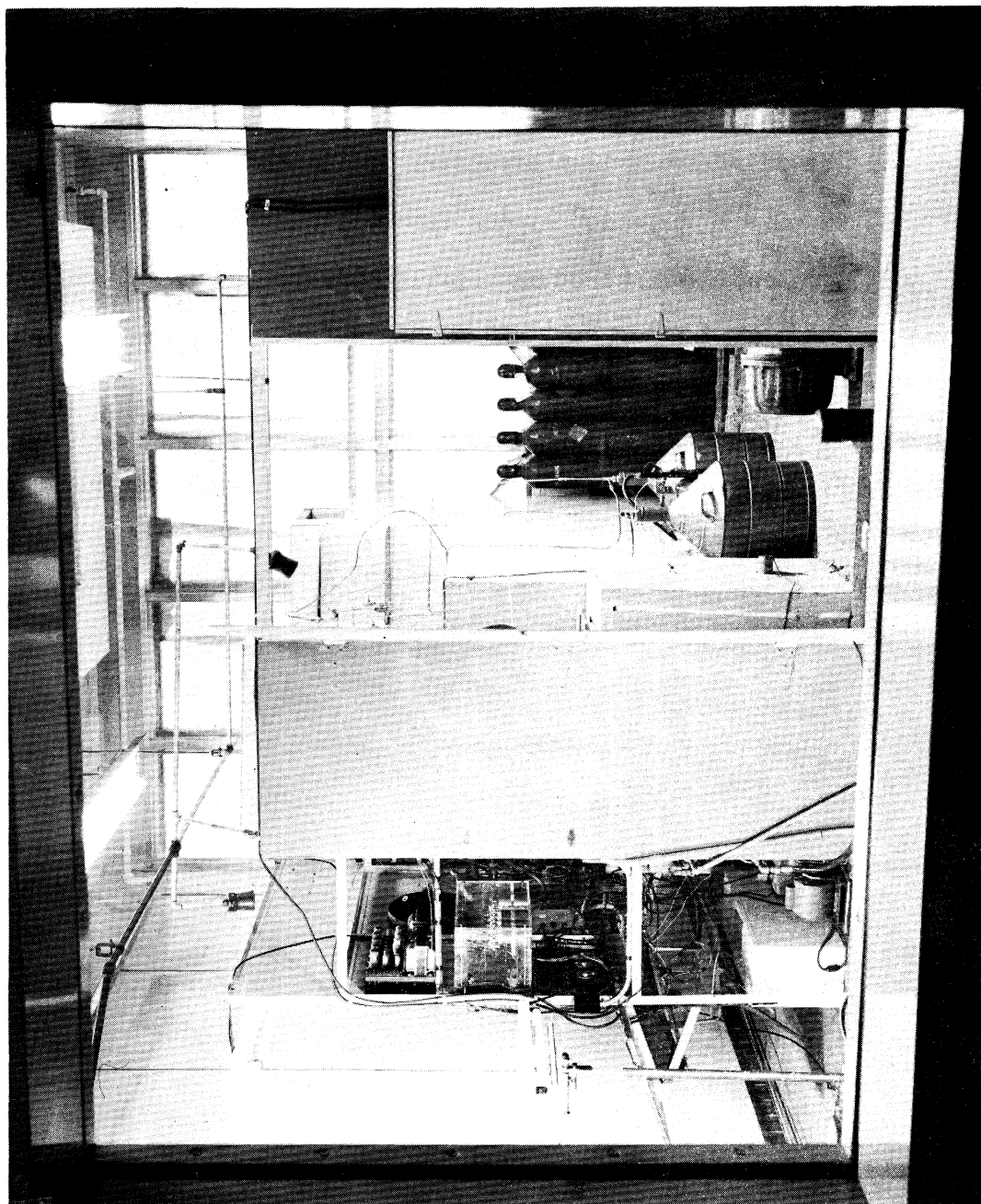


Figure 14. Overall View of Test Cell 247

2. A cold water line.
3. A 115/208 VAC, 4 wire, 3-phase, 150 amp. electrical service.

In addition to the barricade, a number of other safety devices have been installed or were already present in the test cell including:

1. Class ID electrical circuitry inside the barricade.
2. A room ventilation system for removal through an alarm-protected tunnel of any spills of volatile fluid.
3. Comprehensive fusing and grounding of electrical circuitry.
4. Rupture discs in the flow system.
5. A large carbon-dioxide fire system with nozzles located inside and outside the barricade.
6. Plastic shielding in front of all pressure gauges and glassware.

## ISOBARIC SPECIFIC HEAT MEASUREMENTS ON NITROGEN

The flow system and calorimeter were operationally tested by measuring the specific heat of nitrogen at temperatures of  $-50^{\circ}\text{F}$ ,  $-100^{\circ}\text{F}$ , and  $-150^{\circ}\text{F}$ . The pressure range of measurement was from approximately 294 psia to 1176 psia. Nitrogen was selected for the study because it was felt that its isobaric specific heat properties were relatively well known at low temperature and under pressure. It was hoped that the measurements on nitrogen would provide an opportunity to verify the accuracy with which specific heat could be measured with the equipment.

Several trial runs were made with the equipment before it operated satisfactorily enough to obtain data. Some of the difficulties which occurred during operation are briefly reviewed, along with a discussion of the operating characteristics of the system. Following this, data are reported for a group of runs for which the equipment was operated from 15 to 35 hours continuously. The conversion of the data into specific heat values is presented and a comparison is made with values presented in the literature. An attempt is then made to consider some of the uncertainties and errors which were involved in the reported specific heats.

### Discussion of System Performance

The plan of operation was to run the equipment for a sufficient length of time to bring the calorimeter and entering fluid to the desired conditions, introduce a measured amount of electrical energy into the fluid, and then measure the important variables after the calorimeter had stabilized. In the trial runs, some complication arose before the system

was stable enough to warrant the recording of data. During the latter runs in which data was recorded, the system was much more stable; however, a number of upsets and minor difficulties lengthened the process of obtaining data considerably.

In general, the operational characteristics of the system were found to be excellent. Although a number of minor troubles occurred from time to time, only one major difficulty was apparent during the period in which data was taken. This major difficulty was the intermittent failure of the cooling system to maintain a stable supply of constant temperature fluid to the calorimeter.

The cooling system instability was a result of two factors:

1. The liquid nitrogen level controller in the liquid nitrogen cooler failed to provide dependable or sufficiently sensitive control.
2. Excessive heat gain to the flowing fluid occurred between the final cooling step and the point of entry into the calorimeter.

At critical times during the series of measurements the liquid nitrogen level controller failed completely -- resulting in an upset in the system. The re-establishment of steady conditions in such cases required from one to two hours. At other times the nitrogen cooler operation did not fail completely, but was sufficiently unsatisfactory that a continuous slow cycling or drift in the system temperatures and pressures resulted. Data was taken in some cases when the system was drifting slowly -- if it appeared that absolutely steady performance would not be attained in a reasonable length of time.

It was necessary because of heat gains between the cooling system and the calorimeter to remove a great deal more energy from the fluid in the cooling system than had been anticipated. At lower operating temperatures and/or higher operating pressures nitrogen was liquefied in this process. This compounded the problem of instability because the flow to the calorimeter was extremely sensitive to the degree of liquefaction -- which was being continually changed by poor liquid nitrogen level control.

After the equipment had been operated for some time and the calorimeter heat input adjusted, the following criteria of steady state operations were used:

1. Temperature of the fluid leaving the cooling system
2. Difference in temperature between fluid entering the calorimeter bath conditioning coil and the temperature of the bath liquid
3. Difference in temperature between the fluid entering and leaving the calorimeter
4. Pressure at the calorimeter
5. Difference in temperature between the fluid entering the metering bath conditioning coils and the metering bath temperature
6. Pressure at the flow meter
7. Pressure drop across the flow meter
8. Calorimeter insulating vacuum level
9. Several difference thermocouple measurements between internal calorimeter points (See Figure 15, Table VII)
10. Calorimeter heater current and IR drop

11. Miscellaneous observations, most of which were anticipatory of changes, such as: metering bath temperature, low temperature bath controller operation, several temperatures throughout the flow system

It was found that when cooling system operation was satisfactory, the system usually became very steady in operation.

Control of flow rate and pressure by means of the valve manifolds and system storage and buffering was excellent. It was possible to establish any desired pressure up to at least 2,000 psia at the calorimeter, vary the flow rate by several fold, and maintain a satisfactory and steady metering pressure. Short term pressure fluctuations at the flow meter were never in excess of 0.02 inches of mercury. The metering pressure, when cooling system performance allowed, remained constant within 0.05 psi for long periods of time. It was not difficult to obtain all measurements in the metering pressure range of 75 to 100 psia. Calorimeter pressure remained so steady, when cooling system operation did not upset it, that a pressure variation of 0.1 psi could not be detected by means of the pressure balance for 30 minutes at a time.

The metering bath temperature remained constant at the desired 68.0°F at all times. The pressure drop across the flow meter, as determined by a U-tube and cathetometer, remained constant within 0.001 inch of water frequently for 10 to 15 minutes.

The operation of the low temperature calorimeter bath was better than had been anticipated. The average bath temperature remained constant frequently to 0.01°F for an hour and sometimes several hours. The short term control cycle variation around the mean bath temperature was never



more than  $\pm 0.025^{\circ}\text{F}$ . The control cycle occurred over a sufficiently short period of time so that thermal inertia of the conditioning coil and calorimeter prevented detection of any cycling in the initial fluid temperature measurement inside the calorimeter.

The operation of the calorimeter power supply and heater circuit appeared to be excellent. It was possible to quickly adjust to any desired heat input up to the maximum supply output of 60 watts. Instability in the heater current and voltage, due to power supply ripple, was never more than five microvolts as interpreted by the K3 potentiometer at switch positions  $L_1$  and  $L_2$  (Figure 24). The mean value of heater voltage and current remained steady for long periods of time.

During the nitrogen measurements the main calorimeter thermocouple, which measured the temperature rise of the fluid, appeared to function well. On the basis of the calibration obtained, (see Appendix B), it was thought that this measurement was excellent. It was not discovered until after measurements had been completed that a serious temperature difference error had probably occurred. This error was not an observable operating characteristic and hence discussion of this matter will be postponed, (see Discussion of Results and Consideration of Errors). Eventually the failure of the main calorimeter thermocouple was responsible for the termination of the nitrogen investigation. The cause of the failure is not definitely known, but it is suspected that a high voltage was accidentally applied to the thermocouple leads. Along with the preparation of a new thermocouple installation, it appeared wise to make other improvements before proceeding with further measurements.

Two additional difficulties, which had the effect of producing a larger heat leak in the calorimeter than had been anticipated, were encountered during the nitrogen investigation.

One of these difficulties was the inability to maintain a consistently high insulating vacuum level in the calorimeter. It had been calculated that a vacuum level of 10 microns of mercury would correspond to a mean free path of air molecules commensurate with the minimum important distance for heat transfer (by stagnant air conduction between important surfaces) in the calorimeter. The plan was to operate the calorimeter at a vacuum level of about one micron of mercury. It was necessary to make the majority of nitrogen runs, however, at a vacuum level of 3 to 30 microns and three runs were made at much higher pressures. The poor vacuum resulted principally from leakage of nitrogen through the calorimeter heater leads seal (Figure 19), which occurred unless the calorimeter was frequently disassembled and the seal retightened.

The vacuum failure will have to be eliminated for future, more refined measurements. It was not believed that it would seriously prejudice the preliminary evaluation of the system performance. Modifications (see Future Work) should not be too difficult.

The heat leakage problem, due to a poor vacuum level in the calorimeter, was compounded, however, by an inability to consistently operate the isothermal radiation shield (Figure 15). The difference thermocouples IJ, MN, NH, NK (Figure 15) which were used to monitor the shield heater were tied electrically to all of the difference thermocouples shown in Figure 15, except the main thermocouple used for measuring the

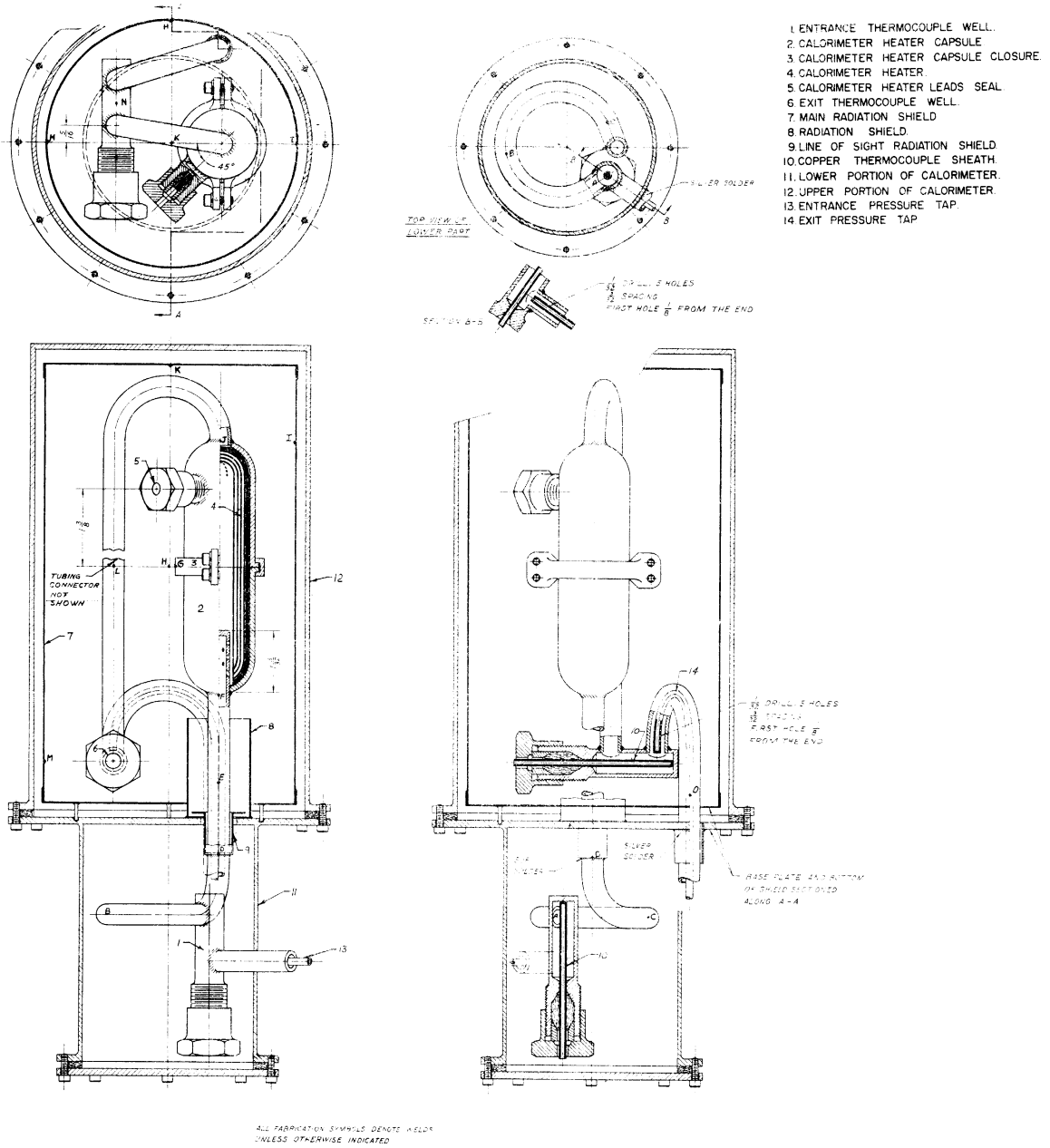


Figure 15. Calorimeter Assembly Drawing

temperature rise of the fluid in the calorimeter. On several occasions poor electrical insulation at a single junction put the entire loop out of commission. In view of frequent failure of these thermocouples and the already complex initial operation of the equipment, any attempt to operate the radiation shield, except for testing purposes, was abandoned.

It was possible to show by measurements on several occasions that the entire shield approached a single temperature very closely. The constancy of readings of difference thermocouples IJ, MN, NH and NK shown in Table III is offered as evidence of a single shield temperature. Similarly, the small readings of these difference thermocouples show that it was possible to maintain an average shield temperature very near the temperature of all the surfaces which the shield was supposed to protect.

It was also possible by means of the several difference thermocouples to show that several potential heat leaks in the calorimeter were of negligible significance, and that good temperature equalization was probably obtained for the fluid flowing through the calorimeter.

Difference thermocouples AB, AC, AD, AE, AF (Figure 15) indicated that heat leakage from the base of the calorimeter heater by conduction to the entrance thermocouple well or to the low temperature bath was essentially zero, see data in Table III.

Difference thermocouples JL and LN (Figure 15) indicated that temperature equalization of the fluid leaving the calorimeter heater and flowing to the exit thermocouple well was probably good, Table III.

Difference thermocouple NO (Figure 15) indicated that no significant heat leakage occurred along the exit high pressure tube, between the exit thermocouple well and the calorimeter bath, Table III.

TABLE III

TYPICAL SET OF READINGS FOR CALORIMETER DIFFERENCE THERMOCOUPLES

Designation of Thermocouple	Reading, Microvolts**
AB	0.2 Rev
AC	0.0
AD	0.1 Emf
AE	2.2 Emf
AF	180.7 Emf
JG	1.9 Rev
NH	1.9 Rev
JI	8.2 Rev
FJ	134.1 Emf
NK	5.4 Rev
LJ	2.5 Emf
NM	1.1 Rev
NL	0.5 Emf
ON	0.7 Rev
Main Calorimeter Thermocouple, 1 2*	1813.1 Emf

\* Main calorimeter junction: 1 inlet, 2 exit.

\*\*NOTE: Order of appearance of letters designating difference thermocouples indicates sense of temperature difference for same polarity (Emf, Rev); e.g., if  $T_A$  is known to be less than  $T_F$  and all other readings have the same polarity, then  $T_A < T_B$ ,  $T_J < T_G$ ,  $T_N < T_M$ , etc.

1 microvolt  $\approx$  .05°F except for main calorimeter thermocouple.

A number of other minor difficulties slowed down the process of obtaining data. High pressure leaks gave difficulty until they were all located. About six of the valves that were operated at the lowest system temperatures had to have their packings retightened from time to time. Freeze-ups occurred in cooling coils and in small valve ports until the practice of circulating the fluid through drying filters for some time prior to cooling was initiated.

#### Data Obtained

Nine values of the isobaric specific heat of nitrogen, each representing two independent measurements at two system flow rates, are reported in Table IV. Also summarized in Table IV, are the important variables for each  $C_p$  determination. A complete listing of the primary data used in calculating  $C_p$  is given in Table XXI of Appendix E.

Determinations of  $C_p$  were also made at  $-75^\circ\text{F}$ , 1176 psia, and  $-125^\circ\text{F}$ , 1176 psia, but are not included in Table IV. At  $-75^\circ\text{F}$ , only one flow rate was possible due to operational difficulties. At  $-125^\circ\text{F}$ , the two flow rates employed were nearly the same. In both cases, it was not possible to establish with reliability the proper correction for heat leakage.

#### Calculation of Specific Heat from Data

The values of specific heat reported in Table IV were calculated from the data by a method analogous to the following:

$$C_p = \frac{Q}{F(\Delta T - \delta T)} + \frac{\delta Q}{F(\Delta T - \delta T)} \quad (17)$$

TABLE IV  
SUMMARY OF ISOBARIC SPECIFIC HEAT DATA ON NITROGEN

Nominal Conditions of Cp Determination	Flow No.	Mass Flow Rate, lb/minute	Reciprocal Mass Flow Rate, 1/F, minutes/lb	Temp. Rise (ΔT-87), °F	Measured Heat Input, Q, Btu/minute	Calculated Heat Leakage Correction, ΔQ, Btu/minute	$\frac{ \Delta Q }{Q} \times 100$	Calorimeter Insulating Vacuum Level (Microns of Mercury)	$\frac{\text{Btu/lb} \cdot \text{°F}}{(\text{Cp})_F}$	$\frac{\text{Btu/lb} \cdot \text{°F}}{C_p}$
-50	1	.2998	3.336	18.37	1.5330	-.0667	4.35	30	.2784	.2668
-50	2	.2171	4.606	18.38	1.1284	-.0677	6.00	12	.2828	
-50	1	.2682	3.729	15.72	1.2565	-.0477	3.80	20	.2980	.2871
-50	2	.1851	5.403	15.85	0.8887	-.0489	5.50	20	.3029	
-50	1	.3095	3.231	17.57	1.8015	-.1035	5.75	15	.3313	.3133
-50	2	.2158	4.634	17.44	1.2762	-.1051	8.24	18	.3391	
-100	1	.2189	4.568	18.58	1.1529	-.0590	5.12	5	.2835	.2697
-100	2	.1668	5.995	18.18	0.8729	-.0586	6.71	5	.2878	
-100	1	.2658	3.762	23.14	1.9092	-.0402	2.11	5	.3104	.3040
-100	2	.2027	4.933	23.76	1.5046	-.0416	2.76	5	.3124	
-100	1	.2064	4.845	18.20	1.3347	-.0737	3.86	380	.3553	.3364
-100	2	.2988	3.347	18.27	1.9077	-.0746	5.59	275	.3495	
-100	1	.3105	3.221	19.48	2.2396	-.1538	6.87	11	.3703	.3465
-100	2	.2353	4.250	19.70	1.7519	-.1588	9.06	3	.3779	
-150	1	.3086	3.240	19.81	1.8663	-.1005	5.39	90	.3053	.2897
-150	2	.2193	4.560	19.66	1.3430	-.1011	7.53	80	.3115	
-150	1	.2237	4.470	19.37	1.6121	-.1070	5.39	250	.3720	.3488
-150	2	.2764	3.618	19.54	1.9852	-.1072	6.65	250	.3676	

- $C_p$  = Isobaric specific heat, Btu/lb - °F  
 $Q$  = Measured electrical energy addition, Btu/min  
 $\delta Q$  = Unmeasured heat leakage, Btu/min  
 $F$  = Mass flow rate, lb/min  
 $\Delta T$  = Temperature rise of the fluid upon addition of electrical energy, °F  
 $\delta T$  = First order approximation for Joule-Thomson effect (expressed as equivalent temperature change), °F

The first term on the right hand side of Equation (17) may be termed  $(C_p)_F$ . It is the apparent isobaric specific heat calculated from the data on the basis of a finite flow rate and before a correction is made for unmeasured energy transfer,  $\delta Q$ . Thus Equation (17) may be re-written:

$$C_p = (C_p)_F \pm \frac{\delta Q}{F(\Delta T - \delta T)} \quad (17a)$$

It has been demonstrated by other investigators<sup>(67,72)</sup> that  $\delta Q$  is frequently nearly independent of  $Q$  and  $F$  and depends primarily on  $\Delta T$ . More precisely, it has been shown by Montgomery and De Vries<sup>(72)</sup> that a plot of  $(C_p)_F$  vs  $1/F^n$  (where  $n$  depends upon the calorimeter) yields a straight line and that  $n$  is frequently equal to 1. On the assumption that  $\delta Q$  is completely independent of  $Q$  and  $F$ , a plot of  $(C_p)_F$  vs  $1/F$  for several values of  $Q$  and  $F$ , but with  $\Delta T$  held constant will yield a straight line. The intercept of this line will be  $C_p$ , the slope  $-\frac{\delta Q}{\Delta T}$ . This is illustrated in Figure 16. In the present



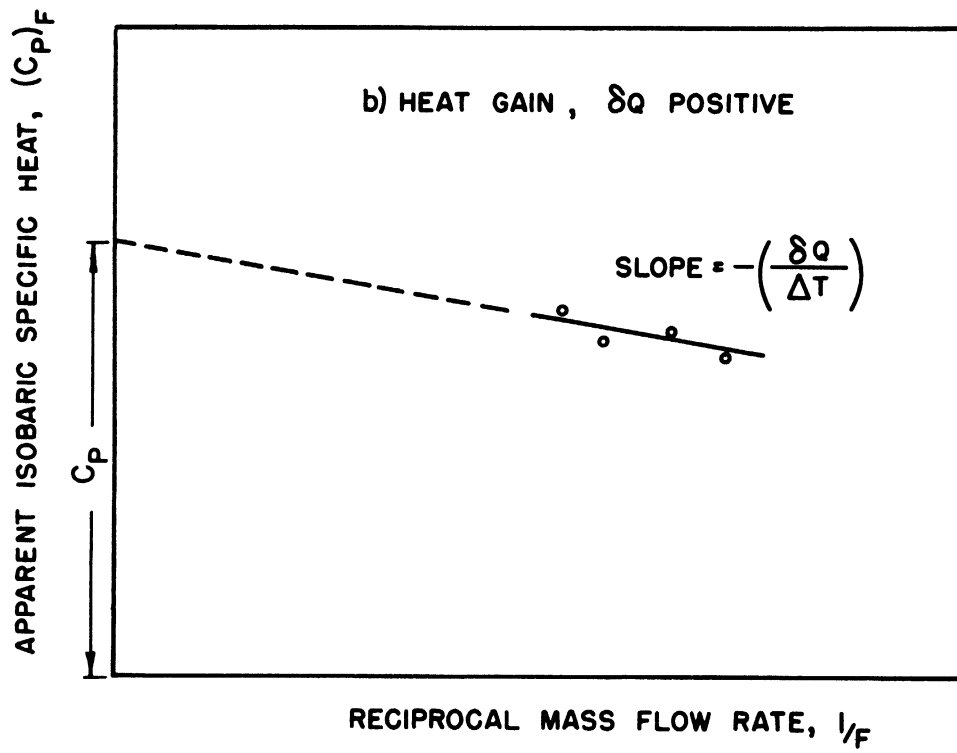
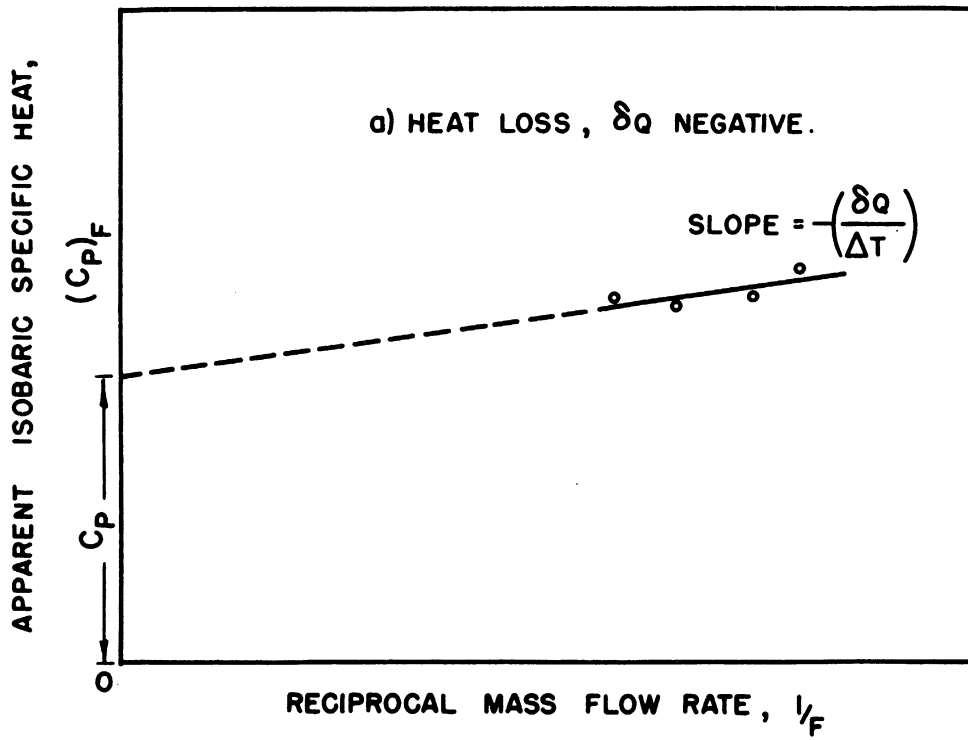


Figure 16. Linear Approximation for Heat Leakage Correction in a Flow Calorimeter

investigation  $\delta Q$  was negative, i.e., a heat loss occurred, since  $C_P$  was less than  $(C_P)_F$  in all cases. The usual convention of signs has been observed. The quantity  $Q$  in Equation (17) is always positive, implying an addition of energy to the system.

It was assumed (for the nitrogen investigation) that a linear plot such as illustrated in Figure 16 was valid. It would have been desirable to test this assumption by employing several flow rates,  $F$ . This was not done, however, in the preliminary nitrogen investigation because of the large amount of time involved in making measurements -- due to poor cooling system operation and other operational difficulties. Only two values of flow rate were used to determine the heat leak correction,  $\delta Q$ . The fact that only two flow rates were used, of course, introduced considerable uncertainty in the determination of the straight line shown in Figure 16, even if the assumption of linearity was valid.

In future investigations it will be necessary to test the assumptions involved in the heat leak correction and attempt to correlate  $\delta Q$  in terms of the significant factors that affect it.

One additional simplification in experimental technique, which was employed, should be pointed out. Because of the time consuming nature of the initial nitrogen determinations, the first order correction  $\delta T$  for the Joule-Thomson effect -- which occurred due to a slight pressure drop in the calorimeter -- was not measured in many cases. The quantity  $\delta T$  was known to be negative (decrease in temperature upon expansion) in the range of the present investigation from the work of Roebuck.<sup>(105)</sup> Thus, a value of  $(C_P)_F$  which was too large was obtained for the cases in which  $\delta T$  was neglected. This had the effect of producing a larger apparent heat loss

in the calorimeter. Measurement of  $\int T$  should take place at the average temperature of a  $C_p$  determination. In the cases in which it was measured (Table XXI) it was measured with the calorimeter at the initial fluid temperature, however. For all cases in which  $\int T$  was measured it was found to be small (maximum 0.3% of  $\Delta T$ ) and negative.

#### Comparison with Literature Values

Table V compares the values of isobaric specific heat of nitrogen measured directly in the present investigation with values calculated from the most recent and complete tabulations of the properties of nitrogen. No direct experimental measurements of  $C_p$  for nitrogen under pressure and at temperatures below about room temperature have been reported. The values obtained from the tables of Bloomer and Rao<sup>(12a)</sup> and National Bureau of Standards Circular 564<sup>(135)</sup> are both based on calculation by means of an equation of state and ideal gas properties.

Bloomer and Rao<sup>(12a)</sup> have tabulated the enthalpy of nitrogen at several pressures from 10 psia to 1500 psia and from temperatures as low as  $-320^\circ\text{F}$  to temperatures as high as  $+500^\circ\text{F}$ . The equation of state employed was a ten constant pressure explicit equation developed by the authors.

The enthalpy data of Bloomer and Rao was first differentiated graphically with respect to temperature to obtain smoothed values of  $C_p$  at a number of tabulated pressures. The values of specific heat, thus obtained, were plotted as a function of pressure at temperatures of  $-50^\circ\text{F}$ ,  $-100^\circ\text{F}$ , and  $-150^\circ\text{F}$  and a smooth curve drawn through the points. Values of specific heat at the pressures of the present investigation were read from the curves and listed in Table V.

TABLE V  
COMPARISON OF ISOBARIC SPECIFIC HEAT DATA FOR NITROGEN WITH LITERATURE VALUES

Nominal Conditions of Cp Determination Temp. °F	Pressure psia	Flow No.	Present Invest. - Btu/lb °F	Bloomer and Rao, Cp Btu/lb °F	N. B. S. Circu- lar 564 Cp, Btu/lb °F	$\left( \frac{\text{Present Invest. - Bloomer \& Rao}}{\text{Bloomer \& Rao}} \right) \times 100$	$\left( \frac{\text{Present Invest. - N. B. S. Circular 564}}{\text{N. B. S. Circular 564}} \right) \times 100$
-50	293.9	1 ]	0.267	.265	0.264	+0.75	+1.14
-50	293.9	2 ]					
-50	587.8	1 ]	0.287	.281	0.281	+2.14	+2.14
-50	587.8	2 ]					
-50	1175.7	1 ]	0.313	.314	0.316	-0.32	-0.95
-50	1175.7	2 ]					
-100	293.9	1 ]	0.270	.271	0.270	-0.37	0.00
-100	293.9	2 ]					
-100	587.8	1 ]	0.304	.298	0.297	+2.01	+2.36
-100	587.8	2 ]					
-100	881.8	1 ]	0.336	.331	0.328	+1.51	+2.44
-100	881.8	2 ]					
-100	1175.7	1 ]	0.346	.366	0.361	-5.46	-4.16
-100	1175.7	2 ]					
-150	293.9	1 ]	0.290	.285	0.287	+1.75	+1.05
-150	293.9	2 ]					
-150	587.8	1 ]	0.349	.349	0.339	0.00	+2.95
-150	587.8	2 ]					

Based on the conclusions of Bloomer and Rao concerning the tabulated enthalpy values it was estimated that all of the specific heats obtained from this source had an accuracy of  $\pm 5$  percent or better.

National Bureau of Standards Circular 564(135) contained the most recent tabulation of the properties of nitrogen. Values of  $C_p$  have been tabulated from 0.01 atmospheres to 100 atmospheres and at temperatures as low as 100°K and as high as 3000°K. A number of the values at low temperature and high pressure were omitted by the authors, however, because it was believed they were of poor accuracy.

A cubic expression in pressure for the compressibility factor was used by the authors of Circular 564 to predict nitrogen behavior. Two of the virial coefficients were determined from an unmodified 6-12 Leonard-Jones function. The third was represented by an empirical equation fitted to PVT data. The constants were adjusted so that PVT data was predicted better at intermediate and higher temperatures - for which the tabulation of Circular 564 was primarily intended. Prediction of low temperature PVT (and other miscellaneous measurements by several investigators) was stated to be relatively poor. The authors of Circular 564 believed that in some temperature and pressure ranges, -- which included several points taken in the present experimental determinations of  $C_p$  -- that the isobaric specific heats tabulated might be in error by as much as 5 or even 10 percent.

Values of specific heat from Circular 564 at -50°F, -100°F, and -150°F were plotted as a function of pressure and a smooth curve drawn through the points. Values of interest at intermediate pressures were obtained from these curves. The curves were extrapolated somewhat to obtain values not reported.

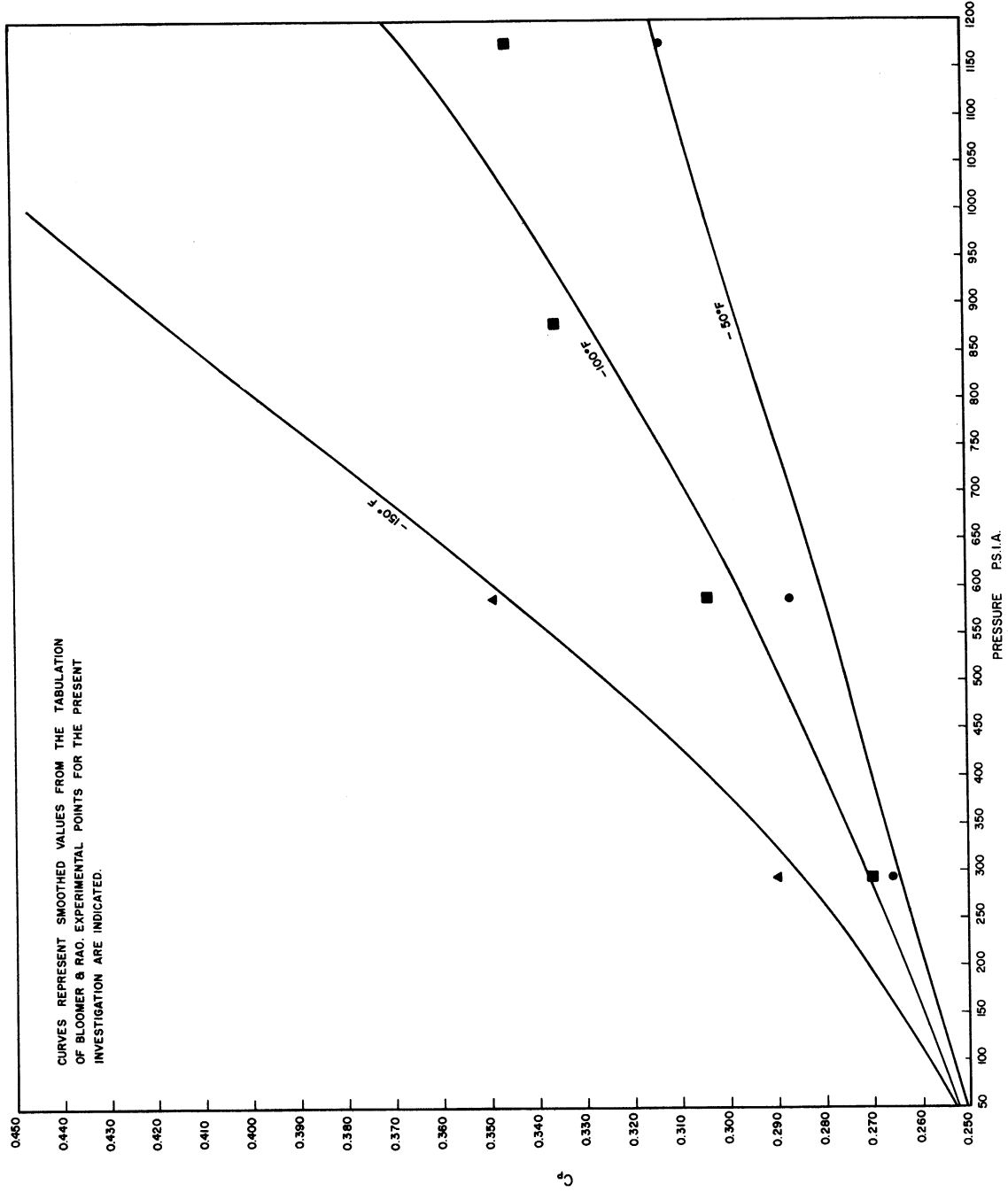


Figure 17. Variation of Isobaric Specific Heat of Nitrogen with Pressure at -50°F, -100°F, and -150°F

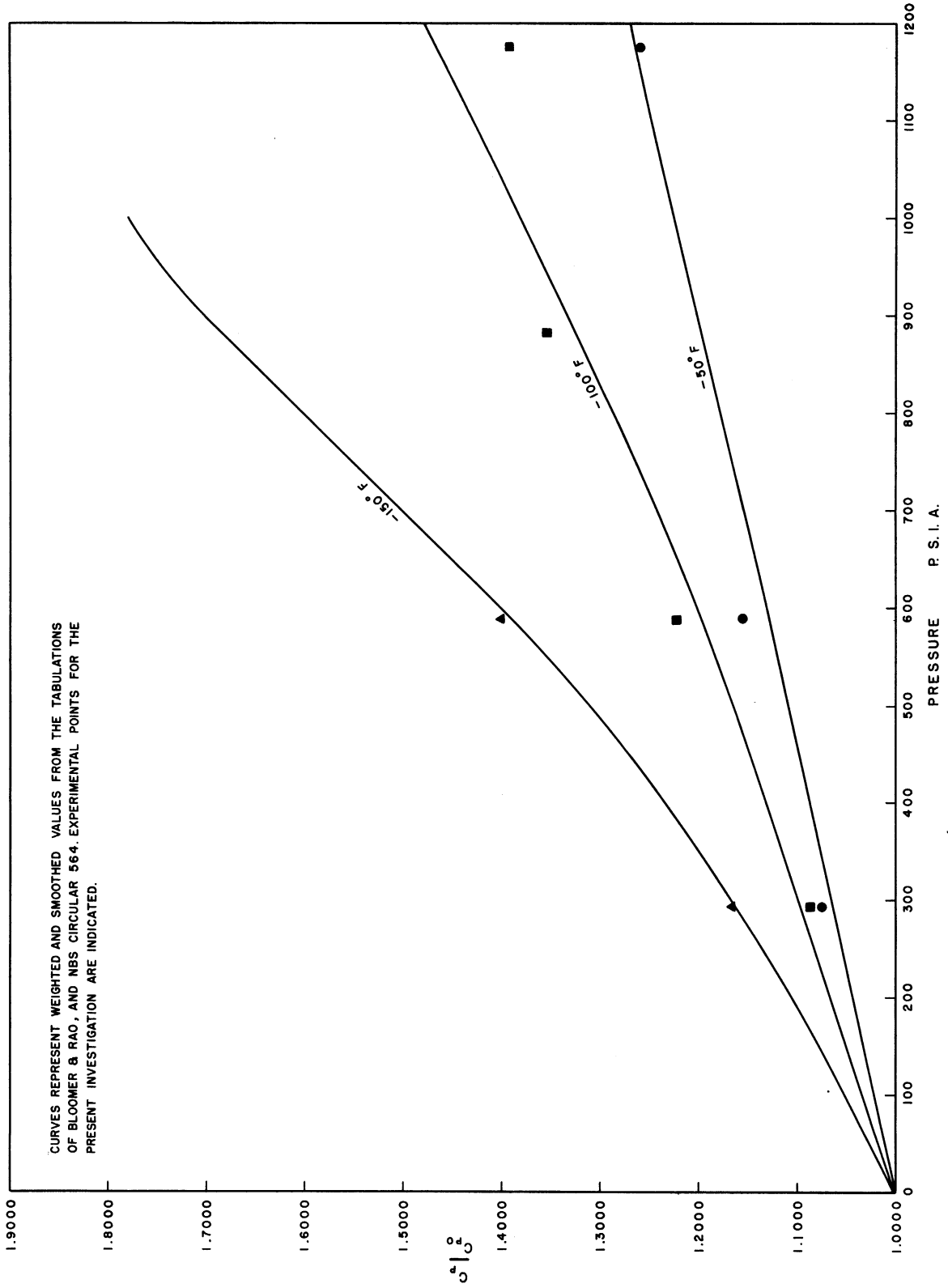


Figure 18. Variation of  $C_p/C_{p_0}$  for Nitrogen with Pressure at  $-50^\circ\text{F}$ ,  $-100^\circ\text{F}$ , and  $-150^\circ\text{F}$

The two tabulations of nitrogen properties discussed are essentially independent in the sense that: the same PVT data was not for the most part used, they were weighted for different ranges of application, and the equations used to represent nitrogen behavior were different.

In view of the agreement between  $C_p$  values from the sources cited and the values determined in the present investigation, it was concluded that the majority of the measured values of  $C_p$  listed in Table V may have an accuracy of 2 or 3 percent. The point at  $-100^\circ\text{F}$ , 1176 psia, measured in the present investigation, was considered to be in error. This conclusion was based on the disagreement with literature values and the unreasonable correction for heat leakage,  $\oint Q$ , which was found for this point.

In Figure 17, the calculated values of  $C_p$  from Bloomer and Rao have been plotted as a function of pressure at lines of constant temperature for the temperatures:  $-50^\circ\text{F}$ ,  $-100^\circ\text{F}$ ,  $-150^\circ\text{F}$ . The values of  $C_p$  obtained in the present investigation are indicated.

Figure 18 shows the variation of  $C_p/C_{p_0}$  as a function of pressure for the temperatures of the present investigation. The curves were drawn using values obtained from both Bloomer and Rae and National Bureau of Standards Circular 564. Since  $C_{p_0}$  did not vary appreciably with temperature in the range of interest, an average value of 0.2484 was used for all temperatures. The experimental points of the present investigation are indicated.

#### Discussion of Results and Consideration of Errors

The comparative values of specific heat for nitrogen from other sources, which were to have served as something of a primary standard, were not thought to be sufficiently accurate for this purpose. It would



have been undoubtedly desirable to have obtained a number of measured values of  $C_p$  at lower pressures and higher temperatures -- where comparative values in the literature are apparently better for nitrogen -- in order to verify overall accuracy.

It is highly probable that the overall accuracy of the nine values of  $C_p$  measured is considerably poorer than the 1% accuracy which had been anticipated. This is thought to be true primarily because of unsteadiness in the system which occurred during the nitrogen measurements and a probable temperature measurement error which is yet to be discussed. The increased heat leakage which occurred due to malfunctioning of the calorimeter insulating vacuum system and inability to operate the isothermal shield were not the primary factors which contributed to uncertainty in the specific heat values obtained.

The fact that the system was frequently unsteady, due to poor cooling system operation, made it impossible to investigate carefully the dependence of the heat leakage correction term,  $\delta Q$ , on the possible variables of importance. It contributed to uncertainty in the uncorrected, apparent values of specific heat,  $(C_p)_F$ , obtained. It also made impractical a careful measurement of the Joule-Thomson correction factor,  $\delta T$ , in Equation (17a).

The temperature measurement error (which has not yet been described) had the effect of increasing the apparent size of  $(C_p)_F$  in Equation (17a) and also the apparent magnitude and uncertainty in the correction term  $\delta Q$ .

It was estimated that with the calorimeter insulating vacuum at the levels indicated in Table IV, the isothermal shield inoperative, and

a rise of 20°F for the fluid flowing through the calorimeter -- that a, heat loss,  $\delta Q$ , amounting to as much as 3 or 4% of the measured heat input,  $Q$ , might occur. A heat loss of only about 1% of  $Q$  was expected on the assumption that the vacuum level and guard operation were satisfactory. This evaluation of heat leaks included heat conduction along the electrical wires entering the calorimeter, radiative heat transfer, and heat transfer by conduction through air in the calorimeter case (Figure 15). Of course, there was considerable uncertainty in some of the heat leaks computed -- in view of the complicated geometry of the problem and the uncertain boundary conditions which were present.

The actual apparent size of the heat leak correction term,  $\delta Q$ , in Equation (17) may be seen from Table IV to have ranged from 2 to 8% of  $Q$  for most cases. A small portion of the discrepancy between the 2 - 8% heat leak which appeared to have occurred and the 2 - 4% estimated heat leak may be attributed to neglecting the term  $\delta T$  in Equation (17) for many of the points reported. Also the uncertainty in  $(C_p)_F$  may have caused some accidentally large values in  $\delta Q$ . Nevertheless, it is difficult to explain the magnitude of the term  $\delta Q$  without assuming that there was some additional factor present. Such considerations led eventually to the investigation of the temperature measurement error previously mentioned, but not described.

The temperature measurement error is believed to have occurred because the thermal resistance to the transfer of heat between the fluid and the two sets of calorimeter thermocouple junctions was an appreciable fraction of the total thermal resistance for heat transfer between fluid at the initial and final temperatures (via the thermocouple wire). Another

contributing factor was probably heat conduction along the two lead wires to the main calorimeter thermocouple.

It can be easily shown that the heat transfer by conduction between the two sets of junctions of the main calorimeter thermocouple via the interconnecting electrical wire was very small -- a few thousandths of a percent of the measured heat addition in the calorimeter,  $Q$ . Nevertheless, the difference in temperature of the junctions need not be the same as the temperature difference of the fluid being measured if certain thermal resistances are high.

We will designate the thermal resistance between calorimeter inlet fluid at temperature  $T_1$  and the inlet junction of the main calorimeter thermocouple  $R_1$ ; the thermal resistance to heat conduction between the inlet and exit junctions we will call  $R_2$ ; the thermal resistance between the calorimeter exit fluid at temperature  $T_2$  and the exit thermocouple junctions we will refer to as  $R_3$ . The true temperature difference of the calorimeter fluid,  $T_2 - T_1$ , will be designated  $\Delta T$  and the temperature difference of the two sets of junctions,  $T_2' - T_1'$ , we will designate as  $\Delta T'$ . The additional problem of heat conduction along the lead wires to the thermocouple will be ignored.

It may be shown that for the conditions stated the percentage error in  $\Delta T'$  (which was taken to be equal to  $\Delta T$  in the calculation of  $C_p$ ), was:

$$\frac{\Delta T' - \Delta T}{\Delta T} \times 100 = \frac{R_1 + R_3}{R_1 + R_2 + R_3} \times 100 \quad (18)$$

It was shown, neglecting all thermal resistances contributing to the sum  $R_1 + R_3$  except that due to the convective resistance between the

fluid and the thermocouple wells, (Figure 21), that the error described was significant. For an estimated heat transfer coefficient of  $6 \frac{\text{Btu}}{\text{Hr-Ft}^2-\text{F}}$  between the thermocouple wells and the fluid the error was computed to be about 2% of  $\Delta T$  ( $\Delta T' < \Delta T$ ). The sign of the error was such that the apparent size of the heat loss in the calorimeter was increased. As explained, this estimate neglected other contributing factors.

Physically, this problem may be eliminated for future investigations rather simply by increasing the resistance term,  $R_2$ , in Equation (18) (increasing the distance between thermocouple junctions) and by a procedure of "tieing down" the thermocouple wires thermally (described in "Future Work").

An attempt to find a completely systematic variation in the corrective factors  $\delta Q$ , in Table IV verified the uncertainty in the values of  $\delta Q$  and the assumption that many factors affected them. It was not possible to predict values of  $\delta Q$  based on the experience of Table IV. Summarizing the several factors which resulted in the unpredictability in  $\delta Q$ :

1. Variations in vacuum level occurred during the measurements. At the vacuum levels present, appreciable variability in heat conduction through air in the calorimeter occurred.
2. The assumption was made that  $\delta Q$  could be obtained from a linear extrapolation of  $(C_p)_F$  versus  $1/F$  (Equation 17a) and this proposition was not tested.
3. The values of  $(C_p)_F$  obtained may have been relatively poor because of poor cooling system operation.

4. The Joule-Thomson correction factor,  $\delta T$ , was not determined for all runs; this altered the apparent size of  $\delta Q$ .
5. An error in measuring  $\Delta T$  showed up in the term  $\delta Q$ .

An estimate was made of the maximum accidental errors which could have occurred in measuring the important variables for determining isobaric specific heat. The analysis is given in Appendix A of the thesis. The results of this analysis are shown in Table VI.

TABLE VI  
ESTIMATE OF MAXIMUM MEASUREMENT ERRORS

Variable	Maximum Percentage Uncertainty
Measured energy addition, $Q$	0.1
Mass flow rate, $F$	0.7
Temperature rise of the fluid, $\Delta T$ (For 20°F increment)	0.3

Since the errors in Table VI are assumed to be random, a simultaneous occurrence is thought to be highly unlikely.

It was estimated that for the following conditions:

1. A heat leakage,  $\delta Q$ , of 1 to 2 percent of  $Q$  (estimated for a vacuum level of 1 micron of mercury in the calorimeter, an operative radiation shield)
2. An uncertainty in  $\delta Q$  of 0.2 percent (estimated on the basis of  $\delta Q$  being 1 to 2 percent of  $Q$ )
3. A simultaneous occurrence of the maximum errors listed in Table VI.

the maximum error in  $C_p$  would be 1.3%. The estimate was made by adding the absolute values of the error terms.

## RECOMMENDATIONS FOR FUTURE WORK

On the basis of the experience which was gained during the design, construction, and operation of the flow system, the need for certain improvements in the equipment and techniques employed have become apparent. Some of these changes should be accomplished prior to the initiation of the study of light hydrocarbon properties. Some can be accomplished simultaneously with this program.

It will be necessary to improve the present cooling system operation. This can be done best by installing a constant temperature bath pre-cooler, scrapping the liquid nitrogen cooler, and doing away with a number of the valves and lines which contribute to a large heat gain in the present cooling system. The constant temperature pre-cooling bath could be constructed along the lines of the present constant temperature bath; however, automatic temperature control may not be necessary.

In replacing the main calorimeter thermocouple, which failed, the distance between the junctions should be increased considerably to lessen heat conduction between them. The thermocouple should also be "tied down" thermally at each end, to a surface at  $T_1$  and one at  $T_2$ , to eliminate heat leakage from or to the junctions.

The present calorimeter vacuum level must be improved. This can be done by finding a suitable ceramic or bonding agent seal for the calorimeter heater leads. The present vacuum line to the calorimeter can also be shortened somewhat and at least one unnecessary valve removed.

The construction of mechanically improved difference thermocouples will make possible the consistent operation of the calorimeter isothermal shield. It will be possible to eliminate a number of the difference thermocouples on the basis of the findings which were made concerning potential heat leaks -- and thus reduce conductive heat transfer through lead wires to the calorimeter.

It would be worthwhile to study the present flow metering method for the purpose of improving a source of considerable inaccuracy. If the present scheme is used in the future, the meter should be recalibrated with a different gas to verify the constants in the metering equation. A high pressure manometer should also be installed to measure the metering pressure in this case. It may be desirable to consider installation of a gasometer or similar device, however. In this case it would be necessary to supply the compressor from a constant pressure reservoir or by means of pressure regulation during the time in which flow is being diverted.

It is considered highly desirable to conduct additional measurements on nitrogen or air in the lower pressure, higher temperature range -- where their properties are better known -- in order to obtain a good estimate of the overall accuracy of the equipment performance.

Installation of barostats or pressure control in the system may be desirable, particularly for Joule-Thomson measurements.

It would be desirable to calibrate or at least check the potentiometer used in the system.



Before isobaric integral latent heat measurement can be initiated the present power supply will have to be enlarged and the calorimeter heater and power measurement circuit modified to handle the larger loads. The flow rate in the system may be decreased for isobaric latent heat measurements (by a factor of about 3 in comparison with flow rates used in specific heat measurements). The estimated maximum power requirement would then be 200 watts.

The Joule-Thomson throttle is essentially ready to be operationally tested. It will be necessary to procure a new set of calibrated weights for the pressure balance, however, in view of the state of the present ones. The pressure balance should be tested against the high pressure mercury manometer at the University of Wisconsin.

## SUMMARY AND CONCLUSIONS

1. A flow system was designed and constructed which incorporates the necessary features for determining several of the thermodynamic properties of gases and liquids at low temperature and high pressure. The system was designed to operate at pressures as high as 2500 psia and at temperatures from 70°F to -280°F.
2. Thorough consideration was given to the design and construction of a flow calorimeter and a Joule-Thomson expansion device.
3. Calibration and preliminary testing of the equipment was accomplished.
4. Isobaric specific heat measurements were made on nitrogen at pressures as high as 1176 psia and temperatures as low as -150°F.
5. Experimentally measured values of the isobaric specific heat of nitrogen showed agreement, generally, of 2% or better with values obtained from the literature.
6. It was concluded that, with slight modification of the equipment, future measurements of isobaric specific heat of an accuracy better than 1% are possible.

APPENDIX A

## DESIGNING THE FLOW SYSTEM

In the overall design of the flow system it was necessary to consider simultaneously a number of factors of importance and their relationships. In view of the anticipated measurement of several different thermodynamic properties over a wide range of conditions, a great deal of flexibility of operation had to be provided and provision had to be made for the accurate measurement of a number of variables.

A study was made of the problems affecting the maintenance of steady conditions at the calorimeter and expansion device. This involved considering means for controlling the supply of fluid to the calorimeter or expansion device as well as the matter of temperature control in the system.

The total cooling requirements and the time required to cool the system by circulation of fluid was an important factor in the overall design problem.

Thorough consideration was given to the problem of selecting the magnitude of the important measured variables for both calorimetric determinations and isenthalpic expansion. The selection of a maximum flow rate in the system is discussed separately, see Sizing the System, page . . . . . The selection of the magnitude of the other measured variables including pressure and temperature changes and calorimeter heat input is presented in conjunction with the important problem of methods for measuring the variables and the accuracy of these measurements. Methods considered for measuring flow rate in the system are also considered in this discussion.

An additional matter which is not included in the discussions which follow is the problem of maintaining a desired combination of flow rates and pressures in the system, having specified the various heat inputs and heat removals in the system and essentially the temperature profile through the system. It was concluded that a reasonable combination of pressures and flows at the calorimeter or expansion device could be obtained in a closed flow cycle, operating with a constant speed compressor, by adjusting various flow resistances (valves) including a recycle flow resistance to the compressor suction, and varying the total fluid content of the system. In this process, it is necessary to allow a small range in compressor suction pressures (and hence flow metering pressure) in order to arrive at a satisfactory combination of the other system variables. This was demonstrated by considering the number of variables necessary to describe the steady state operation of the system and the number of mathematical restrictions relating them.

Maintenance of Steady Conditions at the  
Calorimeter and Joule-Thomson Throttle

Accurate determinations of specific heat or isenthalpic expansion cannot be made unless experimental conditions are quite steady. For flow calorimetry and Joule-Thomson work, this infers:

1. A constant input of material into the system before the calorimeter or Joule-Thomson throttle.
2. A constant cooling and heating of the material as it flows through the system.
3. A maintenance of constant temperature at the calorimeter or Joule-Thomson throttle.

Item one is included in the discussion that follows. A brief discussion of various overall cooling system designs begins on page . . . . . The low temperature bath in which the calorimeter was located is described in Detailed Equipment Design and Description, Appendix A.

#### Flow Rate Control

A number of schemes have been used for controlling the rate of flow of the fluid in direct flow calorimetry. However, not all of these methods are applicable over a range of pressures, or where mixtures are involved.

Typical of one scheme used by several investigators engaged in flow calorimetry of pure gases: controlling the rate of evaporation of the liquefied fluid in a vessel and then utilizing a series of manual and/or automatic control valves for refinement. Among these investigators are Osborne, Stimson and Sligh<sup>(78)</sup> whose very elaborate work at the National Bureau of Standards is an excellent example of this method. In their work on ammonia to twenty atmospheres they used a constant-evaporation vessel and three motor-operated valves to control the pressure in their calorimeter. Valve motor operation was initiated by electrical contacts in a manometer, one side of which was held at a variable reference pressure, while the other side was connected into the calorimeter supply line. The gas leaving the calorimeter was throttled to a lower pressure and then passed through one of several orifices. The downstream pressure from the orifices was controlled roughly by the temperature at which condensation of the ammonia took place for the purpose of weighing. The orifices were operated at critical flow. They were chosen so that with the downstream pressure at

a sufficiently low value the desired flow rate could be obtained at an orifice up-stream pressure of from one to three atmospheres. At calorimeter pressures above three atmospheres, a throttling valve before the orifices controlled flow.

Use of a controlled evaporation procedure is not applicable to mixtures and it poses severe problems for pure substances of very high volatility. The method of operation for the control valves used by Osborne, Stimson, and Sligh and the possibility of using orifices in the system were of interest.

Schrock<sup>(123)</sup> supplied carbon dioxide to a calorimeter from a bank of high pressure cylinders which were heated to compensate for removal of gas. The carbon dioxide was throttled and the pressure at the calorimeter controlled by means of automatic pressure regulators. The flow rate in the system was varied by means of a manually operated high pressure needle valve. A constant pressure reservoir (gasometer) was installed after the calorimeter. This served the dual function of maintaining a constant reduced pressure reservoir and providing a measure of the flow rate in the system.

The method used by Schrock would have been applicable to the present investigation in conjunction with open system operation. Complete open system operation (without re-supplying the source of flow) has the disadvantage of limiting the length of operating time, at relatively large flow rates. Also, unless the material is cheap and can be discarded, a recovery is necessary.

Another scheme for insuring constancy of flow in a closed flow system was employed by Roebuck in his Joule-Thomson work with porous

plugs. (95, 96, 102) Roebuck's system contained a gas compressor. He was able, by bleeding material from the flow system and varying the amount of bleed above and below the porous plugs, to obtain a very constant condition of flow. The amount of bleed was varied to maintain constancy of pressure by means of automatically-operated barostats. These barostats consisted of pistons under load which floated on the system, moving up and down with pressure fluctuations. The motion of the pistons was used to vary the direction and operation of motor-operated valves which controlled the amount of bleed.

It was decided after considering various possible solutions to the problem of providing steady flow to the calorimeter and Joule-Thomson throttle, that the use of a compressor in a closed flow-cycle would offer a number of advantages. Furthermore, it was decided that steadiness of flow could be promoted by damping the system; that is, by making the total volume of the system large in comparison to the rate of flow of fluid through it. This could be done it was thought by floating high pressure cylinders on the system.

Consideration was given to the use of a liquid pump instead of a compressor, but this possibility was rejected. The materials to be studied were gaseous or of fairly low density near room temperature. Since much of the work was to be done in the superheat or relatively low-density regions, a good deal of unnecessary cooling would be involved in reaching suitable densities for pump operation. Furthermore, the pump would have to operate under very difficult mechanical conditions.

The procedure of using a compressor in a closed flow cycle together with system damping, has the following advantages:



1. A relatively large flow rate can be used without the problem of re-supplying the source of flow, occurring in open system operation.
2. A good compressor operates for long periods of time in a relatively steady manner without attention.
3. The rate of flow through a calorimeter or Joule-Thomson throttle may be varied rather easily over a wide range of flow rates by recycling.
4. A high degree of stability of the calorimeter or Joule-Thomson throttle can be obtained by a procedure of damping the system; the degree of damping can be easily varied by adding or removing volume from the system.

It should be pointed out that the scheme for providing a steady flow of fluid, as described, represented an intentional simplification. It was thought desirable to include additional flow control in the form of automatic valves. It was decided, however, that this should be done - if necessary - after the equipment had been operated.

The Total Cooling Requirements of the System and the Time Required to Reach a Condition of Steady State Operation

Factors which were considered in designing the cooling system included:

1. Flow rate in the system.
2. Temperature and pressure range of operation.
3. Total heat capacity of the cooling system.
4. Heat capacity of that portion of the system cooled only by the flow of gas.

5. Efficiency of the cooling operation.

Several different cooling system designs were studied.

Building a Continuous Piece of Refrigeration  
Equipment Using an Air Compressor

Consideration was given to the possibility of using an air compressor to produce large quantities of high pressure air which could then be cooled and expanded to produce the required heat sink. Using such a system, it would have been possible to handle a wide range of cooling requirements by varying the amount and/or degree of expansion of the air. Furthermore, the cooling system would have been continuous in operation with no problem of "batchwise" coolant supply.

It was possible to obtain an air compressor from two different sources at no cost to the project. Physical space requirements, cost of installation, and additional system complexity were considered as negative points, however.

The Cooling and Expansion of High Pressure  
Air Obtained Via a Pipeline to the  
University of Michigan Wind Tunnel Facilities

It was ascertained that, for considerable lengths of time, relatively unlimited sources of high pressure air were available from tanks pumped up at the Aeronautical Engineering facilities for wind tunnel operation. The required air supply for the proposed cooling system would not have appreciably affected, over long periods of time, the extremely large supply at these tanks. A proposal was made that the University install a high pressure air line from the Aeronautical facilities for a distance of about 1000 feet to the Automotive Engineering

Building. Other people at the Automotive Engineering Building were interested in the proposed 2500 to 3000 psi air service. Unfortunately, the project had to be abandoned when the University refused to absorb the cost of such a pipeline.

#### Purchase of a Package Refrigeration Unit

The possibility was briefly considered of buying a package cooler to provide absorption of the required heat. This was never investigated in great detail as a probable cost in excess of 5000 dollars was estimated.

#### Batch Cooling Employing Ice, Dry Ice, and Liquid Nitrogen

This method was eventually adopted for providing the system refrigeration. The main factor which made such a scheme practicable was the availability of liquid nitrogen in large quantity as a coolant at an extremely low price. The Mechanical Engineering Department operated 25 liter per hour liquid nitrogen machine was the potential source of the liquid nitrogen. The physical proximity of this machine to the location of the low temperature hydrocarbon project added to the advantage of low cost, by allowing continuous filling and transferring of metal Dewars during operation of the low temperature calorimetric system, by project personnel. Furthermore, large storage facilities for liquid nitrogen were available, including a 250 liter machine capacity and a 550 liter auxiliary storage capacity, so that a considerable inventory could be built up. A number of fifty liter metal Dewars were available for liquid nitrogen storage in test cell 247 during operation of the equipment.

By employing ice, dry ice, and heat exchange with the fluid leaving the low temperature bath, it was possible to both supply the necessary cooling for intermediate level low temperature work without using liquid nitrogen and conserve liquid nitrogen during very low temperature operation.

A number of alternate paths for flow of the fluid through the cooling system were provided in order that

1. All of the cooling steps would be available regardless of the low temperature bath operating temperature.
2. A number of fluid streams at different temperatures could be mixed in order to approach the desired operating temperature very closely.

#### Sizing the System

The problem of sizing that will be discussed at this time is the overall problem of deciding on a maximum and an average flow rate through the calorimeter and Joule-Thomson throttle. There are a number of factors which bear on this choice. Among those that the author considered are:

1. The effect of magnitude of flow rate on the system cooling requirements.
2. The effect of magnitude of flow rate on accuracy of measurement of flow rate in calorimetric measurements.
3. The effect of magnitude of flow rate on the amount of precisely regulated and controlled power required in specific heat and latent heat measurements.

4. The heat leakage in the calorimeter and the Joule-Thomson throttle.
5. The heat capacity of the calorimeter and Joule-Thomson throttle.

Item one above required calculation of the cooling requirements for various flow rates at the lowest temperature of operation which was anticipated. It also involved a study of various ways for providing this cooling and the cost and complexity or inconvenience of each. Methods considered are discussed on page 111. In general, the availability of large quantities of liquid nitrogen at a low price simplified this problem considerably. The system cooling requirement, although of considerable concern, was not the limiting factor in establishing flow rates in the range of flow rates considered.

Item two above is discussed in connection with methods considered for measurement of flow rate. In general, a sacrifice in metering accuracy by direct weighing (which is more advantageous in a volatile system at low flow rates) was made by specifying a relatively high flow rate.

Item three above was found to be only a slight restriction for the purposes of the present investigation. It would have been possible to select a variety of heat inputs to the calorimeter without being seriously limited by power supply characteristics or cost. For flow calorimetry of an accuracy of the order of 0.1 percent this problem would be much more important, see page 122.

In view of the anticipated measurement of Joule-Thomson throttling, Item four determined the precise maximum flow rate for the system.

This is true because in a conventional measurement of integral isenthalpic throttling an appreciable heat leakage is almost unavoidable (see Detailed Equipment Design and Description, Joule-Thomson Throttle, Appendix A).

For an expansion device of a given physical size and design a maximum heat leakage can be estimated. The magnitude of heat leakage which occurs during measurements cannot be determined with reliability, however.

Therefore, it was desirable to specify a maximum system flow rate which was large enough to make such effects inconsequential.

Estimates were made of the heat leakage expected for a selected calorimeter geometry and set of operating conditions. These estimates provided the necessary information to show that for a given fluid temperature rise in the calorimeter, selected essentially independently, that a satisfactory range of flow rates would fall within the limit imposed by isenthalpic measurements.

In addition to the prevention of heat leakage by various mechanisms, a certain degree of size reduction in the flow calorimeter and Joule-Thomson device was attempted in order to lessen heat leakage - and hence flow rate requirements. In general, however, a scaling which would have resulted in a very meticulous job of constructing pressure seals, installing electrical windings, or temperature measuring devices was avoided.

Item five above was not found to be a limiting factor although considerable effort was expended in reducing the heat capacity of the flow portion of the calorimeter, in order to lessen the time required to reach a steady state; see Detail Equipment Design and Description, Specific Heat Calorimeter, Appendix A.

Accuracy of Measurement of the Several  
Problem Variables; Selection of Magnitude  
of the Variable and Method of Measurement

In a multivariant problem, the percentage accuracy required of the several variables depends on the percentage accuracy with which the final result must be known and the sensitivity of the final results with respect to the individual variables.

Specific Heat Measurements

The accuracy goal set for specific heat measurements was one percent. After a study of the three primary measurements necessary for determining isobaric specific heat, it became apparent that measurement of mass flow rate would be the most difficult. It was felt that, relative to the overall one percent accuracy of specific heat measurements anticipated, the total heat input to the fluid and the temperature change of the fluid passing through the calorimeter could be measured accurately with a minimum of difficulty. The latter statement anticipated, of course, the ability to obtain the necessary degree of system stability. The majority of the one percent overall accuracy margin was reserved for inaccuracy in flow metering and corrections for the various heat leaks.

The problem of the size of the major individual variable with respect to the desired percentage accuracy was given special consideration. The flow rate problem was considered in conjunction with the overall problem of sizing the system. In order to simplify the design of the calorimeter, it was deemed desirable to plan on operating the calorimeter at relatively high flow rates at a sacrifice in metering accuracy which would have been obtainable by direct weighing at lower flow rates.

The size of the average temperature increment was selected after considering its effect upon heat leaks in the calorimeter, problems of temperature equalization after addition of heat to the fluid, rate of change of specific heat with temperature, and the accuracy of measuring instruments. Accurate power measurements, it was felt, could be made over a wide range of power inputs; therefore, the size of power input was determined largely by specifying the other two principle variables and knowing the approximate range of isobaric specific heats for the light hydrocarbons.

Mass Flow Rate, F.--In general, mass flow rate does not appear to be susceptible to any really accurate means of measurement other than a direct weighing procedure, or possibly a direct low pressure volume measurement. The possibility of using a direct weighing procedure was given consideration.

The principal reasons that a weighing procedure was not used were the following:

1. The use of a compressor in the system and the relatively high rate of flow anticipated made the system more amenable to a close cycle operation. By returning the gas to the compressor, it was relatively easy to obtain a steady compressor operation. Supplying the compressor for any period of time from a controlled reservoir is somewhat more difficult, although by no means unmanageable.



2. Equipment for accurate direct weighing is very complex and costly, especially if high flow rates and high volatilities are considered.

If a direct weighing method had been used (with a compressor in the system) the scheme followed would probably have been the following: The system would have been brought to steady state using the closed flow cycle. The flow from the low temperature bath would then have been diverted to a spare weighing vessel and a controlled reservoir opened to the compressor supply tank. After re-establishment of steady state, the flow would have been diverted very quickly to the weighing vessel which was to be used. Upon completion of one measurement, the flow would have been temporarily channeled back into the system until operating variables had been changed and a steady condition once again obtained.

In addition to the inconvenience of such a procedure, the problems of obtaining an accurate measure of the flow rate during the weighing period are formidable. The material would have to be condensed at very low temperatures for a sufficient length of time to reduce the effect of the probable timing error. Due to the relatively high flow rate anticipated for the system, a large mass of fluid would be collected during this time interval. If this very volatile material were allowed to come to room temperature in order to be weighed, the pressure in the weighing vessel would be tremendous. The weight of a vessel capable of safely withstanding the resultant pressure would be such that it would prejudice the accurate determination of the sample weight, even using the tare method.

In order to evaluate the direct weighing method it was necessary to consider the following:

1. The automatic valve and timing circuit which would be necessary and the cost for a given timing accuracy.
2. Design of the weighing vessel.
3. The weighing balance which would be necessary.

Components of the timing circuit would probably have included equipment for generation of a very constant frequency AC signal, a synchronous-interval timer, and the necessary mechanical and electrical components to actuate the automatic valve. A weighing balance of very high accuracy under high loads would be necessary. The weighing vessels would have to be carefully designed from the standpoint of internal vessel volume, total weight, and safety at low temperatures.

Some consideration was given to the possibility of using a gasometer, but the general inconvenience of open system operation - even for a short period of time - made such a scheme unattractive. An additional problem that was considered was the uncertainty involved in correcting for the partial pressure of the confining fluid.

The conclusion was reached that the increase in metering accuracy which might be obtained by direct weighing or the use of a gasometer, in comparison with a flow metering technique, would not compensate for the additional mechanical difficulties or costs involved - for the overall accuracy of  $C_p$  measurements sought (1 percent).

Measurement of Temperature Difference,  $\Delta T$ .--It was decided on the basis of the rate of change of specific heat with temperature for the light hydrocarbons, consideration of heat leakage in the calorimeter, and the experience of previous investigators (67, 78, 126, 136) to select 20°F as an

average  $\Delta T$  for design purposes. The two methods considered for measuring this temperature increment were platinum thermometry and the use of a thermocouple.

It was believed that the use of platinum thermometers to measure the inlet and outlet fluid temperature in the calorimeter or their difference directly would result in a greater ultimate (percentage) accuracy for a temperature increment as large as 20°F, provided an adequate measuring instrument was employed in conjunction with the platinum thermometers. Very small temperature differences might be measured more accurately, it was thought, by the use of thermocouples. It was felt that, although a high degree of accuracy was attainable and desirable in the measurement of  $\Delta T$ , it was not compatible with the overall system design to seek the ultimate accuracy that could be reached with platinum thermometry. The installation of platinum thermometers in the calorimeter represented a more difficult mechanical problem and a much more expensive solution to the problem. Osborne, Stimson, and Sligh<sup>(78)</sup> and other investigators at the National Bureau of Standards<sup>(126,136)</sup> had demonstrated that copper-constantan thermocouples are capable of measuring a  $\Delta T$  of 20°F in calorimetric work with an accuracy of 0.2%.

Copper-constantan was selected for the calorimeter and Joule-Thomson thermocouples because of its wide usage in the low temperature range and hence its well known properties. Certain other base-metal thermocouple materials produce greater electromotive force, however. To increase the size of the emf being measured and, therefore, lessen the measuring instrument requirements, a multiple junction thermocouple was constructed.

The number of junctions was selected on the basis of physical space requirements in the calorimeter, accuracy of the measuring potentiometer, and to some extent the magnitude of the heat leakage between the two sets of junctions by conduction along the interconnecting wires. It was anticipated that six junctions would produce about 2,000 microvolts for a 20°F increment and that this emf could be measured with almost negligible error using the Leeds and Northrup K3 potentiometer which is described in Detailed Equipment Design and Description. The use of several thermocouple junctions was also advantageous from the standpoint of averaging spurious emfs due to inhomogeneity or strains in the thermocouple wire.

#### Power Measurement

The supply of electrical power for flow calorimetry and its measurement is normally perhaps the most straightforward of the several problems encountered. Accurate measurement requires standard resistors; however, the potentiometer need not be an expensive one.

Traditionally, the source of current for precision calorimetric work has been long-life wet cells. This has been true for these reasons:

1. A preference by investigators for DC current because of the ease with which accurate power measurements can be made.
2. The excellent voltage stability of the cells after an appropriate warm-up period and under limited load conditions.
3. Simplicity of use.

The use of batteries was considered in the present investigation but rejected because the large power requirement anticipated was

inconsistent with a reasonable use of batteries, from the standpoint of number of cells, size of the cells, recharging problem, and cost. Instead, it was decided that a good electronically regulated DC power supply would provide sufficient voltage stability for the purposes of the present investigation. It was estimated that for specific heat measurements at the maximum flow rate and maximum  $\Delta T$  of the fluid which would be used, that 60 watts would be adequate for all but measurements very close to the critical point and that measurement of the power with an accuracy of about 0.1% could be expected.

Important considerations in selecting the power supply were power supply voltage, load regulation and maximum ripple. The power supply voltage was chosen on the basis of operating temperature of the calorimeter heater and physical space required for the heater.

#### Joule-Thomson Measurements

No definite accuracy level was established for the Joule-Thomson measurements. It was felt that the attainable accuracy would be largely contingent upon the steadiness of the high and low pressure, before and after the porous plugs, and upon the relative magnitude of heat leaks.

The two primary measured quantities for Joule-Thomson work are a temperature difference,  $\Delta T$ , and a pressure difference,  $\Delta P$ . It was thought that isenthalpic curves should be measured by expanding from a fixed initial pressure and temperature to successively lower pressures. Using this procedure all but the initial pressure increments would be reasonably larger. The size of the increments would depend upon the curvature of the particular isenthalp.

The uncalibrated Leeds and Northrup K3 potentiometer which was to be used for measurements of thermocouple emf has an accuracy in the range of thermocouple measurements of about one microvolt. It was estimated that if a twelve junction difference thermocouple was employed that the minimum voltage measurement -- corresponding to a pressure increment of 100 psi would be approximately 600 to 800 microvolts. The potentiometer error would then be less than 0.2%. The overall  $\Delta T$  error for the minimum pressure increment was estimated as 0.4%. Because of the limit on thermocouple resistance imposed by a sensitive galvanometer, heat leakage along the thermocouple wires, and mechanical complications, twelve junctions were considered to be about the maximum which should be used. The accuracy of measurement of  $\Delta T$  for the larger pressure increments, it was felt, would be contingent upon the particular thermocouple and its calibration.

Difficulties which might arise for larger temperature increments due to heat leakage were considered. It might be necessary to shift initial temperature and pressure conditions and limit the size of the temperature increments. This would be dependent upon the design of the Joule-Thomson device. This instrument, although constructed, was not operationally tested in the present investigation.

In order to measure the pressure increments accurately over a wide range of size and at varying static pressures it was concluded that a differential dead weight pressure balance would be the most satisfactory solution. A high pressure manometer was considered to be out of the question unless a different operating procedure was employed, i.e. successive expansion with small pressure increments and shifting initial conditions. A high pressure manometer had been used by Roebuck<sup>(98)</sup> for measuring large values of  $\Delta P$  under high static pressures, but the construction of such a manometer would have been a tremendous undertaking. Bourdon tube gauges were felt to be too inaccurate for the purpose, even with differential gauges.

Fortunately, this problem was solved when Dr. Roebuck offered to make available to the author the pressure balance used in his earlier Joule-Thomson work. It was felt that an accuracy of 0.1% to 0.2% could be obtained in the measurement of  $\Delta P$  with this instrument for a pressure increment not smaller than 100 psi.

The measurement of  $\Delta T$  for the expanding fluid depends upon a consideration of the size of the pressure increments. It was estimated that the minimum Joule-Thomson coefficient which would be encountered (for the light hydrocarbons) would be about .03°F/psi to .04°F/psi. For a minimum pressure increment of 100 psi this would correspond to a minimum temperature increment of 3°F to 4°F. (On the other hand, the temperature increments may become quite large.) The decision was made to use a multiple junction copper constantan difference thermocouple for determining  $\Delta T$ . The reasons for using a copper-constantan thermocouple in lieu of platinum thermometers has been discussed on page 121.

1. Suction pressure: 4.1 to 6.8 kilograms per square centimeter.
2. Maximum allowable discharge pressure: 170 kilograms per square centimeter. (Each stage is equipped with a pressure gauge and a relief valve.)
3. Fly wheel angular speed: 360 rpm.
4. Capacity: by actual test, 1.63 cubic meters per hour at 6.1 kilograms per square centimeter suction pressure.

The three stages of the compressor are in line, on the same piston rod. The first stage is located between the second (adjacent to the drive mechanism) and the third stage at the opposite end of the compressor. The third stage seal is made by a stuffing box having metallic ring packing; the other two stages are made gas-tight by the piston rings. The piston rod itself is sealed by a multi-part stuffing box with metallic ring packing. The inner-most of the packing makes the tight joint while small quantities of gas which pass through are caught by an oil-ring in the outer packing and led out through a sight glass containing oil. The valves in the compressor are of a simple plate type.

Lubrication of the piston is provided for by a Bösch lubricator which pumps oil from a reservoir. A very special oil was used which had tenacity, the property of emulsifying with water and good spreading properties. An oil separator integral to the compressor has a capacity of two liters.

The drive mechanism of the compressor consists of a fly wheel 710 millimeters in diameter by 80 millimeters in width, a crankshaft with



## DETAILED EQUIPMENT DESIGN AND DESCRIPTION

The purpose of this section is to present, for the benefit of investigators specifically interested in the measurement of thermodynamics properties, a detailed description of some of the experimental techniques employed in the present investigation.

A description or discussion is given of several of the individual pieces of equipment in the flow system, including the calorimeter and Joule-Thomson expansion device. This presentation, while far from complete, is thought to be sufficiently detailed to answer most of the questions which might arise concerning method or equipment.

### Höfer Compressor

The compressor used in this investigation was an Andreas Höfer custom-made apparatus, designed according to the author's specifications. The machine was built in Germany and purchased through the Autoclave Engineers Sales Corporation of Erie, Pennsylvania, representatives for Höfer in this country. It was purchased in preference to several American-made compressors which were investigated. After comparing data on various compressors and consulting with people who owned them, it became apparent that in a laboratory-size compressor, a compressor of German make, Höfer, was superior to any made in the United States. This evaluation included: (1) Price, (2) Operating characteristics, (3) Quietness of operation, (4) Workmanship and dependability, (5) Delivery time, (6) Replacement of parts and maintenance.

The Höfer compressor has three-stages, is double-acting, and of horizontal design. The principle operating characteristics are:

middle, between the carbon and glass wool. The fluid entering the separator flows in from the bottom, above a space reserved for oil drop-out by gravity, but below the brass cylinder. A high pressure drain valve was provided for removal of oil. The fluid passes up through the brass cylinder and out through the exit, slightly above the top end of the filtering cylinder. The first few inches of the inside of the pipe at the top were bored out and an O-ring placed near the top end of the brass cylinder to prevent short-circuiting of fluid around the outside of the filter. The filter was removed and checked periodically for the condition of the carbon and glass wool.

#### Liquid Nitrogen Cooler

The liquid nitrogen cooler consists of two coils made from 3/8 inch x 0.209 inch I.D. copper tubing, located in a 3-1/2 foot high x 9 x 9 inch stainless steel liner. The coils, slightly less than 9 inches O.D., are vertically in tandem and held that way by brass rods. The bottom coil is closely wound and extends over a vertical distance of only about 6 inches. The upper coil is wound as a helix with a pitch of about 3 inches and extends vertically for a distance of some 2-1/2 feet above the bottom coil. During operation the bottom coil is completely submerged in liquid nitrogen and represents a fixed heat removal for a given condition of flow through it.

The liquid nitrogen level is varied with respect to the upper coil in order to obtain some additional control over the heat removal from the flowing fluid at this point. The level of liquid nitrogen is controlled (see Figure 9) by means of a moveable probe extending down to

eccentric, cross head, cross head guide and connecting rod. An oil sump in the frame encloses the driving gear. The cross head and cross head pin are self-lubricating while running.

The compressor is driven by a Westinghouse 10 horsepower, 900 RPM, 220/440 volt, three phase, squirrel cage AC induction motor. Starting is direct, employing an Allen Bradley magnetic, push button actuated switch. Connections to the totally enclosed motor are class ID. (A squirrel cage motor is very desirable with a direct start because of the high starting torque of the compressor under load.) The use of a variable speed motor was considered. However, this additional control over flow rate in the system was not deemed necessary.

#### Secondary Oil Separator

After being compressed, the gas is discharged from the oil separator which is an integral part of the compressor to a secondary oil separator.

The secondary oil separator was added to the system in order to be sure that essentially no compressor oil, entrained by the compressed gas, was carried into other parts of the system. It was constructed from a 2-1/2 foot length of double extra heavy carbon steel pipe. On one end was welded a pipe cap and on the other a welding neck flange (which was sealed by a mating blind flange).

The secondary oil separator contains a removable brass cylinder through which the gas flows in an upward direction. This cylinder contains in the lower half, activated carbon, and in the upper half, glass wool. There are fine mesh screens at each end of the cylinder and in the

middle, between the carbon and glass wool. The fluid entering the separator flows in from the bottom, above a space reserved for oil drop-out by gravity, but below the brass cylinder. A high pressure drain valve was provided for removal of oil. The fluid passes up through the brass cylinder and out through the exit, slightly above the top end of the filtering cylinder. The first few inches of the inside of the pipe at the top were bored out and an O-ring placed near the top end of the brass cylinder to prevent short-circuiting of fluid around the outside of the filter. The filter was removed and checked periodically for the condition of the carbon and glass wool.

#### Liquid Nitrogen Cooler

The liquid nitrogen cooler consists of two coils made from 3/8 inch x 0.209 inch I.D. copper tubing, located in a 3-1/2 foot high x 9 x 9 inch stainless steel liner. The coils, slightly less than 9 inches O.D., are vertically in tandem and held that way by brass rods. The bottom coil is closely wound and extends over a vertical distance of only about 6 inches. The upper coil is wound as a helix with a pitch of about 3 inches and extends vertically for a distance of some 2-1/2 feet above the bottom coil. During operation the bottom coil is completely submerged in liquid nitrogen and represents a fixed heat removal for a given condition of flow through it.

The liquid nitrogen level is varied with respect to the upper coil in order to obtain some additional control over the heat removal from the flowing fluid at this point. The level of liquid nitrogen is controlled (see Figure 9) by means of a moveable probe extending down to

the desired liquid nitrogen level. The probe consists of a stainless steel tube with a copper bulb at the end near the liquid nitrogen level. The stainless tube and copper bulb contain a volatile material such as air, initially under pressure. When the copper bulb is near or in liquid nitrogen the majority of the material in the probe and interconnecting tube is liquefied -- the pressure exerted on a pressure switch is very small. As the liquid nitrogen level falls, the material eventually exerts a pressure sufficient to activate the pressure switch, which in turn operates a solenoid valve and allows air pressure to be applied to the liquid nitrogen dewar.

Gas pressure forces liquid nitrogen through a delivery tube to flow into the stainless liner until such time as the resultant decrease in the bulb temperature drops the pressure in the probe system sufficiently to activate the pressure switch in the reverse direction. At this time, the pressure switch causes the solenoid valve to shut off gas pressure to the dewar and vent the pressuring system.

The process of filling the probe with the proper amount of a suitable material is done by trial and error and depends on the sensitivity of control desired and the range of operation of the pressure switch.

The nitrogen cooler contains about 50 liters of liquid nitrogen when full. It is contained in a plywood box and is insulated with Styrofoam. The heat gain from the atmosphere when the liner is full is equivalent to a loss of about 1.5 liters of liquid nitrogen per hour.

### Interchanger

The interchanger is of double pipe construction and is operated countercurrently. The warmer fluid passes in succession through 16 tubes, each 6 feet long, composed of pieces of  $3/8$  inch O.D. x 0.209 inch I.D. externally finned copper tubing. The colder fluid flows in an annular space between the fins of the inner tubing and comparable lengths of  $1-1/4$  inch O.D. x  $1-1/8$  inch I.D. brass tubing. Appropriate, brazed return bends were employed. The assembled exchanger consists of 8 large U's resting vertically on the closed parts of the U's. The exchanger was placed in a large plywood box and insulated with Styrofoam and Santocel insulation.

### Low Temperature (Calorimeter) Bath

The purpose of the low temperature bath is to:

1. Maintain the outer parts of the calorimeter of Joule-Thomson throttle at any desired temperature level from room temperature to  $-280^{\circ}\text{F}$ .
2. Provide final adjustment of the temperature of the fluid to the calorimeter or Joule-Thomson throttle to a known, constant value.

The low temperature bath consists of a tank containing a vigorously agitated liquid, such as kerosene or iso-pentane, the temperature of which is carefully controlled. The calorimeter and/or Joule-Thomson device are submerged in the liquid. The fluid being studied flows through a conditioning coil located in the bath prior to entering the measuring instruments.

The actual working space in the bath is a 17 inch long x 9 inch wide x 17 inch deep stainless steel box. This liner is located in the center of a 41 inch x 33 inch x 41 inch plywood box. The volume between the stainless liner and the plywood box, except for the space occupied by a removable top, is filled completely with Styrofoam insulation. The Styrofoam block was built from pieces suitably cut, each piece was fitted carefully, and the separate pieces cemented together with a special compound. The entire outside of the cube was wrapped with a double layer of aluminum foil as were the surfaces, inside, defining the unfilled space. Thus, free air space was virtually eliminated and a moisture barrier provided.

The metal tank was fitted with a metal top, split along its length. All tubing, a stirrer shaft, and electrical wiring entering the bath were brought through holes located on the centerline of the top. Two wooden boxes filled with Santocel insulation were made so as to slip down tightly into a wooden chute above the metal top of the tank. The tubing, etc. from the tank exited along the centerline between the boxes, and a small space which remained was filled with glass wool during operation.

The average temperature of the bath was controlled within 0.01°F for long periods of time. The following items were employed in controlling the bath temperature:

1. A cooling coil employing liquid or gaseous nitrogen.
2. Two electrical heaters, one manual and one controller operated.
3. A mechanical stirrer.

4. An automatic bridge-type controller having its primary detecting element located in the bath in the form of a nickel resistance.
5. A platinum resistance thermometer and a copper-constantan thermocouple located in the bath.

A number of methods were considered for controlling the bath temperature. One which was considered: the use of a homemade on-off controller with a sensing element similar to a mercury thermoregulator, but of a design which would have been applicable at very low temperature. Such a device has been used by Roebuck<sup>(94)</sup> for liquid bath control to better than 0.001°C.

Consideration was also given to constructing various control circuits with an AC or DC bridge as the common basic feature. An error signal from such a bridge, which may be varied in magnitude by selection of bridge voltage and bridge impedences, could be suitably amplified and made to control relays, motor positioned rheostats, a saturable core reactor, etc. By proper design, such a system may be provided with almost any sensitivity commensurate with the nature of the control problem, i.e. response times. Examples of the use of bridge circuits for very precise control are given by Roebuck<sup>(97)</sup> and Masi.<sup>(67)</sup>

It was concluded eventually that an industrial controller could be modified to perform the necessary job of control -- thus avoiding the time consuming job of design, construction, and testing of a homemade instrument. The instrument selected was the Brown type 152 Air-O-Line controller. This instrument combines the Wheatstone Bridge-Brown continuous balance system with a final pneumatic control. The Wheatstone Bridge



consists of four resistances in a closed loop, a current source and a means for detecting potential difference. Two of the resistances are equal and constant. A third is in the form of a slide wire and heliopot in series. The remaining resistance is a Driver Harris 99% + nickel alloy winding located in the low temperature bath. It was constructed to have a resistance of 1100 ohms near the maximum operating temperature of the bath.

Any unbalance in the Wheatstone Bridge appears as a DC potential whose magnitude and polarity depends on the relative magnitude of the nickel resistance and the slide wire-heliopot combination. The DC potential is converted to AC and amplified by a voltage amplifier. The voltage amplifier drives a power amplifier which supplies power to a balancing motor. The polarity of the DC controls the phase of the AC so that the balancing motor moves the slide wire in the proper direction to re-establish balance. Final control is pneumatic. The instrument set point and pen are mechanically linked to the nozzles and flappers of a pneumatic instrument. By means of conventional use of nozzles, flappers, bellows, etc. the instrument develops an output pressure of 3 to 20 psi. Control is position proportional with automatic reset. Derivative response was not deemed necessary.

The pneumatic output of the controller is connected to a cono-flow pneumatic current controller. Variation in output pressure from the controller activates a piston in the "current controller". This piston, through mechanical linkage, positions the moving arm of a 170 VA variac. The input to this variac is controlled by a second variac, in series with it, which is located at the panel board. The output of the controller

positioned variac powers a 125 watt, 115 VAC Cenco knife heater located in the low temperature bath. A third variac at the panel board provides adjustment of voltage for the manually operated bath heater, a second 125 watt Cenco heater. Both heaters have been made gas-tight.

By adjusting the heliopot in the Brown controller it is possible to balance the bridge at any temperature corresponding to 0 to 1100 ohms for the nickel winding. The controller set point is found by following the bath temperature by means of a thermocouple or the platinum resistance thermometer. The resistance of the nickel element was not calibrated against temperature. Nickel was selected for the bath winding because of its high coefficient of resistivity, about twice that of platinum at room temperature. The resistance of the nickel winding at any temperature is given by:

$$R_T = R_0 [1 + \alpha (T - T_0)] \quad (19)$$

$R_0$  = Resistance at reference temperature, ohms

$R_T$  = Resistance at temperature T, ohms

$\alpha$  = Integrated mean coefficient of resistivity, ohms/ohm  
degree

Since  $T - T_0$  is negative in the present application ( $T_0$  is the maximum bath temperature of interest) and alpha is positive,  $R_T$  is less than  $R_0$ . The fact that alpha is not constant, but decreases as temperature is lowered, reduces the magnitude of  $R_T$  at a greater than linear rate with temperature. The magnitude of the error signal to which the controller must respond is dependent upon  $dR_T/dT$ . Therefore,  $R_0$  should

be as large as practicable so that  $dR_T/dT$  is large. The size of  $R_0$  in the present application was limited to the input impedance which the controller could handle. It was possible according to Honeywell to use a maximum of about 2,200 ohms with their instrument. It was decided on the basis of a complete consideration of the control problem that 1,100 ohms would be adequate, however. It was thought that if additional sensitivity was needed in the low temperature range, that a second nickel winding having 1100 ohms resistance at some low temperature could be switched into the circuit.

The Honeywell instrument was selected to have a very narrow full scale range of 10 ohms. The accuracy and sensitivity of industrial controllers are based on a percentage of their full scale range. By agreement with Honeywell, a very narrow-ranged instrument was obtained and thus a high accuracy and sensitivity secured. At the same time, an adjustable zero (heliopot) was installed, upon request, so that the instrument could be used over a wide range of conditions. It has been found in practice that the controller proportional band may be reduced to about one percent without instability and that this is equivalent to a short-term control cycle of  $\pm .025^\circ\text{F}$  at the lowest temperatures encountered. Control could probably be improved somewhat, but this is not considered necessary. The periodicity of the temperature variation of the bath fluid and the thermal inertia of the calorimeter and conditioning coil were such that the temperature of the fluid entering the calorimeter was extremely stable.

Agitation of the bath fluid was obtained using an explosion-proof lightning mixer having a 36 inch shaft and two propellers. The

size and shape of the low temperature bath liner and the mixer were selected to obtain a certain desired type of mixing.

The conditioning coil in the low temperature bath was fabricated from 3/8 inch x 0.209 inch copper tubing having a total length of approximately 40 feet. The liquid nitrogen cooling coil was made from 50 feet of 5/16 inch x .032 inch copper tubing. Both are rectangular and are in tandem; the physical arrangement is such that good fluid circulation is maintained around them and around the calorimeter. The liquid nitrogen cooling supply is regulated as illustrated in Figure 9.

### Isobaric Specific Heat Calorimeter

#### Principal Design Considerations

A number of factors are important in the design of a flow calorimeter. It is desirable to reduce, as much as possible, the magnitude of the unmeasured heat leakage to be expected, since any correction for this effect always involves some amount of uncertainty. An uncertainty in a heat leakage correction adds to any uncertainty in the measurement of the primary variables (flow rate, measured energy addition, temperature rise of the fluid) in determining the reliability of  $C_p$  measurements. Similarly, the calorimeter must be designed to eliminate any significant change in kinetic energy of the fluid as it flows between the points which define the system. Pressure drop in the calorimeter must be held to a tolerable level. The heat capacity of the calorimeter is important, particularly if the fluids being studied are gaseous, since excess heat capacity increases the time necessary to reach a condition of steady state.

### Reduction of the Magnitude of Heat Leakage

Heat leakage in a flow calorimeter refers to heat transfer, not directly measured, which occurs between the "system" and the "surroundings". The "system" may be defined as the flow path of the fluid between points of initial and final temperature measurement (between entrance and exit thermocouple wells for the calorimeter illustrated in Figure 15). Between these points, ideally, all energy transfer crossing the boundaries of the system must be accounted for in flow calorimetry. This is never completely accomplished, but it is essential that the unmeasured energy transfer be reduced to a tolerable level.

The principal ways in which heat leakage was avoided in the calorimeter (Figure 15) were the following:

1. The entire calorimeter assembly was located in an environment (low temperature bath), the temperature of which was not greatly different from the temperature of any of the portions of the "system". The bath temperature is essentially identical to the entering fluid temperature.
2. The calorimeter heater and exit thermocouple well were placed in a portion of the calorimeter physically separated from the entrance thermocouple well, since these components were not at the entering fluid temperature.
3. The path for heat conduction along high pressure tubing between the calorimeter heater and the entrance thermocouple well, the heater and the exit thermocouple, was lengthened as much as possible.

4. The calorimeter was evacuated to essentially eliminate any heat transfer by gross convection or conduction through air between components of the "system" and the surroundings.
5. A radiation shield was provided which was to be operated at a temperature near that of all of the components at essentially the exit fluid temperature (calorimeter heater, exit thermocouple well, and high pressure tubing) in order to prevent radiative heat transfer from these components to surfaces at a lower temperature.
6. The diameter and length of electrical wires in the calorimeter were selected to reduce heat conduction, along the wires, between the "system" and the "surroundings" to a tolerable level.

In general, the use of relatively high flow rates in the system and the low operating temperatures anticipated permitted simplifications in shielding techniques.

#### The Heat Capacity of the Calorimeter

Every attempt was made to reduce the heat capacity of the calorimeter, especially that portion which was in contact only with the fluid passing through the system, since excess heat capacity increases the time necessary to reach a steady flow condition. The high pressures which were anticipated in the present investigation made difficult, however, the problem of reducing the weight of certain portions of the calorimeter, while at the same time maintaining the desired large safety factors. Over the

wide range of low temperatures and high pressures involved, it would not have been wise to reduce these safety factors to a bare minimum -- especially in view of the small absolute dimensions of wall thickness considered. A careful study was made of the weights involved, mass flow rates anticipated, and probable heat transfer coefficients from the fluid to the calorimeter. The heat capacity of that portion of the calorimeter in direct contact with the liquid bath was not of great importance.

#### Detailed Description of the Specific Heat Calorimeter

The calorimeter is located in a stirred constant temperature liquid bath, the temperature of which is the initial temperature for the fluid passing through the calorimeter. The thermal inertia of the low temperature bath conditioning coil and calorimeter case was expected to make unimportant any minor short term oscillations in bath temperature.

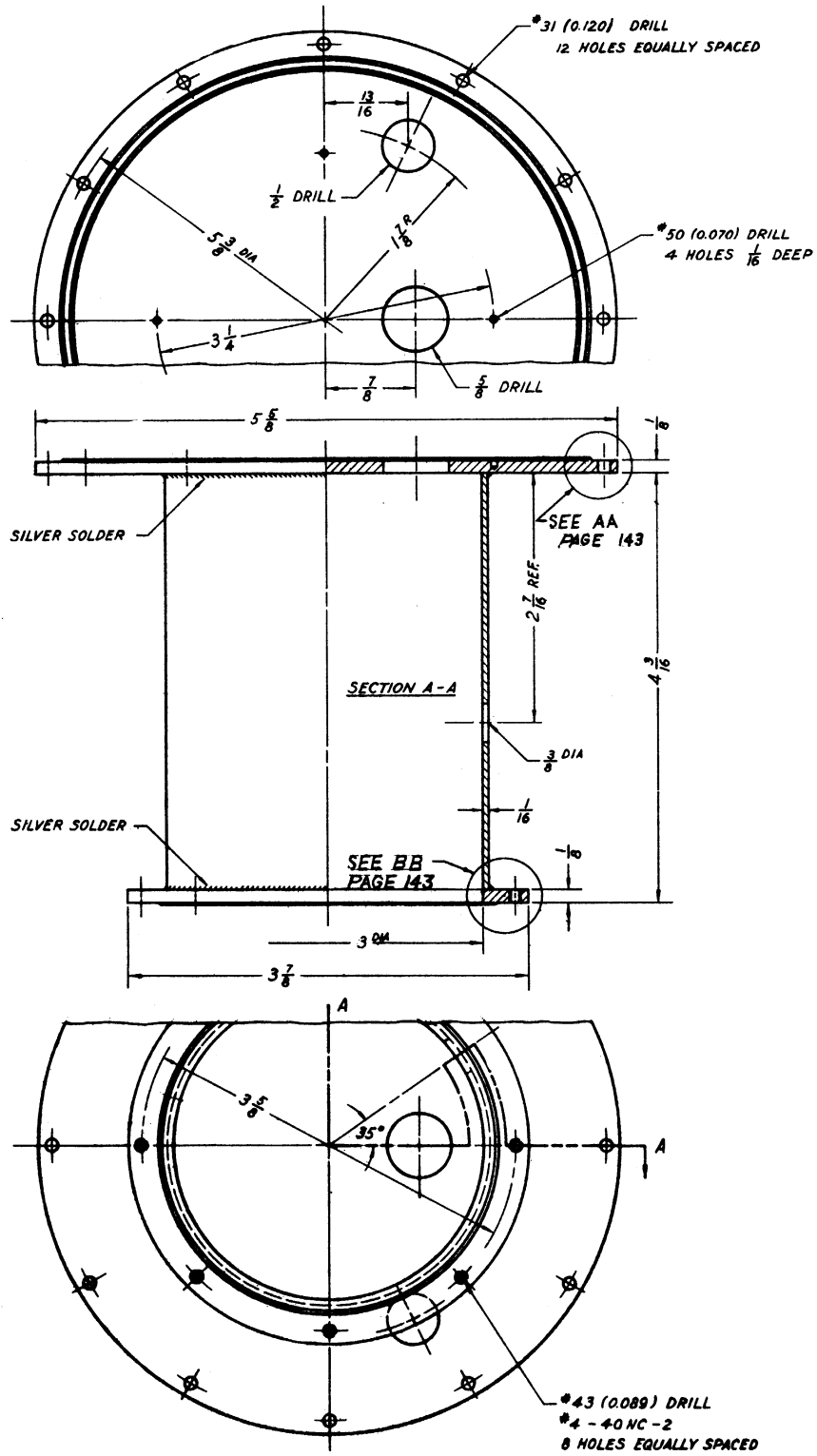
The fluid entering the calorimeter flows through a thermocouple well (lower portion of calorimeter, Figure 15) which is isolated from the calorimeter heater (upper portion of calorimeter, Figure 15) to avoid heat leakage from the heater to the thermocouple well. The calorimeter is evacuated -- energy transfer between the heater and the lower portion of the calorimeter by conduction or convection though air is virtually eliminated. A radiation shield was installed in the line of sight between the heater capsule and the lower portion of the calorimeter to: (1) intercept radiation and conserve it to the system, and (2) prevent radiation from affecting the entrance thermocouple junctions. The fluid flows from the entrance thermocouple upward to the heater capsule where electrical energy is added. The tube conveying the fluid from the

thermocouple well to the heater is of Type 304 18-8 stainless steel, as are the entrance thermocouple well, heater capsule, exit thermocouple well and the remainder of the high pressure tubing in the calorimeter. Stainless steel has a very low thermal conductivity, for a metal, in addition to possessing high strength and resistance to low temperature fracture. The resistance to thermal conduction from the heater capsule to the entrance thermocouple was further increased by lengthening as much as practicable the tubing connecting the heater to the thermocouple well.

Upon entering the heater capsule the fluid passes back and forth through a series of annular spaces, between concentric copper cylinders with hemispherical ends (Figure 19). Alternate ends of these baffles have holes to permit flow. The first three of these baffles were wrapped with a total of 147 ohms of (double glass with binder) insulated No. 26 Nichrome V resistance wire, manufactured by Driver Harris. The heater operates at a maximum of 100 VDC and a maximum 60 watts is dissipated. The fluid flowing through the heater capsule receives energy from several baffle surfaces. This procedure simplifies the job of transferring energy to the fluid, without operating the heater wires at a high temperature. Higher temperature heater operation would have increased the possibility of "hot spots" and could have contributed to heat leaks in the system. The outer three baffles in the heater capsule promote temperature equalization of the fluid.

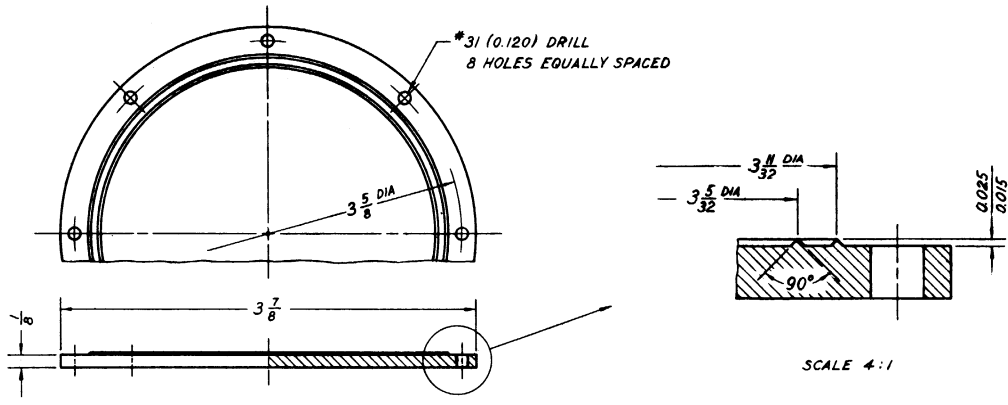
The use of the method of heat addition described is thought to involve a minimum of heat capacity in the process of energy addition and temperature equalization. The baffle arrangement is also satisfactory from the standpoint of pressure drop. The annular surfaces are quite



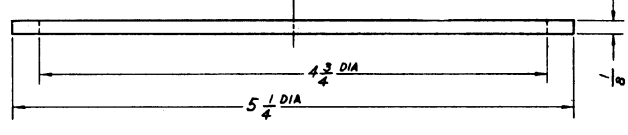
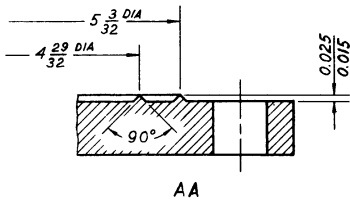


LOWER CASE  
COPPER

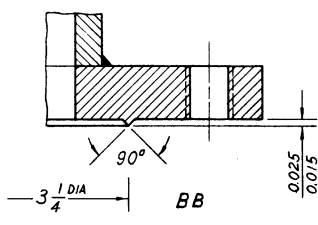
Figure 19. Calorimeter Detail Drawings



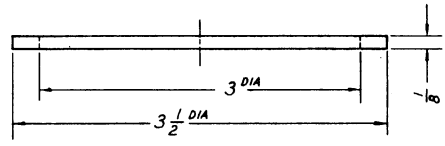
COVER (LOWER CASE)  
COPPER



GASKET (TEFLON)



SCALE 4:1



GASKET (TEFLON)

REQ'D 20 \*A-40NC-2 x 3/8 FIL HD MACH SCR.

Figure 19. Calorimeter Detail Drawings (Cont'd)

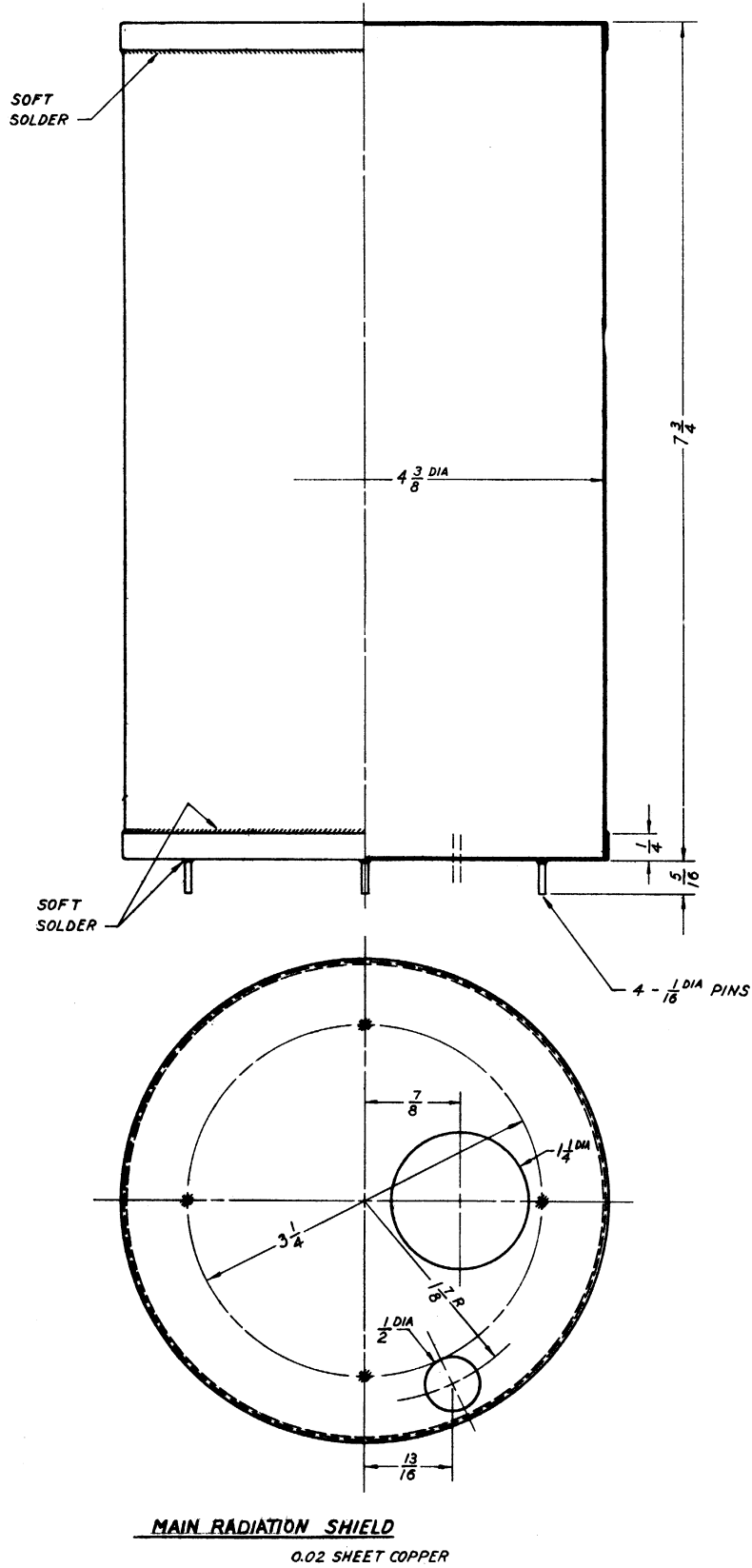


Figure 19. Calorimeter Detail Drawings (Cont'd)

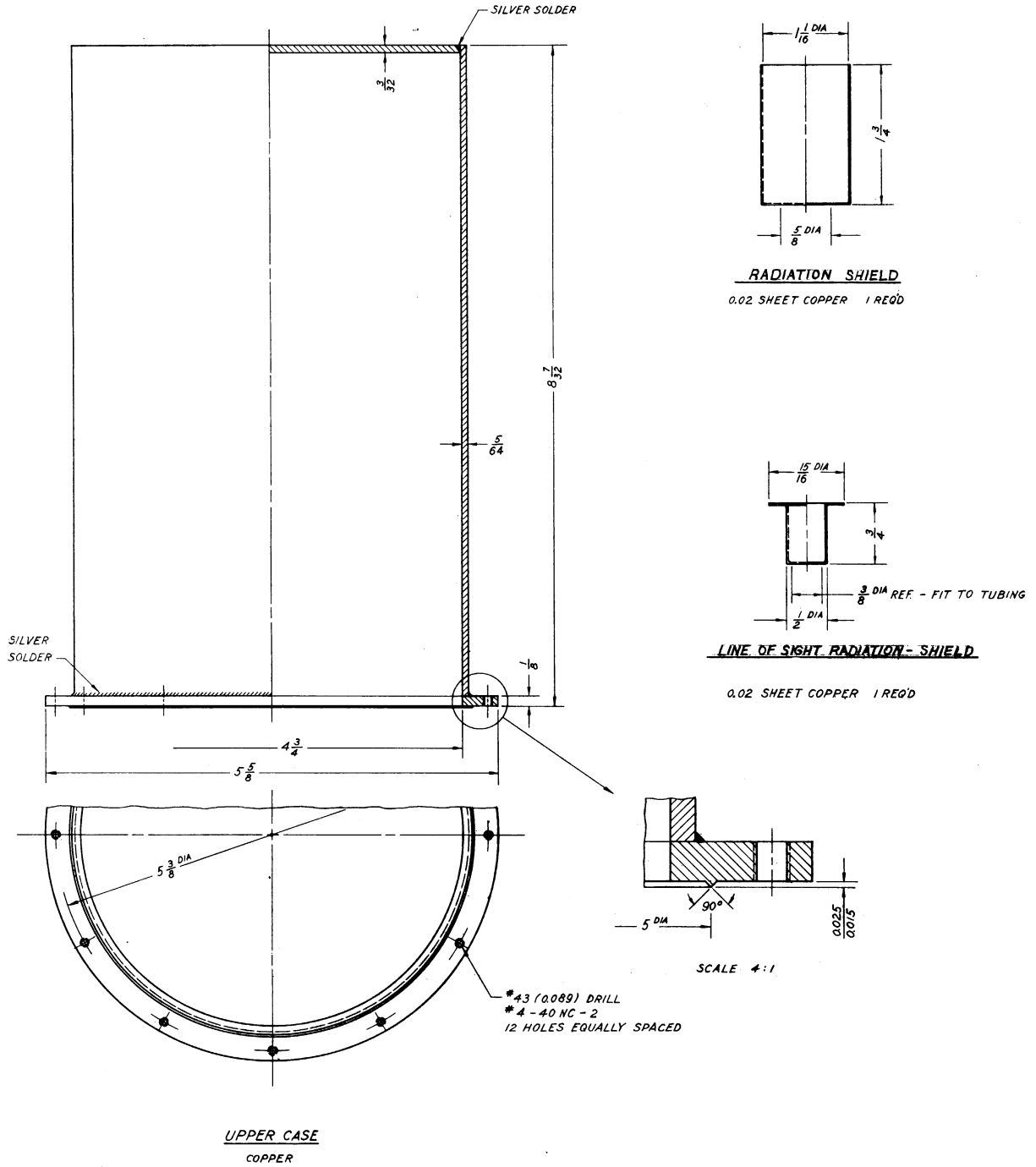
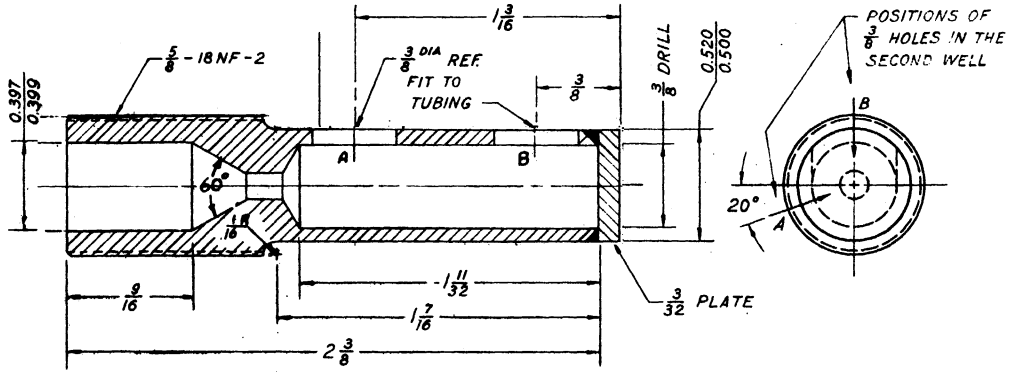
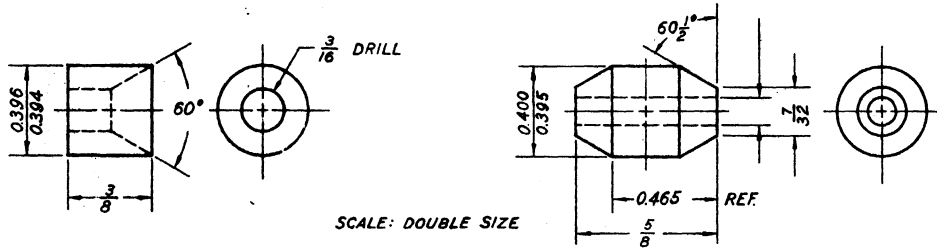


Figure 19. Calorimeter Detail Drawings (Cont'd)



SCALE: DOUBLE SIZE

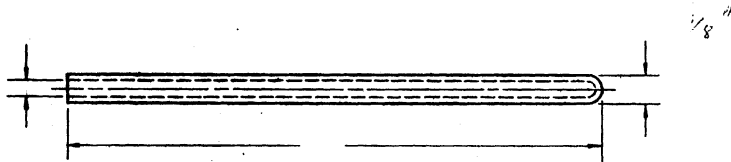
**THERMOCOUPLE WELL**  
304 S.S. 2 REQ'D



SCALE: DOUBLE SIZE

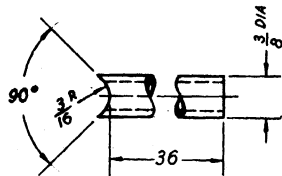
**GLAND**  
304 S.S. 2 REQ'D

**PACKING (TEFLON)**



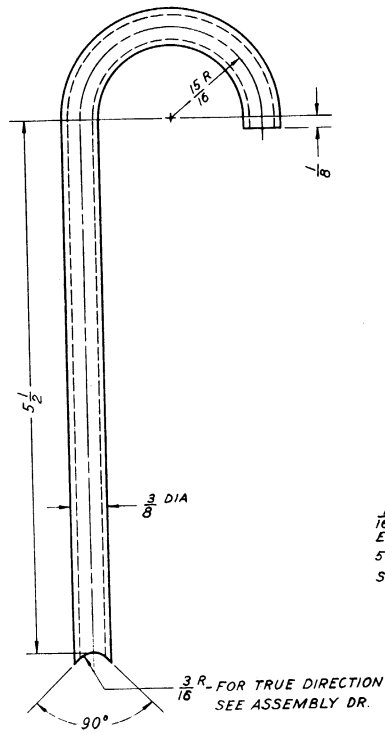
SCALE: DOUBLE SIZE

**COPPER THERMOCOUPLE SHEATH**

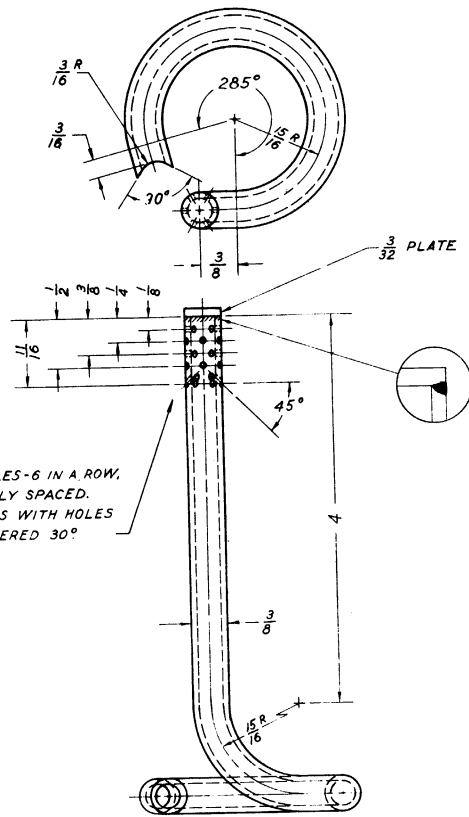


304 S.S. TUBING 1 REQ'D

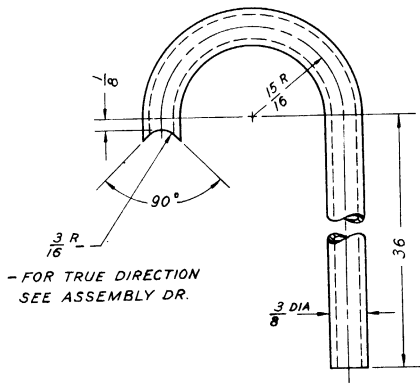
Figure 19. Calorimeter Detail Drawings (Cont'd)



304 S.S. TUBING 1 REQ'D



ENTRANCE TUBE  
304 S.S. TUBING 1 REQ'D



EXIT TUBE  
304 S.S. TUBING 1 REQ'D

Figure 19. Calorimeter Detail Drawings (Cont'd)

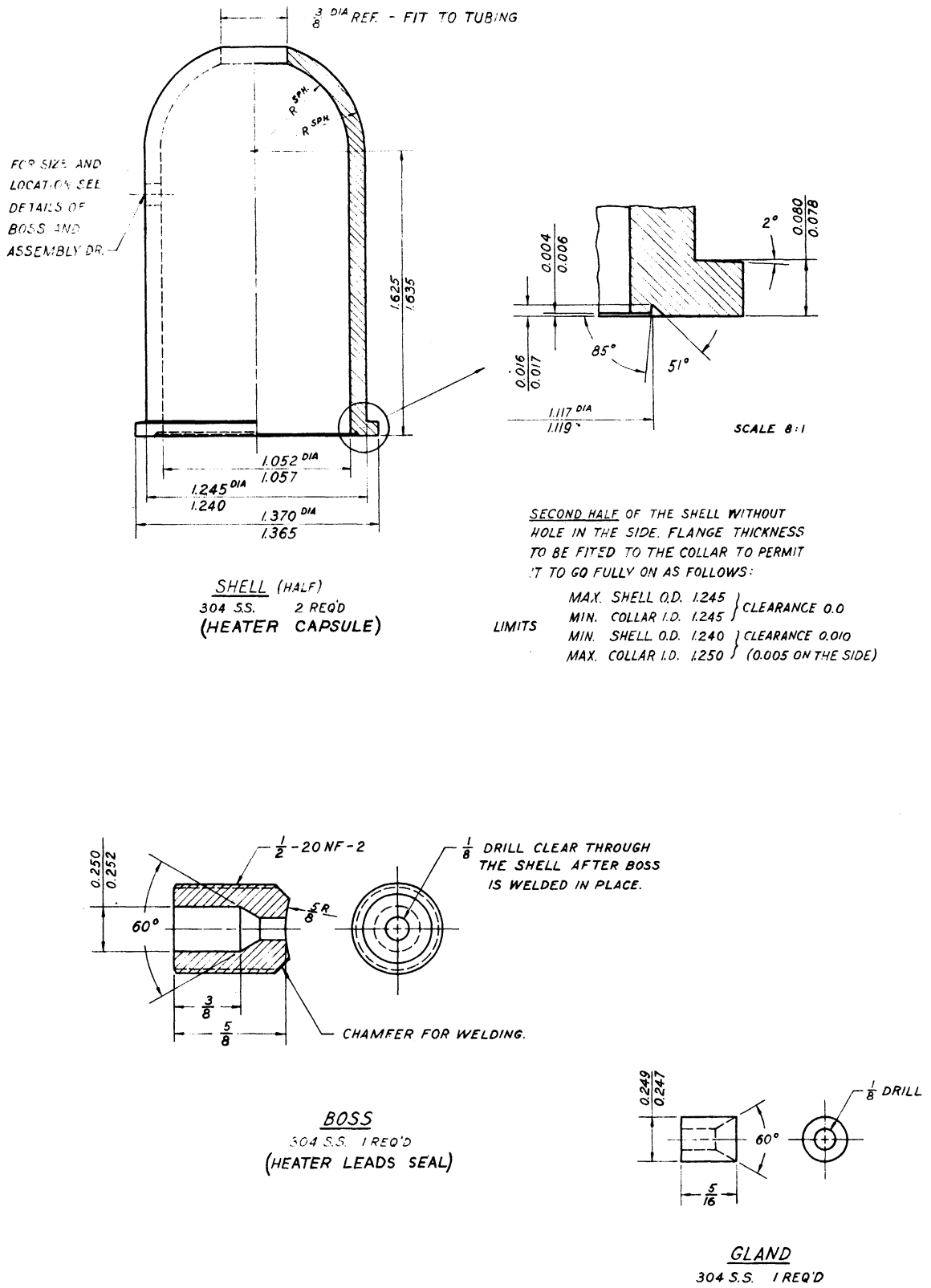
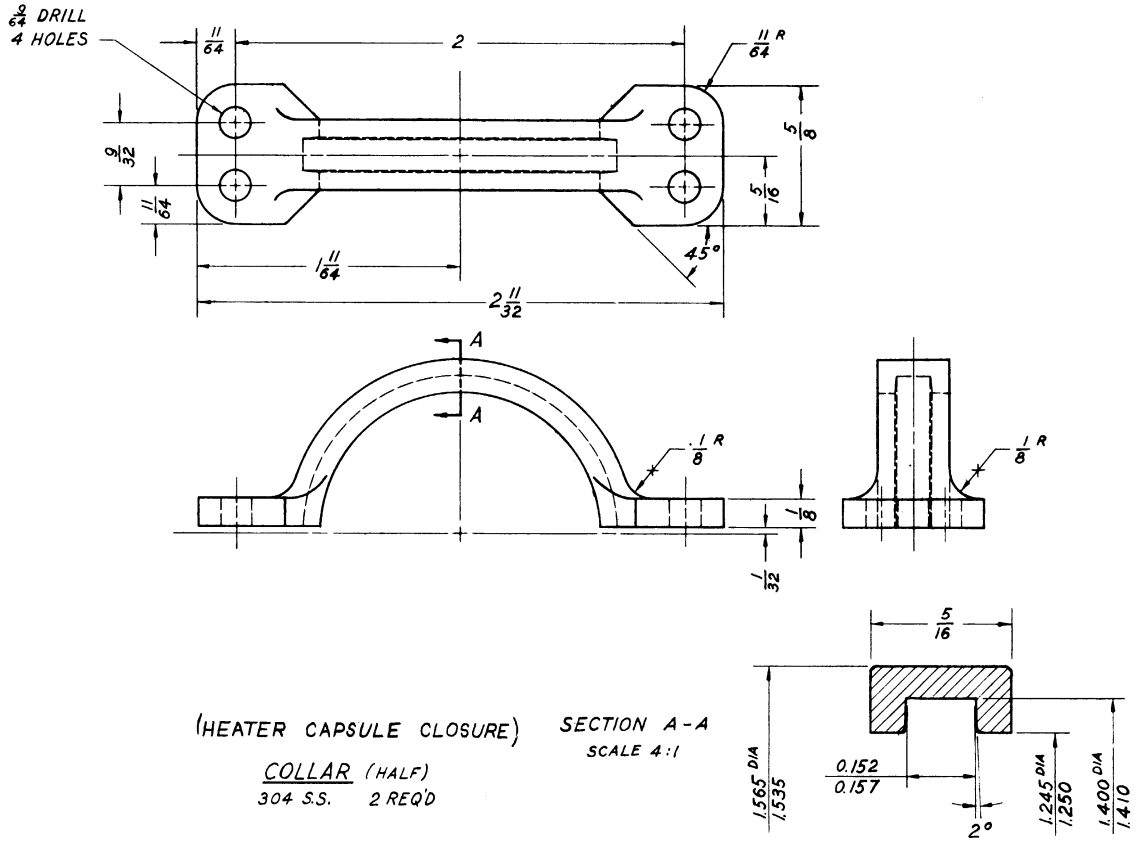
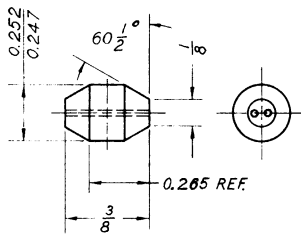


Figure 19. Calorimeter Detail Drawings (Cont'd)

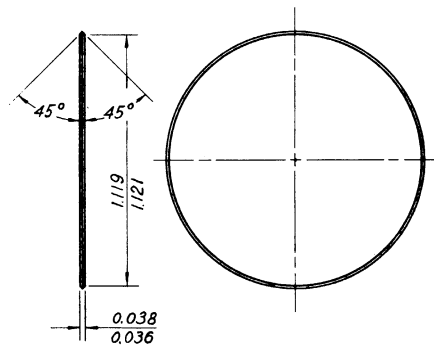


SECOND HALF WITH 4 #5-40NC-2 TAPPED HOLES  
IN PLACE OF 4 3/64 DRILLED HOLES.

BREAK EDGES WHERE SHOWN.



PACKING FOR BOSS  
TEFLON



SEAL RING GASKET FOR HEATER  
CAPSULE CLOSURE  
COPPER

REQ'D 4 #5-40NC-2 x 3/8 SOCKET HD CAP SCR.  
4 #5 MEDIUM LOCK WASHERS.

Figure 19. Calorimeter Detail Drawings (Cont'd)

(BAFFLES CONTINUED)

Figure 19. Calorimeter Detail Drawings (Cont'd)



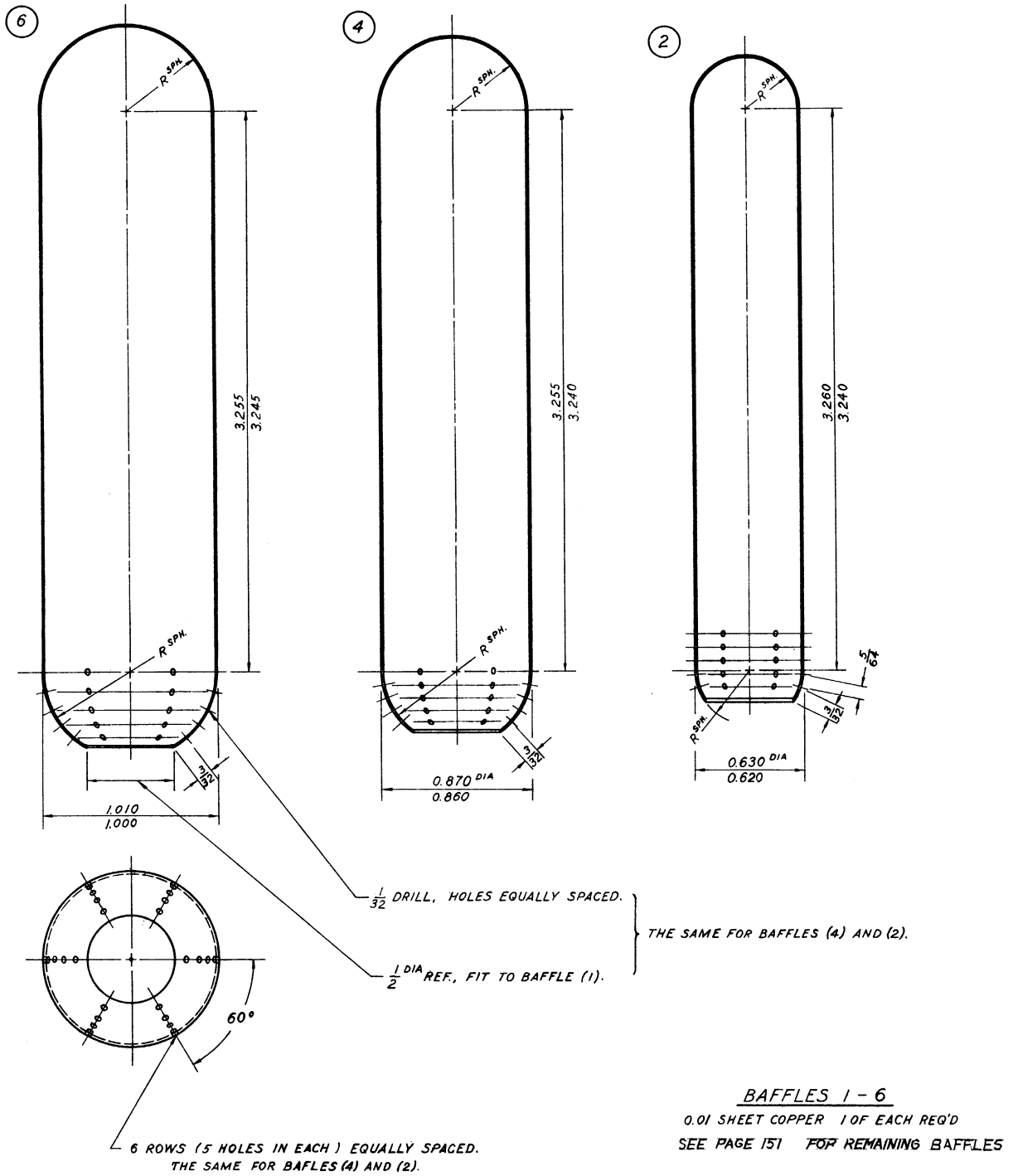
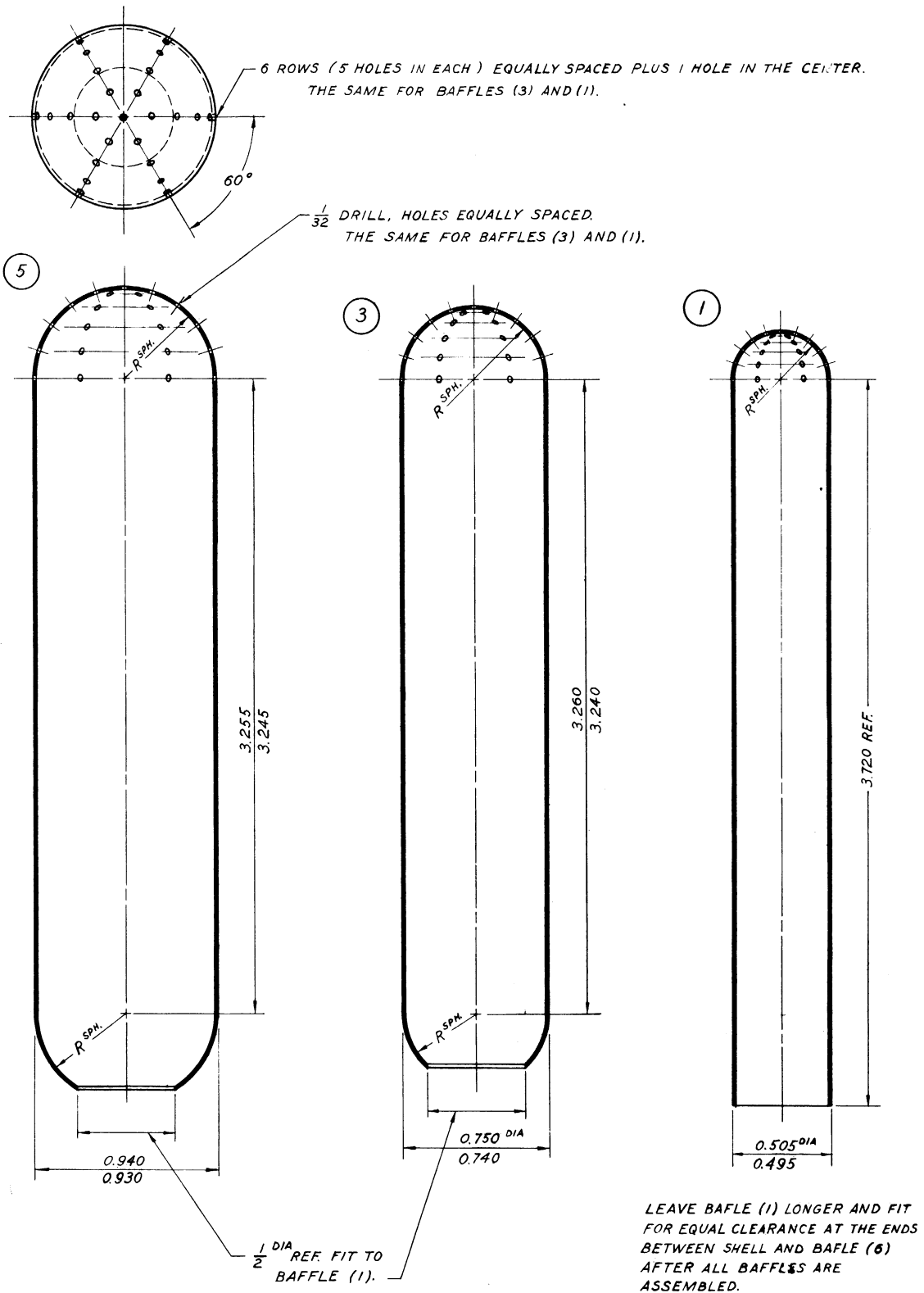


Figure 19. Calorimeter Detail Drawings (Cont'd)



(BAFFLES CONTINUED)

Figure 19. Calorimeter Detail Drawings (Cont'd)

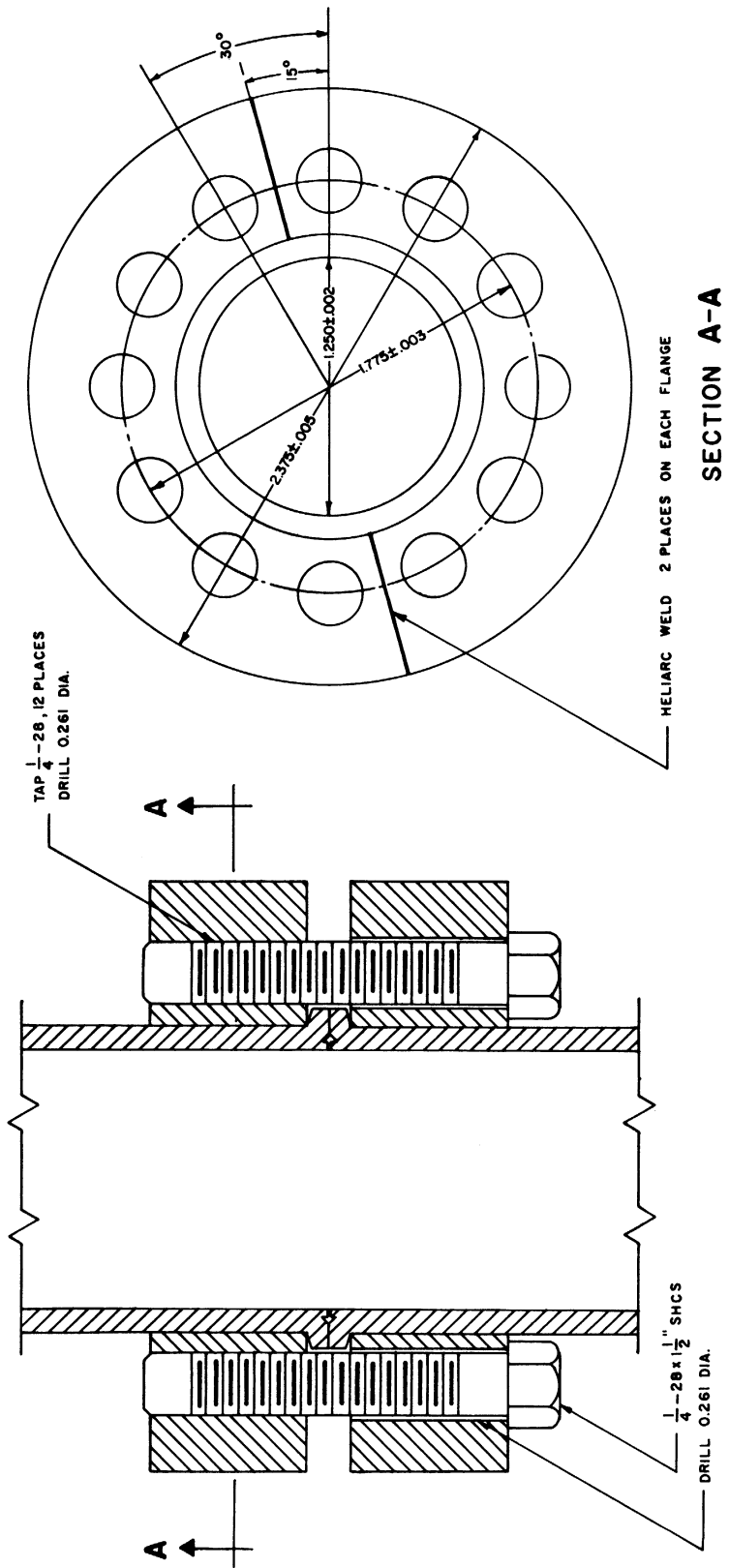
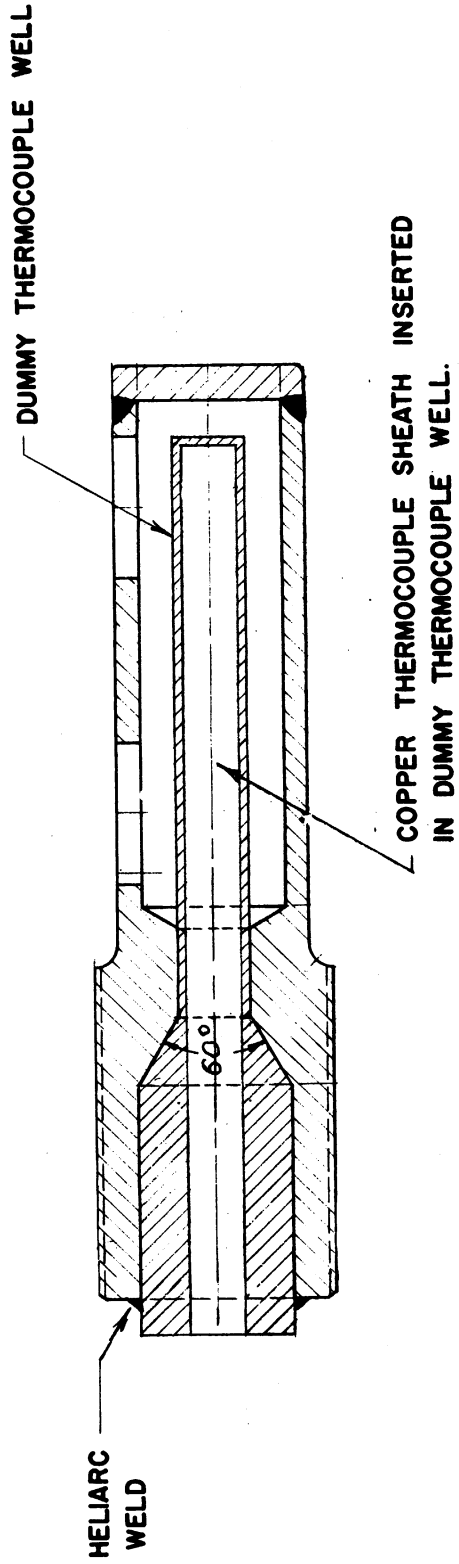


Figure 20. Modified Calorimeter Heater Capsule Closure



NOTE: FOR DIMENSIONS SEE FIG. 19

Figure 21. Modified Calorimeter Thermocouple Wells

smooth, the change-in-direction pressure drops relatively small. The annular area for flow in each pass (over the wires for the first three) was made equal and sufficiently large that pressure drop would be small; at the same time the dimensions were such that good heat transfer to the flowing fluid could be expected.

The fluid enters the heater section through a number of holes in the side of the entrance tube in order to distribute the flow and to prevent a hot spot at the base of the baffles, the only point at which the baffles were anchored to the heater capsule, Figures 15 and 19.

The fluid, after receiving energy within the heater capsule, flows to the exit thermocouple well. The length of this path was increased to promote further temperature equalization of the fluid after energy addition and to prevent a conductive heat leak to the exit thermocouple well along the tubing, Figure 15.

The fluid, after passing through the exit thermocouple well, leaves the calorimeter through a stainless steel tube. This tube was lengthened, somewhat, to prevent conduction from the thermocouple well to the calorimeter bath. The exit tube passes through the calorimeter base without touching it and is brought out of the low temperature bath through a larger concentric stainless steel tube. The annular space between the tubes is evacuated, Figure 15.

The thermocouple wells, heater capsule, and high pressure tubing were chrome plated and polished to lessen heat transfer by radiation. A plating having a lower emissivity or absorbtivity, such as copper, would have been more effective; however, the radiation problem was not considered to be severe at low temperatures.

A large radiation shield surrounds the contents of the upper portion of the calorimeter. This shield is held at approximately the exit fluid temperature by means of an 1100 ohm electrical winding. Not all parts of the calorimeter being thus shielded were expected to be at exactly the same temperature. However, a large variation in temperature over these surfaces was not expected. The radiation shield is copper to promote temperature equalization. Copper-constantan difference thermocouples (Figure 15) made possible the selection of an average shield temperature and the detection of any departure of the shield from an isothermal surface. The shield was supported by three small stainless pins in its base which did not convey away a great deal of energy. Heat transfer from the shield by other mechanisms was small. The shield power requirement did not exceed 3 watts.

The entire calorimeter was evacuated for the purpose of preventing undesired heat transfer by gross convection or stagnant air conduction. (This refers principally to heat transfer between the heater capsule, high pressure tubing or thermocouple well-in the upper portion of the calorimeter - and any other surface at a lower temperature.) In general, heat transfer through air in the calorimeter is continuously reduced as the pressure in the calorimeter is reduced. The residual effect, due to stagnant conduction is not, however, affected until the pressure in the calorimeter is such that the mean free path of air molecules is of the same order of magnitude as the minimum important distance for heat transfer. Calculations showed that for the calorimeter designed, heat transfer by stagnant conduction would remain constant, through air, until a pressure level of about 10 microns was attained. As the pressure

A large radiation shield surrounds the contents of the upper portion of the calorimeter. This shield is held at approximately the exit fluid temperature by means of an 1100 ohm electrical winding. Not all parts of the calorimeter being thus shielded were expected to be at exactly the same temperature. However, a large variation in temperature over these surfaces was not expected. The radiation shield is copper to promote temperature equalization. Copper-constantan difference thermocouples (Figure 15) made possible the selection of an average shield temperature and the detection of any departure of the shield from an isothermal surface. The shield was supported by three small stainless pins in its base which did not convey away a great deal of energy. Heat transfer from the shield by other mechanisms was small. The shield power requirement did not exceed 3 watts.

The entire calorimeter was evacuated for the purpose of preventing undesired heat transfer by gross convection or stagnant air conduction. (This refers principally to heat transfer between the heater capsule, high pressure tubing or thermocouple well-in the upper portion of the calorimeter - and any other surface at a lower temperature.) In general, heat transfer through air in the calorimeter is continuously reduced as the pressure in the calorimeter is reduced. The residual effect, due to stagnant conduction is not, however, affected until the pressure in the calorimeter is such that the mean free path of air molecules is of the same order of magnitude as the minimum important distance for heat transfer. Calculations showed that for the calorimeter designed, heat transfer by stagnant conduction would remain constant, through air, until a pressure level of about 10 microns was attained. As the pressure

decreases below this level, the conductive heat transfer will be reduced linearly. A calorimeter insulating vacuum level of one micron was selected on the basis of this estimate.

The temperature rise of the fluid upon addition of a measured quantity of electrical energy was determined by means of a six junction copper-constantan difference thermocouple between the entering and exiting thermocouple wells. It was decided that a thermocouple measurement of the temperature difference would be adequate; platinum thermometry was not deemed necessary. The average temperature difference of the fluid was selected as 18 to 20°F and a thermocouple with a sufficient number of junctions selected, six, so that accurate measurements might be made with a Leeds and Northrup K3 potentiometer. The use of a number of junctions also had the purpose of averaging the effects of inhomogeneities or strains in individual thermocouple wires.

The constantan wires were No. 30 and the copper wires No. 36. The wires were, generally, kept as small as possible to minimize heat leakage between the exiting and the entering thermocouple wells. Their size was limited somewhat by:

1. The effect of inhomogeneities in constantan.
2. Limitations in resistance which had to be observed in the galvanometer circuit.
3. Danger of kinking or otherwise damaging the wire.

The constantan wire was cotton insulated, and the copper silk insulated. Other types of insulation are better in many respects, but some of them tend to strain thermocouple wire.



Each set of the six bare thermocouple junctions was wrapped with silk thread and staggered along the length of a copper sheath, Figure 15. The sheaths were packed with Apiezon N to promote temperature equalization and as additional electrical insulation between the junctions and the sheaths. The wires were attached so that they could not be easily pulled out of the sheaths and the wire between sheaths made into a bundle and suitably wrapped to protect them from mechanical damage.

In addition to the main calorimeter thermocouple, a loop of No. 30 constantan wire was run between a number of points within the calorimeter. At each measuring point, the constantan wire was bared and a junction made with a single No. 36 copper wire. It was possible by properly connecting these lead wires to rotary selector switches to measure the temperature differences illustrated in Figure 15 and listed in Table VII, and ascertain the point of greater temperature in each case.

The connection of the thermocouple junctions at all points not on the radiation shield was made by tying a portion of the lead wire, and the junction itself, firmly to the surface with nylon thread. Underneath each of these junctions a layer of cigarette paper was placed to isolate the junction electrically from the surface to which it was attached. The tips of the junctions and the cigarette paper were covered with Apiezon N. This aided considerably in keeping the junctions in good thermal contact with the various surfaces, but did not affect the electrical isolation of the junctions.

The thermocouple junctions which were to be attached to the radiation shield were slipped into small copper sheaths which had been

soldered to the inside surface of the shield at the desired points. The bare tips of these junctions were first wrapped with cigarette paper and the inside of the sheaths packed with Apiezon N.

Difference thermocouples AB, AC, AD, AE, AF (Figure 15) are for the purpose of determining whether a temperature gradient exists along any portion of the tube between the entrance thermocouple and the base of the heater capsule. Difference thermocouples IJ, KN, MN, NH are used for adjusting the radiation shield to a proper average temperature and also to indicate the existence of any temperature differences from point to point on the radiation shield. Difference thermocouple FG indicates the approach of the heater capsule closure temperature to the operating temperature of one point on the heater capsule. [The modified heater capsule closure (Figure 20) represents about half of the heat capacity of the high pressure portion of the calorimeter.] Difference thermocouple FJ indicates any difference in temperature between the base and top of the heater capsule. Difference thermocouples JL and LN are for the purpose of detecting heat leakage from the heater capsule to the exit thermocouple well. Difference thermocouple NO is for the purpose of ascertaining whether or not heat leakage is occurring, by conduction, from the exit thermocouple well to the low temperature bath.

A tube (9/16 inch O.D. x 1/2 inch I.D.) was brought out of the side of the top calorimeter case (not shown in Figure 15) for the purpose of evacuating the calorimeter. At the opposite end of this tube, above the low temperature bath, a flanged O-ring connection was made to the main vacuum line.

Three  $1/4$  inch O.D. x  $3/16$  inch I.D. tubes (not shown in Figure 15) were connected below the base plate between the upper and lower portions of the calorimeter for the purpose of bringing the many wires within the calorimeter to a point outside the low temperature bath. One tube was used for the four No. 22 copper lead wires to the calorimeter heater. At a point above the low temperature bath this tube was connected to a cylinder which was filled with Dekhotinsky cement, to form a vacuum seal around the wires. The length of the heater leads and their size, from the point of vacuum seal to the heater capsule, were chosen to minimize heat gain to the calorimeter by conduction from the surroundings and from generation of heat in the leads. Beyond the vacuum seal, the wires were increased in size to reduce heat generation in the current carrying wires and to reduce IR drop in the potential taps.

Another  $1/4$  inch x  $3/16$  inch tube was used to remove the thermocouple lead wires from the calorimeter. The lead wires were tied together and inserted in plastic tubing for their protection. They were handled very carefully to avoid any kinks, which would be sources of spurious emf's in any region where a temperature gradient existed. A procedure similar to that used for the heater leads was employed in vacuum sealing the thermocouple wires. In this case, a removable top on the cylinder used for vacuum sealing was important in protecting the junction points of extensions to the lead wires from a temperature gradient.

A third  $1/4$  inch x  $3/16$  inch tube was employed for removing the radiation shield heater leads. This heater was operated on AC, and it was desirable to isolate the AC as much as possible from the thermocouple

leads. The radiation shield heater was wound bifilarly in order to cancel any inductive effect. Its leads were vacuum sealed in a manner analogous to that previously described for the other wires.

A description of several high pressure, low temperature mechanical seal problems which were encountered in the construction of the calorimeter is given in Mechanical Design, Appendix A.

#### Joule-Thomson Throttle

The accuracy of isenthalpic measurements depends upon the elimination of several undesirable energy effects and upon an accurate measurement of pressure and temperature changes. The measurement of pressure changes and temperature changes for integral isenthalpic measurements is discussed on page 123. The undesirable energy effects which tend to occur are:

1. Heat leakage to or from the flowing fluid between the points of temperature measurement.
2. Heat leakage directly to or from the temperature measuring devices, which although not materially affecting the flowing fluid temperature, may alter the temperature measurements.
3. Translational kinetic energy effects due to gross velocity changes between the temperature measuring devices.
4. Changing conditions of turbulence between the temperature measuring devices.

Items one and two above may be termed heat leakage effects, items three and four kinetic effects. Kinetic effects may be virtually

eliminated in a properly designed expansion device, except at low values of final pressure. Roebuck<sup>(95)</sup> found, however, that it was extremely difficult to separate kinetic and heat leak effects in the range in which the former become significant. Heat leakage effects are difficult to avoid and difficult to estimate in the conventional methods of performing isenthalpic throttling experiments. Consideration was given to the possibility of using a complicated procedure of guarding against heat leakage. However, it was decided that using a radial porous plug technique, a properly scaled expansion device, and relatively large flow rates would be considerably simpler. The radial porous plug technique offers a number of advantages in comparison with other methods which have been employed.

#### Isenthalpic Expansion by Several Different Methods

Vogel, Noel, and Hausen<sup>(46)</sup>, used a wad of asbestos in a steel tube to serve as the flow resistance. This was the classical approach. Brown and Associates<sup>(39,53,62,64,73,82,131)</sup> designed and operated an expansion device consisting of a series of interchangeable orifices in their measurements of the Joule-Thomson effect in hydrocarbons at high temperatures. Attempts have also been made to use a single valve arrangement to produce a variable pressure drop. The author became convinced that an additional method which has been used, the radial porous plug method, described by Burnett and Roebuck<sup>(19)</sup> and Roebuck<sup>(95,96)</sup> and used by Roebuck and co-workers<sup>(95-105)</sup> and Sage and Lacey<sup>(14)</sup>, possessed certain inherent advantages over a linear flow system.

One advantage of the radial porous plug method is that use of a porcelain plug, such as the one which will be described, tends to

eliminate any regions of local high (translational) velocity. The flow through all areas of the plug surface is uniform. Occasional difficulties with inhomogeneity of individual plugs may exist, but, by and large, this can be discovered and the faulty plug eliminated. Higher velocities may exist through pores of a plug, especially near the inner surface, but the net average velocity change through the plug will be very small. Only at very low final pressures do translational kinetic and turbulent effects, based on the experience of Roebuck, become significant.

The second principal advantage of the radial porous plug method is the greater ease with which heat transfer to the surroundings can be eliminated, in comparison with a linear flow method. This matter is explained in a discussion of the radial plug method.

#### Radial Porous Plug Method of Isenthalpic Expansion

The porous plugs, which were manufactured for the present research by the Coors Porcelain Company of Golden, Colorado, are semi-glazed porcelain cylinders with one closed hemispherical end. The plugs, which are interchangeable, are held vertically in the expansion device (Figure 22). Fluid at the initial pressure and temperature enters the chamber surrounding the plug at the top (Figure 22). The volume inside the plug contains the fluid at the lower pressure and final temperature. Fluid leakage around the base of the plug is prevented by means of an O-ring seal, although a small amount of leakage is not important.

During isenthalpic measurements the final temperature of the fluid upon expansion may be lower or higher than the initial temperature. The large majority, if not all, of the states which would be encountered

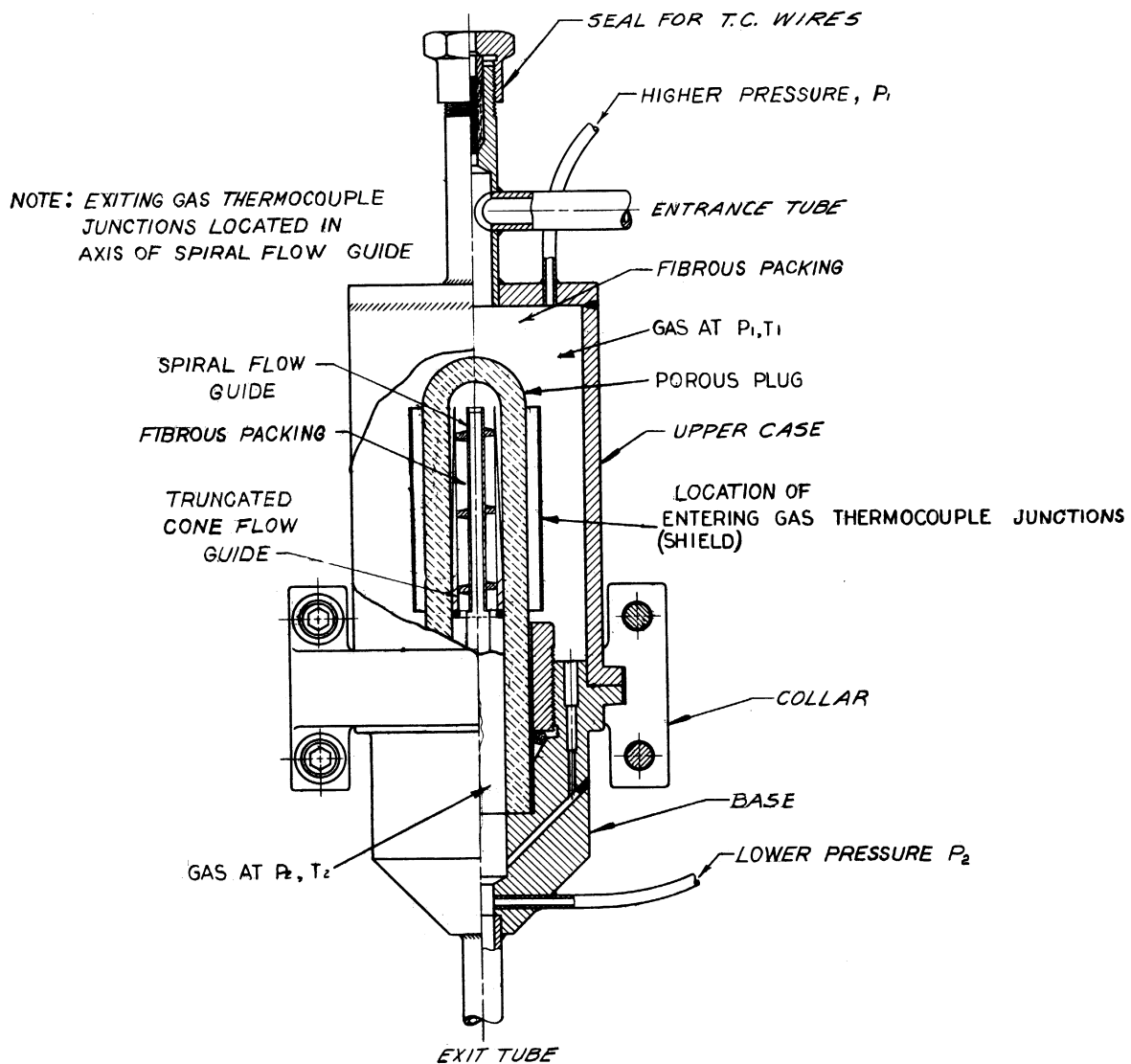


Figure 22. Joule-Thomson Throttle Assembly Drawing

for the light hydrocarbons over the range of temperatures and pressures anticipated in the present research would result in a decrease in temperature with isenthalpic expansion. Therefore, the problem will be discussed for this case. The method is equally applicable, however, for the case where an increase in temperature with isenthalpic expansion occurs; in fact, in general the problem is somewhat simpler under these conditions.

The temperature of the fluid within the outer plug chamber (Figure 22) is approximately at the temperature of the surroundings, since the entire expansion device is immersed in a stirred constant temperature liquid bath through which the fluid flows in a conditioning coil prior to entering the Joule-Thomson device. More precisely, the radial variation in temperature at a given position along the plug should be very small after a certain, small, radial distance from the outer plug surface is reached. (The fact that a radial temperature variation does exist, however, will be explained at a later point in the discussion.) A fibrous material is packed around the outside of the porous plug so as to fill the plug chamber completely (Figure 22). This packing serves two functions. It eliminates gross convection currents within the outer plug chamber. Secondly, it prevents radiation of energy between the plug surroundings and the outer plug surface.

We will ignore for a moment any heat transfer by conduction along the length of the plug, from the plug base, and also by conduction to the outer plug surface due to the presence of the fibrous packing. It is apparent that under these conditions, and with the further assumption that the fluid and plug material have no thermal conductivity, that



a fluid-determined temperature gradient would exist between the outer surface of the plug and its inner surface. Furthermore, under these conditions, the magnitude of the temperature gradient would be much greater near the inner surface of the plug. This is so because the major portion of the pressure drop is near the inner surface of the plug (a proportionate increase in specific volume of the fluid occurs with pressure drop and the same mass flow must pass every radial cross section of the plug).

Since the fluid and plug do have thermal conductivity, heat will be moved forward in the direction of flow. This in turn will tend to more nearly equalize the temperature of radial positions through the plug -- since energy for forward conduction is supplied at each point by the heat capacity of the fluid. Thus, the fluid temperature will drop at a greater rate than it would be simply expanding. This implies that energy will be moved forward, also, from the fluid near the outside surface of the plug and to some extent by the small conductivity of the porous packing. Therefore, a temperature gradient exists for some distance away from the plug surface, i.e., the outer plug surface is at a lower temperature than the bath fluid, the fibrous packing, or the fluid approaching the plug.

If we continue to neglect for the present conduction from the plug base to the plug, the following observations may be made:

1. The plug is physically separated from the surroundings (the low temperature bath) and fibrous insulation discourages gross convective heat transfer or heat transfer by radiation between the surroundings and the plug.

2. The surroundings are at a temperature not greatly different from that of the outer plug surface.
3. If the fluid near the plug is replaced at a sufficiently high rate and/or if its heat capacity is sufficiently high, the temperature gradient in the outer plug chamber would be very small at a small distance from the outer plug surface.
4. The temperatures of fluid elements in the outer plug chamber, along the length of the plug, would be the same at equal radial positions.

It is true that it would be possible in a linear flow system such as used by Brown and Associates (39,53,62,64,73,82,131) or Vogel, Noel, and Hausen<sup>(46)</sup> to both insulate the device and also adjust the temperature of the surroundings to a point near that of the measurements. In the work of Brown and Associates, the device was well insulated but the temperature of the surroundings was not adjusted to the temperature of the measurements. A large amount of insulation was required and, even so, a tremendous flow rate to offset the effect of heat transfer with the surroundings. In the work of Vogel, Noel, and Hausen<sup>(46)</sup>, the temperature of the surroundings was adjusted, but the system was not isolated, and the temperature along the steel tube boundary of this system did not match the gradient through the asbestos. In general, in a system that is not radial, but linear, the temperature gradient along the boundaries must be matched along the entire length of the flow resistance if no heat leakage is to occur. In the radial problem that we have considered thus far, this would not have to be the case. A uniform boundary condition of the surroundings over the length of the plug would suffice.

In the practical application of the radial technique, other difficulties occur. One difficulty is that, since the porous plug has the property of thermal conductivity and since the temperature of the plug is lower than that of the plug support or base, heat will tend to flow upward along the walls of the porous plug. It is possible to combat this effect by using a device, such as is shown in the interior of the plug in Figure 22, which divides the flow through the plug. The flow below the internal division passes through the plug near its base and carries away heat flowing from the plug support, without contacting the sensitive portion of the device measuring the expanded gas temperature. This procedure, while it solves one problem, introduces a second; the fluid being wasted at the plug base carries away energy from the fluid being used. Not contacting the fluid being wasted with the second temperature measuring device would not matter if the radial temperature distribution near the exterior plug surface was truly independent of linear position along the plug. Since, however, there is a component of flow toward the base of the plug the fluid temperature at a given radial position will decrease from the top to bottom of the plug and part of the energy of the fluid being used will be lost -- by conduction to the fluid flowing through the lower portion of the plug. The use of a small portion of the flow to eliminate heat gains through the plug base is a compromise.

The temperature of the fluid before passing through the porous plug may be measured at several points. Roebuck<sup>(95)</sup> measured this initial fluid temperature just as it entered a plug chamber. This will not, of course, give the average temperature just before passing through the plug.

The error will depend on the size of the heat leaks involved and the replacement of heat capacity at a point by the flowing fluid.

In view of the fact that a multiple junction copper constantan difference thermocouple was to be used to measure the temperature change of the fluid, it was thought to be convenient to distribute one set of the junctions around the exterior surface of the plug. By placing the entrance thermocouple junctions on a thin surface of aluminum foil, around the portion of the exterior plug surface above the point of internal division (see Figure 22), something of an average fluid temperature immediately before passing through the plug may be obtained. This will not be the proper average temperature, however, for the following reasons: the junctions are subject to some heat transfer other than with the fluid about to enter the plug, different residence times of fluid masses are not properly averaged by the junctions thermally connected by the aluminum foil, part of the fluid effecting the junctions will not, at least immediately, enter the plug above the internal division of flow. Nevertheless, this was thought to be the best simple procedure for measurement of the initial fluid temperature. The use of aluminum foil for the location of the thermocouple junction aids somewhat in retarding heat transfer by radiation between the surroundings, the thermocouples, and the exterior plug surface.

The flow through different portions of the interior surface of the plug may be conveniently mixed inside the plug prior to passing the exit junctions of the thermocouple (located in the axis of the spiral flow guide, Figure 22). The portion of the flow which enters the plug above the internal division of flow returns to the inside hemispherical top of

the plug, joins the flow through the top, and then flows down around the helix. The fins and hollow axis of the helix are copper. The hollow tube which supports the helix (inserted into the axis of the helix) is constructed of stainless steel, Figure 22.

If the flow through various portions of the plug surface were not mixed, the measured temperature difference would generally tend to be too low. This is because the flow entering near the top of the plug would be in contact with the temperature measuring device longer than the flow which entered at any position closer to the plug base and hence would, exert the most influence. The flow entering near the top of the plug is at a higher temperature than fluid entering at any position along the plug since it is this portion of fluid that has lost the least heat prior to passage through the plug. Mixing the fluid prior to passing the exit thermocouple junctions also tends to minimize the problem of inhomogeneity in the plug surface.

In regard to the internal flow guide arrangement, it should be observed that the design included an effort to maintain a constant velocity of flow inside the plug at all points. Specifically, the following precautions were taken:

1. The annular area for flow between the interior surface of the plug and the surface of the truncated-cone flow guide was made very nearly proportional to the amount of fluid flowing, at each longitudinal position.
2. The cross sectional area for flow around the helix was made such that the fluid velocity would be the same as would occur at all points inside the plug.

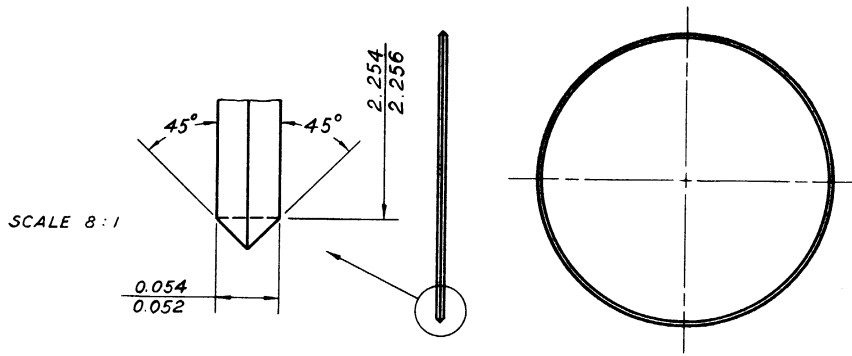
Other mechanical details of the Joule-Thomson device need only be mentioned briefly.

Pressure taps, as shown in Figure 22, were installed for measuring the pressure change of the fluid and also the absolute pressure of each measurement. It was intended that a dead weight pressure balance be used for this purpose. It was not thought that any appreciable difference in pressure would exist between the points of location of the taps and the pressures existing at the points of temperature measurement.

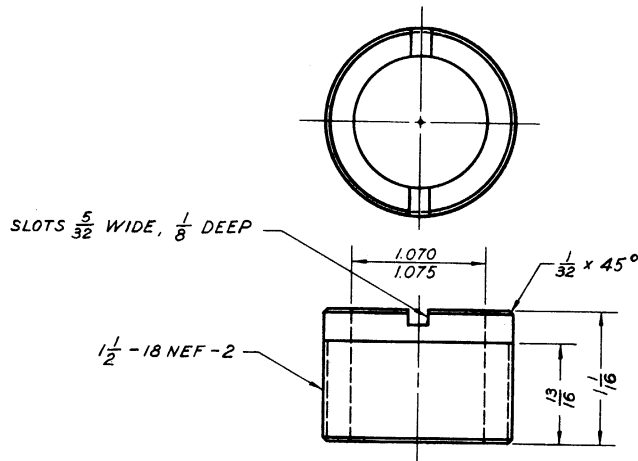
Each of the set of interchangeable porous plugs was fitted with a tight stainless steel sleeve around its base. The sleeves were cemented to the porcelain plugs with a bonding agent. The pressure seal between the high and low pressure sides of the plug consisted of a Teflon O-ring compressed against the metal sleeve of the plug as shown in Figures 22 and 23. The higher pressure on the outside of the plug aids in producing this pressure seal.

The thermocouple wires will be brought from the higher to the lower pressure sides of the plug through a series of holes drilled in the lower stainless steel base. A copper and constantan wire would be brought through each of the 12 holes and sealed near the top of the lower base by means of a bonding agent or ceramic-type material. This phase of the construction was not completed during the present portion of the investigation. The method described for sealing the thermocouples will involve a number of problems, including the possibility of straining the thermocouple wire. It may be necessary to remove the wires from the expansion device through a different type pressure seal.

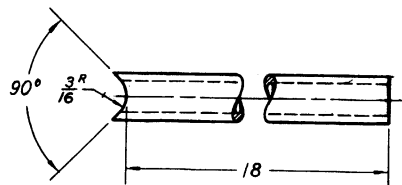




SEAL RING  
COPPER 1 REQ'D



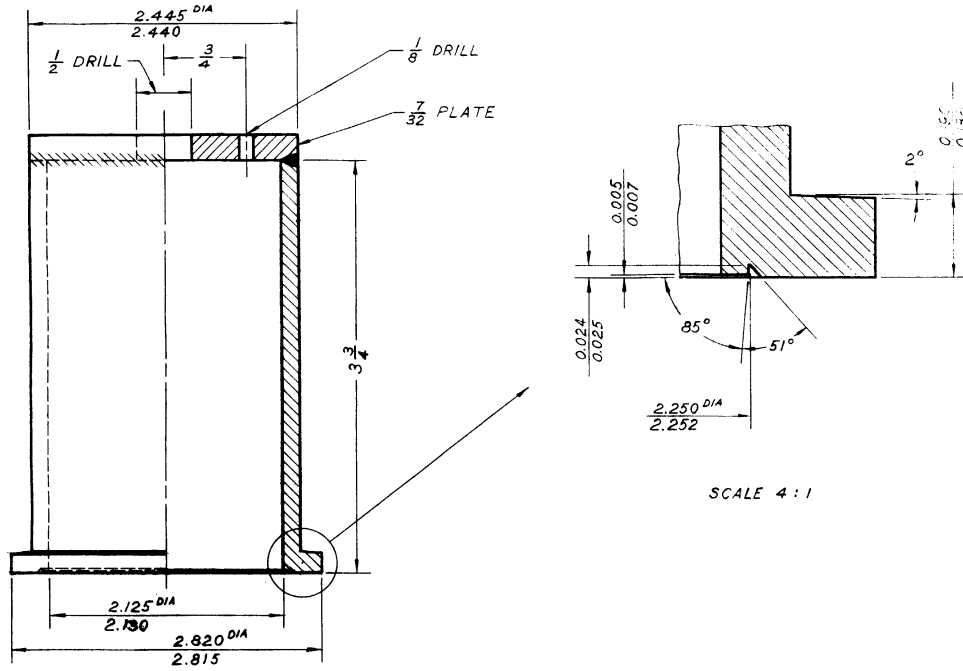
NUT  
304 SS 1 REQ'D



ENTRANCE TUBE  
 $\frac{3}{8}$  OD,  $\frac{1}{4}$  ID, 304 SS TUBING 1 REQ'D

Figure 23. Joule-Thomson Throttle Detail Drawings (Cont'd)

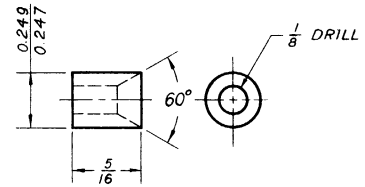




SCALE 4 : 1

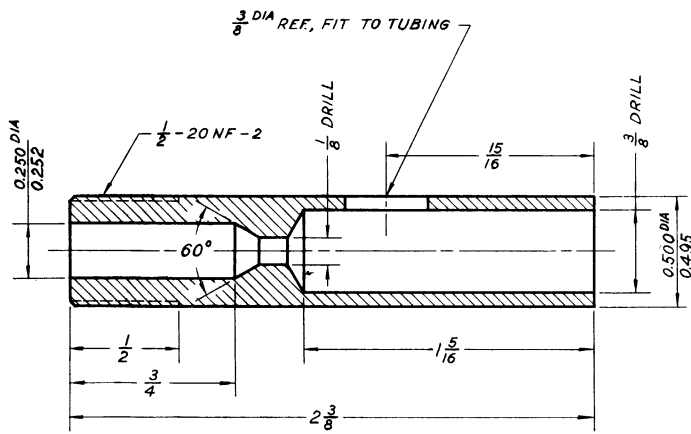
**SHELL (UPPER CASE)**

304 SS 1 REQ'D  
SCALE FULL SIZE



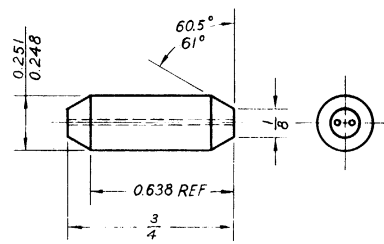
**GLAND**

304 SS 1 REQ'D  
SCALE 2 : 1



**SEAL FOR THERMOCOUPLE WIRES**

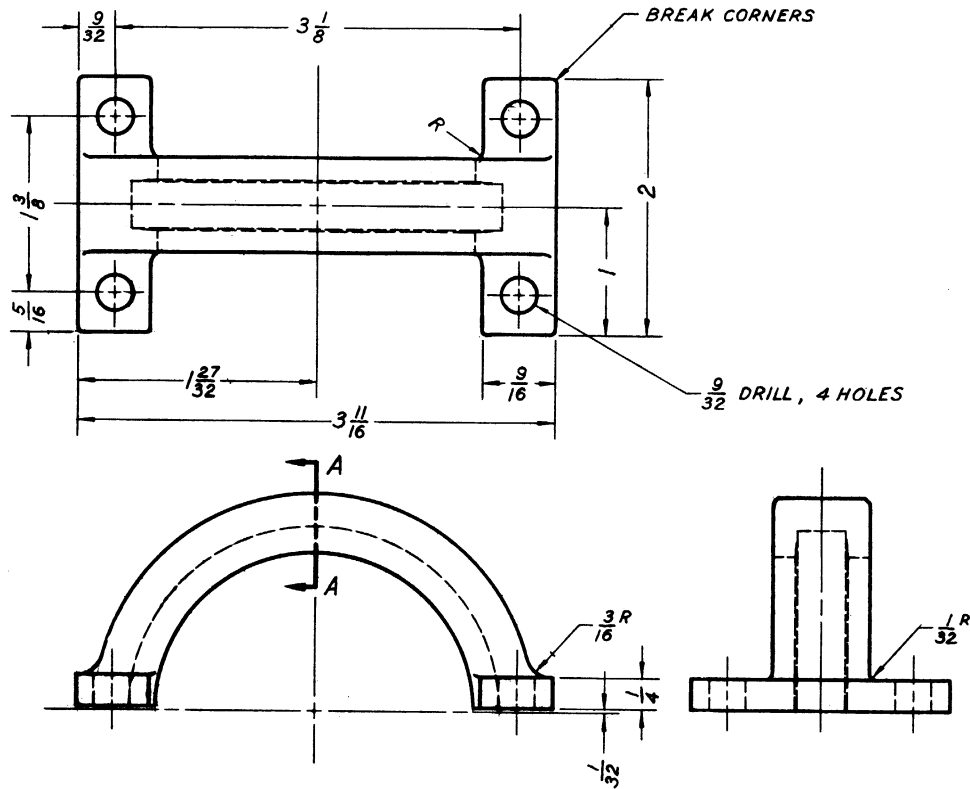
304 SS 1 REQ'D  
SCALE 2 : 1



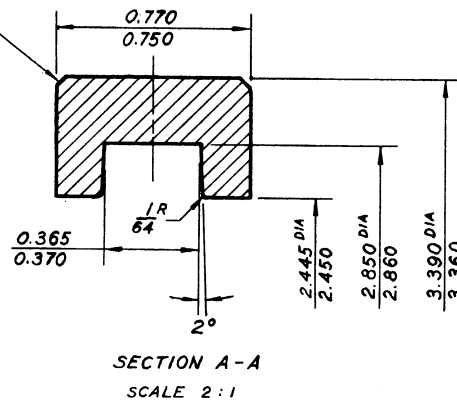
**PACKING**

TEFLON 1 REQ'D  
SCALE 2 : 1

Figure 23. Joule-Thomson Throttle Detail Drawings (Cont'd)



**COLLAR (HALF)**  
 304 SS 1 REQ'D  
 SCALE FULL SIZE



OTHER HALF WITH 4  $\frac{1}{4}$ -20NC-2 TAPPED  
 HOLES IN PLACE OF 4  $\frac{9}{32}$  DRILLED HOLES.

REQ'D 4  $\frac{1}{4}$ -20NC-2  $\times$   $\frac{5}{8}$  SOCKET HD. CAP SCR.  
 4  $\frac{1}{4}$  MEDIUM LOCK WASHERS.

Figure 23. Joule-Thomson Throttle Detail Drawings (Cont'd)

The two copper lead wires from the multiple junction thermocouple will be removed from the plug chamber through a glass-impregnated Teflon seal (shown in Figure 23) or a ceramic seal.

#### Vacuum System

In order to reduce the heat transfer between portions of the calorimeter at different temperatures a vacuum system was provided consisting of the following items: a Cenco Hy-Vac 7 vacuum pump; a Cenco OD-25 all metal diffusion pump; metal tubing and valves; a cold trap; a Lippincot McLeod gauge.

The vacuum pump has a free air displacement of 70 liters per minute, a pumping speed of 0.525 liters per second at one micron of mercury, and a guaranteed vacuum of 0.1 microns of mercury. The diffusion pump has a pumping speed of 28 liters per second at  $10^{-4}$  millimeters of mercury using Cenco DC 702 silicone oil.

Connections from the vacuum pump to the diffusion pump were made with brass tubing. Brass tubing having an internal diameter of 1-3/8 inches was extended from the diffusion pump to a flanged connection with the calorimeter vacuum line. A metal tubing connection was made to the main vacuum line so that rubber tubing could be extended to the McLeod gauge. All metal tubing joints were silver soldered and then coated with Glyptol.

#### Precision Electrical Measurements

It was necessary to purchase a potentiometer for the widely different problems of low voltage thermocouple measurements and higher voltage measurements associated with the calorimeter power circuit (Figure 24)

and platinum resistance thermometer circuit (Figure 25). It was felt that a White potentiometer (0-100,000 microvolts), manufactured by Leeds and Northrup, would be suitable for this purpose. It was learned, however, that this potentiometer had been removed from the market. After a study of other potentiometers available, it was decided that a Leeds and Northrup Model K3 would be satisfactory. The principal features of the K3 potentiometer are listed in Table XXIII of Appendix E,

#### Low Voltage Measurements

Because of the anticipated high accuracy thermocouple measurements the matter of thermal emf's, AC pickup, and other spurious emf's was given careful consideration. The following principal items were of interest in considering the applicability of the Model K3 potentiometer to low voltage measurements:

1. Switch contacts in the K3 potentiometer which are in direct series with the emf terminals are made thermally astatic.
2. Attenuation of thermal emf's is accomplished before they appear in the measuring circuit.
3. External connections to the potentiometer are made to copper binding posts.
4. A divided circuit permits a true potentiometer zero.
5. The wiring plan is arranged to minimize inductance loop effects.
6. The potentiometer is shielded to avoid electrostatic problems.

7. The potentiometer has guarded circuits to prevent leakage currents between certain critical points and the guards may be extended to external circuits.

The potentiometer guard system was extended to the potentiometer battery, the standard cell, and the galvanometer. This was done by placing each of these accessories on a sheet of polystyrene situated on a copper plate, and employing guarded leads. The guards were connected to the copper plates on one end and to appropriate potentiometer binding posts on the other end. The battery and standard cell were housed in closed wooden boxes.

Selection of the particular circuit to be read with the potentiometer was made by means of two Leeds and Northrup type 31-3 rotary selector switches (two pole 12-position switches) connected in series. The various circuits which were measured by the potentiometer are listed in Table VII.

The Leeds and Northrup 31-3 switch is a shorting switch: as the shaft is rotated the brushes make contact with the next segment before leaving the previous segment. The stationary contacts are of solid silver while the brushes are a silver alloy. Contact resistance is less than 0.001 ohms, maximum impedance less than 0.03 microhenries, capacitance between points less than 0.5 micro-micro-farads. Transient thermal emf on switching at normal speeds is less than 1.0 microvolt.

Both selector switches as well as all attendant circuitry for precision thermocouple, platinum resistance thermometer, and calorimeter power measurements are housed in a lucite box. The front side of the box is part of a piece of linen bakelite which serves as an electrical panel

TABLE VII  
POTENTIOMETRIC SWITCH POSITIONS

Potentiometric Switch Position	Measurement	Indicated Schematically
L1	Calorimeter heater voltage	Figure 24
L2	Calorimeter power supply current	" 24
L3	Platinum thermometer current	" 25
L4	Platinum thermometer voltage	" 25
L5	System difference thermocouple 5a	" 7
L6	System difference thermocouple 8a	" 7
L7	Calorimeter difference thermocouple AB	" 15
L8	" " " AC	" 15
L9	" " " AD	" 15
L10	" " " AE	" 15
R1	" " " AF	" 15
R2	" " " JG	" 15
R3	" " " NH	" 15
R4	" " " JI	" 15
R5	" " " FJ	" 15
R6	" " " NK	" 15
R7	" " " LJ	" 15
R8	" " " NM	" 15
R9	" " " NL	" 15
R10	" " " ON	" 15
R11	Main calorimeter difference thermocouple 12*	" 15

\* Main calorimeter junction: 1 inlet, 2 exit

NOTE: Order of appearance of letters designating calorimeter difference thermocouples indicates sense of temperature difference for same potentiometric polarity; e.g. if L7, R4, R11 have same polarity and Temperature 2 > Temperature 1 - then Temperature B > Temperature A, Temperature I > Temperature J, etc.

for the entire system (Figure 12). The rotary switches, standard resistors, heliopot, etc., are mounted inside the plastic box. Operation of the switches and heliopot is accomplished at the top of the bakelite panelled-front by means of knobs attached to the respective shafts, which are brought through the bakelite. Wiring inside the plastic box was accomplished with No. 12 heavy copper buss bar wire in order to minimize resistance in certain portions of the circuit where it is important.

The lucite box has the following purposes:

1. To insure that circuit components where dissimilar metal contacts, inhomogeneities, or strains occur are at the same temperature.
2. To maintain circuit resistances at a relatively constant, known temperature.
3. To prevent dust and other contaminants from depositing on the standard resistors, switches, etc.
4. To protect the relatively delicate circuitry from damage.

Connections to components external to the lucite box were made with a series of pure copper binding posts which were brought through the lucite box and bakelite panel. Connections on the inside of the box to the binding posts were made by soldering with a special thermal-free solder. Connections were made to the binding posts on the outside by means of copper lugs and threaded copper nuts. All wires which were brought to the components inside the lucite box were copper.

### Potentiometer Standard Cell

A Leeds and Northrup No. 7308 Eppley unsaturated standard cell was employed. It's voltage tends to change at the rate of about 100 microvolts per year (0.01%), but for the present investigation it was considered preferable to a saturated cell which has a much higher temperature coefficient and would require an oil bath.

### Potentiometer Battery

A Leeds and Northrup No. 7597 2-volt low discharge cell with about 200 amp-hours of service before recharging was used.

### Galvanometer

The galvanometer is a Leeds and Northrup high sensitivity DC reflecting type instrument, Model 2284-X. It was built to specifications in order to obtain the desired high sensitivity, a fairly high critical damping resistance, and a reasonable period. These characteristics are: Sensitivity, 0.14 microvolts per millimeter at one meter; CDRX, 190 ohms; Period, 6.0 seconds. The internal resistance of the galvanometer is approximately 30 ohms.

The galvanometer reading device consists of a telescope, a scale, and a fluorescent light. The telescope was mounted on a heavy metal stand which could be leveled. The telescope was placed at a distance of 3 meters from the galvanometer, giving an effective galvanometer sensitivity of about 0.05 microvolts per millimeter. Initially it was planned to employ a calibrated White potentiometer and a calibrated deflection technique of galvanometer operation. Since a Leeds and Northrup K3 potentiometer with a slidewire was used instead, a null method of



galvanometer operation was employed. In view of the fact that a null method was used, careful critical damping of all measuring circuits and the use of properly curved scale were not necessary; there was no problem of maintaining linearity of galvanometer deflections.

The galvanometer was mounted on an extremely elaborate galvanometer stand consisting of a heavy steel plate and a system of springs and dashpots. This stand was constructed to combat a severe vibration problem in the Automotive Engineering Building caused by the operation of a number of large test engines, the liquid nitrogen machine, and the compressor used in the present investigation.

#### Calorimeter Power Supply and Power Measurement

The power supply used in the present investigation was a Lambda model 65M electronically regulated DC power supply. The DC voltage output may be varied continuously from 0 to 100 VDC. The maximum current is 600 milliamperes. Line regulation is better than 0.15% or 0.3 volts (whichever is greater) and load regulation is better than 0.25% or 0.3 volts. Ripple and noise is less than 5 millivolts rms. Either side of the output may be grounded. The maximum power consumption by the power supply is 585 watts at 105-125 VAC.

#### Calorimeter Heater Circuit

A double pole switch places the power supply in series with rheostats of maximum resistance 720 ohms, 90 ohms, 5.6 ohms, 1.0 ohm, the calorimeter heater of approximately 147 ohms resistance at room temperature, and a 0.1 ohm (nominal) standard resistor (Figure 24).

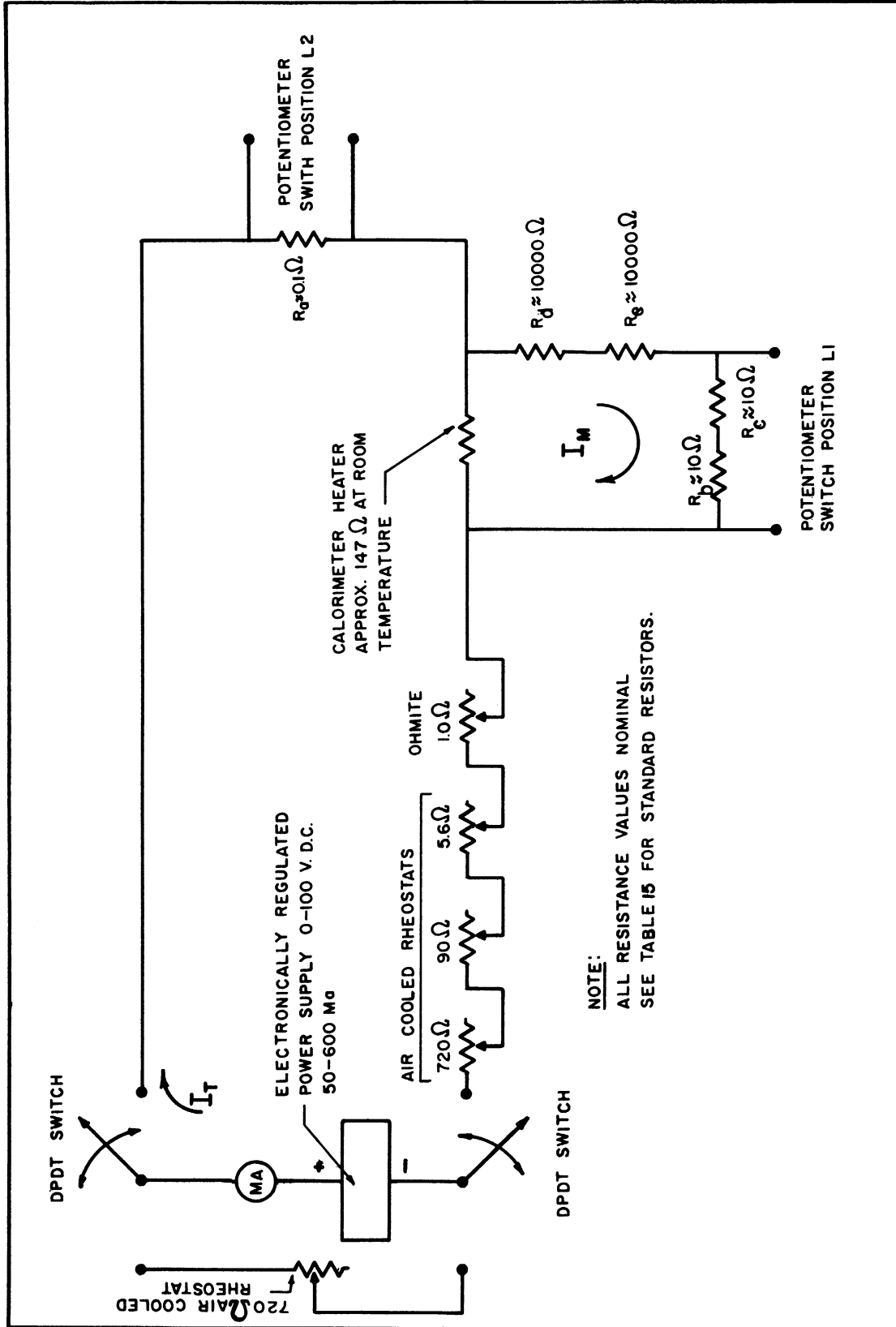


Figure 24. Calorimeter Heater Circuit

Adjusting the control rheostats permits setting the flow of current through the calorimeter heater very accurately, once the power supply voltage has been chosen. Approximate adjustment of this current can be made by observing the power supply ammeter.

The power being dissipated in the DC calorimeter heater is measured by determining the current flowing through the heater and the voltage drop across it and applying the relation:

$$W_C = E_C I_C \quad (20)$$

$W_C$  = Power dissipated in the calorimeter heater, watts

$E_C$  = Voltage drop across calorimeter heater, volts

$I_C$  = Current passing through calorimeter heater, amperes

The resistance of each of the standard resistors shown in Figure 24 may be expressed as:

$$R_T = R_{25} [1 + a(T-25) + \beta (T-25)^2] \quad (21)$$

$R_T$  = Resistance at temperature T, absolute ohms

$R_{25}$  = Resistance at 25°C, absolute ohms

T = Temperature, degrees centigrade

$a, \beta$  = Constants

No temperature correction was made in the present investigation for the changes in resistance due to temperature, of the standard resistors, i.e. it was assumed that  $R_T = R_{25}$  in Equation (21). This involved no significant error in determining  $E_C$  and  $I_C$ , Equation (20).

The quantity  $E_C$  in Equation (20) is given by:

$$E_C = \left( \frac{R_b + R_c + R_d + R_e}{R_b + R_c} \right) E_{L_1} \quad (22)$$

$E_C$  = Voltage drop across calorimeter heater, volts

$E_{L_1}$  = Voltage measured at switch position  $L_1$ , volts

(Figure 24)

$R_b, R_c, R_d, R_e$  = Resistance of standard resistors at 25°C, absolute ohms (Figure 24, Table XV)

There was no error of importance because of IR drop in the wires of the multiplying loop, Figure 24. Separate potential taps were run from the calorimeter heater. The wire size of the potential taps is No. 22 for a short distance inside the calorimeter. Beyond the vicinity of the calorimeter the wire size was increased to No. 12. A Buss bar was placed between the two 10 ohms resistors and between the two 10,000 ohms resistors. This is particularly important in the case of the 10 ohms resistors ( $R_b, R_c$ ) since inspection of Equation (22) reveals that a small unknown resistance in this portion of the measuring loop could result in a serious error in measuring the calorimeter heater voltage drop.

At potentiometer balance there is no flow of current into the potentiometer circuit via switch position  $L_1$ , Figure 24.

The total current flowing through the loop containing the power supply (Figure 24) may be calculated from the relation:

$$I_T = \frac{E_{L_2}}{R_a} \quad (23)$$

$I_T$  = Current flowing through power supply, amperes

$E_{L_2}$  = Voltage measured at switch position  $L_2$ , volts

(Figure 24)

$R_a$  = Resistance of standard resistor at 25°C, ohms  
(Figure 24, Table XV)

The net current flowing through the calorimeter heater may be found by subtracting the current flowing through the measuring loop,  $I_M$ , from the total current flowing through the power supply:

$$I_C = I_T - I_M \quad (24)$$

$I_C$  = Current passing through calorimeter heater, amperes

$I_T$  = Total current flowing through power supply loop, amperes

$I_M$  = Measuring current, amperes

$I_M$  is given by:

$$I_M = \frac{E_{L1}}{R_b + R_c} \quad (25)$$

Measurement of the Operating  
Temperature of the Low Temperature Bath

The initial temperature for calorimetric measurements was determined by means of a platinum resistance thermometer located in the low temperature bath. The potentiometric method of platinum thermometry was employed, Figure 25. The resistance of the platinum at temperature T was determined from the relation:

$$R_T = \frac{E_P}{I_P} \quad (26)$$

$R_T$  = Resistance of the platinum coil at temperature T,  
absolute ohms

$E_P$  = Voltage drop across the platinum coil, volts

$I_P$  = Current passing through the platinum coil, amperes

A two volt, low discharge cell was the source of the measuring current. Several hours prior to operation, the double pole, double throw switch shown in Figure 25 was placed in the warm-up position. This placed a 2,000 ohm helipot in series with the battery and a milliammeter. After

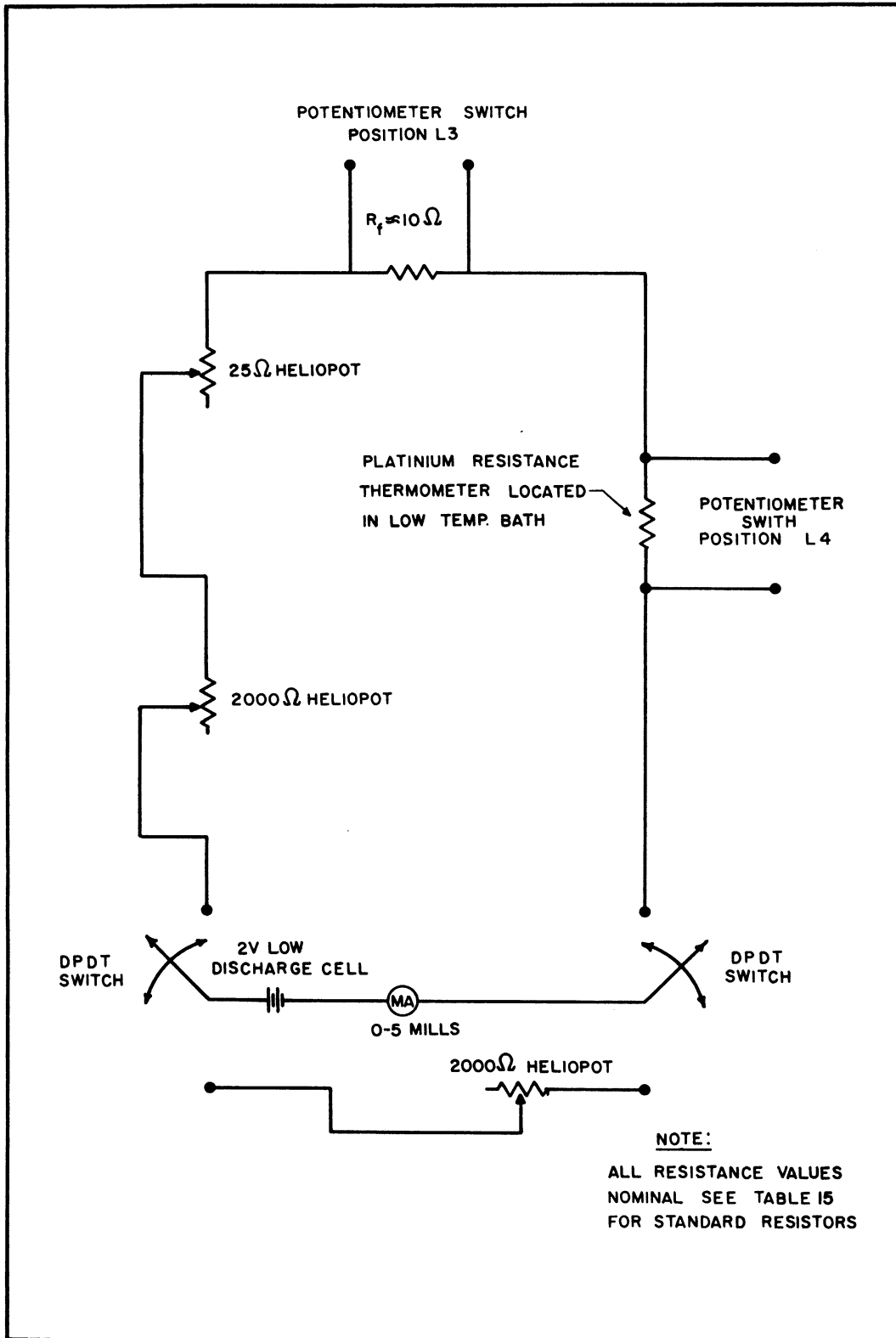


Figure 25. Platinum Resistance Thermometer Circuit

the current had stabilized, and before measurements were begun, the switch was positioned so as to place a 2,000 ohm heliopot, a 25 ohm heliopot, a 10 ohm standard resistor, and the resistance thermometer in series with the current source and milliammeter.

The current,  $I_P$ , through the platinum resistance thermometer was calculated from the known value of resistance of the standard resistor and the voltage drop across it:

$$I_P = \frac{E_{L3}}{R_f} \quad (27)$$

$I_P$  = Current passing through the platinum coil,  
amperes

$E_{L3}$  = Voltage measured at switch position  $L_3$ , volts  
(Figure 25)

$R_f$  = Resistance of standard resistor, absolute ohms  
(Figure 25, Table XV)

The voltage drop across the platinum coil was measured directly at potentiometric switch position  $L_4$ :

$$E_P = E_{L4} \quad (28)$$

Separate potential taps were run to the four terminal resistance thermometer.

#### Measurement of Flow Rate

It was desirable to have an approximate indication of surges and drifts in flow rate on the low pressure side of the system. It was necessary to have also an accurate measure of the mass flow rate through

the calorimeter. In order to accomplish the former objective an orifice was placed in the line from the metering bath to the compressor supply tank, Figure 7. Pressure taps from the upstream and downstream sides of the orifice were connected to a high pressure mercury manometer which could be used to measure a pressure difference as large as 36 inches of mercury. Shutoff valves were placed on both sides of the manometer. A similar valve was installed between the low and high pressure sides for equalizing the pressure on the mercury prior to opening or closing the shut-off valves.

In order to obtain an accurate measure of the mass flow rate through the calorimeter a linear flow meter was installed. A description of the method of calibration and operation of the meter is given in Calibration of the Equipment, Appendix B and Sample Calculation of Iso-baric Specific Heat, Appendix D. A description of the flow metering system is given in the discussion that follows. In general, the metering temperature was held constant but the metering pressure was allowed to vary in order to obtain a satisfactory combination of system operating variables. It was necessary therefore to calibrate the meter at several pressures. Accurate measurement of metering pressure and temperature were necessary during operation of the flow system in order to determine accurately the viscosity and density of the fluid.

#### Linear Flow Meter

The primary element of the metering system is a National Instrument Laboratory's linear flow meter. This flow meter consists basically of a number of small, identical flow channels through which the gas flows



at a very low Reynolds number. The flow gives rise to a small pressure drop which is measured by means of a U-tube containing water and a cathetometer. The pressure drop across the meter is very nearly proportional to flow rate, hence the name linear flow meter.

Mathematically, the relation between volumetric flow rate and differential pressure in a simple flow restriction may be expressed as:

$$\Delta P = b\mu\dot{V} + a\dot{V}^2 \quad (29)$$

$\Delta P$  = Pressure drop across the flow restriction

$\mu$  = Viscosity of the fluid being metered at metering temperature and pressure

$\dot{V}$  = Volumetric flow rate

$a, b$  = Calibration constants

[Equation (29) was expressed in terms of mass flow rate and fluid density at the metering pressure and temperature for convenience, see Calibration of the Equipment, Appendix B.] If a flow element is constructed so that  $a \approx 0$ , the element is termed linear. On the other hand, if  $b \approx 0$  the meter is termed a square root or Bernoulli element. With an orifice and other Bernoulli type instruments it is sometimes difficult to maintain a sufficiently high Reynolds number at low flow rates and errors due to viscosity become large. Similarly, if a linear element is operated above its maximum designated flow rate, errors due to gas density become important. In metering problems involving the very accurate measurement of small quantities of a gas, and where an upper-bound can be placed on the flow rate to be measured, it is thought to be easier to design a reliable

linear meter. For an instrument such as the National Instrument Laboratory's linear meter, all that is required for a very high degree of linearity is that the Reynolds number be less than about 400.

Relative to the purposes of the present investigation, a linear flow meter offers certain advantages in comparison with a Bernouli type element:

1. Calibration of a linear element does not depend on upstream conditions of turbulence or velocity profile.
2. Slight variations in flow can be averaged more easily in a linear meter than in a Bernouli meter.
3. The flow rate through a linear meter may be reduced from the maximum value specified (by compressor output in the present investigation) to a zero flow rate with no adverse effects due to a low Reynolds number, as would occur in a Bernouli element.
4. The flow rate through the meter may be reduced to practically zero with no appreciable loss in metering accuracy due to a changing meter sensitivity.

The maximum allowable flow rate through the linear element which was employed in the present investigation was approximately 0.3 lb/min. This corresponded to a maximum pressure differential across the meter of 10 inches of water. A National Instrument Laboratory's U-tube and cathetometer used to measure the pressure difference across the flow meter (Figure 7) had an overall accuracy of about  $\pm 0.0015$  inches of water, thus allowing an accuracy of 0.1% in measurement of pressure difference down to 1.5 inches of water.

### U-Tube and Cathetometer

The U-tube consists of two 3/4 inch glass legs, each 12 inches long, connected by a small channel at the bottom. The two glass legs are rated for a safe working pressure of 150 psia. A plastic shield was installed for protection of personnel, however. Two sliding carriages, with coarse and fine position adjustment are used to determine the water level in each of the legs of the U-tube. The reading mechanism includes a fixed scale between the two legs of the U-tube for determining tenths of an inch and two fixed scales and verniers for determining hundredths and thousandths of an inch of water differential.

### Measurement of Metering Pressure

The pressure on the low pressure side of the flow meter is measured using a sixteen inch Heise Bourdon tube gauge having a full scale range of 150 psig. The smallest subdivisions on the gauge are 0.05 psi and the gauge can be read easily to 0.01 psi. The gauge has an estimated accuracy of 0.15 psi over the full range with careful calibration and use. A device was installed in the line to the pressure gauge to prevent a pressure in excess of 140 psig being applied to the gauge. Shut-off valves and an equalizing valve were installed for the U-tube and pressure gauge, Figure 7. Another valve was installed for venting the U-tube and pressure gauge.

### Control and Measurement of Metering Temperature

In order to insure a constancy of metering temperature, the linear flow element was installed in a constant temperature water bath. Gas destined for the meter flowed through a section of high pressure

tubing which had been wrapped with an electrical resistance heater and which contained a thermocouple installation. It then passed through a coil of copper tubing in the water bath. The power dissipation in the electrical heater was controlled by means of a variac so that the flowing gas temperature approached closely the temperature of the metering bath. The approach to metering bath temperature was observed in two ways. First, the flowing gas temperature was measured by means of a copper-constantan thermocouple installed in the line after the electrical heater and before the water bath and read as position 8b on a Honeywell indicating potentiometer. Secondly, the voltage generated between this flowing gas junction and a copper-constantan junction located in the water bath was measured using the Leeds and Northrup K3 potentiometer at potentiometric switch position 16, Table VII. This measurement is designated 8a in Figure 7. The dual function of the flowing gas junction was controlled by means of a copper double pole, double throw switch -- thermally insulated to prevent spurious emf's due to dissimilar metal contacts at the switch.

The constant temperature metering bath consists of a large carbon steel tank with an 18-8 type 304 stainless steel liner. The outside dimensions are 32 inches x 32 inches x 28 inches (depth) and the inside dimensions 28 inches x 28 inches x 26 inches (depth). The bath temperature is controlled by means of a mercury thermoregulator, a relay, two 250 watt heaters, a cooling coil, and a centrifugal stirrer. The bath temperature can be controlled to within 0.02°F. Measurement of the bath temperature is accomplished with a calibrated mercury-in-glass thermometer completely submerged in the bath liquid.

### Measurement of System Pressures

A number of Bourdon tube pressure gauges and a differential pressure balance were employed in measuring system pressures. A 3,000 psig gauge was installed at the panel board for the purpose of indicating the discharge pressure of the Hofer compressor. A 2,000 psi gauge was installed to measure the compressor suction pressure. Replacement with a 200 psi gauge was planned, but never carried out. Two 3,000 psi gauges were installed to indicate the approximate pressures at the calorimeter and Joule-Thomson throttle, Figure 26. At the panel board, a series of five 3,000 psi cylinder gauges indicated the pressures in the five high pressure supply and buffering cylinders, Figure 7.

### Calorimetric and Joule-Thomson Pressure Measurements

Absolute pressures at the calorimeter and Joule-Thomson throttle as well as the pressure drop across the porous plugs during isenthalpic measurements may be determined by means of a differential dead weight pressure balance, Figure 26. Fluid is admitted to two sides of the pressure measuring system from the upstream and downstream sides of the flow devices or the low pressure side of the system may be opened to the atmosphere. Bleed valves allow venting the pressure after measurement with the differential dead weight pressure balance.

The pressure balance was loaned through the courtesy of Dr. J.R. Roebuck of the Physics Department of the University of Wisconsin. The mechanical details of the pressure balance have been previously described by Roebuck<sup>(93)</sup> who built the instrument. It has since been modified somewhat. Basically, the instrument balances, by means of a set of calibrated

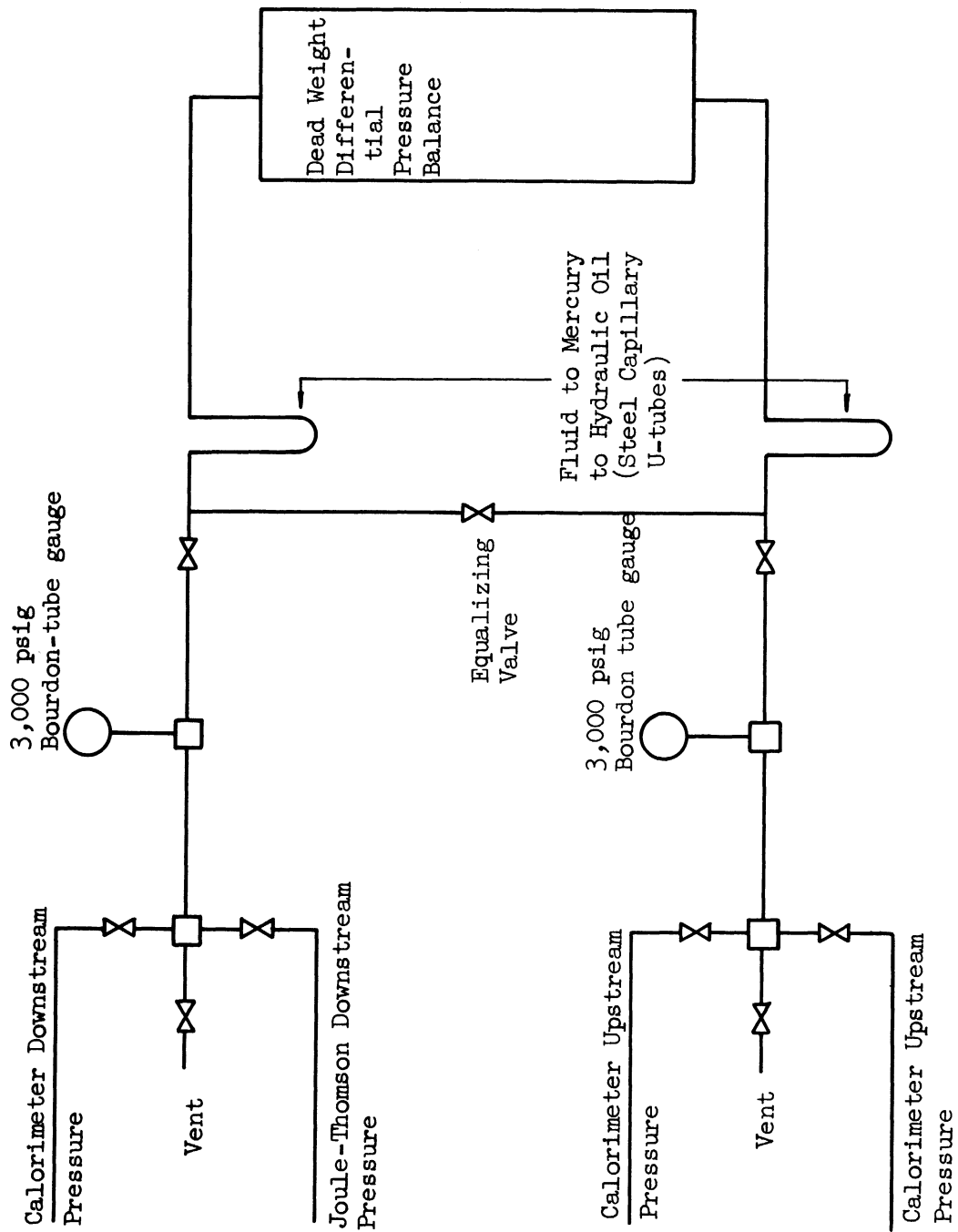


Figure 26. Calorimeter and Joule-Thomson Pressure Measurements

weights, the difference in pressure applied at the opposite ends of a vertical piston, Figure 11.

Two high pressure cylinders are held on a common axis by means of a cast iron frame so that the opposite ends of the piston move into or out of them. The contents of each cylinder are made pressure tight with respect to the moving piston by a stuffing box. At the center of the piston is located a cylindrical drum which rotates the piston, to eliminate static friction at the stuffing boxes. The drum is turned through a system of pulleys and belts by an electric motor. There are two belts attached to the drum; one is the drive belt, the other pulling from the opposite direction is under nearly equal tension to that of the drive belt and prevents any net force being exerted at  $90^\circ$  to the vertical piston. The top of the cylindrical drum has a set of ball bearings which carry through gimbals - a steel U, a vertical rod, and a pan holding the weights. The gimbals are prevented from rotating by means of an arm which allows only vertical motion.

All of the weight which bears on the moving piston except the calibrated load is balanced by means of a counter-balancing weight. A cylindrical extension to the counter-balancing weight is located in mercury so that an exact equilibrium position may be obtained for the piston. This position is indicated on a scale by a pointer attached above the cylindrical drum.

The higher of the two pressures applied to the piston is exerted on the bottom piston cylinder and the lower pressure on the top piston cylinder. The fluid pressure from the system is piped to a large steel block which is part of the pressure balance. This block contains a number of valves, compartments, and interconnecting passages. Two steel, small

capillary U-tubes extend down from the bottom of the block. The inside of this control block is divided into two sides, high pressure and low pressure. On the high pressure side of the block fluid from the corresponding system pressure tap is admitted to a compartment so that it exerts pressure on a mercury reservoir, through mercury in one of the U-tubes, to mercury in a corresponding compartment on the opposite side of the block. Oil, above the mercury in the second compartment is piped to the lower piston cylinder. The same arrangement exists in another part of the block for the low pressure. The lines to the control block may be shut off and a valve opened for the purpose of equalizing fluid pressures. The small capillary U-tubes serve to suppress blowing-of-the-mercury in the system in case of improper procedure. Electrical contacts are provided for equalizing the height of mercury in the two U-tubes.

The piston which is very precisely machined, surface hardened, and ground was measured very carefully to determine its diameter. There was no diameter variation along its length of as much as .0001 inches. The average piston diameter was found to be approximately 0.2479 inches. One pound load on the pan is equivalent to a pressure difference of 20.717 psi applied to the ends of the piston.

#### Measurement of System Temperatures

A number of system temperatures, indicated in Figure 7, are determined using a Honeywell electronic precision indicator. This instrument is a self-balancing potentiometer having twelve channels. The moving scale, calibrated for copper-constantan thermocouples, covers the range +150°F to -350°F.



## MECHANICAL DESIGN

It is not intended that a detailed discussion of all of the mechanical problems pursuant to the construction of the low temperature equipment be given. Such a discussion would require a tremendous amount of space and would represent only one possible solution to the various practical problems which arose. It is the purpose of this section to outline only a few of the techniques and procedures followed.

### Piping and Vessels

The majority of the high pressure lines in the system were 1/8 inch x 1/16 inch, 3/8 inch x 1/4 inch or 1/2 inch x 3/8 inch seamless Type 304 18-8 stainless tubing. The particular size was determined by the flow if the service was not static. Static pressure taps were for the most part 1/8 inch x 1/16 inch. The majority of high pressure fittings were from the Autoclave Tubeline or Speedline series both of which have ermeto type connections. Ermeto connections are simple and quick to make in comparison with other connections, such as the coned-joint, and provided tight seals over a wide range of temperatures and pressures.

In some areas where pressurized lines would not be subjected to low temperatures, seamless carbon steel tubing and fittings were used. In these instances, the fittings were galvanized and the tubing coated to prevent rusting.

Most of the valves necessary to operate the equipment, as well as a large percentage of the remaining fittings, were located at a valve switchboard for convenience of operation, testing, and maintenance. This switchboard was situated at one end of the control panel (Figure 12). It consists of a large stainless steel box connected to the panel board

in the rear. The front and top of this box are open. Access to the valves is at the open front of the box, a corresponding area of the panel board having been cut out. The valves and fittings inside the stainless box are supported by guy wires extended overhead. This procedure allows for expansion and contraction during heating and cooling of the numerous fittings. The valve switchboard was packed with glass wool during low temperature operation. For the purpose of testing for leaks, a canvas waterproof cover could be put over the front of the valve switchboard and the entire contents of the stainless steel box filled with water.

All of the cold lines which were piped from the valve switchboard to the equipment on the other side of the barricade were placed in a series of connecting chutes and troughs (See Figure 10, overhead) in order to expedite the job of insulating them.

All of the high pressure valves in the system are one of the following types: (1) Autoclave Tubeline, (2) Autoclave Speedline, (3) Hoke metering, or (4) Norman metering. The Autoclave Tubeline valves were used as high pressure cutoff valves. The Autoclave Speedline valves were used for approximate metering purposes. The Hoke metering valves were used to provide relatively fine adjustment of flow rates. The Norman valves provided very sensitive, final flow control.

Other general tubing and piping procedures included:

1. Arrangement for conservation of working space and ease of maintenance, e.g., installation of much of the piping in the pit, below the floor level of the room.
2. Ample use of clamps and other pipe supports.

3. Welding of all high pressure threaded connections which did not have to be disassembled.
4. Use of sealants, such as Permatex, for high pressure threaded connections which had to be disassembled.

#### Pressure Testing

Hydrostatic testing of such items as the compressor supply tank, secondary oil separator, calorimeter, and Joule-Thomson throttle were made at a minimum of 1-1/2 times the maximum operating pressures.

Once the system had been assembled, the low and high pressure sides were tested for leakage with nitrogen; the high pressure side at about 2300 psi and the low pressure side at 800 psi. The valve switch-board was submerged in water for detection of leaks; the remainder of the connections in the system were soaped. After the majority of leaks had been found, the system was pressurized and left under pressure for several hours. The pressure was then re-measured to see if there had been any significant change. This procedure was repeated until the system pressures (high and low) did not change significantly for a 48-hour period. It was, however, necessary to repeat leak tests of the system periodically to insure that low temperature operation had not induced new leaks.

#### AC Power

An estimate was made of the power required for the initial equipment installation. It was found necessary to have about 80 amps available in 110 to 120 VAC single phase power and about 30 amps of 208 to 220 VAC three phase power.

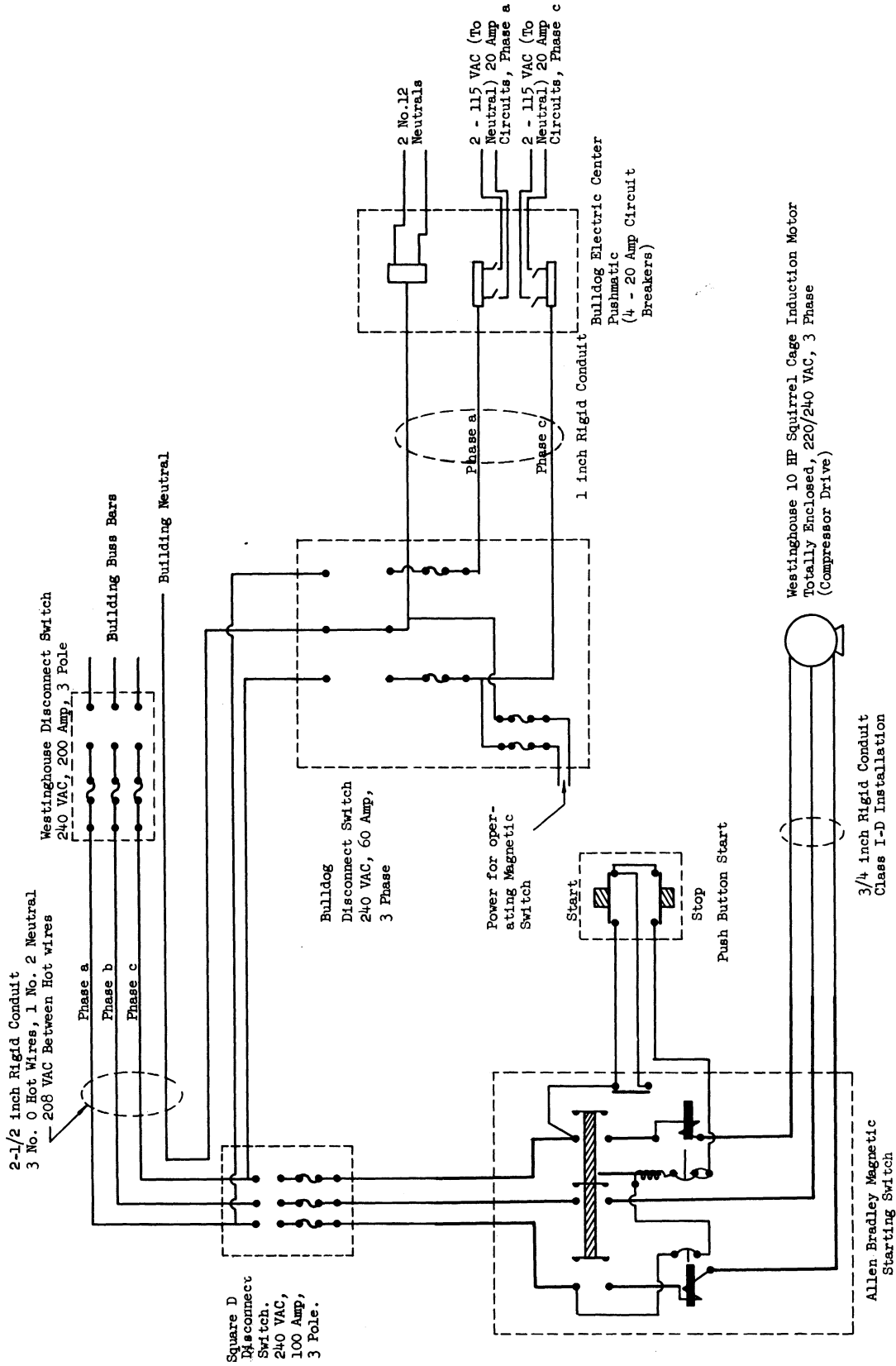


Figure 27. Primary Distribution of AC Power in Test Cell 247

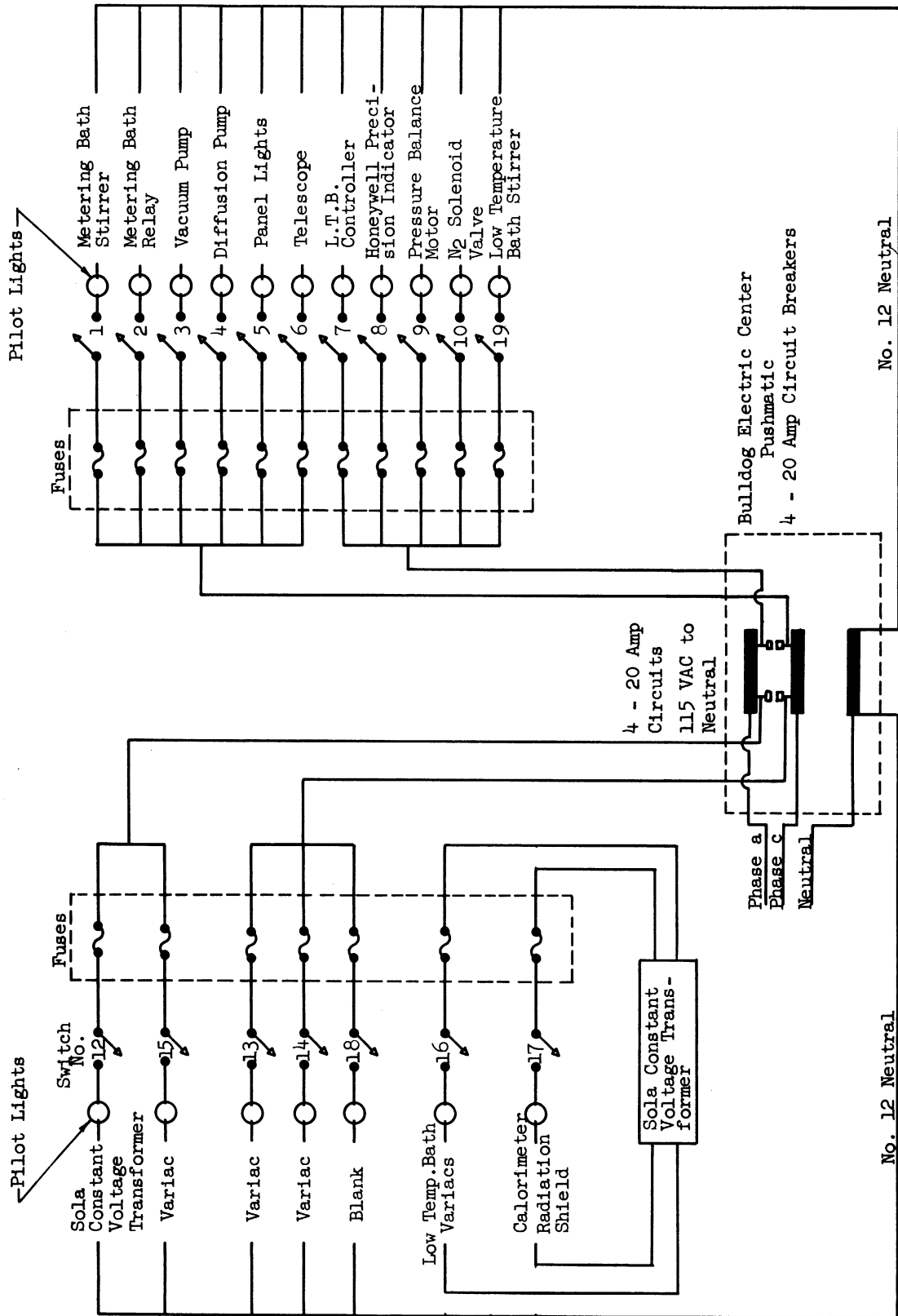


Figure 28. 115 VAC Single Phase Circuitry in Test Cell 247

It was decided that a four wire, three phase, 150 amp service with 208 VAC (rms) available between hot wires and 115 VAC (rms) available between any of the three hot wires and the neutral would provide the necessary service with adequate additional capacity in case of addition to the equipment. This service was run from the building buss bars on the floor above Cell 247, in a 2-1/2 inch rigid conduit (Figures 27 and 28).

#### Low Temperature, High Pressure Mechanical Problems

The combination of variable low temperatures and high pressures present in the experimental work introduced a number of closure and other mechanical seal problems. The exact nature of these problems depended on the type of closure or seal involved. Some or all of the following factors were usually of importance in defining the problem:

1. The geometry of the seal or closure.
2. The necessity for movement relative to the seal.
3. The thermal coefficients of expansion of the materials involved in the seal.
4. The flowing property of the materials under load at low temperature.
5. The freedom of movement of various parts under the influence of a changing temperature or pressure.

One example of a low temperature, high pressure seal problem encountered is that of high pressure ermeto type connections. In this instance, the seal itself is between metals of the same or similar properties and there is no appreciable movement of components at the point

of seal, provided that expansion and contraction is allowed for, between the various fittings. This is illustrated by the construction of the valve switchboard in which the large number of connected fittings are allowed as much flexibility as possible, by not rigidly attaching the fittings to mountings but suspending them by guy wires. The geometry and metallurgy of the ermeto type seal has been well tested for constant temperature and pressure sealing. The original compression applied to the ermeto sleeves by means of nuts is sufficient, since widely different coefficients of thermal expansion do not exist at the point of seal. The important factor in this problem, as stated, was stress on the seal resulting from contraction or expansion of interconnecting tubing.

Another example of the low temperature, high pressure seal problem is offered by the numerous valve packings which were subjected to various pressures and temperatures. Here, the problem is more difficult because of the necessity for maintaining a seal with relative movement between valve stem and packing. The solution of this problem required the use of a packing material which would flow under conditions of low temperature and which would allow the valve stem to be moved. Several materials would be suitable for this purpose at higher temperatures. At low temperatures most of these materials quickly lose their flowing property, however, and become too rigid for this kind of application. Furthermore, many of these materials tend to contract and expand under the influence of temperature at a greatly different rate than metals involved in the seal. Thus, under low temperature conditions the packing may not compensate properly for changing loads or a tendency to change its dimensions. It was found that Teflon or glass impregnated Teflon packings

were the most suitable under conditions of low temperature. Teflon is a good valve packing material and remains more pliable at low temperatures than does any other suitable valve packing material which was investigated. Adding glass to the Teflon greatly reduces its coefficient of thermal expansion (which in ordinary Teflon is much greater than for the common metals).

In a particular seal problem, thermal contraction, which occurs in most materials with lowering of temperature, may tend to improve or impair a seal -- depending on the geometry of the problem and the materials involved. However, it may be stated that in many instances where a packing is involved, lowering of temperature results in a "loosening up" of the seal. On the other hand, in many cases where temperature increases, there is a tendency to "tighten up". Thus, the problems associated with thermal coefficients of expansion are frequently more severe at low temperatures than at moderately high temperatures. As stated, the low temperature problem is often compounded by a loss in the flowing property of materials. In the valve packing example, as in various other associated problems, it is therefore often necessary to tighten seals at, or near the lowest temperature which will be encountered.

There were a number of similar problems, basically, to that of valve packings, but without the movement of a part with respect to the seal. These included such difficulties as sealing thermocouple or other electrical wires through a region of high pressure to one of low pressure.

In the case of thermocouples, it was often possible to avoid the problem by placing the thermocouple junctions in a thermocouple well which was sealed at the high pressure end and around the outside by means of



welding or integral part machining. Thus, the thermocouple junctions themselves were not in a region of high pressure. This procedure could, of course, affect the thermocouple readings if proper care is not taken. It is also possible to seal "dummy" thermocouple wells around the outside by means of a metal-to-metal compression seal. This is illustrated by common designs of such manufacturers of high pressure laboratory apparatus as Autoclave Engineers and American Instrument Company. In this case, the thermocouple well is, of course, removable.

The problem of bringing electrical wires through a region of pressure difference under conditions of a variable temperature is more difficult. A pressure seal has to be maintained and at the same time the wires have to be insulated from each other or ground. Rigid seals, often ceramic, are manufactured for the purpose of bringing wires through a pressure gradient. Typically, they may consist of a ceramic center in which a wire or wires have been sealed, and a metal boundary provided for insertion and sealing of the assembly into, for example, a drilled metal hole. This type of arrangement works admirably at constant temperature. With a wide variation in temperatures, however, the ceramic material may tend to crack or break away from the metal retainer or wires unless coefficients of thermal expansion are well matched. Another way in which the problem of electrical wires may be handled is illustrated by the calorimeter heater leads seal (Figure 19). Here, a 15% glass impregnated Teflon packing was used. The wires were brought through the Teflon and load applied to the packing by means of a packing gland, spring arrangement, and a packing nut. The "spring", consisting of Bellville washers served the purpose of tightening the packing as a lowering of

temperature caused it to shrink. The amount of leakage through this particular seal was very small. The seal would have been satisfactory for many purposes. However, in view of the requirements of a high vacuum in the calorimeter case, the packing required frequent tightening and was considered inadequate for this particular application.

Another type of low temperature, high pressure seal problem which was encountered was that of pressure vessel closure over a range of low temperatures and high pressures. This is typified by the calorimeter heater capsule closure. Originally, a design was employed which reduced the heat capacity of the closure as much as possible. This closure (see Figure 19), however, was unsatisfactory over a range of temperatures. The final solution consisted of a simple flange type closure (see Figure 20). With this arrangement, the linear contraction of the flange bolts provided for a tightening action as the temperature of operation was lowered. In addition, the triangular gaskets used were machined from pure nickel, one of the few common metals having: (1) a lower coefficient of thermal expansion than Type 303 stainless steel of which the flange bolts were made, (2) the property of retaining its ability to be plastically deformed repeatedly at low temperature, (3) a high Young's Modulus, but a lower hardness than Type 304 stainless steel from which the closure was machined.

Two additional low temperature seal problems which did not involve high pressures were:

1. Vacuum seal of the calorimeter case in the presence of liquid hydrocarbons (illustrated in Figure 19).

2. Permanent installation and sealing of a platinum resistance thermometer in the low temperature bath, in the presence of liquid hydrocarbons.

#### Low Temperature Insulation

Styrofoam board insulation was used for insulating the low temperature bath, carbon dioxide cooler, nitrogen cooler, and heat exchanger. Pieces of Styrofoam were cut from rough "lumber" and fitted to the desired rectangular parallelepiped geometry of the cooling boxes. The pieces of Styrofoam were cemented together using a special sealant -- for the purpose of preventing air gaps and water infiltration. Exterior and interior surfaces of the boxes were coated with the sealant, and a double layer of aluminum foil cemented to the styrofoam in order to produce a moisture barrier. Infiltration of moisture can result in a considerable impairment of the insulating properties of low temperature insulation. The aluminum foil also serves to reduce heat transfer by radiation. The Styrofoam "blocks" were encased in a plywood box which was painted and sealed at the corners with cloth tape, mainly in order to provide rigidity and for protection of the insulation against mechanical damage. All of the cold, high pressure lines between the cooling system and the valve switchboard were placed in a single trough in order to simplify the job of insulating. The trough was filled with random scraps of Styrofoam and Santocel powder insulation.

Since it was frequently necessary to have access to the fittings in the valve switchboard, these fittings were insulated by stuffing glass wool around them.

Low Temperature Freeze-Ups

Freezing of moisture present in the fluids being tested sometimes resulted in formation of a barrier to flow in the system. This occurred particularly in cooling coils and upon expansion through the smaller valve ports. This difficulty was lessened by:

1. Utilizing very dry gas for the experiments.
2. Repeated evacuation of the system.
3. Circulation of the fluid through silica gel filters for some time before beginning cooling operations.

Consideration was given to introducing a cold trap in the system, but this precaution was not necessary.

Freeze-up of air used in transferring liquid nitrogen from Dewars was experienced. This problem was solved by heating the incoming air, at the nitrogen delivery tubes, with electrical resistance windings.

APPENDIX B

## CALIBRATION OF THE EQUIPMENT

The accuracy of specific heat measurements depended in good measure upon calibrations of the flow meter and the main calorimeter thermocouple.

The flow meter was calibrated by the National Instrument Laboratory, the manufacturer of the meter. By maintaining the meter in a bath at 20°C and employing the same pressure range for measurement as for calibration, the only variables remaining were gas viscosity and density. The calibration was made with a methane gas of measured viscosity. The methane density and nitrogen properties at 20°C were taken from the literature.

The main calorimeter thermocouple was calibrated against a platinum resistance thermometer. One set of junction of the thermocouple and the platinum thermometer were located in a copper block, the temperature of which was carefully regulated. The other set of thermocouple junctions was held at the ice point temperature.

### Linear Flow Metering Equipment

The meter employed to determine the flow rate in the system was a National Instrument Laboratory's Vol-O-Flow element.

The basic flow equation for this instrument may be expressed as:

$$\frac{\rho \Delta P}{F} = bu + aF \quad (29a)$$

$\rho$  = Density of the fluid being metered at metering pressure and temperature, lb/ft<sup>3</sup>

$\Delta P$  = Pressure drop across the element, inches of water  
at 20°C

$F$  = Mass flow rate, lb/min

$b$  = A geometric constant of the meter proportional to  
length<sup>-3</sup>

$\mu$  = Viscosity of the fluid being metered at the metering  
pressure and temperature, micropoises

$q$  = A geometric constant of the meter proportional to  
length<sup>-4</sup>

Calibration of the flow meter was performed by the National Instrument Laboratory of Washington, D.C. on a sample of gas having the analysis shown in Table VIII.

TABLE VIII

ANALYSIS OF GAS USED IN CALIBRATING FLOW METER

Component	Mol Percent
Methane	99.4
Nitrogen	0.2
Ethane	0.3
Propane	0.1
	<hr/> 100.0

Approximately 1200 standard cubic feet of this gas were obtained through the courtesy of Tennessee Gas Transmission Company, Gulf Oil Corporation, and Dr. Riki Kobayashi of Rice Institute. The gas analysis was

made by mass spectrometer by Gulf Oil Corporation. This gas had been obtained for the purpose of measuring the enthalpy of methane and methane binaries.

It is important to observe that the constants a and b in Equation (29a) are peculiar to the geometry of the particular meter being calibrated but do not in any way depend on the gas which is being metered. Thus, once the meter has been calibrated for one gas, using it for metering any other gas depends only upon an accurate knowledge of the gas viscosity and density at metering conditions. The constants a and b do vary with pressure and temperature, however, since the geometry of the meter is sensitive to variation in pressure and temperature.

It was entirely practicable and advisable in the calorimetric system to maintain a single constant metering temperature. This simplified both the problems of calibrating and operating the meter. Unfortunately, however, the same was not true of the metering pressure. It was necessary that the metering pressure, which was essentially the same as the compressor suction pressure, be allowed to vary from run to run in order that a satisfactory combination of the other operating variables might be obtained. At the time of calibration of the meter the necessary pressure variation at the meter for a reasonable ease of system adjustment could only be estimated. It was decided to allow for a pressure variation of about 70 psi or from 60 to 130 psia. This exceeded the specified operating range of the compressor slightly, which was 60 to 100 psia. It was found, during the nitrogen investigation, that it was necessary to allow a pressure variation at the meter of only about 30-40 psi between the various runs. The temperature of calibration of the meter



was selected as 20°C and a multiple pressure calibration from 60 to 130 psi requested.

The viscosity of the gas sample used for calibrating the meter was determined independently in an ultra-low Reynold's number element by National Instrument Laboratory. The viscosity of the sample was expressed at one atmosphere pressure as:

$$\mu_{1,T} = 106.10 [1 + .00302 (T-20)] \quad (30)$$

$\mu_{1,T}$  = Viscosity of calibrating gas in micropoises at 1 atm and temperature T.

T = Temperature in degrees centigrade.

The magnitude of the temperature variation of viscosity at one atmosphere (near 20°C) was valuable in estimating the desired accuracy of temperature control and measurement at the flow meter, but in all experimental measurements, which were made with nitrogen, an attempt to obtain a metering temperature of exactly 20°C was made. No temperature correction was applied to the viscosity of nitrogen for metering bath temperature variations. The pressure variation of viscosity of the calibrating gas was expressed by National Instrument Laboratories as:

$$\mu_{P,T} = \mu_{1,T} K \quad (31)$$

where  $\mu_{P,T}$  = The viscosity in micropoises at pressure P, psia, and temperature T, °C

$\mu_{1,T}$  = The viscosity in micropoises at atmospheric pressure and temperature T, °C

$K$  = A correction factor given as a function of pressure (Figure 29)

The pressure variation of viscosity was found along a path of 20°C and hence would not have applied exactly at a different temperature. For small changes in temperature this error would have been negligible. As it was, the temperature of operation was almost exactly 20°C.

The density of the calibrating gas was expressed as:

$$\rho = \rho_0 \times \frac{P}{14.696} \times \frac{273.18}{T} \times \frac{1}{Z} \quad (32)$$

$\rho$  = Density at pressure P and temperature T

$\rho_0$  = Density at 1 atm and 0°C (0.04499 lb/ft<sup>3</sup>)

$P$  = Pressure in psia

$T$  = Temperature in °K

$Z$  = Compressibility factor at pressure P and temperature T

The density at 1 atm and 0°C of the gas sample was computed from a knowledge of the average molecular weight and assuming the ideal gas law to hold. The author supplied tabulated values and graphs for the compressibility factor of methane obtained from the literature<sup>(112)</sup> and these values were used in preparation of a graph giving Z as a function of pressure at 20°C (Figure 30). It was assumed that methane behavior would be sufficiently well approximated by the behavior of the calibrating gas.

Examination of Equation (29a) indicates that, knowing density at a particular temperature and pressure and measuring mass flow rate as a function of pressure drop would yield the necessary information for

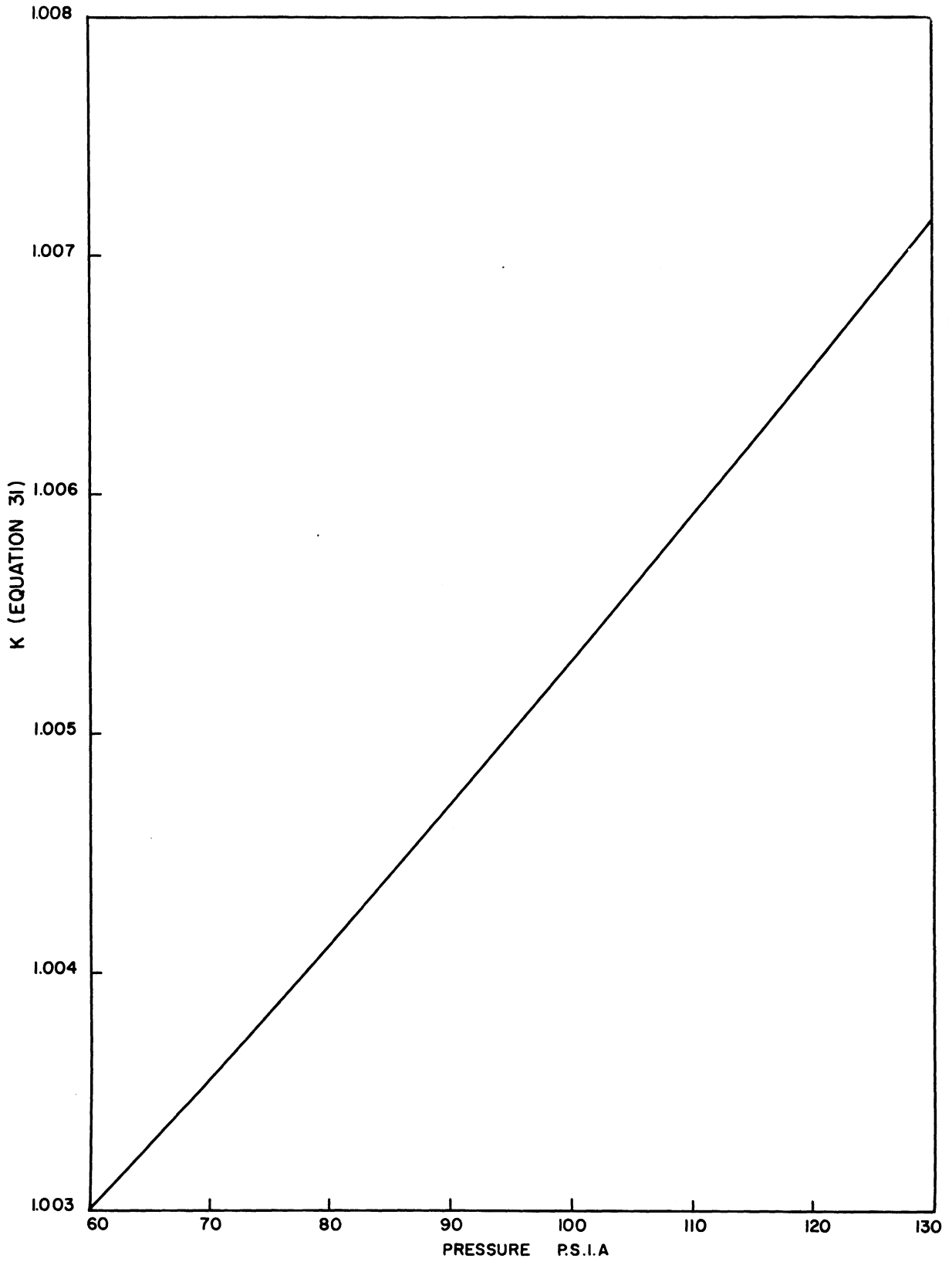


Figure 29. Pressure Correction to Methane Viscosity for Flowmeter Calibration

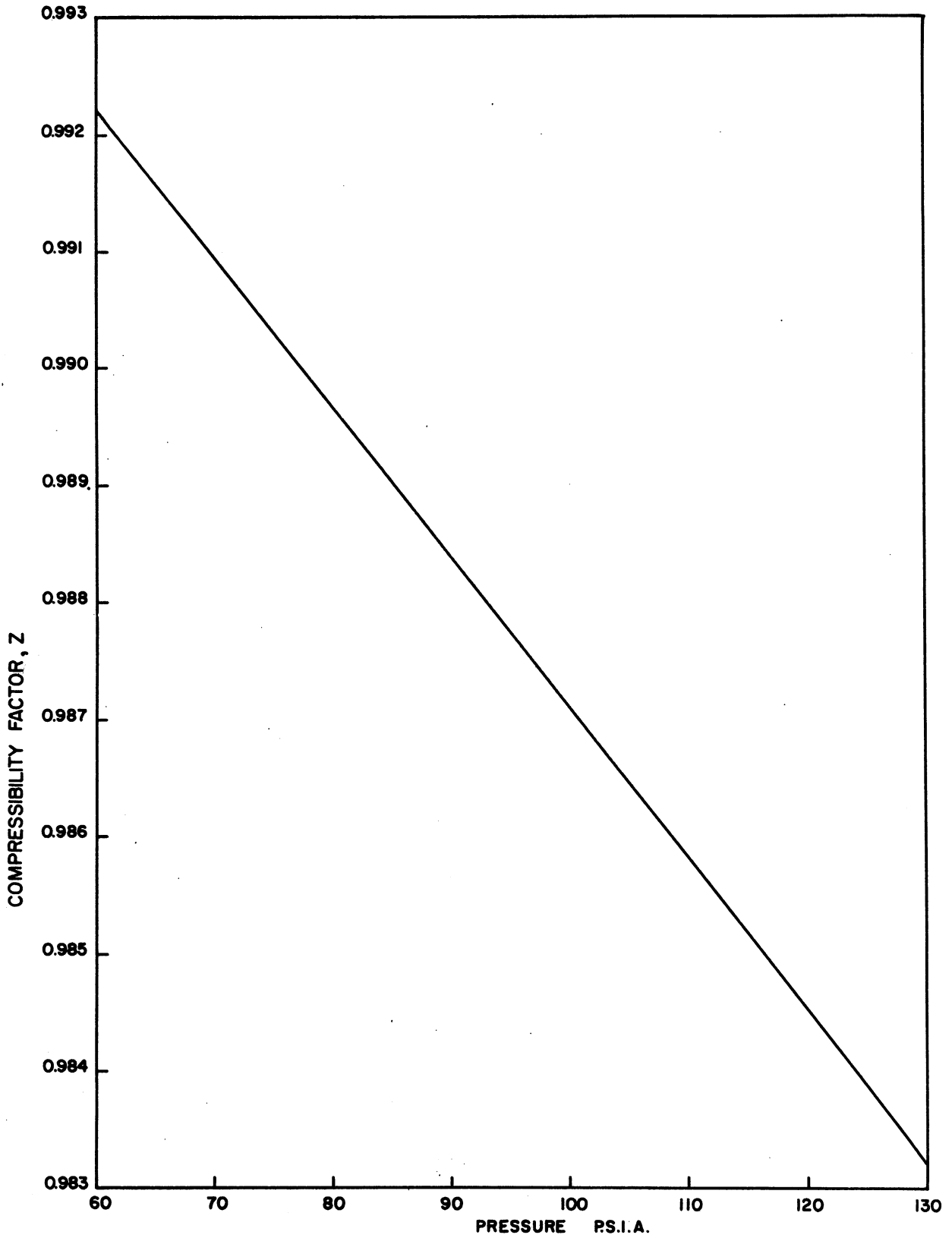


Figure 30. Compressibility Factors for Methane at 20°C

obtaining the values of  $b\mu$  and  $a$  - at the conditions of the measurement. This is illustrated in Figure 31. The mass flow rate was determined by measuring the volumetric flow rate through the meter at a low pressure and applying a corresponding low pressure density. Thus, Equation (29a) may be expressed for the purposes of calibration as:

$$\frac{\rho \Delta P}{\rho_0 \dot{V}_0} = b\mu + a\rho_0 \dot{V}_0 \quad (29b)$$

$\rho$  = Density of calibrating gas at the pressure and temperature of the calibration

$\Delta P$  = Corrected pressure drop across the flow meter

$\mu$  = Viscosity of the calibrating gas at the pressure and temperature of the calibration

$\dot{V}_0$  = Volumetric flow rate measured at essentially atmospheric pressure and a convenient temperature

$\rho_0$  = Density of the calibrating gas at the pressure and temperature of measurement of  $\dot{V}_0$

The normal procedure which is used by National Instrument Laboratory is: to measure the viscosity of the calibrating sample at the pressure and temperature of calibration and then to measure  $\Delta P$  across the instrument to be calibrated as a function of flow rate at ten flow rates over the full range of the meter. The meter which was employed in the flow system has a maximum capacity of 0.3 lb/min so that flow calibration points were taken at approximately 0.03, .06, ..., 0.30 lb/min.

Measurements of viscosity of the calibrating gas were made at 60, 70, 80, 90, 100, 110, 120, and 130 psia and 20°C. Complete (ten point) flow rate measurements were made, however, only at 60 and 130 psia, 20°C.

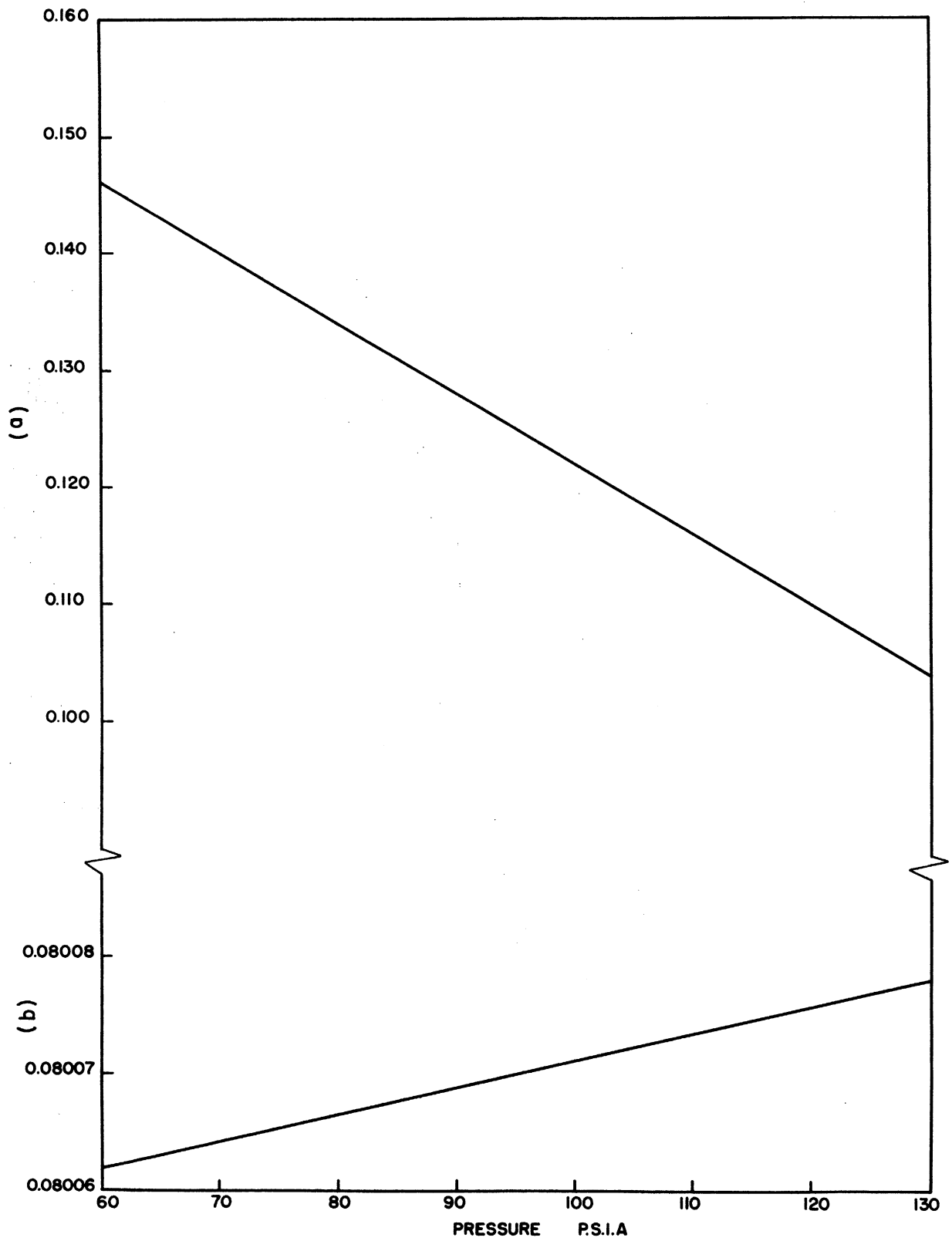


Figure 31. Pressure Correction to Flowmetering Calibration Constants at 20°C

The best values of  $b\mu$  and  $a$  in Equation (29a) (in the least mean squares sense) were determined from the flow calibration data at 60 and 130 psia, 20°C. The values  $\mu$  at 60 and 130 psia, 20°C were applied to the values of  $b\mu$  found, in order to calculate the corresponding values of  $b$ .

It was known from previous experience on the part of National Instrument Laboratory that the pressure variation of  $b$  was very small (the actual variation found in  $b$  over the pressure range 60 psia, 20°C is shown in Figure 32). Therefore, the values of  $b$  at the intermediate pressures of 70, ..., 120 psia were found by interpolating linearly between the values at 60 and 130 psia.

The interpolated values of  $b$  were applied to measured values of  $\mu$  to determine the values of  $b\mu$  at intermediate pressures and 20°C. A single flow measurement, at approximately maximum flow rate for the meter, was also made at each of the intermediate pressures and 20°C. From a knowledge of  $b\mu$  and one value of  $\rho \Delta P/F$  at the intermediate pressures, values of the slope,  $a$ , in Equation (29a) could be calculated. The difference between a mass flow calculated using Equation (29a) and one calculated neglecting the second item on the right hand side of Equation (29a) was never more than about 0.2 percent for the experimental work on nitrogen. Therefore, errors in the values of the constant,  $a$ , at intermediate pressures were inconsequential.

The accuracy of flow metering for gases other than the calibration gas will depend principally on the accuracy of knowledge of the calibration constant  $b$ , the viscosity of the gas, and the pressure at which

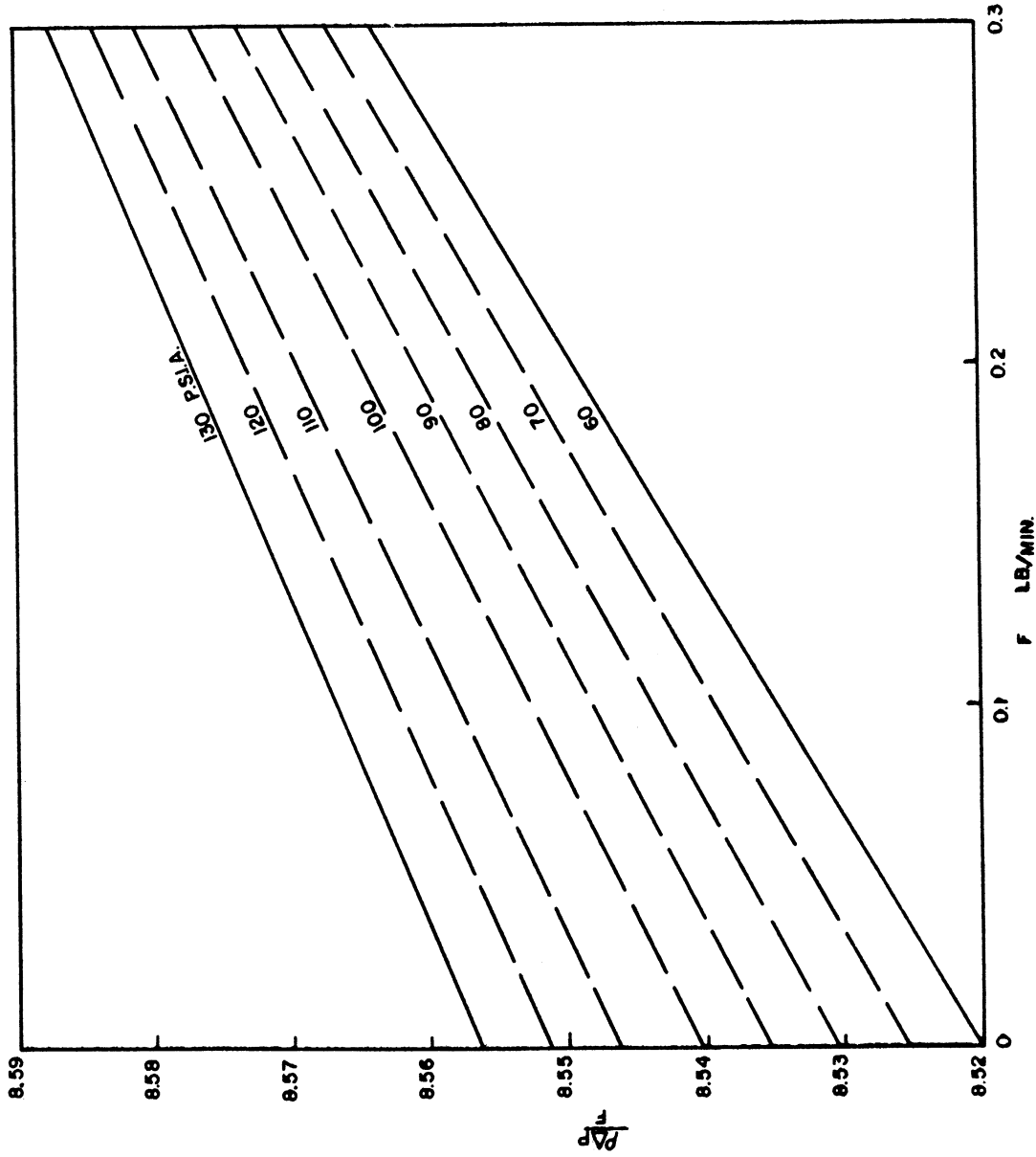


Figure 32. Calibration Curves for Linear Flowmeter at 20°C and Several Pressures



the metering is carried out. A discussion of the estimated accuracy of the flow meter calibration and the estimated accuracy of flow rate measurements during the nitrogen investigation is given in Appendix C, Measurement Error Analysis.

Main Calorimeter Thermocouple

The temperature change of the fluid flowing through the calorimeter was determined by means of a six junction copper-constantan difference thermocouple.

The emf-temperature relationship of this thermocouple was expressed as:

$$E_T = a + bT + cT^2 + dT^3 \quad (33)$$

$E_T$  = The emf developed across the thermocouple when one set of junctions was at temperature T and the other set at the ice point temperature.

$a, b, c, d$  = Constants.

$T$  = Temperature, ( $^{\circ}\text{F} + 460.00$ ), an arbitrary scaling.

The voltage measurements were made during calibration with a Leeds and Northrup, White-double potentiometer, range 0 to 100,000 microvolts. The temperature of the working junctions was ascertained by using a Leeds and Northrup platinum thermometer calibrated by the National Bureau of Standards, the White potentiometer, and necessary circuitry for the potentiometric method of platinum thermometry.

A detailed description of the potentiometric circuitry used in the calibration will not be given since it was quite similar to that used

by the author in measuring the operating temperature, the potentiometer, potentiometer accessories and platinum thermometer circuitry were part of the equipment used by Dr. E. F. Westrum of the Chemistry Department in the measurement of very low temperature heat capacities of solids.

The important differences between the emf measurements made during thermocouple calibration and those made during the nitrogen investigation, using a Leeds and Northrup K3 potentiometer, were:

1. The White potentiometer had been calibrated.
2. A calibrated deflection procedure of potentiometer-galvanometer operation was employed in the thermocouple calibration whereas a null method was used in later thermocouple measurements.

One set of junctions of the thermocouple, encased in a copper sheath, was placed in a Dewar flask containing crushed ice and distilled water. A cork top was placed in the Dewar flask and the sheath submerged for some distance in the ice.

The other set of junctions and the capsule-type platinum thermometer were located in a six inch length of two inch diameter electrolytic copper bar stock. The opposite ends of the barstock were drilled the required diameters for insertion of the thermometer and sheath along the axis of the bar stock. The ends of the sheaths and the thermometer were brought within one-eighth inch of each other at the longitudinal center of the copper. Each was coated with Apiezon N to insure good thermal contact with the copper.

The copper bar stock was wrapped with a suitable electrical resistance winding. The copper bar, thus prepared, was placed inside

two concentric cylinders. The first was made from brass tubing and suitable end pieces. The outer cylinder was a two pound coffee can. The copper bar stock and the brass cylinder were equipped with small stainless steel feet so that their bottom ends were an inch or so from the bottoms of the cylinders in which they were housed.

The entire arrangement was placed inside a large styrofoam block, about 3 feet x 3 feet x 3 feet, located inside a plywood box. A space was left in the center of the styrofoam for inserting the coffee can and a styrofoam top which could be fitted in above the can. The only access to the coffee can was through two stainless steel tubes. One tube passed through the tops of the coffee can and brass cylinder to bring the electrical heater wires, thermocouple leads, and platinum thermometer leads to the outside. The other tube travelled as far as the annular space between the coffee can and brass cylinder for the purpose of introducing liquid nitrogen to this area.

Liquid nitrogen was added to the space between the coffee can and the brass cylinder until the temperature of the copper bar stock was well below the lowest temperature of measurement. After this temperature was reached, it was found to be sufficient simply to introduce cold nitrogen gas from the supplying Dewar continuously through the stainless tube.

By means of two variacs, in series, it was possible to precisely adjust the AC power dissipation in the bar stock winding. It was found, after some experimentation, that if energy was added for a short time to the winding and then the power turned off, that the temperature of the block would increase for a period of time, but at a decreasing rate. As the nitrogen cooling took effect the rate of increase in temperature of

the copper would decrease until, for a period of one to two minutes, there would be very little change in temperature. The bar stock would then begin to decrease in temperature.

It was during the period when the temperature of the copper was changing very, very slowly that measurements of temperature and thermocouple emf were made. The rate of temperature change under these conditions was always less than 0.1 °F/ minute.

The general procedure was to measure, during the period of nearly constant temperature, the thermocouple emf and platinum thermometer variables several times as a function of time. This was done in such a way that at least two thermocouple voltage measurements would be bracketed by a minimum of three platinum thermometer readings. It was possible by means of linear interpolation to report the temperature indicated by the platinum thermometer at the same time that the thermocouple voltage had been read.

After practice, it was possible to conduct the entire series of measurements during the period of time in which the rate of temperature drift of the copper was very small. It was necessary to measure the platinum thermometer current only before and after each set of measurements since this did not change rapidly with a change in platinum resistance; frequently, it did not change at all. One observer was responsible for making the potentiometer readings of voltage drop across the platinum thermometer and thermocouple emf. Another controlled the liquid nitrogen supply, heater operation, and at the time of measurement noted on an electrical timer, graduated in hundredths of a second, the time at which measurements were made. A calibrated deflection method of potentiometer-galvanometer operation was used. The potentiometer operator followed the

small drift in emf indicated by a crosshair on a lighted scale and telescope. The galvanometer deflection read by the potentiometer operator and the time read by the other observer were well co-ordinated.

During the period of measurement, the galvanometer's electrical null and sensitivity were determined. The galvanometer sensitivity was determined by measuring the shift from galvanometer null which occurred when unit steps of unbalance were made with the lowest potentiometer decade switch.

The AC heater and heater leads in the vicinity of the thermocouple and platinum thermometer did not affect readings -- since they were never energized during emf readings.

The procedure in determining thermocouple emf as a function of temperature:

1. Both sets of thermocouple junctions were placed at the ice point and essentially no spurious voltage due to inhomogeneity or strains in the wire was found.
2. Measurements of platinum thermometer voltage and thermocouple emf were made as a function of time. A sufficient number were made so that temperature and emf could be referenced by linear interpolation to a common time.
3. Corrections which had been obtained in calibration of the potentiometer were applied to all potentiometer emf measurements.
4. Platinum thermometer resistance was calculated from emf measurements and the National Bureau of Standards

certified value of a standard resistance used in the platinum thermometer circuit.

5. Temperatures at which measurements had been made were calculated from a knowledge of the resistance of the platinum by means of the Callendar equation.
6. Measurements of temperature and thermocouple emf were put on a common time basis. (Table IX)

The next step in preparing the thermocouple for use was to obtain a least mean squares fit of the emf, temperature data for Equation (33). This problem was programmed and solved on the IBM 650 computer operated by the University. The constants are listed in Table X. Making use of the IBM 650 computer, a tabulation of temperature versus thermocouple emf was made at 0.05°F temperature increment.

#### Low Temperature Bath Platinum Resistance Thermometer

The low temperature bath thermometer No. 1216653 was calibrated by Leeds and Northrup. The Callendar equation which expresses the relation between resistance and temperature is given by:

$$T = 100 \frac{R_T - R_0}{R_{100} - R_0} + \delta \left( \frac{T}{100} - 1 \right) \frac{T}{100} \quad T \leq 0^\circ\text{C} \quad (34a)$$

$$T = 100 \frac{R_T - R_0}{R_{100} - R_0} + \delta \left( \frac{T}{100} - 1 \right) \frac{T}{100} + \beta \left( \frac{T}{100} - 1 \right) \left( \frac{T}{100} \right)^3 \quad (34b)$$

$T > 0^\circ\text{C}$

The constant,  $\delta$ , requires a third temperature point in addition to the ice and steam points; the boiling point of sulfur was used. The constant  $\beta$  requires, additionally a subzero point; for this purpose the boiling point of oxygen was used.

TABLE IX  
MAIN CALORIMETER THERMOCOUPLE CALIBRATION DATA

Temperature (°F)	Measured Thermocouple Emf with one set of Junctions at 32.00°F (Microvolts)	Deviation *Calculated-Measured (Microvolts)
-268.84	29,960.6	+1.4
-251.25	28,750.6	+1.2
-234.70	27,540.6	+4.7
-217.45	26,220.6	-1.7
-196.28	24,500.5	-3.4
-186.01	23,630.5	-5.4
-173.51	22,540.5	-8.4
-142.83	19,699.3	+5.2
-129.63	18,422.2	+3.6
-113.83	16,845.3	+2.6
- 97.79	15,192.6	+0.9
- 81.01	13,406.7	+1.1
- 64.86	11,633.3	+3.6
- 48.91	9,841.9	-3.2
- 34.80	8,210.2	-2.0
- 15.51	5,920.0	-0.2
+ 2.85	3,680.0	-0.2
+ 32.00	0.6	+2.6

\* Calculated values based on Equation (33) and constants of Table X.

Date of Calibration: August 1957

TABLE X  
MAIN CALORIMETER THERMOCOUPLE CALIBRATION CONSTANTS

Constants in Equation (33)	Value
a	+37.926543
b	- 1.5089629 x 10 <sup>-2</sup>
c	- 1.4729216 x 10 <sup>-4</sup>
d	+ 4.3284023 x 10 <sup>-8</sup>

The values of the constants in Equations (34a, 34b) for thermometer No. 1216653 are listed in Table XIV of Appendix E.

#### Standard Electrical Resistors

The values of resistance for the standard resistors used in the calorimeter heater circuit (Figure 24) and the platinum thermometer circuit (Figure 25), as determined by Leeds and Northrup, are listed in Table XV of Appendix E.

#### Heise Bourdon Tube Gauge

Calibrations of the Heise Bourdon tube gauge used in flow metering are reported in Tables XVI and XVII of Appendix E.

#### Potentiometer Standard Cell

A calibration of the cadmium unsaturated-type cell used in conjunction with the Leeds and Northrup K3 potentiometer is given in Table XVIII of Appendix E.

#### Differential Pressure Balance Weights

The weights used with the differential pressure balance on loan from the University of Wisconsin were calibrated. The corrections were of no importance in ascertaining the pressure of specific heat measurements because of their small magnitude. The conditions of the weights are such that a new set will have to be obtained prior to commencement of Joule-Thomson studies. Hence, the calibrations are not reported.



APPENDIX C

$E_{L_2}$  = Voltage measured at potentiometric switch position  $L_2$ , volts (Figure 24).

$R_a, R_b, R_c, R_d, R_e$  = Standard resistances, absolute ohms (Figure 24, Table XV).

The values of the resistances as computed from Table XV were:

$$R_a = 0.099999 \quad (\pm .01\%), \text{ ohms} \quad (35)$$

$$R_b + R_c = 19.9996 \quad (\pm \text{approximately } .01\%), \text{ ohms} \quad (36)$$

$$R_b + R_c + R_d + R_e = 20,019.6 \quad (\pm \text{approximately } .01\%), \text{ ohms} \quad (37)$$

The maximum potentiometric error in  $E_{L_1}$  and  $E_{L_2}$  are given by Leeds and Northrup for the uncalibrated middle range of the K3 potentiometer as:

$$\text{True value of } E_{L_1} \text{ or } E_{L_2} = \pm (.015\% \text{ of } E_{L_1} \text{ or } E_{L_2} + 2 \text{ microvolts}) \quad (38)$$

The accuracy of these measurements was further limited, however, by power supply ripple, which caused a maximum instability of 5 microvolts at potentiometric switch positions  $L_1$  and  $L_2$ .

An additional estimated uncertainty of two ohms occurred in the quantity  $(R_b + R_c + R_d + R_e)$  due to the fact that the resistance of the calorimeter heater potential leads was not carefully measured.

It was not possible to make a maximum likelihood estimate of the error in the quantity  $W$  in Equation (20), nor was it possible without making a large number of assumptions to estimate a confidence interval for  $W$ . In order to establish a confidence interval corresponding to any realistic confidence level, say 0.95 or 0.99, required a knowledge

## MEASUREMENTS ERROR ANALYSIS

An estimate was made of the maximum indeterminate errors expected in the measurement of the three important variables for determining  $C_p$ : the mass flow rate,  $F$ ; the measured heat addition,  $Q$ ; and the temperature rise of the fluid in the calorimeter,  $\Delta T$ . This estimate corresponds to the establishment of confidence intervals having confidence levels of essentially 1.00.

### Power Measurement

The power input to the DC calorimeter heater was computed from the equations:

$$W_C = E_C I_C \quad (20)$$

$$E_C = \left( \frac{R_b + R_c + R_d + R_e}{R_b + R_c} \right) E_{L_1} \quad (22)$$

$$I_C = \left( \frac{E_{L_2}}{R_a} - \frac{E_{L_1}}{R_b + R_c} \right) \quad (24a)$$

$W_C$  = Power dissipated in calorimeter heater, watts.

$E_C$  = Voltage drop across calorimeter heater, volts.

$I_C$  = Current through calorimeter heater, amperes.

$E_{L_1}$  = Voltage measured at potentiometric switch position  $L_1$ , volts (Figure 24).

of the standard deviation or error distribution of the quantities which determined W.

An estimate was made of the maximum (indeterminate) error which could occur in W for a simultaneous occurrence of maximum errors in the quantities which determined W. This corresponded to assuming a combination of errors of very low probability or the establishment of a confidence interval with a confidence level of essentially 1.00. In other words, very wide bounds were placed on the error which could occur in W due to indeterminate factors. This estimate of error was, therefore, expected to be much greater than the most common error -- or than the error that would occur 95 times out of 100.

The quantity W may be expressed in terms of the pertinent variables and the maximum errors of appreciable probability in these variables as:

$$W_c = \frac{(R_b + R_c + R_d + R_e) + \epsilon_1}{(R_b + R_c) + \epsilon_2} (E_{L_1} + \epsilon_3) \left[ \frac{E_{L_2} + \epsilon_4}{R_a + \epsilon_5} - \frac{E_{L_1} + \epsilon_3}{(R_b + R_c) + \epsilon_2} \right] \quad (39)$$

= Maximum error estimate for the variable to which it is added in Equation (38), in appropriate units.

Values of  $E_{L_1}$  and  $E_{L_2}$  were selected corresponding to the minimum power input to the calorimeter during the nitrogen investigation.

These values were

$$E_{L_1} = 0.047608 \text{ volts} \quad (40a)$$

$$E_{L_2} = 0.032470 \text{ volts} \quad (40b)$$

In accordance with the previous discussion and using the values of  $E_{L1}$  and  $E_{L2}$  listed above, values were computed for  $\epsilon$ :

$$\epsilon_1 = \pm 4.0 \text{ ohms} \quad (41a)$$

$$\epsilon_2 = \pm 0.0020 \text{ ohms} \quad (41b)$$

$$\epsilon_3 = \pm .000014 \text{ volts} \quad (41c)$$

$$\epsilon_4 = \pm .000012 \text{ volts} \quad (41d)$$

$$\epsilon_5 = \pm 0.000010 \text{ ohms} \quad (41e)$$

In computing the value of  $\epsilon_1$ , Equations (39), (41a), the uncertainty in calorimeter heater potential lead resistance was added to the error given by Equation (37).  $\epsilon_3$  and  $\epsilon_4$  were computed from Equation (38), and the maximum additional uncertainty of 5 microvolts resulting from power supply ripple. A value of 5 microvolts was known to be high in view of the averaging effect of this short term ripple, apparent during measurements. The instability could be followed at highest galvanometer sensitivity of approximately 0.05 microvolts per millimeter and averaged at the second highest sensitivity of approximately 1.0 microvolt per millimeter.

The maximum error in W may be estimated from Equation (39) in several ways. The quantity W may be expressed as a perfect differential or the equation may be multiplied out and products of two error terms neglected, in view of the magnitude of the  $\epsilon$ 's.

The mean value for W in Equation (39),  $\epsilon = 0$ , is  $W = 15.345$  watts or Equation (20) using the values of  $E_{L1}$  and  $E_{L2}$  listed in Equations (40a) and (40b). The maximum error in W for this example [computed from

Equation (39) was  $W = (15.345 \pm \text{approximately } 0.1\%)$ , watts. Therefore, an uncertainty of  $\pm 0.1\%$  of  $W$  was taken as an estimate of the confidence interval corresponding to a confidence level of essentially 1.00.

#### Measurement of $\Delta T$

The temperature rise of the fluid flowing through the calorimeter was determined by means of a six junction copper-constantan difference thermocouple. The thermocouple calibration has been described in Appendix B, Calibration of the Equipment. The emf of the thermocouple was expressed as a cubic in temperature:

$$E_T = a + bT + cT^2 + dT^3 \quad (33)$$

It was impossible, based on a single calibration of the thermocouple, to estimate the reproducibility of the data which was obtained. It was also essentially impossible to explain the deviation of data points from values computed from Equation (33), by separating the effects of determinate and indeterminate errors, and deviation caused by the inexactness of the chosen representation.

The magnitudes of the emf deviations between data points and Equation (33) for the case of one junction at 32.00°F and the other at temperature  $T^\circ\text{F}$  are given in Table IX. The discrepancies are very small when one considers the size of the emf's measured. These deviations can become important, however, if one is interested in determining a relatively small value of  $\Delta T$  from Equation (33).

It was thought that the magnitude of the determinate errors in measuring the absolute temperature of the platinum calibrating thermometer and the emf produced by the thermocouple were small. The

platinum thermometer which was used had been calibrated by the National Bureau of Standards. The standard resistor used in the platinum thermometer circuit and the White potentiometer employed for measuring emf's had also been calibrated. The uncertainty in the White potentiometer, Leeds and Northrup model 7623, uncalibrated, is about  $\pm$  (0.02% + 1 microvolt). This would represent an error of about the same size as the deviations shown in Table IX; however, it was assumed that the calibrated potentiometer error was much smaller.

The indeterminate errors in this type of calibration were probably chiefly due to the following:

1. Inequality in the temperature of the platinum resistance thermometer and the working thermocouple junctions during measurements -- due to thermal inertia of the system.
2. Inhomogeneities or strains in the thermocouple, which produced spurious emfs.

Any error which occurred in the calibration due to thermal lag could not be estimated. The effect of imperfections in the thermocouple was tested by placing both sets of junctions at the ice point and subjecting the interconnecting wire to different temperatures. In no case was the resultant emf produced greater than 0.6 microvolts. The fact that a multiple junction thermocouple, rather than a single junction thermocouple, was employed no doubt had an averaging effect on any spurious emf's. Ideally, the thermocouple should have been recalibrated at the time of original calibration and the working and ice point junctions interchanged. This would have been a severe test of reproducibility.

The effect of change in calibration of the thermocouple over the operating period of the present investigation was believed to have been very small. Investigators(2,125) have found that a low temperature copper-constantan thermocouple, carefully handled, remains very stable for years.

The question arose in view of the large number of calibration points (Table IX), over the temperature range  $-269^{\circ}\text{F}$  to  $32^{\circ}\text{F}$ , as to the relative accuracy of determining  $\Delta T$  (during measurements of  $C_p$ ) directly from the calibration data and determining  $\Delta T$  from Equation (33) obtained by least squares regression. In other words, was the data better than the function assumed for representation? Higher order curve fits were carried out and the representation did not improve. However, thermocouple data need not be represented exactly by any finite polynomial, such as Equation (33), and certainly not by one with a relatively small number of terms.

The nature of the deviations of data points from values predicted by Equation (33) are shown graphically in Figure 33. Figure 33 clearly indicates that the deviations were not random. It was assumed that these deviations were a complicated superposition of determinate and random errors upon the behavior of the cubic expression.

The maximum deviation indicated in Table IX was 8.4 microvolts, equivalent to an emf error of 0.037% relative to the ice point. The average error, in any sense, was considerably smaller. The deviations were plotted in Figure 33 and the difference in  $\Delta T$  obtained from the data and from Equation (33) compared for  $20^{\circ}\text{F}$  intervals at the temperatures of the nitrogen data. Discrepancies of 7.4 microvolts at  $-150^{\circ}\text{F}$ ,



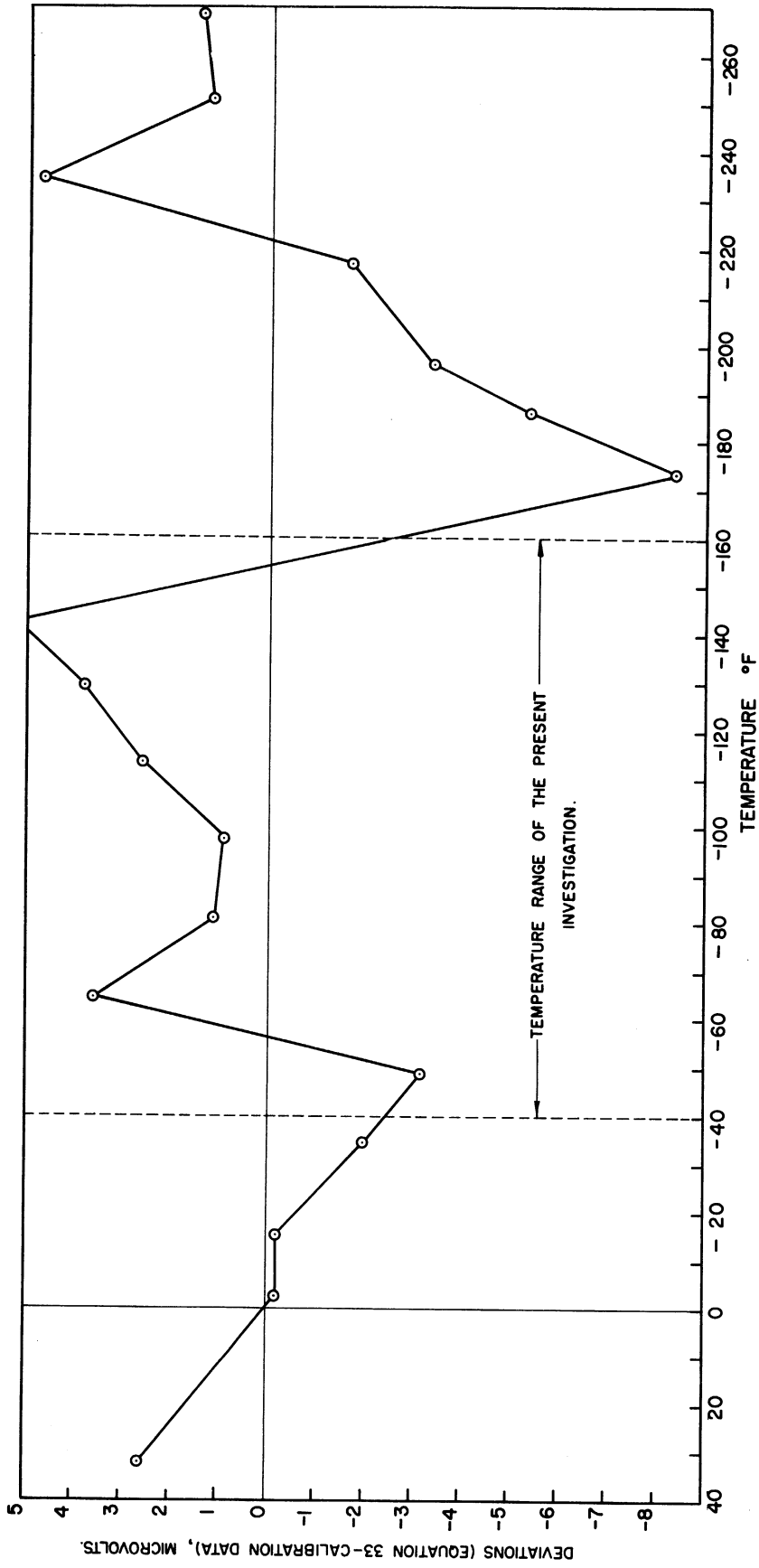


Figure 33. Deviations of Calorimeter Thermocouple Data from a Fitted Curve

1.7 microvolts at  $-125^{\circ}\text{F}$ , 1.2 microvolts at  $-100^{\circ}\text{F}$ , 2.5 microvolts at  $-75^{\circ}\text{F}$ , and 4.1 microvolts at  $-50^{\circ}\text{F}$  were found. A temperature increment of  $20^{\circ}\text{F}$  was equivalent to an emf of about 2000 microvolts, so that the maximum possible percentage discrepancy between  $\Delta T$ 's calculated from Equation (33) and obtained directly from the data was approximately:

$$\frac{\Delta T_{\text{Equation (33)}} - \Delta T_{\text{data}}}{\Delta T_{\text{data}}} \times 100 = \frac{\left(\frac{7.4}{2,000} \times 20^{\circ}\text{F}\right) \times 100}{20^{\circ}\text{F}} = 0.37\% \quad (42)$$

The decision was made to use values of  $\Delta T$  obtained from Equation (33) rather than to determine them directly from the data. This procedure was expedited by tabulating values of emf and temperature at  $0.05^{\circ}\text{F}$  intervals using an IBM 650 computer.

On the basis of investigations at the Bureau of Standards, Scott<sup>(125)</sup> concluded that for a typical single junction copper-constantan thermocouple calibrated at three temperatures between the ice point and  $-190^{\circ}\text{C}$  that the calibration reproducibility and correspondence to the absolute temperature scale, based on a standard cubic equation for copper-constantan thermocouples, were equivalent to an emf error of 2 microvolts or less. This did not refer to the ultimate accuracy which had been obtained.

An uncertainty of 2 microvolts for a single junction thermocouple would be equivalent to 12 microvolts for a 6 junction thermocouple. It was estimated from a consideration of the averaging effect of the spurious emf's by the several junctions, the care with which measurements had been made, the number of calibration points, and the deviations of Table IX that the correspondence of the calibration to the true curve

of means was better than 10 microvolts at all points. It was also estimated that the probability was very small that recalibration would yield a difference in emfs for any 20°F increment that differed by as much as 6 microvolts.

The additional uncertainty in emf which was introduced by the use of the uncalibrated K3 potentiometer during specific heat measurements was only about 1 microvolt for a 20°F temperature interval. It was thought that no appreciable, residual, spurious emf's arose in the K3 associated potentiometer circuitry. Precautions to avoid this problem were elaborate.

The conclusion was that the maximum error in measuring  $\Delta T$  during the nitrogen investigation was about 0.3% of  $\Delta T$  for a 20°F increment.

Osborne, Stimson, and Sligh<sup>(78)</sup> in determining the specific heat of ammonia by flow calorimetry compared values of  $\Delta T$  measured by a single junction copper-constantan thermocouple directly to values of  $\Delta T$  measured by means of a platinum thermometer for 18-20°F increments. These comparisons, which involved a large number of measurements, showed an average discrepancy of 0.2%. Other investigators<sup>(136)</sup> have demonstrated accuracies of this level using copper-constantan thermocouples in flow calorimetry.

#### Flow Rate Measurement

The mass flow rate in the calorimetric system was computed from the equation:

$$\Delta P = \frac{b\mu F}{\rho} + \frac{aF^2}{\rho} \quad (29c)$$

$\Delta P$  = Pressure drop through flow meter, standard inches of water (20°C).

$\mu$  = Viscosity of the fluid being metered at the temperature and pressure of the measurement, micropoises.

$\rho$  = Density of the fluid being metered at the temperature and pressure of the measurement, lb/ft<sup>3</sup>.

a, b = Calibration constants.

F = Mass flow rate, lb/min.

Prior to undertaking an estimate of the error which occurred in the quantity F in Equation (29b), the assumption was made that neglecting the term  $\frac{aF^2}{\rho}$  would not have an appreciable effect on this error analysis. This assumption was based on the fact that neglecting the term  $\frac{aF^2}{\rho}$  in Equation (29c) changed the computed values of F by less than 0.2% in all cases considered in the nitrogen investigation. Thus, the flow metering equation was assumed to be:

$$\Delta P = \frac{b\mu F}{\rho} \quad (29d)$$

An analysis of the maximum error in determining F, corresponding to a confidence level of essentially 1.00, was made based on Equation (29d) in a manner similar to that carried out for estimation of heat input error. Solving for F in Equation (29d):

$$F = \frac{\rho \Delta P}{b\mu} \quad (29e)$$

If maximum errors  $\epsilon_6, \epsilon_7, \epsilon_8, \epsilon_9$  occurred in the quantities  $\rho, \Delta P, b, \mu$  respectively, then F was given by:

$$F = \frac{(\rho + \epsilon_6)(\Delta P + \epsilon_7)}{(b + \epsilon_8)(\mu + \epsilon_9)} \quad (29f)$$

$\epsilon$ 's = Estimated maximum errors in the quantities to which they are added.

The error,  $\epsilon_b$ , in the calibration constant,  $b$ , is invariant with respect to the use of Equation (29c) to compute  $F$ ; it does not vary from measurement to measurement. The quantities  $a$  and  $b$  in Equation (29c) were determined by National Instrument Laboratory using a sample of methane which the author supplied. Constants  $a$  and  $b$  were determined from a series of measurements by means of a least squares regression analysis (see Calibration, Appendix B). It was impossible without a knowledge of the individual data points obtained by National Instrument Laboratory to estimate the precision of their measurements, nor was it possible to estimate directly the accuracy of the determination of  $b$  without a knowledge of data points for several repeated calibrations. It was possible, however, to estimate the maximum error, corresponding to a high probability, which could have occurred in  $b$  computed from Equation (29d), for one data point, due to indeterminate errors. This estimate was based on maximum error estimates for the quantities  $\mu$ ,  $F$ ,  $\rho$ ,  $\Delta P$  as determined for the calibrating fluid. This procedure did not yield what was felt to be a very realistic uncertainty in  $b$ , however, in view of the fact that maximum errors were used and the averaging effect of the least mean squares regression was neglected. Furthermore, the close agreement in the values of  $b$  determined at two pressures (see Calibration of the Equipment, Appendix B) tended to indicate a high precision of measurements in the calibration of the meter.

Based on a consideration of the factors discussed and estimates of calibration accuracy obtained from National Instrument

Laboratory, the value of  $b$  was believed to have a maximum uncertainty of less than 0.2%. Accordingly, for the purpose of a maximum error estimate for  $F$  in Equation (29f), the quantity  $\epsilon_8$  was taken to be  $\pm .002b$ .

The error which occurred in the measurement of the quantity  $\Delta P$  in Equation (29f) during the nitrogen investigation was estimated to be less than 0.1% of  $\Delta P$  with a confidence level of essentially 1.00. The National Instrument Laboratory had determined that the overall error in measuring the difference in liquid levels in the precision u-tube, cathetometer combination employed for the nitrogen investigation was less than 0.0015 inches. The difference in water levels in the two legs of the u-tube measured during the nitrogen investigation varied from 5 to 10 inches. Thus, the maximum error in the uncorrected measurement of pressure differential, termed  $\Delta h$  in Equation (44) (Sample Calculation, Appendix D), was expected to be approximately 0.015 to 0.030% of  $\Delta h$ . The uncertainties in the correction applied to  $\Delta h$  to determining  $\Delta P$ , Equation (44), were not of appreciable magnitude. An overall maximum error was assigned to  $\Delta P$  for the purpose of a maximum error analysis for  $F$  in Equation (29f), such that  $\epsilon_7 = \pm .001 \Delta P$ .

The values for the viscosity of nitrogen were taken from the data of Kestin and Pilarczyk.<sup>(56)</sup> A study of the precision of this data and a comparison with values computed from an expression derived by means of theoretical treatment in terms of molecular constants<sup>(48)</sup> led to the estimate that the viscosity of nitrogen was known (in the pressure and temperature range of interest) with an accuracy of about 0.1%. The value of  $\epsilon_9$  in Equation (29f) was taken to be:  $\epsilon_9 = \pm 0.001 \mu$ .

The density of nitrogen was computed from the equation:

$$\rho = \frac{P M_W}{Z R T} \quad (43)$$

$\rho$  = Density lb/ft<sup>3</sup>.

$M_W$  = Molecular weight, lb mass/lb mole.

$Z$  = Compressibility factor.

$R$  = Universal gas constant,  $10.732 \frac{\text{psia} \cdot \text{ft}^3}{\text{lb mole} \cdot ^\circ\text{R}}$ .

$T$  = Absolute temperature, degrees Rankine.

$P$  = Pressure, psia.

The compressibility factors for nitrogen were obtained from the compilation of Sage and Lacey<sup>(112)</sup> and are thought to be of an accuracy of  $\pm 0.1\%$ . The error in measuring the metering temperature (during the nitrogen investigation) was less than .04%. The accuracy of pressure measurement with the Heise Bourdon tube gauge was taken as  $\pm 0.2\%$ . It can be shown that the resultant uncertainty in  $\rho$  in Equation (29f) is less than 0.35% with a high level of confidence. The maximum error in  $\rho$  in Equation (29f) was taken as:  $\epsilon_G = .0035$ .

A consideration of the maximum errors in the individual terms in Equation (29f) led to the conclusion that the maximum error in mass flow rate,  $F$ , corresponding to a confidence level of essentially 1.00, was  $\pm 0.7\%$ .

APPENDIX D



SAMPLE CALCULATION OF ISOBARIC SPECIFIC HEAT

The apparent isobaric specific heat,  $(C_p)_F$ , was computed from the following equation:

$$(C_p)_F = \frac{Q}{F(\Delta T - \delta T)} \quad (17b)$$

$(C_p)_F$  = Apparent isobaric specific heat, Btu/lb °F.

Q = Measured heat addition, Btu/min.

F = Mass flow rate, lb/min.

$\Delta T$  = Temperature rise of the fluid, °F.

$\delta T$  = Correction term for Joule-Thomson effect, °F.

The data point: -50°F, 294 psia, flow 1 (Table XXI) will be used to illustrate the calculation of the quantities on the right hand side of Equation (17b). The necessary data for the calculation is summarized in Table XI.

TABLE XI

SUMMARY OF DATA: -50°F, 294 PSIA, FLOW 1

Variable	Value
$\Delta h$	8.837 inches of water
Tr	24.10 °C
Pmu	83.69 psig
Bu	29.22 inches of mercury
Tm	68.0 °F
$E_{L1}$	0.063354 volts
$E_{L2}$	0.042856 volts
$E_{L3}$	0.020193 volts
$E_{L4}$	0.040944 volts
$E_{R11}$	2093.1 microvolts

Calculation of Mass Flow Rate, F

The mass flow rate, F, in Equation (17b) was determined from the relation:

$$\Delta P = \frac{b\mu F}{\rho} + \frac{aF^2}{\rho} \quad (29c)$$

$\Delta P$  = Corrected pressure drop across a linear flowmeter, standard inches of water, 20°C.

a = A calibration "constant" at metering temperature, T<sub>m</sub>, and corrected metering pressure, P<sub>m</sub>.

b = A calibration "constant" at metering temperature, T<sub>m</sub>, and corrected metering pressure, P<sub>m</sub>.

$\mu$  = Viscosity of fluid being metered at the metering temperature, T<sub>m</sub>, and corrected metering pressure, P<sub>m</sub>.

F = Mass flow rate, lb/min.

$\rho$  = Density at metering pressure and 20°C, lb/ft<sup>3</sup>.

Calculation of Corrected Pressure Drop,  $\Delta P$

The corrected pressure drop across the meter,  $\Delta P$ , in standard inches of water, 20°C, was calculated from  $\Delta h$ , the difference in water levels in the two legs of the U-tube (as measured by the cathetometer) by means of an equation supplied by National Instrument Laboratory:

$$\Delta P = \Delta h \left[ 1 - 189 \times 10^{-6} (T_r - 20) - 5.3 \times 10^{-6} (T_r - 20)^2 - 0.000177 \left[ 1 - \frac{(g_s - g_a)}{g_s} \right] \left[ 1 - \frac{P_{gr}}{P_{wr}} \right] \right] \quad (44)$$

$\Delta P$  = Corrected pressure drop across flowmeter, standard inches of water, 20°C.

$\Delta h$  = Apparent pressure drop across flowmeter, inches of water measured at temperature  $T_r$ .

$T_r$  = Room temperature, degrees centigrade.

$g_s$  = Standard acceleration of gravity, gals.

$g_l$  = Local acceleration of gravity, gals.

$\rho_{gr}$  = Density of gas in the U-tube above the water at temperature  $T_r$ , lb/ft<sup>3</sup>.

$\rho_{wr}$  = Density of water in the U-tube at temperature  $T_r$ , lb/ft<sup>3</sup>.

The first bracket on the right hand side of Equation (44) combines a correction for the linear thermal expansion of the cathetometer (metal) scale and a correction for the change in density with temperature of the water in the U-tube, both referred to 20°C. The second bracket in Equation (44) contains a correction for the variation in the acceleration of gravity at different geographical points. The third bracket in Equation (44) represents a correction for the head of gas (in this case nitrogen) displacing the water in the short leg of the manometer.

Local gravity at the Natural Science Building on the Main Campus of the University of Michigan is 980.314 gals. The elevation of this building is 876 feet above sea level and its latitude is 42°, 16.6 minutes north. The proper correction to convert this value to local gravity at the North Campus Automotive Building is: subtract 0.00007 gals. for each foot of added elevation; add 0.0013 gals. for each mile north. These corrections were not applied for the nitrogen work. The value of local gravity at the Automotive Building was taken to be:

$$g_l = 980.314 \text{ gals}$$

The density of nitrogen over water in the U-tube was computed from the following equation:

$$\rho_{gr} = \frac{P_m M_w}{Z R T_r} \quad (43a)$$

$P_m$  = Corrected metering pressure (low pressure side of the meter), psia.

$M_w$  = Molecular weight lb/lb mole (nitrogen, 28.016)

$R$  = Universal gas constant,  $10.732 \frac{\text{psia-ft}^3}{\text{lb mole-}^\circ\text{R}}$

$T_r$  = Room temperature, degrees Rankine

$Z_r$  = Compressibility factor of nitrogen at temperature,  $T_r$ , and corrected metering pressure,  $P_m$ .

The corrected metering pressure,  $P_m$ , in Equation (43a) was computed from the uncorrected value,  $P_{mu}$ :

$$P_m = P_{mu} + \gamma_H + B_u + \gamma_B \quad (45)$$

$P_{mu}$  = Uncorrected metering pressure, psig (Table XI or XXI).

$\gamma_H$  = Correction obtained from calibration of the pressure gauge used in metering (Heise Bourdon tube gauge), psi (Table XVII, Appendix E).

$B_u$  = Uncorrected barometric pressure, psia.

$\gamma_B$  = Temperature correction to barometric pressure for changes in the density of mercury, psi (Table XIX, Appendix E).

Substitution of the values of  $P_{mu}$ ,  $\gamma_H$ ,  $B_u$ , and  $\gamma_B$  in Equation (45) in the proper units yielded a value of  $P_m$ :

$$P_m = 97.99 \text{ psia}$$

The density of nitrogen over water in the U-tube,  $\rho_{gr}$ , Equation (43a), was calculated for  $P_m = 97.99$  psia, a value of  $T_r = 534.97^\circ R$  obtained by proper conversion of the value listed in Table XI, a value of  $Z_r = 0.9992$  obtained from a tabulation by Sage and Lacey<sup>(112)</sup>, and the values for the constants  $R$  and  $M_w$ :

$$\rho_{gr} = 0.4785$$

The density of water,  $\rho_{wr}$ , in Equation (44) was found to be:

$$\rho_{wr} = 62.31 \text{ lb/ft}^3$$

Substituting the values of  $\Delta h$ ,  $T_r$ ,  $g_s$ ,  $g_l$ ,  $\rho_{gr}$ , and  $\rho_{wr}$  in Equation (44) ( $\Delta h = 8.837$  inches of water,  $T_r = 24.10^\circ C$ ,  $g_s = 980.665$  gals.,  $g_l = 980.314$  gals.,  $\rho_{gr} = 0.4785 \text{ lb/ft}^3$ ,  $\rho_{wr} = 62.31 \text{ lb/ft}^3$ ) a value was obtained for  $\Delta P$ , the corrected pressure drop across the meter:

$$\Delta P = 8.742 \text{ inches of water at } 20^\circ C$$

#### Metering Constants a and b in Equation (29c)

The quantities  $a$  and  $b$  in Equation (29c) were obtained from Figure 31:

$$a = 0.1232$$

$$b = 0.0800706$$

#### Calculation of Density of Fluid in Equation (29c)

The value of  $\rho$  in Equation (29c) was computed from the equation:

$$\rho = \frac{P M_w}{Z R T_m} \quad (43b)$$

$Z_m$  = Compressibility factor of nitrogen at the metering bath temperature  $T_m$ , and the corrected metering pressure,  $P_m$ .

$T_m$  = Metering bath temperature, degrees Rankine (Table XI)

Substituting values of  $P_m = 97.99$  psia,  $M_w = 28.016$  lb/lb mole,  $Z_m = 0.9986$  from Sage and Lacey<sup>(112)</sup>,  $R = 10.732 \frac{\text{psia-ft}^3}{\text{lb mole } ^\circ\text{R}}$ , and  $T_m = 527.6$  °R (Table XI):

$$\rho = 0.4855 \text{ lb/ft}^3$$

#### Calculation of Viscosity of Fluid in Equation (29c)

The viscosity of nitrogen in Equation (29c) was computed from the equation of Kestin and Pilarczyk<sup>(56)</sup>:

$$\frac{\mu_{P,T}}{\mu_{1,T}} = 1 + 88.79 \times 10^{-6} (P-14.7) + 9.168 \times 10^{-10} (P-14.7)^2 + 10.86 \times 10^{-12} (P-14.7)^3 \quad (46)$$

$\mu_{P,T}$  = Viscosity of nitrogen at pressure, P, and temperature, T, micropoises.

$\mu_{1,T}$  = Viscosity of nitrogen at atmospheric pressure and temperature, T, micropoises.

P = Pressure, psia (in this case,  $P = P_m$ )

T = Temperature, degrees centigrade [in this case,  $T = (T_m \div 1.8 + 32.00) ^\circ\text{F}$ ]

From Kestin and Pilarczyk<sup>(56)</sup>,  $\mu_{1,20.0^\circ\text{C}} = 175.0$  micropoises. Substituting  $\mu_{1,T} = 175.0$  micropoises and  $P = 97.99$  psia in Equation (46):

$$\mu_{P,T} = \mu_{97.99 \text{ psia}, 20^\circ\text{C}} = 176.34 \text{ micropoises}$$

Summary of Variables in Equation (29c)

The variables in Equation (29c) which have been calculated are summarized in Table XII.

TABLE XII

INTERMEDIATE MASS FLOW RATE VARIABLES  
FOR EXAMPLE CALCULATION

Variable	Value
$\Delta P$	8.742 inches of water, 20°C
a	0.1232
b	0.0800706
$\mu$	176.34 micropoises
$\rho$	0.4855 lb/ft <sup>3</sup>

The mass flow rate, F, in Equation (29c) was computed from the values of  $\Delta P$ , a, b,  $\mu$ ,  $\rho$  listed Table XII:

$$F = 0.2998 \text{ lb/min.}$$

Calculation of Measured Heat Addition, Q

The measured heat addition, Q, was computed from the relations:

$$Q = \frac{E_C I_C}{17.58} \quad (20a)$$

Q = Measured heat addition, Btu/min.

$E_C$  = Calorimeter heater IR drop, volts

$I_C$  = Calorimeter heater current, amperes

$$E_C = \left( \frac{R_b + R_c + R_d + R_e}{R_b + R_c} \right) E_{L1} \quad (22)$$

$E_{L_1}$  = Potentiometric reading  $L_1$  (Figure 24), volts.

$R_b, R_c, R_d, R_e$  = Resistance of standard resistors  
(Figure 24, Table XV), absolute ohms, 25°C.

$$I_C = \left( \frac{E_{L_2}}{R_a} - \frac{E_{L_1}}{R_b + R_c} \right) \quad (24a)$$

$E_{L_2}$  = Potentiometric reading  $L_2$  (Figure 24), volts.

$R_a$  = Resistance of standard resistor, absolute ohms, 25°C.

No correction was made for the temperature change of resistance of the standard resistors, since this effect was inconsequential for the present purposes. Substituting the values of  $E_{L_1}$  and  $E_{L_2}$  from Table XI and the values of  $R_a, R_b, R_c, R_d, R_e$  from Table XV in Equations (22) and (24a) and solving for  $Q$  in Equation (20a):

$$Q = 1.533 \text{ Btu/min.}$$

#### Calculation of Fluid Temperature Rise, $\Delta T$

The temperature change of the fluid was determined from an IBM 650 tabulation of thermocouple emf versus temperature, relative to the ice point temperature, at 0.05°F temperature increments. The calorimeter thermocouple equation was:

$$E_T = a + bT + cT^2 + dT^3 \quad (33)$$

$E_T$  = Thermocouple emf with one set of junctions at 32.00°F and the other set at temperature  $T$ , millivolts.

$T$  = Temperature, (°F + 460.00, an arbitrary scaling)

$a, b, c, d$  = Constants obtained from calibration data (see Calibration of the Equipment, Appendix B, Table X).



The initial fluid temperature in the calorimeter,  $T_1$ , was used, in conjunction with the tabulation of values based on Equation (33), to find a value of  $E_{T_1}$ . It was possible to find  $E_{T_2}$  from the value for  $E_{T_1}$  by applying the emf of the difference thermocouple,  $E_{R_{11}}$ .

Calculation of Initial Fluid Temperature,  $T_1$

The initial fluid temperature was measured using a platinum resistance thermometer. The resistance of platinum at temperatures below the ice point temperature is given by the Callendar equation in the form:

$$T = 100 \frac{R_T - R_0}{R_{100} - R_0} + \delta \left( \frac{T}{100} - 1 \right) \frac{T}{100} + \beta \left( \frac{T}{100} - 1 \right) \left( \frac{T}{100} \right)^3 \quad (34b)$$

$T$  = Temperature, degrees centigrade, ( $T \leq 0$ ).

$R_T$  = Resistance of platinum coil at temperature  $T$ , absolute ohms.

$R_0, R_{100}, \delta, \beta$  = Calibration constants (see Calibration of the Equipment, Appendix B, and Table XIV).

An IBM 650 tabulation of  $R_T$  versus  $T$  at 0.05°F temperature increments was employed in determining values of  $T$  from values of  $R_T$ . Values of  $R_T$  were computed from the equation:

$$R_T = \frac{E_P}{I_P} \quad (26)$$

$E_P$  = Voltage drop across platinum coil, volts.

$I_P$  = Current through platinum coil, amperes.

$$E_P = E_{L_4} \quad (\text{Figure 25}) \quad (28)$$

$I_P$  was found by determining the voltage drop across a standard resistor:

$$I_P = \frac{E_{L3}}{R_f} \quad (27)$$

$E_{L3}$  = Potentiometric measurement (Figure 25), volts.

$R_f$  = Resistance of standard resistor (Figure 25, Table XV), absolute ohms.

For the example problem from Table XI,  $E_{L3} = 0.020193$  volts,  $E_{L4} = 0.040944$  volts; from Equations (27), (28), (26):

$$R_T = 20.2763 \text{ absolute ohms}$$

The value of  $T_1$  corresponding to  $R_T = 20.2763$  absolute ohms was:

$$T_1 = -59.83^\circ\text{F}$$

The corresponding value of  $E_{T1}$  from the IBM 650 tabulation of thermocouple data was:

$$E_{T1} = 11,074.9 \text{ microvolts}$$

#### Calculation of Exit Fluid Temperature, $T_2$

The thermocouple emf (relative to the ice point temperature for the fluid leaving the calorimeter at a higher temperature,  $T_2$ ) is given by:

$$E_{T2} = E_{T1} - (E_{T1} - E_{T2}) \quad (33a)$$

The value of  $E_{T2}$  for the example problem was calculated from Equation (33a);  $E_{T1} = 11,074.9$  microvolts,  $E_{T1} - E_{T2} = E_{R11}$  (Table XI) = 2093.1 microvolts:

$$E_{T2} = 8,981.8 \text{ microvolts}$$

From the IBM 650 tabulation, the value of  $T_2$  corresponding to  $E_{T_2} = 8,981.8$  microvolts was:

$$T_2 = -41.46^\circ\text{F}$$

The temperature rise of the fluid in the calorimeter,  $\Delta T$ , is given by:

$$\begin{aligned} \Delta T &= T_2 - T_1 \\ &= -41.46^\circ\text{F} - (-59.83^\circ\text{F}) \\ &= 18.37^\circ\text{F} \end{aligned}$$

Calculation of Joule-Thomson Correction Term,  $\sigma T$

The Joule-Thomson correction term,  $\sigma T$ , in Equation (17b) was not measured for the example. It was calculated for other data points in a manner analogous to that used for determining  $\Delta T$  - or by simply adding the thermocouple voltages corresponding to  $\Delta T$  and  $\sigma T$  (taking into account polarities) in view of the magnitude of  $\sigma T$  and  $dE_T^2/dT^2$  (Equation 33).

Calculation of Isobaric Specific Heat,  $C_p$ ,  
from Apparent Isobaric Specific Heat,  $(C_p)_F$

The variables in Equation (17b) which have been calculated are summarized in Table XIII. The corresponding values for flow rate 2 at  $-50^\circ\text{F}$  and 294 psia are also given.

TABLE XIII

SUMMARY OF VARIABLES USED IN COMPUTING  $C_p$  FOR EXAMPLE CALCULATION

Variable	Flow 1	Flow 2
Mass Flow Rate, $F$ , lb/min	0.2998	0.2171
Measured Energy Addition, $Q$ , Btu/min	1.533	1.128
Temperature Rise of the Fluid, $\Delta T$ , $^\circ\text{F}$	18.37	18.38
Reciprocal Mass Flow Rate, $1/F$ , min/lb	3.336	4.606

The values of  $(C_P)_F$  computed from Equation (17b) using the quantities summarized in Table XIII were:

$$(C_P)_{F_1} = 0.2784 \text{ Btu/lb } ^\circ\text{F}$$

and

$$(C_P)_{F_2} = 0.2828 \text{ Btu/lb } ^\circ\text{F}$$

The isobaric specific heat,  $C_P$ , was obtained from an extrapolation of these values of  $(C_P)_F$  versus  $1/F$  (See Isobaric Specific Heat Measurements on Nitrogen, Data Obtained)

$$C_P = (C_P)_{F_1} - \frac{\Delta(1/F)}{1/F_1} [(C_P)_{F_2} - (C_P)_{F_1}] \quad (17c)$$

The value for  $C_P$  at  $-50^\circ\text{F}$ , 294 psia was found to be:

$$C_P = 0.2668.$$

Corrections were not applied for the small error in  $C_P$  due to the fact that the arithmetic mean temperature and pressure of measurement were not the same as the nominal conditions,  $-50^\circ\text{F}$ , 294 psia. The arithmetic mean temperature was computed as  $T_{\text{avg}} = T_1 + \frac{\Delta T}{2}$  (Table XXII). The pressure at the entrance to the calorimeter was measured using a dead weight differential pressure balance. One pound weight was equivalent to a pressure difference of 20.717 psi. The weights were calibrated; however, the corrections were negligible for the present purposes.

APPENDIX E

TABLE XIV  
CALIBRATION CONSTANTS FOR PLATINUM RESISTANCE  
THERMOMETER, SERIAL NO. 1216653

Constants in Equations (3a, b)	Value
$R_0$	25.502 ohms
$\frac{R_{100} - R_0}{100R_0}$	0.00392656
$\alpha$	1.492
$\beta$	0.1104

Calibration by: Leeds and Northrup Company  
Date of Calibration: May 23, 1957

TABLE XV  
CALIBRATED RESISTANCES OF STANDARD RESISTORS

Designation in Figure Indicated	Leeds and Northrup Catalog No.	Designation Serial No.	Nominal Resistance ohms	Date of Calibration	$R_{25^\circ C}$ (ohms)	Accuracy $R_{25^\circ C}$ (Percent)	$\alpha$ $\frac{\text{ohms}}{\text{ohm}^\circ C}$	$\beta$ $\frac{\text{ohms}}{\text{ohm}^\circ C^2}$	
Ra	Figure 24	4221-C	1309523	0.1	May '57	0.0999999	0.01	+0.000004	-0.0000005
Rb	Figure 24	4025-C	1196105	10	April '57	9.9995	0.005	+0.000011	-0.0000005
Rc	Figure 24	4025-C	1310053	10	May '57	10.0001	0.005	+0.000005	-0.0000005
Rd	Figure 24	4040-C	1227955	10,000	April '57	9999.8	0.005	+0.000001	-0.0000005
Re	Figure 24	4040-C	1227969	10,000	April '57	9999.8	0.005	+0.000001	-0.0000005
Rf	Figure 25	4025-C	1311656	10	May '57	10.0001	0.005	+0.000006	-0.0000005

Calibration Performed by: Leeds and Northrup

TABLE XVI  
FIRST CALIBRATION OF HEISE GAUGE

Dead Weight or Hg Col. Reading (psi)	Gauge Reading (Deviation)
7.5	-
15.0	-
22.5	-
30.0	-
37.5	-
45.0	-
52.5	-
60.0	-
67.5	-
75.0	-
82.5	-
90.0	-
97.5	-
105.0	-
112.5	-
120.0	-
127.5	-
135.0	-
142.5	-
150.0	-

Remarks: Corrections indicated for error of 0.15 psi  
or more.

Maximum hysteresis: 0.08 psi

Temperature of test: 70°F

Gauge No: 15714

Calibration by: Heise Bourdon Tube Co., Inc.

Date: October 1957

TABLE XVII  
SECOND HEISE GAUGE CALIBRATION

Gauge Pressure (psig)	Correction to be Added Algebraically to Gauge Reading (psi)
29.90	+0.04
39.25	+0.07
49.85	+0.05
59.85	+0.03
69.83	+0.03
79.88	-0.04
89.78	+0.05
99.78	-
109.90	-0.01
119.90	-0.05
129.90	-0.07
139.85	-0.04

Maximum hysteresis: 0.10 psi

Temperature of test: 78°F

Gauge No.: 15714  
Calibration by: Richard C. Faulkner  
Date: August 19, 1958

TABLE XVIII  
CALIBRATION OF POTENTIOMETER STANDARD CELL

Eppley Standard Cell No.	Emf
650924	1.01928 (+ .01%) @ 24°C

Calibrated by: The Eppley Laboratory, Inc.  
Date of Calibrations: February 14, 1957



TABLE XIX

TEMPERATURE CORRECTIONS TO BAROMETRIC PRESSURE

Temperature, °F	Corrections to be Subtracted from Barometric Reading (Inches of Mercury)
35	.02
40	.03
45	.04
50	.06
55	.07
60	.08
65	.10
70	.11
75	.13
80	.14
85	.15
90	.17
95	.18
100	.19

TABLE XX

ANALYSIS OF NITROGEN USED IN  
ISOBARIC SPECIFIC HEAT MEASUREMENTS

Component	Percentage
Nitrogen	99.4+
Oxygen	0.2+
Argon	0.2-
Carbon Dioxide	0.2+

NOTE: Spectrographic Analysis.

TABLE XXI  
RAW DATA NITROGEN SPECIFIC HEADS

Nominal Conditions of Cp Determination Temp. °F	Flow No.	P <sub>11</sub> Volts	E <sub>12</sub> Volts	E <sub>11</sub> (Vanle-Thomson) Microvolts	E <sub>13</sub> Volts	Correction to be Added to Nominal Pressure of Cp Measurement (Pentons psi)	E <sub>14</sub> Volts	Uncorrected Barometric Pressure, Inches Hg	Room Temp. °C	Metering Temp. °F	h <sub>1</sub> Inches	h <sub>2</sub> Inches	Uncorrected Metering Pressure (psig)	Calorimeter Inletting Vacuum Level (Microns of Mercury)	Comments
-50	293.9	1	.063354	.042896	2093.1	-	.020193	29.22	24.10	68.0	1.439	10.276	83.69	30	
-50	293.9	2	.054350	.036772	2094.0	-	.020191	29.23	23.64	68.0	1.437	9.309	76.65	12	
-50	587.8	1	.057231	.038884	1786.5	-	.020191	29.25	23.40	68.0	1.546	10.175	75.35	20	
-50	587.8	2	.048157	.032695	1802.0	-	.020191	29.26	23.40	68.0	2.833	8.886	73.80	20	Calorimeter Shield on System Unsteady
-50	587.8	3	.048159	.032631	1920.8	-	-	29.26	23.60	68.0	2.836	8.884	71.67	18	
-50	1175.7	1	.068571	.046529	2000.6	-1.6	.020281	29.47	20.00	68.0	1.324	10.383	84.19	15	
-50	1175.7	2	.057693	.039176	1986.6	-4	.020276	29.51	22.80	68.0	2.327	9.396	73.52	18	
-50	1175.7	3	.057700	.039158	2089.0	-	.020275	29.51	22.90	68.0	2.331	9.396	73.00	15	Calorimeter Shield on
-100	293.9	1	.054492	.037466	1934.0	-	.020249	29.11	24.85	68.0	1.571	10.158	59.05	5	
-100	293.9	2	.047608	.032470	1893.0	+5	.020249	29.11	24.95	68.0	3.582	8.210	88.50	5	
-100	587.8	1	.070430	.048008	2420.4	-6	.020249	29.13	25.00	68.0	1.518	10.207	74.00	5	
-100	587.8	2	.062520	.042621	2486.5	+8	.020249	29.12	24.90	68.0	2.529	9.196	73.38	5	
-100	881.8	1	.058884	.040141	1896.7	0	.020257	29.09	23.00	67.9	2.303	9.529	66.78	275	
-100	881.8	2	.070405	.047946	1904.0	0	.020257	29.05	22.80	68.0	1.394	10.331	82.70	380	
-100	1175.7	1	.078268	.052003	2032.4	-4	.020339	29.44	22.10	68.0	1.372	10.343	85.56	11	
-100	1175.7	2	.067460	.045992	2094.8	+13	.020340	29.44	22.10	68.0	2.588	9.134	89.37	3	
-150	293.9	1	.069581	.047501	1855.2	+19	.020148	29.40	21.00	68.0	1.227	10.484	81.85	90	
-150	293.9	2	.059010	.040305	1841.1	+15	.020150	29.46	20.80	68.0	2.225	9.493	72.48	80	
-150	587.8	1	.064650	.044159	1820.6	+6	.020150	29.46	20.70	68.0	2.324	9.396	76.73	250	
-150	587.8	2	.071745	.049002	1836.8	+8	.020150	29.46	20.70	68.0	1.342	10.366	73.88	250	
-75	1175.7	1	.064420	.043961	1990.9	-15	.020366	29.24	21.35	68.0	1.433	10.279	67.55	12	
-75	1175.7	2	-	-	1924.0	+8	-	29.24	21.20	68.0	1.462	10.253	71.05	17	
-125	1175.7	1	.079033	.053929	1836.4	-	.020122	29.46	20.70	68.0	1.374	10.331	81.85	-	

TABLE XXII  
INTERMEDIATE CALCULATIONS, NITROGEN SPECIFIC HEAT DATA

Nominal Conditions of Cp Determination	Nominal Conditions Pressure, psia	Flow No.	Calorimeter Bath Temp. °F	( $\Delta T$ - $\Delta T$ ) °F	Avg. Temp. of Cp Measurement °F	Avg. Pressure of Cp Measurement psia	Mass Flow Rate, F lb/minute	Reciprocal Mass Flow Rate, 1/F minutes/lb	Measured Power Addition, Q Btu/minute	(Cp)F Btu/lb °F	$\Delta Q$   Btu/min	Cp Btu/lb °F
-50	293.9	1	-59.83	18.37	-50.65	293.3	.2998	3.3356	1.5330	.2784	.0667	.2668
-50	293.9	2	-59.83	18.38	-50.64	294.8	.2171	4.6062	1.1284	.2828	.0677	.2668
-50	587.8	1	-59.82	15.72	-51.96	588.7	.2682	3.7286	1.2565	.2980	.0477	.2871
-50	587.8	2	-59.82	15.85	-51.90	588.0 to 587.7	.1851	5.4025	0.8887	.3029	.0489	.2871
-50	587.8	3	-59.82	16.88	-51.38	586.6	.1806	5.5371	0.8873	.2911	--	--
-50	1175.7	1	-59.59	17.57	-50.81	1174.9	.3095	3.2310	1.8015	.3313	.1035	.3133
-50	1175.7	2	-59.54	17.44	-50.82	1175.3	.2158	4.6339	1.2762	.3391	.1051	.3133
-50	1175.7	3	-59.55	18.33	-50.38	--	.2090	4.7847	1.2757	.3330	--	--
-100	293.9	1	-110.18	18.58	-100.89	294.7	.2189	4.5683	1.1529	.2835	.0590	.2697
-100	293.9	2	-110.18	18.18	-101.09	294.4	.1668	5.9952	0.8729	.2878	.0586	.2697
-100	587.8	1	-110.18	23.14	-98.61	587.2	.2658	3.7622	1.9092	.3104	.0402	.3040
-100	587.8	2	-110.18	23.76	-98.30	588.6	.2027	4.9334	1.5046	.3124	.0416	.3040
-100	881.8	1	-109.52	18.20	-100.42	881.8	.2064	4.8450	1.3347	.3553	.0737	.3364
-100	881.8	2	-109.52	18.27	-100.38	881.8	.2988	3.3467	1.9077	.3495	.0746	.3364
-100	1175.7	1	-109.83	19.48	-100.09	1175.3	.3105	3.2206	2.2396	.3703	.1538	.3465
-100	1175.7	2	-109.83	19.70	-99.98	1177.0	.2353	4.2499	1.7519	.3779	.1588	.3465
-150	293.9	1	-159.50	19.81	-149.60	295.8	.3086	3.2404	1.8663	.3053	.1005	.2897
-150	293.9	2	-159.48	19.66	-149.65	295.4	.2193	4.5600	1.3430	.3115	.1011	.2897
-150	587.8	1	-159.49	19.37	-149.81	588.4	.2237	4.4703	1.6121	.3720	.1070	.3488
-150	587.8	2	-159.49	19.54	-149.22	588.6	.2764	3.6179	1.9852	.3676	.1072	.3488
-75	1175.7	1	-84.51	18.23	-75.40	1174.2	.2516	3.9746	1.6040	.3497	--	--
-75	1175.7	2	-84.51	17.63	-75.70	1176.5	.2606	3.8373	1.6159	.3517	--	--
-125	1175.7	1	-134.73	18.53	-125.47	--	.2987	3.3478	2.4067	.4348	--	--



## BIBLIOGRAPHY

1. American Petroleum Institute, Selected Values of Thermodynamic Properties of Hydrocarbons, Carnegie Press (1953).
2. Aston, J. G., Temperature, Its Measurement and Control in Science and Industry, Reinhold Corp., New York, 219-227 (1941).
3. Aston, J. G., Fink, H. L., Bestul, A. B., Pace, E. L., and Szasz, G.J., J. Am. Chem. Soc., 68, 52 (1946).
4. Aston, J. G. and Messerly, G. H., J. Am. Chem. Soc., 62, 1917 (1940).
5. Balke, W. H. and Kay, W. B., Ind. Eng. Chem., 24, 291 (1932).
6. Barkeley, C. H., Valentine, J. L., and Hurd, C. O., Trans. Am. Inst. Chem. Eng., 43, 25 (1947).
7. Benedict, M., Webb, G. B., and Rubin, L. C., J. Chem. Phys., 8, 334 (1940).
8. Benedict, M., Webb, G. B., and Rubin, L. C., J. Chem. Phys., 10, 747 (1942).
9. Benham, A. H., Ph.D. Thesis, University of Michigan (1956).
10. Bloomer, O. T., Eakin, B. E., Ellington, R. T., and Gami, O. C., Inst. Gas Tech. Res. Bull., No. 21 (1955).
11. Bloomer, O. T., Gami, D. C., and Parent, J. D., Inst. Gas Tech. Res. Bull., No. 22 (1953).
- 12a. Bloomer, O. T. and Rao, K. N., Inst. Gas Tech. Res. Bull., No. 18 (1952).
- 12b. Brickwidde, F. G., Moskow, M., and Aston, J. G., U.S. Nat. Bur. Stds. J. Res., 37, 263 (1946).
13. Budenholzer, R. A., Botkin, D. F., Sage, B. H., and Lacey, W. N., Ind. Eng. Chem., 34, 878 (1942).
14. Budenholzer, R. A., Sage, B. H., and Lacey, W. N., Ind. Eng. Chem., 31, 369 (1939).
15. Budenholzer, R. A., Sage, B. H., and Lacey, W. N., Ind. Eng. Chem., 31, 1288 (1939).
16. Budenholzer, R. A., Sage, B. H., and Lacey, W. N., Ind. Eng. Chem., 32, 384 (1940).

17. Budenholzer, R. A., Sage, B. H., and Lacey, W. N., Ind. Eng. Chem., 35, 1214 (1943).
18. Burcik, E. J., Eyster, E. H., and Yost, D. M., J. Chem. Phys., 9, 118 (1941).
19. Burnett, E. S. and Roebuck, J. R., Phys. Rev., 30, 529 (1910).
20. Callendar, H. L., Trans. Roy. Soc. (London), A199, 55 (1902).
21. Canjar, L. N. and Edmister, W. C., Chem. Eng. Prog. Symposium Ser. No. 7, 49, 73 (1953).
22. Canjar, L. N. and Edmister, W. C., Chem. Eng. Prog. Symposium Ser. No. 7, 49, 93 (1953).
23. Canjar, L. N., Goldman, M., and Marchman, H., Ind. Eng. Chem., 43, 1186 (1951).
24. Canjar, L. N., and Peterka, V. J., Am. Inst. Chem. Eng. J., 2, 343 (1956).
25. Chu, I. C., Mueller, N. L., Bunche, R. M., and Jennings, A. S., Pet. Proc., 5, 1202 (1950).
26. Dailey, B. P. and Felsing, W. A., J. Am. Chem. Soc., 65, 42 (1943).
27. Dana, L. I., Jenkins, A. C., Burdick, J. N., and Timm, R. C., Refrig. Eng., 12, 387 (1926).
28. Dennison, D. M., Rev. Mod. Phys., 12, 175 (1940).
29. DeVries, T. and Collins, B. T., J. Amer. Chem. Soc., 63, 1343 (1941).
30. Dodge, B. F., Chemical Engineering Thermodynamics, McGraw-Hill, New York, 130, 134, (1944).
31. Dodge, B. F., Chemical Engineering Thermodynamics, McGraw-Hill, New York, 392-394 (1944).
32. Edmister, W. C., Am. Inst. Chem. Eng. J., 1, 38 (1955).
33. Egan, C. J. and Kemp, J. D., J. Am. Chem. Soc., 59, 1264 (1937).
34. Eucken, A. and Berger, W., Z. ges. Kälteind., 9, 145 (1934).
35. Eucken, A. and Fried, F., Physik, 29, 4 (1924).
36. Eucken, A. and Lude, K. V., Z. Phys. Chem., B5, 413 (1929).
37. Eucken, A. and Parts, A., Z. Phys. Chem., B20, 184 (1933).

38. Eucken, A. and Weigert, K., Z. Phys. Chem., B23, 265 (1933).
39. Fekula, G. M., Ph.D. Thesis, University of Michigan (1942).
40. Frank, A. and Clusius, K., Z. Phys. Chem., B36, 291 (1937).
41. Frank, A. and Clusius, K., Z. Phys. Chem., B42, 395 (1939).
42. Giaque, W. F. and Clayton, J. O., J. Am. Chem. Soc., 55, 4875 (1933).
43. Glasstone, S., Thermodynamics for Chemists, D. Van Nostrand, New York (1950).
44. Guggenheim, E. A., Proc. Roy. Soc. (London), A148, 304 (1935).
45. Guggenheim, E. A., Trans. Faraday Soc., 33, 151 (1937).
46. Hausen, H., Z. Für Tech. Phys., 371-7, 444-52 (1926).
47. Heuse, W., Ann. Phys., 59, 86 (1919).
48. Hilsenrath, J. and Touloukian, Y. S., Trans. Am. Soc. Mech. Eng., 76, 967 (1954).
49. Holborn, L. and Jacob, M., Akad. der Wissencheften, Berlin Ber., 213 (1914).
50. Hougen, O. A. and Watson, K. M., Chemical Process Principles, Part 2, Thermodynamics, John Wiley and Sons, Inc., New York, 605-12 (1949).
51. Johnston, H. L. and Davis, C. O., J. Am. Chem. Soc., 56, 271 (1934).
52. Katz, D. L. and Rzasa, M. J., Bibliography for Physical Behavior of Hydrocarbons Under Pressure and Related Phenomena, J. W. Edwards, Inc., Ann Arbor, Michigan (1946).
53. Kemp, H. S., Ph.D. Thesis, University of Michigan (1944).
54. Kemp, J. D. and Egan, C. J., J. Am. Chem. Soc., 60, 1521 (1938).
55. Kennedy, E. R., Sage, B. H., and Lacey, W. N., Ind. Eng. Chem., 28, 718 (1936).
56. Kestin, J. and Pilarczyk, K., Trans. Am. Soc. Mech. Eng., Vol. 76, 987 (1954).
57. Kilpatrick, J. E. and Pitzer, K. S., U.S. Nat. Bur. Stds. J. Res., 37, 163 (1946).

58. Kistiakowsky, G. B., Locher, J. R., and Ransom, W. W., J. Chem. Phys., 8, 970 (1940).
59. Kistiakowsky, G. B. and Rice, W. W., J. Am. Chem. Soc., 58, 766 (1936).
60. Kistiakowsky, G. B. and Rice, W. W., J. Chem. Phys., 7, 281 (1931).
61. Kistiakowsky, G. B. and Rice, W. W., J. Chem. Phys., 8, 610 (1940).
62. Konz, P. R., Ph.D. Thesis, University of Michigan (1937).
63. Lewis, G. N. and Randall, M., Thermodynamics and the Free Energy of Chemical Systems, McGraw-Hill, New York (1923).
64. Lindsay, J. D. and Brown, G. G., Ind. Eng. Chem., 27, 817 (1935).
65. Martin, J. J., Unpublished Notes on Thermodynamics, University of Michigan.
66. Masi, J. F., Trans. Am. Soc. Mech. Eng., 76, 1067 (1954).
67. Masi, J. F. and Petkof, B., U.S. Nat. Bur. Stds. J. Res., 48, 179 (1952).
68. Matthews, C. S. and Hurd, C. O., Trans. Am. Inst. Chem. Eng., 42, 55 (1946).
69. McHenry, E. V. and Graham, M., Biochem. J., 29, 2013 (1935).
70. Millar, R. W., J. Am. Chem. Soc., 45, 874 (1923).
71. Miller, O. N., Ph.D. Thesis, University of Michigan (1934).
72. Montgomery, J. B. and DeVries, T., J. Am. Chem. Soc., 64, 2372 (1942).
73. Moore, D. A., Ph.D. Thesis, University of Michigan (1952).
74. Osborne, N. S., U.S. Nat. Bur. Stds. J. Res., 4, 609 (1930).
75. Osborne, N. S., U.S. Nat. Bur. Stds. J. Res., 6, 881 (1931).
76. Osborne, N. S. and Ginnings, D. C., U.S. Nat. Bur. Stds. J. Res., 39, 453 (1947).
77. Osborne, N. S., Stimson, H. F., and Ginnings, D. C., U.S. Nat. Bur. Stds. J. Res., 23, 197 (1937).
78. Osborne, N. S., Stimson, H. F., and Sligh, T. S., Jr., U.S. Nat. Bur. Stds. J. Res., 20, 119 (1925).



79. Papadopoulos, A., Pigford, R. L., and Friend, L., Chem. Eng. Prog. Symposium Ser. No. 7, 49, 119 (1953).
80. Parks, G. S., Shomate, C. H., Kennedy, W. D., and Crawford, B. L., Jr., J. Chem. Phys., 5, 359 (1937)
81. Partington, J. R. and Shilling, N. G., The Specific Heat of Gases, Earnest Binn Ltd., London (1924).
82. Pattee, E. C. and Brown, G. G., Ind. Eng. Chem., 26, 511 (1934).
83. Pitzer, K. S., Ind. Eng. Chem., 36, 829 (1944).
84. Pitzer, K. S., J. Am. Chem. Soc., 63, 2413 (1941).
85. Pitzer, K. S. and Kilpatrick, J. E., Chem. Rev., 39, 435 (1946).
86. Plank, R. and Kanbeitz, J., Z. ges. Kälteind., 43, 209 (1936).
87. Powell, T. M. and Giaque, W. F., J. Am. Chem. Soc., 61, 2366 (1939).
88. Prengle, H. W., Greenhaus, L. R., and York, R., Chem. Eng. Prog., 44, 863 (1948).
89. Redlich, O. and Kister, A. T., Chem. Eng. Prog. Symposium Ser. No. 2, 48, 49 (1952).
90. Redlich, O. and Kister, A. T., Ind. Eng. Chem., 40, 341 (1948).
91. Redlich, O. and Kister, A. T., J. Chem. Phys., 15, 849 (1947).
92. Roebuck, J. R., J. of Appl. Phys., 23, 119 (1952).
93. Roebuck, J. R., Phys. Rev., 2, 301 (1913).
94. Roebuck, J. R., Private Communications (1956-57).
95. Roebuck, J. R., Proc. Am. Acad. Arts and Sci., 60, 537 (1925).
96. Roebuck, J. R., Proc. Am. Acad. Arts and Sci., 64, 287 (1930).
97. Roebuck, J. R., Rev. Sci. Inst., 3, 93 (1932).
98. Roebuck, J. R. and Ibsen, H. W., Rev. Sci. Inst., 25, 46 (1954).
99. Roebuck, J. R., Murrell, T. A., and Miller, E. E., J. Am. Chem. Soc., 64, 400 (1942).
100. Roebuck, J. R. and Osterberg, H., J. Am. Chem. Soc., 60, 341 (1938).
101. Roebuck, J. R. and Osterberg, H., J. Chem. Phys., 8, 627 (1940).

102. Roebuck, J. R. and Osterberg, H., Phys. Rev., 43, 60 (1933).
103. Roebuck, J. R. and Osterberg, H., Phys. Rev., 45, 332 (1934).
104. Roebuck, J. R. and Osterberg, H., Phys. Rev., 46, 785 (1934).
105. Roebuck, J. R. and Osterberg, H., Phys. Rev., 48, 450 (1935).
106. Sage, B. H., Private Communication (1956).
107. Sage, B. H., Evans, H. D., and Lacey, W. N., Ind. Eng. Chem., 31, 763 (1939).
108. Sage, B. H., Kennedy, E. R., and Lacey, W. N., Ind. Eng. Chem., 27, 1484 (1935).
109. Sage, B. H., Kennedy, E. R., and Lacey, W. N., Ind. Eng. Chem., 28, 601 (1936).
110. Sage, B. H. and Lacey, W. N., Ind. Eng. Chem., 29, 658 (1937).
111. Sage, B. H. and Lacey, W. N., Ind. Eng. Chem., 30, 673 (1938).
112. Sage, B. H. and Lacey, W. N., Thermodynamic Properties of the Lighter Paraffin Hydrocarbons and Nitrogen, Am. Pet. Inst., New York (1950).
113. Sage, B. H., Webster, D. C., and Lacey, W. N., Ind. Eng. Chem., 29, 1188 (1937).
114. Sage, B. H., Webster, D. C., and Lacey, W. N., Ind. Eng. Chem., 29, 1309 (1937).
115. Sage, B. H., Webster, D. C., and Lacey, W. N., Ind. Eng. Chem., 35, 922 (1943).
116. Scatchard, G., Chem. Rev., 44, 7 (1949).
117. Scatchard, G., Trans. Faraday Soc., 33, 160 (1937).
118. Scatchard, G., and Raymond, C. L., J. Am. Chem. Soc., 60, 1278 (1938).
119. Scatchard, G. and Tichnor, L. B., J. Am. Chem. Soc., 74, 3724 (1952).
120. Scheele, K. and Heuse, W., Ann Phys., 37, 79 (1912).
121. Scheele, K. and Heuse, W., Ann. Phys., 40, 473 (1913).

122. Scheele, K. and Heuse, W., Ann. Phys., 59, 86 (1919).
123. Schrock, V. E., Nat. Adv. Comm. Aer., Tech. Note 2838 (1952).
124. Scott, R. B., Private Communications (1956).
125. Scott, R. B., Temperature, Its Measurement and Control in Science and Industry, Reinhold Corp., New York, 206-218 (1941).
126. Scott, R. B. and Mellors, J. W., U.S. Nat. Bur. Stds. J. Res., 34, 243 (1945).
127. Stearns, W. V. and George, E. J., Ind. Eng. Chem., 35, 602 (1943).
128. Stiehl, J. G., Hobson, M., and Weber, J. H., J. Am. Inst. Chem. Eng., 2, 389 (1956).
129. Templeton, D. H., Davies, D. D., and Felsing, W. A., J. Am. Chem. Soc., 66, 2033 (1944).
130. Trautz, M. and Ader, H., Z. Phys. Chem., 89, 1 (1934).
131. Tripathi, G., Ph.D. Thesis, University of Michigan (1949).
132. Tsao, C. C. and Smith, J. M., Chem. Eng. Prog. Symposium Ser. No. 7, 49, 107 (1953).
133. U.S. Nat. Bur. Stds., Selected Values of Properties of Hydrocarbons, Circular C461 (1947).
134. U.S. Nat. Bur. Stds., Selected Values of Chemical Thermodynamic Properties, Circular 500 (1952).
135. U.S. Nat. Bur. Stds., Table of Thermal Properties of Gases, Circular 564 (1955).
136. Wacker, P. F., Cheney, R. K., and Scott, R. B., U.S. Nat. Bur. Stds. J. Res., 38, 651 (1947).
137. Waddington, G., Private Communication (1956).
138. Waddington, G. Todd, S. S., and Huffman, H. M., J. Am. Chem. Soc., 69, 22 (1947).
139. Wagman, D. D., Kilpatrick, J. E., Taylor, W. J., Pitzer, K. S., and Rossini, F. D., U.S. Nat. Bur. Stds. J. Res., 34, 243 (1945).
140. Weber, J. H., Am. Inst. Chem. Eng. J., 1, 210 (1955).
141. Weber, J. H., and Hobson, M., Pet. Proc., 12, 153 (1957).